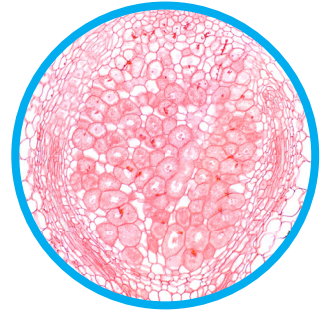
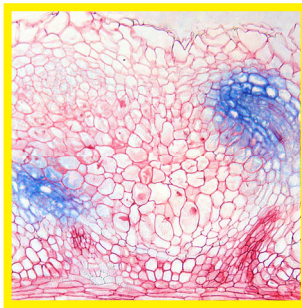
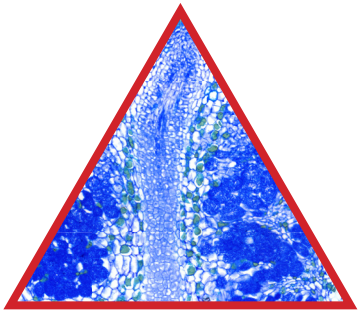


Evolution of Legume Nodule Type

Defeng Shen 2019

Evolution of Legume Nodule Type



Defeng Shen

PROPOSITIONS

1. Legume- and actinorhizal-type nodules share a common evolutionary origin, and the latter is the ancestral type.
(this thesis)
2. *Medicago truncatula* NOOT1 specifies a nodular boundary formation between root vasculature and infected tissue.
(this thesis)
3. The expression pattern of *Nick4* described by Wong et al. (2019, PNAS **116**, 14339-14348) is not reliable, as the authors did not show that the promoter construct can complement the nodulation phenotype of the *nick4* mutant.
4. Di Mambro et al. (2019, Current Biology **29**, 1199-1205) did not demonstrate the biochemical basis by which dexamethasone can activate a cytosolic protein.
5. Overexposure to public opinion restricts independent thinking.
6. Social inequality aggravates ingroup vigilance.

Propositions belonging to the thesis, entitled

Evolution of Legume Nodule Type

Defeng Shen

Wageningen, 2 December 2019

Evolution of Legume Nodule Type

Defeng Shen

Thesis committee

Promotor

Prof. Dr T. Bisseling

Professor of Molecular Biology, Wageningen University & Research

Co-Promotor

Dr R. Geurts

Associate professor, Laboratory of Molecular Biology, Wageningen University & Research

Other members

Prof. Dr F. P. M. Govers, Wageningen University & Research

Dr P. Ratet, Institute of Plant Sciences Paris-Saclay (IPSS2), CNRS,
Gif-sur-Yvette, France

Prof. Dr M. E. Schranz, Wageningen University & Research

Prof. Dr J. Xu, Radboud University, Nijmegen

This research was conducted under the auspices of the Graduate School Experimental Plant Sciences.

Evolution of Legume Nodule Type

Defeng Shen

Thesis

submitted in fulfilment of the requirements for the degree of doctor

at Wageningen University

by the authority of the Rector Magnificus

Prof. Dr A. P. J. Mol,

in the presence of the

Thesis Committee appointed by the Academic Board

to be defended in public

on Monday December 2, 2019

at 4:00 p.m. in the Aula.

Defeng Shen

Evolution of Legume Nodule Type

196 pages

PhD thesis, Wageningen University, Wageningen, NL (2019)

With references, with summary in English

ISBN: 978-94-6395-208-8

DOI: 10.18174/506450

CONTENTS

OUTLINE	7
CHAPTER 1	
General Introduction	11
CHAPTER 2	
The <i>Medicago truncatula</i> Nodule Identity Gene <i>NODULE ROOT1</i> Is Required for Coordinated Apical-Basal Development of the Root	33
CHAPTER 3	
A Homeotic Mutation Changes Legume Nodule Ontogeny into Actinorhizal-type Ontogeny	67
CHAPTER 4	
Conserved Functions of <i>NODULE ROOT1</i> Genes in Actinorhizal-type and Legume-type Nodules Formed by <i>Parasponia andersonii</i> and <i>Medicago truncatula</i>	111
CHAPTER 5	
<i>PanNODULE ROOT1</i> Is a <i>BLADE-ON-PETIOLE</i> Gene that Regulates Branching, Stipule Formation and Leaf Patterning in the Tropical Cannabaceae Tree <i>Parasponia andersonii</i>	141
CHAPTER 6	
General Discussion	173
SUMMARY	189
ACKNOWLEDGMENTS	192
CURRICULUM VITAE	193

OUTLINE

Plant growth requires nitrogen, which can be acquired from the soil, for example, in the form of nitrate and ammonia. However, fixed nitrogen is often a limiting factor for plant growth. To overcome this problem, some plants form root nodules hosting nitrogen-fixing bacteria, which can directly convert atmospheric nitrogen into ammonia. All nodulating plants are part of the Nitrogen-Fixing Clade (NFC), which consists of four orders: Fabales, Rosales, Cucurbitales and Fagales. Within the NFC, members of the legume family (Fabaceae, order Fabales) and *Parasponia* (Cannabaceae, order Rosales) form root nodules with a wide range of bacteria, collectively known as rhizobia; Plants that nodulate with *Frankia* bacteria are called actinorhizal plants, forming actinorhizal nodules. Although *Parasponia* forms a rhizobial symbiosis, the ontogeny of *Parasponia* nodules is similar to that of actinorhizal nodules. Therefore, actinorhizal-type nodules include *Parasponia* nodules. Nodulating is very common in the legume family of order Fabales, but only occurs in 9 out of 24 families in the other three orders. Also, the ontogeny of legume-type and actinorhizal-type nodules has been regarded as fundamentally different. Therefore, it has been hypothesized that the nitrogen-fixing root nodule symbiosis evolved several times (in parallel) in the NFC, twice with rhizobia, eight times with *Frankia*.

Nitrogen-fixing root nodule symbiosis plays a critical role in sustainable agriculture because it reduces the need for nitrogen fertilizers. Understanding the evolutionary relationship between the two types of nitrogen-fixing root nodules is essential for engineering biological nitrogen-fixation in crops. This has been a long-term goal of plant synthetic biologists to improve food production. The objective of this thesis is to analyze the functions of the *NODULE ROOT1* gene in two plant species forming different types of root nodules to dissect the evolutionary relationship between legume-type and actinorhizal-type nodules.

In **CHAPTER 1**, I introduced the current knowledge concerning legume-type and actinorhizal-type nodule development. I focused on the differences and similarities in the ontogeny and molecular mechanisms controlling the formation of these two types of nodules. Based on the feature that both actinorhizal species and several legume mutants in genes orthologous to *NOOT1* can form nodule roots at the nodule apex, I proposed that *NOOT1* could be a key to determine the evolutionary relationship between these two nodule types.

Outline

In **CHAPTER 2**, the function of Medicago *MtNOOT1* during root development was studied. We show that *Mtnoot1* mutant roots grow faster due to an enlarged root apical meristem. Also, *Mtnoot1* mutant roots are thinner than wild-type and delayed in xylem cell differentiation. The affected spatial development of *Mtnoot1* mutant roots correlates with delayed induction of genes involved in xylem cell differentiation. In *Mtnoot1* mutant roots, the zone that is susceptible to rhizobium-secreted Nod factors is basipetally shifted. Our data show that Medicago *MtNOOT1* regulates the root apical meristem size and vascular differentiation, demonstrating that Medicago *MtNOOT1* not only maintains nodule identity, but also coordinates the development of roots.

In **CHAPTER 3**, we analysed the development of actinorhizal-type nodules formed by two plant species (*Parasponia andersonii* and *Alnus glutinosa* (Betulaceae, order Fagales)), and found that their nodule ontogeny is more similar to legume-type nodules than previously described. In actinorhizal-type nodules, pericycle-derived cells only form nodule vasculature. We also showed that in Medicago *Mtnoot1* mutant nodules, vasculature is formed by the pericycle-derived cells, similar to the ontogeny of actinorhizal-type nodule vasculature. This demonstrates that knocking out a single gene can (partially) convert a legume-type nodule into an actinorhizal-type nodule. These findings suggest that these two types of nodules share a common evolutionary origin and the actinorhizal-type nodule is ancestral.

In **CHAPTER 4**, we investigated the function of Medicago *MtNOOT1* orthologous gene in *P. andersonii* (Parasponia) (*PanNOOT1*) by generating CRISPR/Cas9 mutants. In Parasponia *Pannoot1* mutants, nodule roots are formed at the apex of nodules, similar to nodules of legume *noot1* mutants. This indicated that the actinorhizal-type ontogeny of nodule vasculature in Medicago *Mtnoot1* nodules is not sufficient to cause the switch of nodule vasculature to root development. We further showed that Parasponia *PanNOOT1* and Medicago *MtNOOT1* control nodule identity of the vasculature meristem in a cell autonomous manner. In addition, Parasponia *PanNOOT1* and Medicago *MtNOOT1* share conserved functions in regulating nodule meristem development and intracellular colonization of rhizobia in the host cells.

In **CHAPTER 5**, the function of Parasponia *PanNOOT1* in regulating shoot architecture was studied. We showed that the axillary bud emergence and outgrowth are delayed in *Pannoot1* mutants, resulting in reduced axillary branch growth. Also, stipule formation is disturbed and organ fusion between

the stem and the petiole occurs in the *Pannoot1* mutants. We further showed that knock-out of *PanNOOT1* affects the proximal-distal patterning and adaxial-abaxial patterning of leaves, displaying shorter petioles with downwardly curled vasculature and additional abaxialized vasculatures. Our data demonstrated that *PanNOOT1* encodes a *BOP* gene, required for axillary branch development, stipule formation and leaf patterning in the tropical tree *Parasponia*.

In **CHAPTER 6**, I discussed the findings obtained in this thesis, together with recent studies regarding evolutionary aspects of root nodules. I also discussed the general functions of NOOT1, and proposed the ancestral function of NOOT1 in the NFC.

CHAPTER 1

General Introduction

Defeng Shen

Laboratory of Molecular Biology, Department of Plant Sciences, Wageningen University, Droevendaalsesteeg 1, 6708 PB Wageningen, The Netherlands.



1. Nitrogen-fixing Clade

Plants can host nitrogen-fixing bacteria by forming novel lateral root organs, named root nodules. Nitrogen-fixing root nodule symbiosis only occurs in the nitrogen-fixing clade (NFC), which is composed of four orders; Fabales, Fagales, Cucurbitales and Rosales. Legumes (order Fabales) and the non-legume genus *Parasponia* (order Rosales) form nodules with rhizobium bacteria. Other plants that can establish a nitrogen-fixing nodule symbiosis are the actinorhizal plants (orders Fagales, Cucurbitales and Rosales). They can form nodules with *Frankia* bacteria. It has been hypothesised that nodulation evolved multiple times (in parallel) in the NFC; eight times with *Frankia* and twice with rhizobium (Figure 1). The two major reasons supporting this hypothesis are: first, the ontogeny of legume and actinorhizal nodules is fundamentally different and it seems unlikely that they could have a common ancestor; second, species forming actinorhizal nodules are rather rare in the three orders in which they occur and independent gain of nodulation seems more parsimonious than massive loss (Soltis et al., 1995; Swensen, 1996; Doyle, 2011). In this introduction, I will first give an overview of the current knowledge concerning legume and actinorhizal nodule development.

2. Legume Nodules

The Leguminosae (Fabaceae) is the third-largest angiosperm family (LPWG, 2017) and most of its members can form nodules with rhizobium (Teder et al., 2018). Rhizobium is the collective name of Gram-negative bacteria that can form root nodules on legumes and *Parasponia*. They belong to different genera, for example, *Rhizobium*, *Bradyrhizobium*, *Sinorhizobium* and *Mesorhizobium* (Peter et al., 1996). Legume nodules are generally divided into indeterminate and determinate nodules based on whether they form a persistent nodule meristem or not. In determinate nodules, a meristem is formed at the periphery of the primordium, leading to a spherical nodule shape. This meristem disappears at an early stage of nodule development (Hirsch, 1992; Pawlowski and Bisseling, 1996). In this thesis I have studied indeterminate legume nodules and therefore I will describe its anatomy in more detail. In indeterminate nodules a meristem is formed at the apex of the primordium, and it persists to add cells to the different nodule tissues throughout the lifetime of the nodule. By this indeterminate growth nodules obtain an elongated shape and the central tissue shows a developmental gradient with the youngest cells adjacent to the nodule meristem

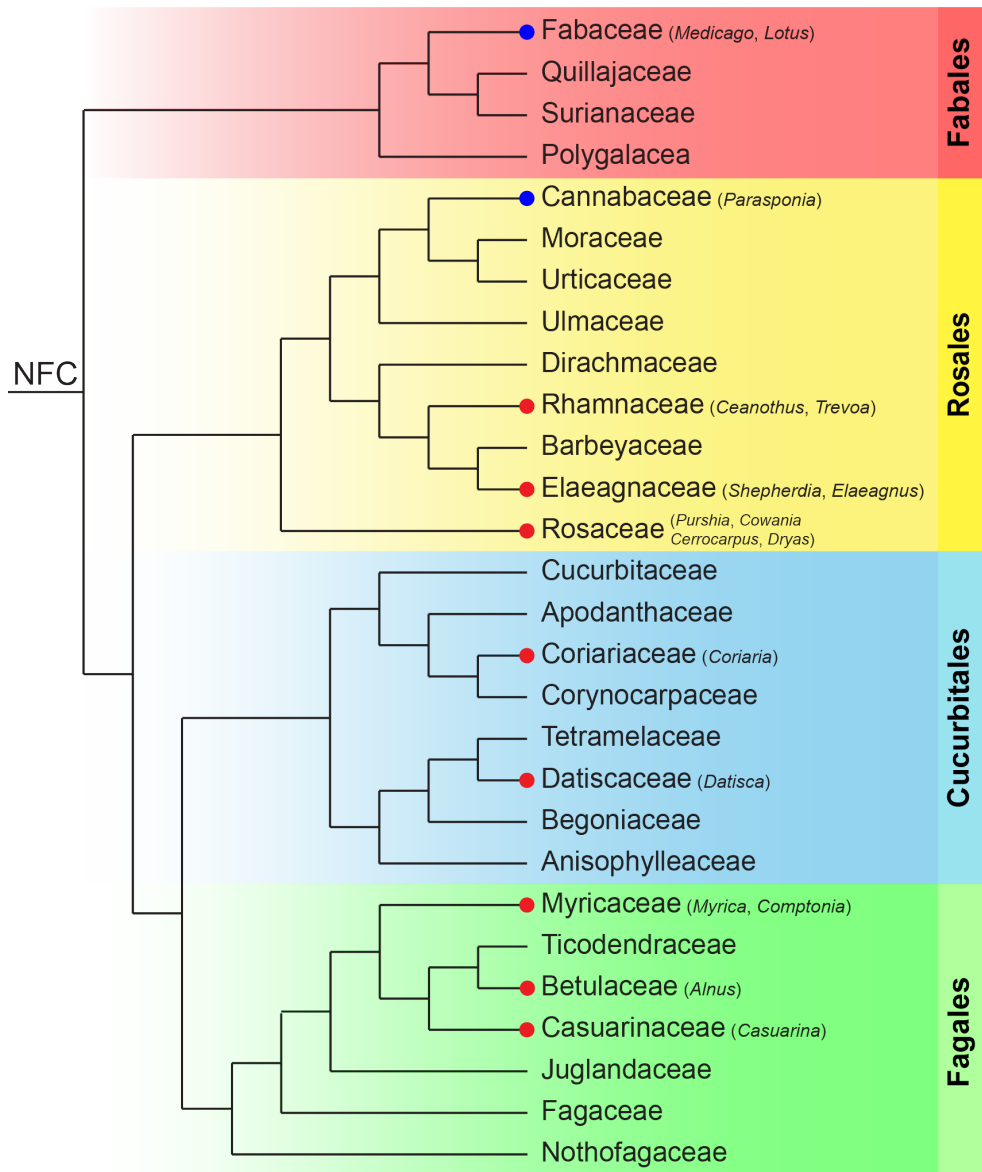


Figure 1. Nitrogen-fixing Clade (NFC). Root nodule symbioses only occur in the NFC, which is composed of four orders; Fabales, Rosales, Cucurbitales and Fagales. The occurrence of rhizobial symbiosis is indicated with blue circles and *Frankia* symbiosis with red circles. When within a family, symbiosis occurs only in one or a few genera, then these are indicated in parentheses. The exception is Fabaceae (legume) family, in which nodulation is very common. *Medicago* and *Lotus* are indicated as model legumes. Phylogenetic tree of the NFC is based on Sun et al., 2016, distribution of nodulating plants based on Tedersoo et al., 2018.

and the oldest cells at the proximal region near to the root attachment point. The zonation of indeterminate nodules is shown in Figure 2. In the nodule meristem, cells actively divide and are not infected by rhizobia. In the infection zone, cells derived from the nodule meristem become infected by rhizobia. Plant cells and rhizobia gradually enlarge and differentiate, which in both cases involves endoreduplication. In the fixation zone differentiated rhizobia (bacteroids) start to fix nitrogen. In the senescence zone, nitrogen fixation ceases and the cells are degraded (Pawlowski and Bisseling, 1996). The model legumes *Lotus japonicus* (Lotus) and *Medicago truncatula* (Medicago) form determinate and indeterminate nodules, respectively. In this thesis I have focused on Medicago and in the following paragraphs, I will focus on this model species unless otherwise indicated.

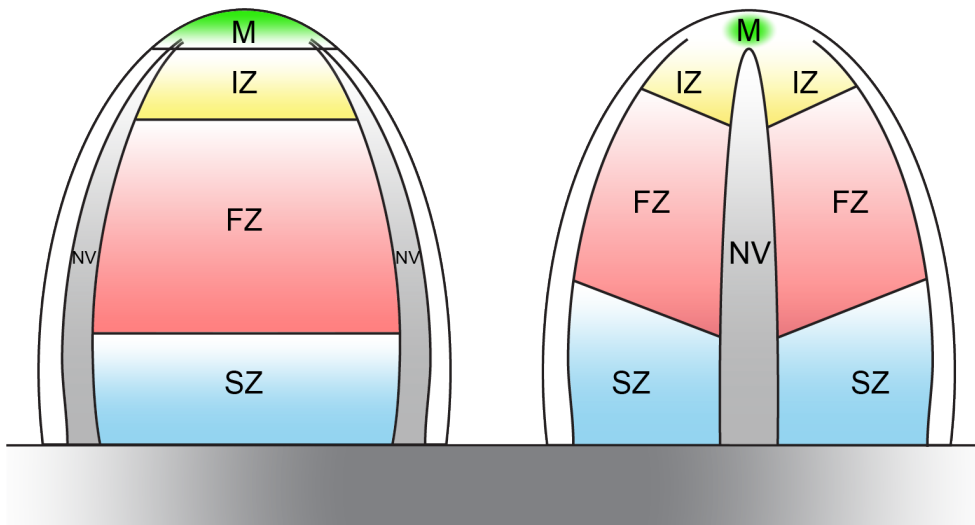


Figure 2. The Zonation in Legume Indeterminate Nodules and Actinorhizal-type Nodules.

Left side: the zonation of legume indeterminate nodules. In the nodule meristem (M), cells remain mitotically active and are not infected by rhizobia. In the infection zone (IZ), cells derived from the nodule meristem become infected by rhizobia, which are released from infection threads. Plant and rhizobium cells gradually enlarge and differentiate. In the fixation zone (FZ), the infected cells are fully packed with differentiated rhizobia (bacteroids), which fix nitrogen. In the senescence zone (SZ), nitrogen fixation ceases, and bacteroids disintegrate and plant cells are degraded. Nodule vasculatures (NV) are located at the periphery of the central tissue.

Right side: The zonation of actinorhizal-type nodules. Actinorhizal-type nodules are coralloid organs composed of multiple lobes. Shown here is a simplified nodule zonation with one lobe. Actinorhizal-type nodules have a central nodule vasculature (NV), with infected cells in the expanded cortex. In the nodule meristem (M), cells

Continued on next page

2.1 Formation of Indeterminate Legume Nodules

The formation of legume nodules involves two coordinated processes: nodule organogenesis and bacterial infection. These two processes are triggered by Nodulation (Nod) factors. Nod factors are lipochitooligosaccharides (LCOs) secreted by rhizobium bacteria in response to specific compounds, often flavonoids, secreted by plant roots (Limpens et al., 2015). Rhizobia attach to the root hairs and induce root hair curling. In this way rhizobia become entrapped at the root hair tips in a closed cavity. There infection threads are initiated by local cell wall hydrolysis and invagination of the plasma membrane, subsequently they grow by tip growth. ROS production is presumed to facilitate the oxidative cross-linking of the infection thread matrix to allow the formation of a tube-like infection thread (Gage, 2004; Brewin, 2004). The infection threads traverse the root hair and outer cortex cells and reach the mitotically activated inner cortical cells (Gage, 2004; Brewin, 2004; Xiao et al., 2014).

Medicago nodule organogenesis starts with anticlinal cell division in pericycle cells opposite protoxylem poles. Subsequently, inner cortical cells (layers C4 and C5) start to divide anticlinally. Cell division is later induced in endodermis, and it continues in C4 and C5. When the infection thread has reached the middle cortical layer (C3), cells of this layer are mitotically activated. This allows the infection thread to pass the C3 layer, and by continued division C3 forms a multi-layered (future) meristem, which is not infected by rhizobia. When C4 and C5 have formed about eight cell layers, and the endodermis and pericycle have formed six to eight cell layers, all these cell layers stop dividing. The C4- and C5-derived cells become penetrated by infection threads from which rhizobia are released (Xiao et al., 2014). During this release they become surrounded by the plant-derived peribacteroid membrane. In this way an organelle-like structure, called symbiosome, is formed (Ivanov et al., 2010). The C4- and C5-derived cells at the periphery of the primordium, start to differentiate to form peripheral

Continued

are actively dividing, adding cells to be infected and supporting the growth of the central vasculature. In the infection zone (IZ), cells become gradually filled with branching *Frankia* hyphae. In the fixation zone (FZ) of most host plants, *Frankia* develop vesicles where nitrogen fixation occurs. In the senescence zone (SZ), *Frankia* hyphae and vesicles are degraded. In the nodules formed by actinorhizal Cucurbitales, the infected cells form an uninterrupted domain, on one side of the nodule vasculature. The drawing on the zonation of actinorhizal-type nodules is based on Pawlowski and Demchenko, 2012.

1
tissues including vascular bundles. The meristem at the apex starts to add cells to the nodule central tissue as well as the peripheral tissues including vasculature, by which the nodule grows (Xiao et al., 2014). The process of infection thread penetration and symbiosome formation continues in the nodule and occurs in the cell layer adjacent to the meristem. Upon release the symbiosomes divide and start to enlarge. Meanwhile, the infected host cells differentiate and enlarge involving endoduplication, which is mediated by cell cycle regulator *ccs52* (Cebolla et al., 1999). At the transition from infection to fixation zone the expression of nitrogen fixation (*nif*) genes encoding nitrogenase subunits is induced and nitrogen fixation starts (Yang et al., 1991; de Maagd et al., 2011). This transition seems to involve a molecular switch as it is associated with several other changes that occur within one cell layer. This includes accumulation of starch (Vasse et al., 1990), major rearrangement of actin skeleton (Gavrin et al., 2015), collapse of vacuole (Gavrin et al., 2014). Further, endoduplication ceases when cells start to fix nitrogen and the expression of *ccs52* is drastically reduced in the fixation zone (Cebolla et al., 1999).

2.2 Nod Factor Signalling Pathway

Genetic studies on the model legumes *Medicago* and *Lotus* have revealed a set of genes, that encode components of the Nod factor signalling pathway. Nod factors are perceived by two types of LysM domain receptor kinases (LysM-RKs) (MtLYK3/MtNFP in *Medicago* and LjNFR1/LjNFR5 in *Lotus*) (Madsen et al., 2003; Radutoiu et al., 2003; Limpens et al., 2003; Arrighi et al., 2006; Mulder et al., 2006; Smit et al., 2007). Nod factor receptors trigger nuclear calcium oscillations by activating a signalling cascade, which includes a plasma membrane-localized leucine-rich repeat receptor kinase (MtDMI2 in *Medicago*, LjSYMRK in *Lotus*) (Endre et al., 2002; Stracke et al., 2002), nuclear membrane-localized cation channels (potassium-permeable channels: MtDMI1 in *Medicago*, LjCASTOR and LjPOLLUX in *Lotus*; and calcium channels: MtCNGCs in *Medicago*), and several components of the nuclear pore complex (e.g. LjNUP85 and LjNUP133 in *Lotus*) (Ané et al., 2004; Kanamori et al., 2006; Saito et al., 2007; Charpentier et al., 2008, 2016). Nuclear calcium oscillations are decoded by a nuclear localized calcium- and calmodulin-dependent protein kinase (MtDMI3 in *Medicago*; LjCCaMK in *Lotus*) (Levy, 2004; Tirichine et al., 2006). This kinase activates the transcriptional activator MtIPD3/LjCYCLOPS, which subsequently induces the expression of downstream genes (Messinese et al., 2007; Yano et al., 2008).

The above described part of the Nod factor signalling pathway (common symbiosis signalling pathway), has been proposed to be co-opted from the more ancient arbuscular mycorrhiza (AM) symbiosis. This is because all these Nod factor signalling components, except the Nod factor receptors, are also required for AM symbiosis. As Myc factors and Nod factors are structurally very similar, it has been proposed that the receptors involved in perceiving these factors are similar (Limpens et al., 2015). This hypothesis is in agreement with the fact that Myc factors might be perceived by MtNFP, as the induction of lateral root formation by Myc factors in *Medicago* is dependent on MtNFP (Maillet et al., 2011). Furthermore, MtNFP is required for the early transcriptional changes induced by Myc factors (Czaja et al., 2012). However, *Mtnfp* and *Ljnf5* knockout mutants are not impaired in AM colonization (Amor et al., 2003; Radutoiu et al., 2003), suggesting that additional LysM-RK(s) closely related to MtNFP and LjNFR5 is (are) involved in Myc factor perception. In line with this, *Mtlyk3* and *Ljnf1* mutants have a slightly reduced mycorrhizal infection (Zhang et al., 2015). The involvement of additional Myc factor receptors is also supported by the fact that MtLYR1, a paralog of MtNFP, is upregulated upon mycorrhization (Gomez et al., 2009; Hogeekamp et al., 2011; Gaude et al., 2012), suggesting potential functions in the mycorrhizal association. Therefore, it has been hypothesized that duplication of ancestral (LysM-RKs) Myc factor receptor genes enabled neofunctionalization to evolve Nod factor receptors, while maintaining Myc factor perception (Op den Camp et al., 2011). Consistent with this, a homolog of MtLYK3/LjNFR1 in *Parasponia andersonii* has been recently identified that plays a role in AM and root nodule symbioses (R Geurts, pers. comm.).

The primary downstream target of MtIPD3/LjCYCLOPS is the gene encoding the transcription factor NODULE INCEPTION (MtNIN/LjNIN) (Singh et al., 2014), which has been shown to be specifically expressed during nodulation and it is essential for infection thread formation and nodule organogenesis (Schauser et al., 1999; Marsh et al., 2007). In *nin* null mutants, excessive root hair curling and deformation are induced by rhizobia, but infection thread as well as nodule organogenesis are blocked (Schauser et al., 1999; Marsh et al., 2007). Dominant active forms of the CCaMK protein or a phosphomimetic version of CYCLOPS can induce spontaneous nodule organogenesis and this is dependent on NIN (Gleason et al., 2006; Tirichine et al., 2006; Singh et al., 2014). In the weak *nin* alleles *daphne* (*Lotus*) and *daphne-like* (*Medicago*), the promoter region of *NIN* is mutated. Both weak *nin* alleles have a dramatically increased number of infection threads, but nodule formation is absent (Yoro

1 et al., 2014; Liu et al., 2019). This shows that rhizobial infection and nodule organogenesis can be uncoupled. A detailed study of the promoter region of *Medicago NIN* revealed that the 5 kb region upstream of the *NIN* start codon is sufficient for the epidermal infection process, but nodule organogenesis requires a remote upstream *cis*-regulatory region to induce the expression of *NIN* in the pericycle. This remote region contains putative cytokinin response elements and is conserved in legume species. The gene encoding cytokine receptor 1, which is essential for nodule primordium formation, as well as the B-type cytokine response regulator *RR1* are expressed in the pericycle cells prior to the induction of *NIN* in the pericycle (Liu et al., 2019). Taken together, it is very likely that *NIN* expression is initially triggered by cytokinin signalling in the pericycle and this initiates nodule primordium formation. So, at early stages of nodule primordium formation the expression of *NIN* is induced at two positions (and in different ways): first, induction of *NIN* in the epidermis cells to initiate infection thread formation; second, activation of *NIN* in the pericycle cells by cytokinin signalling to initiate nodule organogenesis. At later stages of primordium formation, the expression of *NIN* extends to the dividing cortical cells. *NIN* is closely related to *NIN*-LIKE PROTEINs (NLPs), which are widely present in vascular plants. *NIN* is orthologous to *Arabidopsis* NLP1 which is involved in nitrate signalling. *NIN* has lost the nitrate signalling domain and its expression became under control of the Nod factor signalling cascade (Suzuki et al., 2013; Chardin et al., 2014; Van Zeijl et al., 2015). Its recruitment into the nodule formation process represents a major step in the evolution of legume nodulation.

NIN activates the expression of *Nuclear transcription factor Y subunit A-1* (*MtNF-YA1/LjNF-YA1*) (Soyano et al., 2013). In *Medicago*, *MtNF-YA1* is necessary for rhizobial infection and proper formation of nodule meristem (Combiér et al., 2006; Xiao et al., 2014; Laporte et al., 2014); In *Lotus*, *LjNF-YA1* is required for normal nodule organogenesis (Hossain et al., 2016). *MtNF-YA1* can positively regulate the expression of *ethylene response factor required for nodulation 1* (*ERN1*), which encodes an AP2/ERF transcription factor and is essential for infection thread formation (Andrianakaja et al., 2007; Middleton et al., 2007; Cerri et al., 2012).

Nodule formation also requires several other genes. For example, *Rhizobium-directed polar growth* (*RPG*) is required for infection thread progression in root hairs, where it controls the process of polar growth (Arrighi et al., 2008). Two GRAS-domain transcription factors *NSP1* and *NSP2* are also essential for

infection and nodule organogenesis (Kaló et al., 2005; Smit et al., 2005). In *Medicago* epidermis cells, they promote the expression of *ERN1* and infection marker *Early nodulin 11* (Cerri et al., 2012).

2.3 General Aspects of Legume Nodule Formation

Above I described different aspects of legume nodule development and focused on the model plant *Medicago*. However, most of what I described is in general relevant for most legumes although variations on the described processes occur.

The infection by infection threads that start in the epidermis seems to be the most advanced form of infection. However, rhizobia can enter the roots without forming such infection thread in some legumes. For example, in *Lupinus albus* infections occur between epidermal cells (González-Sama et al., 2004). Further, rhizobia can also enter through natural cracks at the lateral/adventitious root base in an intercellular manner, known as ‘crack-entry’. This is for example the case in some *Sesbania* and *Aeschynomene* species (Sprent, 2007).

Nodule ontogeny and anatomy is well conserved within the Leguminosae. In all cases they have a central infected tissue and peripheral vascular bundles. The central tissue is derived from the mitotically activated cortical cells. The determinate and indeterminate nodule type are different with respect to the persistence of the meristem.

In all studied legume species, the rhizobia are hosted intracellularly. In most cases they are in symbiosomes that are not attached to the infection threads. However, in some species of the basal legume genus *Chamaecrista* rhizobia are present in fixation threads. These are extensions of infection threads that can fill a major part of infected cells (Naisbitt et al., 1992). These intracellular fixation threads are very similar to the mode of intracellular infection in actinorhizal nodules (see below). In symbiosomes as well as fixation threads a symbiotic interface is created as no or very little matrix is present in between the membrane of the host and that of the rhizobia. In *Medicago*, it has been shown that the formation of this symbiotic interface involves the recruitment of a symbiosis-specific exocytosis pathway involved in arbuscule formation in the AM symbiosis (Ivanov et al., 2012). In line with the common symbiosis signalling pathway, that is also recruited from the AM symbiosis, I hypothesise that this symbiosis-specific exocytosis pathway is widely used in the legume family during nodule formation.

1 In all legumes that have been studied the common symbiosis signalling pathway is essential. This pathway is activated after perception of Nod factors. In the few cases that root nodule formation is activated by rhizobia that do not make Nod factors, e.g. some *Aeschynomene* species (Okazaki et al., 2016), members of the common symbiosis signalling pathway are still essential for nodulation (Fabre et al., 2015). This suggests that in these species a new receptor evolved that can (also) activate the common symbiosis signalling pathway. In addition to the common symbiosis signalling pathway, NIN has been shown to be a key player in nodule organogenesis and infection, in all species that have been studied. In case of parallel evolution of actinorhizal nodules it will be interesting to see whether the same genes have been recruited or whether it involved a different evolutionary trajectory.

3. Actinorhizal Nodules

In contrast to rhizobial symbiosis, the actinorhizal species occur in markedly more plant families, which belong to three different orders (Fagales, Cucurbitales and Rosales) (Soltis et al., 1995; Swensen, 1996). While the vast majority of the legume species can establish a nodule symbiosis, the number of species that can form actinorhizal nodules is rather low. The phylogenetic relationship of genera containing actinorhizal plants is in general rather distant and genera with actinorhizal species can be part of a family with many genera without actinorhizal species. For example, in the Betulaceae family *Alnus* spp. can form nodules, whereas their close relatives *Betula* spp. do not (Bousquet et al., 1989). This scattered occurrence of actinorhizal species is one of the arguments used to support the hypothesis that actinorhizal nodulation evolved several times independently (Soltis et al., 1995; Swensen, 1996; Doyle, 2011) (Figure 1).

Nodule formation on actinorhizal plants is induced by *Frankia* bacteria. They are filamentous Gram-positive bacteria, which can be phylogenetically divided into three main clusters. Strains from *Frankia* Cluster I can nodulate most actinorhizal plants of the order Fagales. The strains from Cluster II, which is sister to the other *Frankia* clusters, have a broad range of host plants belonging to four families within the orders Rosales and Cucurbitales. *Frankia* Cluster III strains nodulate plants from two families of the order Rosales, and two genera from the order Fagales. Actinorhizal nodules are coralloid organs composed of multiple lobes. Each lobe has a central vascular system, and infected cells in the expanded cortex. Due to the apical meristem of each lobe, the infected cortical

cells are arranged in a developmental gradient, similar to indeterminate legume nodules. The cells in the apical meristem remain mitotically active, adding cells to be infected and supporting the growth of the central vasculature. Adjacent to the meristem is the infection zone, where the cells become gradually filled with branching *Frankia* hyphae. Subsequently, in the nitrogen fixation zone of most host plants, *Frankia* develop vesicles where nitrogen fixation can take place. In the infected cells of the senescence zone, *Frankia* hyphae and vesicles are degraded (Pawlowski and Demchenko, 2012; Santi et al., 2013) (Figure 2).

3.1 Actinorhizal Nodule Formation

Several studies have indicated that actinorhizal nodules originate from root pericycle cells. Upon *Frankia* infection, mitotic activity is induced in the pericycle cells opposite to protoxylem poles. It has been concluded that these cells form nodule primordia from which the nodules develop. These nodules resemble modified lateral roots. However, they are different from lateral roots, for example, they do not form a root cap nor an epidermis. The nodule vasculature is at the central position of this lateral root-like nodule, of which cortex cells are infected by *Frankia* in an intracellular manner (Pawlowski and Bisseling, 1996; Pawlowski and Demchenko, 2012). Similar to nodules formed by some basal legumes (e.g. *Chamaecrista*), actinorhizal infection threads form fixation threads that fill the infected cells and stay attached to the infection threads. *Frankia* in the fixation threads form vesicles. There nitrogenase is formed to fix nitrogen, and the vesicles provide a compartment that protects nitrogenase against oxygen damage (Pawlowski and Demchenko, 2012).

The infection processes vary among actinorhizal plants of different orders. In Fagales, the infection process is intracellular, similar to the root hair infection process described for legumes like *Medicago* and *Lotus*. The infection threads traverse the root hair and grow towards mitotically activated cortical cells. These cells are colonized by infection threads, forming the so-called “prenodule”. It has been described that infection threads grow from the prenodule to the cortex of nodule primordium, where they are hosted in an intracellular manner. The prenodule will not merge with the mature nodule (Callaham and Torrey, 1977; Callaham et al., 1979; Torrey and Callaham, 1979; Burgess and Peterson, 1987; Racette and Torrey, 1989). In Rosales, the infection process of actinorhizal nodules is intercellular. *Frankia* bacteria directly penetrate the middle lamella between intact root epidermis cells and progressively colonize the intercellular

spaces of the root cortex (Miller and Baker, 1985; Racette and Torrey, 1989; Liu and Berry, 1991a, 1991b; Valverde and Wall, 1999). *Frankia* hyphae are surrounded by pectin-rich compounds, which are secreted by epidermal and cortical cells. These compounds are possibly an equivalent of the cell wall-like material of infection threads formed during intracellular infection (Liu and Berry, 1991a). Concomitantly, *Frankia* hyphae grow from the root cortex towards to the newly formed cortex of the primordium through the intercellular spaces. The infection process is hardly studied in actinorhizal species of the Cucurbitales, because they are infected by non-culturable *Frankia* bacteria (Pawlowski and Demchenko, 2012).

Although *Parasponia* spp. form nodules with rhizobia, the nodule structure and development resemble those of actinorhizal nodules. Rhizobia enter the root through the intercellular space of epidermis and cortex. It has been described that mitotically activated root cortical cells form a pre-nodule, which is infected by intracellular infection threads. Subsequently, infection threads infect the cortex of pericycle-derived nodule primordia with a lateral root-like organization (Lancelle and Torrey, 1984, 1985). Similar to *Frankia* in actinorhizal nodules, rhizobia are hosted in fixation threads (Lancelle and Torrey, 1984, 1985; Op den Camp et al., 2011, 2012).

Based on the shared features between actinorhizal nodules and *Parasponia* nodules, they are collectively referred to as actinorhizal-type nodules. The common features of actinorhizal-type nodules are that pericycle-derived nodule primordia develop into mature nodules with a central vasculature and infected cells are located at the periphery. In these cells, nitrogen-fixing bacteria surrounded by a plant-derived membrane are intracellularly accommodated.

3.2 Shared Common Signalling Pathway

In legumes the common symbiosis signalling pathway and NIN play a key role in infection and nodule organogenesis. Therefore, it has been tested whether this is also the case in plants forming actinorhizal-type nodules. These studies focused on *Casuarina glauca* (order Fagales) and *Datisca glomerata* (order Cucurbitales), because these species can be transformed. They belong to different orders and because of their phylogenetic position within the NFC they can represent plants in which nodulation evolved independently. The common symbiosis signalling component SYMRK has been studied in both *C. glauca* and *D. glomerata*. These studies involved knock-down approaches which

showed that SYMRK is essential for nodulation in both species (Gherbi et al., 2008; Markmann et al., 2008). This suggests that in both cases the common symbiosis signalling pathway has been recruited to support nodule formation. Further, similar to legumes, an auto-active version of CgCCaMK can induce spontaneous nodules in *C. glauca*. This construct can also induce nodule formation in *Discaria trinervis* (Svistoonoff et al., 2013). As *D. trinervis* belongs to the order Rosales, it suggests that also in this order the common symbiosis signalling pathway is important for nodulation. As mentioned above, *PanNFP* is also required for nodulation in *P. andersonii* (Parasponia) (Op den Camp et al., 2011) as this receptor activates the common symbiosis signalling pathway in legumes, this suggests that this is also the case in Parasponia.

Similar to legumes, NIN is also needed for nodule formation in *C. glauca*, as downregulation of *CgNIN* reduces nodule number (Clavijo et al., 2015). Further, *NIN* is induced in nodules of *D. glomerata* and *P. andersonii* (Demina et al., 2013; van Velzen et al., 2018), suggesting a common role for NIN in the formation of these actinorhizal-type nodules. Therefore, the common symbiosis signalling pathway and nodule-specific *NIN* both might play an important role in actinorhizal-type nodule formation.

The involvement of the common symbiosis signalling pathway in actinorhizal nodulation suggests that *Frankia* makes LCO molecules similar to Nod factor. However, the non-characterized signal molecules of Cluster I *Frankia* strains (ACN14a and Ccl3) that induce symbiotic responses are hydrophilic and resistant to chitinase degradation, in contrast to the properties of Nod factors, that are amphiphilic and chitinase sensitive (Chabaud et al., 2016). Further, broad host range *Rhizobium* sp. NGR234 strain and its purified Nod factors cannot elicit root hair deformation on *A. glutinosa*, suggesting that *A. glutinosa* does not recognize Nod factors (C  r  monie et al., 1999). Intriguingly, *nodABC*-like genes have been identified in the genome of Cluster II *Candidatus Frankia datisc  e* Dg1 strain, a microsymbiont of *D. glomerata* (Persson et al., 2015). However, no strain from Cluster II is culturable, which hinders the identification of *Frankia* LCOs. Although the presence of LCOs has not yet been confirmed, it is tempting to propose that Nod factor-like molecules produced by Dg1 trigger actinorhizal nodule formation in *D. glomerata*. As the *Frankia* strains from Cluster II form the basal group of the symbiotic *Frankia* clusters, it has been hypothesised that the last common ancestor of the symbiotic *Frankia* strains contained the canonical *nod* genes, but these are subsequently lost in the progenitor of *Frankia* Clusters I and III (Persson et al., 2015). This is consistent with the absence of these

nod-like genes in *Frankia* Clusters I and III. Therefore, it appears that similar to legume-rhizobium symbiosis, the genetic components of the common symbiosis signalling pathway and (at least) *NIN* were also recruited during the evolution of actinorhizal-type nodules. If the evolution of the root nodules is indeed in parallel in different lineages, this would require a convergent recruitment of *NIN* and the common symbiosis signalling pathway in actinorhizal plants and legumes multiple times.

4. Legume-type Nodules vs. Actinorhizal-type Nodules

In summary, legume-type nodules are stem-like with a peripheral vascular system and infected cells in the central tissue; actinorhizal-type nodules are root-like with a central vasculature and infected cortex at the periphery (Pawlowski and Demchenko, 2012). The ontogeny of these two nodule types is fundamentally different. Therefore, they cannot share a single evolutionary origin. Hence, it has been postulated that a genetic predisposition event leading to a precursor state for nodulation evolved in the youngest common ancestor of the NFC. This precursor state allowed the parallel evolution of nodulation in different descendant lineages (Soltis et al., 1995; Swensen, 1996; Doyle, 2011). However, the involvement of both the common symbiotic signalling pathway and *NIN* in all studied nitrogen-fixing symbioses is most parsimonious when this process evolved only once. Therefore, it is essential to reinvestigate whether the arguments used for parallel evolution are supported by sufficient experimental data.

Actinorhizal-type nodules and lateral roots share a similar developmental program, it is not surprising that some actinorhizal-type nodules (e.g. the nodules of *C. glauca*, *Myrica gale*, *Coriaria arborea*, *D. glomerata*) can form so-called nodule roots (Pawlowski and Bisseling, 1996). This suggests that the apical meristem of a nodule lobe can change its identity and forms roots. Such nodule to root identity conversion can also occur in a legume mutant. Knockout of *NODULE ROOT1* (*MtNOOT1*) gene in Medicago, or its orthologous genes in pea (*PsCOCHLEATA1* (*PsCOCH1*)) and Lotus (*LjNOOT-BOP-COCH-LIKE1* (*LjNBCL1*)) can all lead to root outgrowth at the nodule apex (Ferguson and Reid, 2005; Couzigou et al., 2012; Magne et al., 2018). Therefore, I hypothesize that *NOOT1* could be a key to determine the evolutionary relationship between these two nodule types. In this thesis, I compared the nodule and lateral root developmental programs in two species forming actinorhizal-type nodules

(*Alnus glutinosa* and *P. andersonii*) together with the nodule organogenesis of *Medicago Mtnoot1* mutants (**CHAPTER 3**). To understand the intrinsic identity of actinorhizal-type nodule vasculatures, I analysed the function of *P. andersonii* *NOOT1* (*PanNOOT1*) during nodule development (**CHAPTER 4**). Further, to better understand the role of *NOOT1* in symbiosis, I analysed the non-symbiotic function of *MtNOOT1* during root development (**CHAPTER 2**) and the function of *PanNOOT1* during shoot development (**CHAPTER 5**).

REFERENCES

- Amor, B. Ben, Shaw, S.L., Oldroyd, G.E.D., Maillet, F., Penmetsa, R.V., Cook, D., Long, S.R., Denarie, J., and Gough, C.** (2003). The *NFP* locus of *Medicago truncatula* controls an early step of Nod factor signal transduction upstream of a rapid calcium flux and root hair deformation. *Plant J.* **34**: 495–506.
- Andriankaja, A., Boisson-Dernier, A., Frances, L., Sauviac, L., Jauneau, A., Barker, D.G., and de Carvalho-Niebel, F.** (2007). AP2-ERF Transcription Factors Mediate Nod Factor-Dependent *Mt ENOD11* Activation in Root Hairs via a Novel *cis* -Regulatory Motif. *Plant Cell* **19**: 2866–2885.
- Ané, J.-M. et al.** (2004). *Medicago truncatula* *DMI1* required for bacterial and fungal symbioses in legumes. *Science* **303**: 1364–1367.
- Arrighi, J.-F. et al.** (2006). The *Medicago truncatula* Lysine Motif-Receptor-Like Kinase Gene Family Includes *NFP* and New Nodule-Expressed Genes. *Plant Physiol.* **142**: 265–279.
- Arrighi, J.-F., Godfroy, O., de Billy, F., Saurat, O., Jauneau, A., and Gough, C.** (2008). The *RPG* gene of *Medicago truncatula* controls *Rhizobium*-directed polar growth during infection. *Proc. Natl. Acad. Sci.* **105**: 9817–9822.
- Bousquet, J., Girouard, E., Strobeck, C., Dancik, B.P., and Lalonde, M.** (1989). Restriction fragment polymorphisms in the rDNA region among seven species of *Alnus* and *Betula papyrifera*. *Plant Soil* **118**: 231–240.
- Brewin, N.J.** (2004). Plant Cell Wall Remodelling in the Rhizobium–Legume Symbiosis. *CRC. Crit. Rev. Plant Sci.* **23**: 293–316.
- Burgess, D. and Peterson, R.L.** (1987). Development of *Alnus japonica* root nodules after inoculation with *Frankia* strain HFPAr13. *Can. J. Bot.* **65**: 1647–1657.
- Callaham, D., Newcomb, W., Torrey, J.G., and Peterson, R.L.** (1979). Root Hair Infection in Actinomycete-Induced Root Nodule Initiation in Casuarina, Myrica, and Comptonia. *Bot. Gaz.* **140**: S1–S9.
- Callaham, D. and Torrey, J.G.** (1977). Prenodule formation and primary nodule development in roots of *Comptonia* (Myricaceae). *Can. J. Bot.* **55**: 2306–2318.
- Cebolla, A., Vinardell, J.M., Kiss, E., Oláh, B., Roudier, F., Kondorosi, A., and Kondorosi, E.** (1999). The mitotic inhibitor *ccs52* is required for endoreduplication and ploidy-dependent cell enlargement in plants. *EMBO J.* **18**: 4476–4484.
- Cérémonie, H., Debellé, F., and Fernandez, M.P.** (1999). Structural and functional

- comparison of *Frankia* root hair deforming factor and rhizobia Nod factor. *Can. J. Bot.* **77**: 1293–1301.
- Cerri, M.R., Frances, L., Laloum, T., Auriac, M.-C., Niebel, A., Oldroyd, G.E.D., Barker, D.G., Fournier, J., and de Carvalho-Niebel, F.** (2012). *Medicago truncatula* ERN Transcription Factors: Regulatory Interplay with NSP1/NSP2 GRAS Factors and Expression Dynamics throughout Rhizobial Infection. *Plant Physiol.* **160**: 2155–2172.
- Chabaud, M., Gherbi, H., Pirolles, E., Vaissayre, V., Fournier, J., Moukouanga, D., Franche, C., Bogusz, D., Tisa, L.S., Barker, D.G., and Svistoonoff, S.** (2016). Chitinase-resistant hydrophilic symbiotic factors secreted by *Frankia* activate both Ca²⁺ spiking and *NIN* gene expression in the actinorhizal plant *Casuarina glauca*. *New Phytol.* **209**: 86–93.
- Chardin, C., Girin, T., Roudier, F., Meyer, C., and Krapp, A.** (2014). The plant RWP-RK transcription factors: Key regulators of nitrogen responses and of gametophyte development. *J. Exp. Bot.* **65**: 5577–5587.
- Charpentier, M., Bredemeier, R., Wanner, G., Takeda, N., Schleiff, E., and Parniske, M.** (2008). *Lotus japonicus* CASTOR and POLLUX Are Ion Channels Essential for Perinuclear Calcium Spiking in Legume Root Endosymbiosis. *Plant Cell* **20**: 3467–3479.
- Charpentier, M., Sun, J., Martins, T.V., Radhakrishnan, G. V, Findlay, K., Soumpourou, E., Thouin, J., Véry, A.-A., Sanders, D., Morris, R.J., and Oldroyd, G.E.D.** (2016). Nuclear-localized cyclic nucleotide-gated channels mediate symbiotic calcium oscillations. *Science* **352**: 1102–5.
- Clavijo, F. et al.** (2015). The *Casuarina NIN* gene is transcriptionally activated throughout *Frankia* root infection as well as in response to bacterial diffusible signals. *New Phytol.* **208**: 887–903.
- Combiér, J.-P.P., Frugier, F., De Billy, F., Boualem, A., El-Yahyaoui, F., Moreau, S., Vernié, T., Ott, T., Gamas, P., Crespi, M., and Niebel, A.** (2006). *MtHAP2-1* is a key transcriptional regulator of symbiotic nodule development regulated by microRNA169 in *Medicago truncatula*. *Genes Dev.* **20**: 3084–8.
- Couzigou, J.-M.J. et al.** (2012). *NODULE ROOT* and *COCHLEATA* Maintain Nodule Development and Are Legume Orthologs of *Arabidopsis BLADE-ON-PETIOLE* Genes. *Plant Cell* **24**: 4498–4510.
- Czaja, L.F., Hogekamp, C., Lamm, P., Maillet, F., Martinez, E.A., Samain, E., Dénarié, J., Küster, H., and Hohnjec, N.** (2012). Transcriptional Responses toward Diffusible Signals from Symbiotic Microbes Reveal *MtNFP*- and *MtDMI3*-Dependent Reprogramming of Host Gene Expression by Arbuscular Mycorrhizal Fungal Lipochitooligosaccharides. *Plant Physiol.* **159**: 1671–1685.
- Demina, I. V., Persson, T., Santos, P., Plaszczyca, M., and Pawlowski, K.** (2013). Comparison of the Nodule vs. Root Transcriptome of the Actinorhizal Plant *Datisca glomerata*: Actinorhizal Nodules Contain a Specific Class of Defensins. *PLoS One* **8**: e72442.
- Doyle, J.J.** (2011). Phylogenetic Perspectives on the Origins of Nodulation. *Mol. Plant-Microbe Interact.* **24**: 1289–1295.
- Endre, G., Kereszt, A., Kevei, Z., Mihacea, S., Kaló, P., and Kiss, G.B.** (2002). A receptor kinase gene regulating symbiotic nodule development. *Nature* **417**: 962–966.

- Fabre, S., Gully, D., Poitout, A., Patrel, D., Arrighi, J.-F., Giraud, E., Czernic, P., and Cartieaux, F.** (2015). The Nod factor-independent nodulation in *Aeschynomene evenia* required the common plant-microbe symbiotic “toolkit.” *Plant Physiol.* **169**: 2654–2664.
- Ferguson, B.J. and Reid, J.B.** (2005). *Cochleata*: Getting to the root of legume nodules. *Plant Cell Physiol.* **46**: 1583–1589.
- Gage, D.J.** (2004). Infection and Invasion of Roots by Symbiotic, Nitrogen-Fixing Rhizobia during Nodulation of Temperate Legumes. *Microbiol. Mol. Biol. Rev.* **68**: 280–300.
- Gaude, N., Bortfeld, S., Duensing, N., Lohse, M., and Krajinski, F.** (2012). Arbuscule-containing and non-colonized cortical cells of mycorrhizal roots undergo extensive and specific reprogramming during arbuscular mycorrhizal development. *Plant J.* **69**: 510–528.
- Gavrin, A., Jansen, V., Ivanov, S., Bisseling, T., and Fedorova, E.** (2015). ARP2/3-Mediated Actin Nucleation Associated With Symbiosome Membrane Is Essential for the Development of Symbiosomes in Infected Cells of *Medicago truncatula* Root Nodules. *Mol. Plant. Microbe. Interact.* **28**: 605–614.
- Gavrin, A., Kaiser, B.N., Geiger, D., Tyerman, S.D., Wen, Z., Bisseling, T., and Fedorova, E.E.** (2014). Adjustment of Host Cells for Accommodation of Symbiotic Bacteria: Vacuole Defunctionalization, HOPS Suppression, and TIP1g Retargeting in *Medicago*. *Plant Cell* **26**: 3809–3822.
- Gherbi, H., Markmann, K., Svistoonoff, S., Estevan, J., Autran, D., Giczey, G., Auguy, F., Péret, B., Laplaze, L., Franche, C., Parniske, M., and Bogusz, D.** (2008). SymRK defines a common genetic basis for plant root endosymbioses with arbuscular mycorrhiza fungi, rhizobia, and *Frankia* bacteria. *Proc. Natl. Acad. Sci. U. S. A.* **105**: 4928–4932.
- Gleason, C., Chaudhuri, S., Yang, T., Muñoz, A., Poovaiah, B.W., and Oldroyd, G.E.D.** (2006). Nodulation independent of rhizobia induced by a calcium-activated kinase lacking autoinhibition. *Nature* **441**: 1149–1152.
- Gomez, S.K., Javot, H., Deewatthanawong, P., Torres-Jerez, I., Tang, Y., Blancaflor, E.B., Udvardi, M.K., and Harrison, M.J.** (2009). *Medicago truncatula* and *Glomus intraradices* gene expression in cortical cells harboring arbuscules in the arbuscular mycorrhizal symbiosis. *BMC Plant Biol.* **9**: 10.
- González-Sama, A., Lucas, M.M., De Felipe, M.R., and Pueyo, J.J.** (2004). An unusual infection mechanism and nodule morphogenesis in white lupin (*Lupinus albus*). *New Phytol.* **163**: 371–380.
- Hirsch, A.M.** (1992). Developmental biology of legume nodulation. *New Phytol.* **122**: 211–237.
- Hogekamp, C., Arndt, D., Pereira, P.A., Becker, J.D., Hohnjec, N., and Küster, H.** (2011). Laser Microdissection Unravels Cell-Type-Specific Transcription in Arbuscular Mycorrhizal Roots, Including CAAT-Box Transcription Factor Gene Expression Correlating with Fungal Contact and Spread. *Plant Physiol.* **157**: 2023–2043.
- Hossain, M.S. et al.** (2016). *Lotus japonicus* NF-YA1 Plays an Essential Role During Nodule Differentiation and Targets Members of the *SHI/STY* Gene Family. *Mol. Plant-Microbe Interact.* **29**: 950–964.
- Ivanov, S., Fedorova, E., and Bisseling, T.** (2010). Intracellular plant microbe

associations: secretory pathways and the formation of perimicrobial compartments. *Curr. Opin. Plant Biol.* **13**: 372–7.

Ivanov, S., Fedorova, E.E., Limpens, E., De Mita, S., Genre, A., Bonfante, P., and Bisseling, T. (2012). *Rhizobium*-legume symbiosis shares an exocytotic pathway required for arbuscule formation. *Proc. Natl. Acad. Sci.* **109**: 8316–8321.

Kaló, P. et al. (2005). Nodulation signaling in legumes requires NSP2, a member of the GRAS family of transcriptional regulators. *Science* **308**: 1786–1789.

Kanamori, N. et al. (2006). A nucleoporin is required for induction of Ca²⁺ spiking in legume nodule development and essential for rhizobial and fungal symbiosis. *Proc. Natl. Acad. Sci.* **103**: 359–364.

Lancelle, S.A. and Torrey, J.G. (1984). Early Development of *Rhizobium*-Induced Root-Nodules of *Parasponia rigida*. I. Infection and Early Nodule Initiation. *Protoplasma* **123**: 26–37.

Lancelle, S.A. and Torrey, J.G. (1985). Early development of *Rhizobium*-induced root nodules of *Parasponia rigida*. II. Nodule morphogenesis and symbiotic development. *Can. J. Bot. Can. Bot.* **63**: 25–35.

Laporte, P., Lepage, A., Fournier, J., Catrice, O., Moreau, S., Jardinaud, M.-F., Mun, J.-H., Larrainzar, E., Cook, D.R., Gamas, P., and Niebel, A. (2014). The CCAAT box-binding transcription factor NF-YA1 controls rhizobial infection. *J. Exp. Bot.* **65**: 481–94.

Levy, J. (2004). A Putative Ca²⁺ and Calmodulin-Dependent Protein Kinase Required for Bacterial and Fungal Symbioses. *Science* **303**: 1361–1364.

Limpens, E., Franken, C., Smit, P., Willemse, J., Bisseling, T., and Geurts, R. (2003). LysM Domain Receptor Kinases Regulating Rhizobial Nod Factor-Induced Infection. *Science* **302**: 630–633.

Limpens, E., van Zeijl, A., and Geurts, R. (2015). Lipochitooligosaccharides Modulate Plant Host Immunity to Enable Endosymbioses. *Annu. Rev. Phytopathol.* **53**: 311–334.

Liu, J., Rutten, L., Limpens, E., van der Molen, T., van Velzen, R., Chen, R., Chen, Y., Geurts, R., Kohlen, W., Kulikova, O., and Bisseling, T. (2019). A Remote *cis*-Regulatory Region Is Required for *NIN* Expression in the Pericycle to Initiate Nodule Primordium Formation in *Medicago truncatula*. *Plant Cell* **31**: 68–83.

Liu, Q. and Berry, A.M. (1991a). Localization and characterization of pectic polysaccharides in roots and root nodules of *Ceanothus* spp. during intercellular infection by *Frankia*. *Protoplasma* **163**: 93–101.

Liu, Q.Q. and Berry, A.M. (1991b). The infection process and nodule initiation in the *Frankia*-*Ceanothus* root nodule symbiosis - A structural and histochemical study. *Protoplasma* **163**: 82–92.

LPWG (2017). A new subfamily classification of the leguminosae based on a taxonomically comprehensive phylogeny. *Taxon* **66**: 44–77.

de Maagd, R.A., Yang, W.-C., Goosen-de Roo, L., Mulders, I.H.M., Roest, H.P., Spaik, H.P., Bisseling, T., and Lugtenberg, B.J.J. (2011). Down-Regulation of Expression of the *Rhizobium leguminosarum* Outer Membrane Protein Gene *ropA* Occurs Abruptly in Interzone II-III of Pea Nodules and Can Be Uncoupled from *nif* Gene Activation. *Mol. Plant-Microbe Interact.* **7**: 276–281.

- Madsen, E.B., Madsen, L.H., Radutoiu, S., Olbryt, M., Rakwalska, M., Szczygłowski, K., Sato, S., Kaneko, T., Tabata, S., Sandal, N., and Stougaard, J.** (2003). A receptor kinase gene of the LysM type is involved in legume perception of rhizobial signals. *Nature* **425**: 637–640.
- Magne, K., George, J., Berbel Tornero, A., Broquet, B., Madueño, F., Andersen, S.U., and Ratet, P.** (2018). *Lotus japonicus* NOOT-BOP-COCH-LIKE1 is essential for nodule, nectary, leaf and flower development. *Plant J.* **94**: 880–894.
- Maillet, F. et al.** (2011). Fungal lipochitooligosaccharide symbiotic signals in arbuscular mycorrhiza. *Nature* **469**: 58–64.
- Markmann, K., Giczey, G., and Parniske, M.** (2008). Functional Adaptation of a Plant Receptor- Kinase Paved the Way for the Evolution of Intracellular Root Symbioses with Bacteria. *PLoS Biol.* **6**: e68.
- Marsh, J.F., Rakocevic, A., Mitra, R.M., Brocard, L., Sun, J., Eschstruth, A., Long, S.R., Schultze, M., Ratet, P., and Oldroyd, G.E.D.** (2007). *Medicago truncatula* NIN Is Essential for Rhizobial-Independent Nodule Organogenesis Induced by Autoactive Calcium/Calmodulin-Dependent Protein Kinase. *Plant Physiol.* **144**: 324–335.
- Messinese, E., Mun, J.-H., Yeun, L.H., Jayaraman, D., Rougé, P., Barre, A., Lounnon, G., Schornack, S., Bono, J.-J., Cook, D.R., and Ané, J.-M.** (2007). A Novel Nuclear Protein Interacts With the Symbiotic DMI3 Calcium- and Calmodulin-Dependent Protein Kinase of *Medicago truncatula*. *Mol. Plant-Microbe Interact.* **20**: 912–921.
- Middleton, P.H. et al.** (2007). An ERF Transcription Factor in *Medicago truncatula* That Is Essential for Nod Factor Signal Transduction. *Plant Cell* **19**: 1221–1234.
- Miller, I.M. and Baker, D.D.** (1985). The initiation, development and structure of root nodules in *Elaeagnus angustifolia* L. (*Elaeagnaceae*). *Protoplasma* **128**: 107–119.
- Mulder, L., Lefebvre, B., Cullimore, J., and Imberty, A.** (2006). LysM domains of *Medicago truncatula* NFP protein involved in Nod factor perception. Glycosylation state, molecular modeling and docking of chitooligosaccharides and Nod factors. *Glycobiology* **16**: 801–809.
- Naisbitt, T., James, E.K., and Sprent, J.I.** (1992). The evolutionary significance of the legume genus *Chamaecrista*, as determined by nodule structure. *New Phytol.* **122**: 487–492.
- Okazaki, S. et al.** (2016). Rhizobium-legume symbiosis in the absence of Nod factors: Two possible scenarios with or without the T3SS. *ISME J.* **10**: 64–74.
- Op den Camp, R., Streng, A., De Mita, S., Cao, Q., Polone, E., Liu, W., Ammiraju, J.S.S., Kudrna, D., Wing, R., Untergasser, A., Bisseling, T., and Geurts, R.** (2011). LysM-type mycorrhizal receptor recruited for rhizobium symbiosis in nonlegume *Parasponia*. *Science* **331**: 909–912.
- Op den Camp, R.H.M., Polone, E., Fedorova, E., Roelofsen, W., Squartini, A., Op den Camp, H.J.M., Bisseling, T., and Geurts, R.** (2012). Nonlegume *Parasponia andersonii* Deploys a Broad Rhizobium Host Range Strategy Resulting in Largely Variable Symbiotic Effectiveness. *Mol. Plant-Microbe Interact.* **25**: 954–963.

- Pawlowski, K. and Bisseling, T.** (1996). Rhizobial and Actinorhizal Symbioses: What Are the Shared Features? *Plant Cell* **8**: 1899–1913.
- Pawlowski, K. and Demchenko, K.N.** (2012). The diversity of actinorhizal symbiosis. *Protoplasma* **249**: 967–979.
- Persson, T. et al.** (2015). *Candidatus* Frankia Datiscae Dg1, the Actinobacterial Microsymbiont of *Datisca glomerata*, Expresses the Canonical *nod* Genes *nodABC* in Symbiosis with Its Host Plant. *PLoS One* **10**: e0127630.
- Peter, J., Young, W., and Haukka, K.E.** (1996). Diversity and phylogeny of rhizobia. *New Phytol.* **133**: 87–94.
- Racette, S. and Torrey, J.G.** (1989). Root nodule initiation in *Gymnostoma* (Casuarinaceae) and *Shepherdia* (Elaeagnaceae) induced by *Frankia* strain HFPGP11. *Can. J. Bot.* **67**: 2873–2879.
- Radutoiu, S., Madsen, L.H., Madsen, E.B., Felle, H.H., Umehara, Y., Grønlund, M., Sato, S., Nakamura, Y., Tabata, S., Sandal, N., and Stougaard, J.** (2003). Plant recognition of symbiotic bacteria requires two LysM receptor-like kinases. *Nature* **425**: 585–592.
- Saito, K. et al.** (2007). NUCLEOPORIN85 Is Required for Calcium Spiking, Fungal and Bacterial Symbioses, and Seed Production in *Lotus japonicus*. *Plant Cell* **19**: 610–624.
- Santi, C., Bogusz, D., and Franche, C.** (2013). Biological nitrogen fixation in non-legume plants. *Ann. Bot.* **111**: 743–67.
- Schauser, L., Roussis, A., Stiller, J., and Stougaard, J.** (1999). A plant regulator controlling development of symbiotic root nodules. *Nature* **402**: 191–195.
- Singh, S., Katzer, K., Lambert, J., Cerri, M., and Parniske, M.** (2014). CYCLOPS, a DNA-binding transcriptional activator, orchestrates symbiotic root nodule development. *Cell Host Microbe* **15**: 139–52.
- Smit, P., Limpens, E., Geurts, R., Fedorova, E., Dolgikh, E., Gough, C., and Bisseling, T.** (2007). Medicago LYK3, an Entry Receptor in Rhizobial Nodulation Factor Signaling. *Plant Physiol.* **145**: 183–191.
- Smit, P., Raedts, J., Portyanko, V., Debellé, F., Gough, C., Bisseling, T., and Geurts, R.** (2005). NSP1 of the GRAS protein family is essential for rhizobial Nod factor-induced transcription. *Science* **308**: 1789–1791.
- Soltis, D.E., Soltis, P.S., Morgan, D.R., Swensen, S.M., Mullin, B.C., Dowd, J.M., and Martin, P.G.** (1995). Chloroplast gene sequence data suggest a single origin of the predisposition for symbiotic nitrogen fixation in angiosperms. *Proc. Natl. Acad. Sci. U. S. A.* **92**: 2647–2651.
- Soyano, T., Kouchi, H., Hirota, A., and Hayashi, M.** (2013). NODULE INCEPTION Directly Targets *NF-Y* Subunit Genes to Regulate Essential Processes of Root Nodule Development in *Lotus japonicus*. *PLoS Genet.* **9**: e1003352.
- Sprent, J.I.** (2007). Evolving ideas of legume evolution and diversity: A taxonomic perspective on the occurrence of nodulation: Tansley review. *New Phytol.* **174**: 11–25.
- Stracke, S., Kistner, C., Yoshida, S., Mulder, L., Sato, S., Kaneko, T., Tabata, S., Sandal, N., Stougaard, J., Szczyglowski, K., and Parniske, M.** (2002). A plant receptor-like kinase required for both bacterial and fungal symbiosis. *Nature* **417**: 959–962.
- Sun, M., Naeem, R., Su, J.X., Cao, Z.Y., Burleigh, J.G., Soltis, P.S., Soltis, D.E.,**

- and Chen, Z.D. (2016). Phylogeny of the Rosidae: A dense taxon sampling analysis. *J. Syst. Evol.* **54**: 363–391.
- Suzuki, W., Konishi, M., and Yanagisawa, S. (2013). The evolutionary events necessary for the emergence of symbiotic nitrogen fixation in legumes may involve a loss of nitrate responsiveness of the NIN transcription factor. *Plant Signal. Behav.* **8**: e25975.
- Svistoonoff, S. et al. (2013). The Independent Acquisition of Plant Root Nitrogen-Fixing Symbiosis in Fabids Recruited the Same Genetic Pathway for Nodule Organogenesis. *PLoS One* **8**: e64515.
- Swensen, S.M. (1996). The evolution of actinorhizal symbioses: evidence for multiple origins of the symbiotic association. *Am. J. Bot.* **83**: 1503–1512.
- Tedersoo, L., Laanisto, L., Rahimlou, S., Toussaint, A., Hallikma, T., and Pärtel, M. (2018). Global database of plants with root-symbiotic nitrogen fixation: NodDB. *J. Veg. Sci.* **29**: 560–568.
- Tirichine, L. et al. (2006). Dereglulation of a Ca²⁺/calmodulin-dependent kinase leads to spontaneous nodule development. *Nature* **441**: 1153–1156.
- Torrey, J.G. and Callaham, D. (1979). Early nodule development in *Myrica gale*. *Bot. Gaz.* **140**: S10–S14.
- Valverde, C. and Wall, L.G. (1999). Time course of nodule development in the *Discaria trinervis* (Rhamnaceae) - *Frankia* symbiosis. *New Phytol.* **141**: 345–354.
- Vasse, J., De Billy, F., Camut, S., and Truchet, G. (1990). Correlation between ultrastructural differentiation of bacterioids and nitrogen fixation in alfalfa nodules. *J. Bacteriol.* **172**: 4295–4306.
- van Velzen, R. et al. (2018). Comparative genomics of the nonlegume *Parasponia* reveals insights into evolution of nitrogen-fixing rhizobium symbioses. *Proc. Natl. Acad. Sci. U. S. A.* **115**: E4700–E4709.
- Xiao, T.T., Schilderink, S., Moling, S., Deinum, E.E., Kondorosi, E., Franssen, H., Kulikova, O., Niebel, A., and Bisseling, T. (2014). Fate map of *Medicago truncatula* root nodules. *Development* **141**: 3517–3528.
- Yang, W.-C., Horvath, B., Hontelez, J., Van Kammen, A., and Bisseling, T. (1991). *In situ* Localization of *Rhizobium* mRNAs in Pea Root Nodules: *nifA* and *nifH* Localization. *Mol. Plant-Microbe Interact.* **4**: 464–468.
- Yano, K. et al. (2008). CYCLOPS, a mediator of symbiotic intracellular accommodation. *Proc. Natl. Acad. Sci. U. S. A.* **105**: 20540–20545.
- Yoro, E., Suzaki, T., Toyokura, K., Miyazawa, H., Fukaki, H., and Kawaguchi, M. (2014). A Positive Regulator of Nodule Organogenesis, NODULE INCEPTION, Acts as a Negative Regulator of Rhizobial Infection in *Lotus japonicus*. *Plant Physiol.* **165**: 747–758.
- Van Zeijl, A., Op Den Camp, R.H.M., Deinum, E.E., Charnikhova, T., Franssen, H., Op Den Camp, H.J.M., Bouwmeester, H., Kohlen, W., Bisseling, T., and Geurts, R. (2015). Rhizobium Lipo-chitooligosaccharide Signaling Triggers Accumulation of Cytokinins in *Medicago truncatula* Roots. *Mol. Plant* **8**: 1213–1226.
- Zhang, X., Dong, W., Sun, J., Feng, F., Deng, Y., He, Z., Oldroyd, G.E.D., and Wang, E. (2015). The receptor kinase CERK1 has dual functions in symbiosis and immunity signalling. *Plant J.* **81**: 258–267.

CHAPTER 2

The *Medicago truncatula* Nodule Identity Gene *NODULE ROOT1* Is Required for Coordinated Apical-Basal Development of the Root


Defeng Shen, Olga Kulikova, Kerstin Guhl, Henk Franssen, Wouter Kohlen, Ton Bisseling and René Geurts*

Laboratory of Molecular Biology, Department of Plant Sciences, Wageningen University, Droevendaalsesteeg 1, 6708 PB Wageningen, The Netherlands.

*Corresponding author: rene.geurts@wur.nl.



ABSTRACT



Legumes can utilize atmospheric nitrogen by hosting nitrogen-fixing bacteria in special lateral root organs, called nodules. Legume nodules have a unique ontology, despite similarities in the gene networks controlling nodule and lateral root development. It has been shown that *Medicago truncatula* *NODULE ROOT1* (*MtNOOT1*) is required for the maintenance of nodule identity, preventing the conversion to lateral root development. *MtNOOT1* and its orthologs in other plant species -collectively called the NOOT-BOP-COCH-LIKE (NBCL) family-specify boundary formation in various aerial organs. However, *MtNOOT1* is not only expressed in nodules and aerial organs, but also in developing roots, where its function remains elusive. We show that *Mtnoot1* mutant seedlings display accelerated root elongation due to an enlarged root apical meristem. Also, *Mtnoot1* mutant roots are thinner than wild-type and are delayed in xylem cell differentiation. We provide molecular evidence that the affected spatial development of *Mtnoot1* mutant roots correlates with delayed induction of genes involved in xylem cell differentiation. This coincides with a basipetal shift of the root zone that is susceptible to rhizobium-secreted symbiotic signal molecules. Our data show that *MtNOOT1* regulates the size of the root apical meristem and vascular differentiation. Our data demonstrate that *MtNOOT1* not only functions as a homeotic gene in nodule development but also coordinates the spatial development of the root.

INTRODUCTION

Legume plants (Fabaceae) can form unique lateral root organs to host nitrogen-fixing rhizobium bacteria, known as nodules. Legume nodules originate from root cells upon rhizobium-induced lipo-chitooligosaccharide (LCO) signalling. In the legume model *Medicago truncatula* (medicago) LCO signalling induces cell divisions in the pericycle and endodermis, followed by a coordinated mitotic activation of cortical cells. This will give rise to nodule primordia (Xiao et al., 2014). When fully developed, a medicago nodule possesses a large central zone with cells harbouring nitrogen-fixing rhizobia, surrounded by peripheral vascular bundles and a meristem at the apex allowing indeterminate growth (Xiao et al., 2014).

Legume nodule formation is controlled by a network of transcriptional regulators, among which NODULE INCEPTION (NIN) is a master regulator (Schauser et al., 1999; Marsh et al., 2007). *NIN* expression is activated upon LCO signalling in a small zone of the root with elongating root hairs (Desbrosses and Stougaard, 2011; Yano et al., 2008; Vernié et al., 2015; Van Zeijl et al., 2015). Expression of *NIN* in the root pericycle and dividing cortical cells is essential and sufficient to trigger nodule organogenesis (Soyano et al., 2013; Vernié et al., 2015; Liu et al., 2019). Legumes recruited a BTB/POZ-ankyrin domain containing protein of the NOOT-BOP-CHOCLEATA-LIKE (NBCL) family to maintain nodule identity in the newly formed primordium (Couzigou et al., 2012; Magne et al., 2018b, 2018a). Knockout mutations in this gene – in medicago named *NODULE ROOT1* (*MtNOOT1*)- cause a homeotic switch from nodule organogenesis towards lateral root formation (Couzigou et al., 2012). This underlines the important functioning of *MtNOOT1* in nodule development. Besides nodules, *MtNOOT1* is also expressed in young root tissue (Benedito et al., 2008; Holmes et al., 2008). However, its functioning during root development remains elusive.

MtNOOT1 is orthologous to the *Arabidopsis thaliana* (arabidopsis) *BLADE-ON-PETIOLE1* (*AtBOP1*) and *AtBOP2* genes. Studies in arabidopsis have revealed that BOP proteins function as co-transcriptional regulators involved in plant boundary formation (Reviewed in (Aida and Tasaka, 2006; Khan et al., 2014; Žádníková and Simon, 2014; Hepworth and Pautot, 2015; Wang et al., 2016)). For example, *AtBOP1* and *AtBOP2* can promote expression of *LATERAL ORGAN BOUNDARIES* (*LOB*) genes to repress brassinosteroid signalling, which subsequently restricts cell growth and division in the boundary domain between the shoot apical meristem and lateral organs such as leaves (Jun et al., 2010; Bell et al., 2012). *AtBOP1* and *AtBOP2* also control proximal-distal leaf patterning by repressing the expression of genes that promote meristematic activity (Ha et al., 2003, 2007). Knockout mutations in *AtBOP1/AtBOP2* lead to ectopic outgrowths of blade tissue along the petioles of cotyledons and leaves, due to misexpression of meristematic genes (Ha et al., 2003, 2007). Additionally, *AtBOP1* and *AtBOP2* are essential for abscission zone (AZ) formation at the junction between the leaving organ and the main plant body (McKim et al., 2008). In line with this, a complete loss of floral organ abscission is observed in the arabidopsis *Atbop1;Atbop2* double mutant (McKim et al., 2008).

Similar to arabidopsis, mutations in orthologous *BOP* genes in the legumes medicago *MtNOOT1*, pea (*Pisum sativum*) *COCHLEATA1* (*PsCOCH1*), and lotus (*Lotus japonicus*) *LjNBCL1* affect leaf patterning and AZ formation (Couzigou

et al., 2016). Arabidopsis *Atbop1;Atbop2* double mutants do not form stipules (McKim et al., 2008; Ichihashi et al., 2011), which are also simplified or reduced in the medicago *Mtnoot1* mutant and at early nodes of the pea *Pscoch1* mutant (Couzigou et al., 2012). In the lotus *Ljnbcl1* mutant, nectary glands (proposed modified stipules) are completely absent (Magne et al., 2018b). Furthermore, in the medicago *Mtnoot1*, pea *Pscoch1* and lotus *Ljnbcl1* mutants, the abscission of petals is impaired (Couzigou et al., 2016), similar to what is observed in arabidopsis *Atbop1;Atbop2* (McKim et al., 2008). This indicates that the function of NBCL proteins in boundary specification in the proximal region of the leaf and in AZ formation is well-conserved. In addition, MtNOOT1 and PsCOCH1 function during the root nodule development by defining the boundary between nodule meristem and nodule vasculature (Couzigou et al., 2012). Taken together, NBCL proteins play a conserved role in defining boundaries in various developmental contexts.

Studies on NBCL genes in roots are limited. In arabidopsis it was shown that AtBOP1 and AtBOP2 play a negative role in differentiation of lignified fibres in hypocotyl and tap root (Liebsch et al., 2014a; Woerlen et al., 2017). In arabidopsis and medicago, *AtBOP1*, *AtBOP2* and *MtNOOT1* are expressed also in the root tip (Woerlen et al., 2017; Benedito et al., 2008; Holmes et al., 2008), though their functioning in root development has not been unveiled yet. Here, we examined the function of *MtNOOT1* in primary root development. We show that *MtNOOT1* is involved in defining the position of the transition zone between the apical meristem and the elongation/differentiation zone, and is required for coordinated development of the root along the apical-basal axis.

RESULTS

The Primary Root of the Medicago *Mtnoot1* Mutant Is Longer

According to *Medicago truncatula* Gene Expression Atlas (He et al., 2009), the *MtNOOT1* gene (Medtr7g090020) is highest expressed in root tips, surpassing the expression in many nodule samples that have been analysed (Supplementary Figure 1). This suggests a non-symbiotic function of *MtNOOT1* in the root. To investigate this, we compared wild-type and *Mtnoot1* mutant seedlings (tnk507) when grown *in vitro*, and observed that the growth of the *Mtnoot1* primary root is accelerated compared to wild-type (Supplementary Figure 2). To obtain insight in the timing of the increase in primary root growth

of the *Mtnoot1* mutant, we measured the root length at different time points (2 Days After Germination (DAG), 4 DAG and 6 DAG). This showed that the primary roots of the *Mtnoot1* mutants are markedly longer at 4 and 6 DAG when compared to wild-type seedlings (Fig. 1a-b). At 2 DAG no differences in root length was detected, suggesting that the observed differences in root length of the *Mtnoot1* mutant is not due to an earlier or faster germination. A similar result was obtained by analysing a second *Mtnoot1* mutant allele (NF2717) (Couzigou et al., 2012; Magne et al., 2018a) (Supplementary Figure 3a).

Studies in arabidopsis show that accelerated primary root growth can correlate with increased length of the root apical meristem (RAM) (Dello loio et al., 2007; loio et al., 2008). Therefore, we measured the length of the RAM at 6 DAG. Since both *Mtnoot1* mutant lines showed a similar root length phenotype, our analysis was focused on a single mutant allele; *tnk507*. We found that the RAM of this *Mtnoot1* mutant is significantly larger than that of wild-type seedlings (Fig. 1c). A larger RAM can be the result of an increase in cell number or an increase in cell length. To quantify cell numbers in the medicago RAM is technically difficult due to the relatively thick root when compared to arabidopsis. To distinguish between both scenarios that can cause larger RAM, we therefore measured the length of 10 cortical cells at the proximal part of the RAM. We found that the average size of cortical cells in the RAM is not affected by the *Mtnoot1* mutation (Fig. 1d). This suggests that an increase in cell number in the RAM of the *Mtnoot1* mutant underlies its accelerated growth. Taken together, these results suggest that *MtNOOT1* either represses cell division in the RAM or/and promotes cell differentiation in the transition zone of the root.

***MtNOOT1* Is Expressed in the Transition Zone and Root Vasculature**

The accelerated primary root growth prompted us to determine the precise location of *MtNOOT1* expression. Since we were unable to identify a functional promoter region of *MtNOOT1*, we decided to perform RNA *in situ* hybridization on longitudinal sections of root tips (1-2 mm) of wild-type seedlings at 6 DAG. This showed that *MtNOOT1* is highly expressed in the region between the RAM and the elongation/differentiation zone and barely in the rest of the RAM (Fig. 2a). A magnification of the region with the most intense signals showed that *MtNOOT1* is expressed in the transition zone and the distal part of the elongation/differentiation zone (Fig. 2b). This suggests that *MtNOOT1* controls the size of the RAM by promoting cell differentiation in the transition zone.

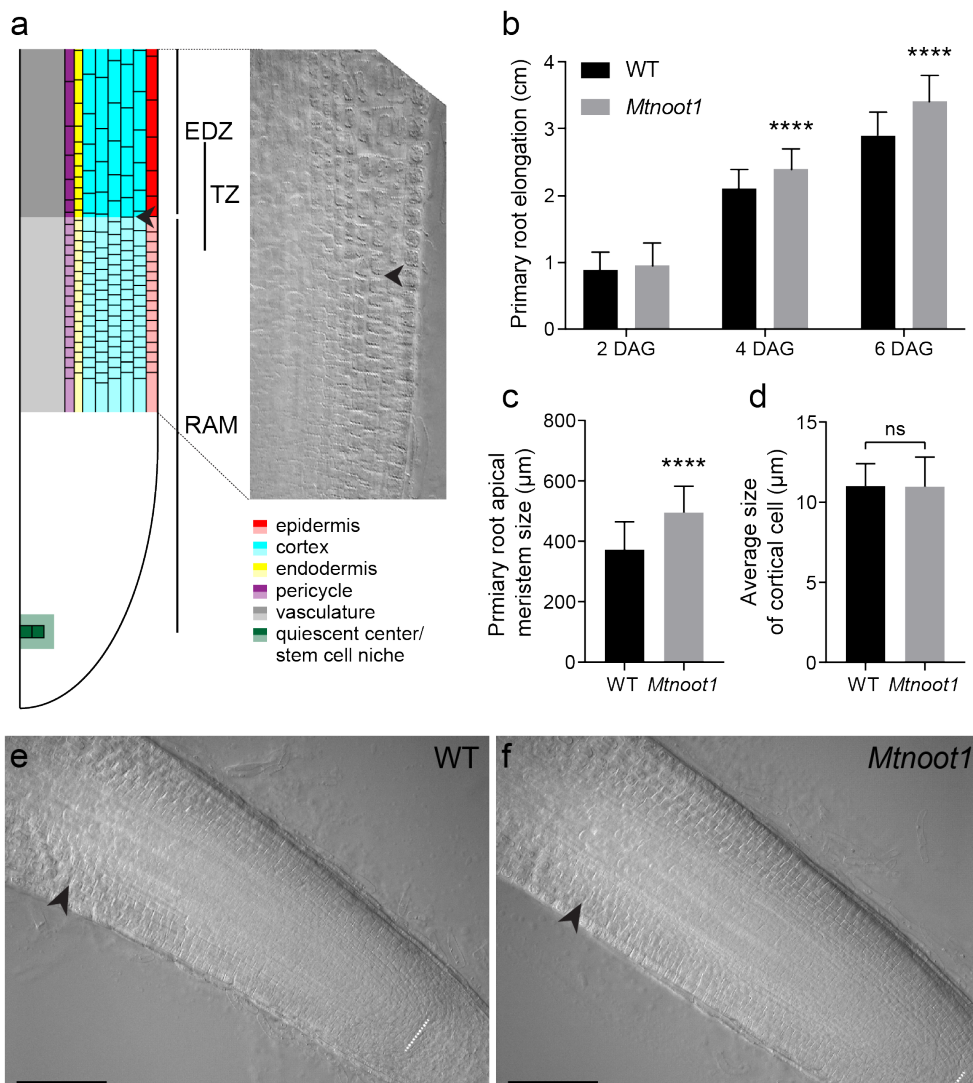


Figure 1. The Primary Root of the Medicago *Mtnoot1* Mutant Is Longer Than Wild-type Root. **a** Schematic representation of the zonation in a medicago primary root. Left panel: the size of the root apical meristem (RAM) is determined from the stem cell niche till the elongation/differentiation zone (EDZ). The apical border of the EDZ is defined by the first elongated cortex cell of second cortical layer, as indicated by arrowhead. Note that the exact position of the RAM-EDZ boundary can vary depending on the cell type, marking a region that named transition zone (TZ) (Dello Iorio et al., 2007; Iorio et al., 2008). Cell types are indicated by colour coding. Right panel: Normaski image of the distal region of the RAM and apical region of the EDZ of a primary root at 6 Days After Germination (DAG). Arrowhead indicates the boundary between the RAM and the EDZ of the second layer of cortical cells. **b** Root length of the medicago *Mtnoot1* *tnk507* mutant is markedly longer at 4 DAG and 6

Continued on next page

Since it has been shown that AtBOP1 and AtBOP2 play a role in vasculature differentiation (Khan et al., 2012; Liebsch et al., 2014b; Woerlen et al., 2017), we questioned whether *MtNOOT1* may play a similar role in medicago roots. To investigate this, we first examined whether *MtNOOT1* is expressed in the root vasculature. We divided the first 2 cm of young seedling roots (without visible lateral roots or primordia) into four zones of each ~5 mm long (basipetally, from zone 1 to zone 4, of which zone 1 includes the RAM till the mature root cells with elongated root hairs). These root segments correspond to different stages of vascular development and were used to conduct qRT-PCR studies (Fig. 2c). This showed that *MtNOOT1* is expressed in all four zones, with relatively the lowest level of expression in zone 1 and the highest level in zone 4 (Fig. 2c). This is consistent with Gene Expression Atlas data (Supplementary Figure 1). RNA *in situ* hybridization on a cross section of wild-type zone 4 segment showed that *MtNOOT1* transcripts mainly occur in the procambium cells of the vasculature (Fig. 2d). This suggests that *MtNOOT1* could also play a role in root vasculature development in medicago.

The Primary Root of the *Mtnoot1* Mutant Is Delayed in Xylem Cell Differentiation

As *MtNOOT1* is expressed in the root vasculature, we investigated whether the *Mtnoot1* mutant is affected in root vasculature development. Preliminary observations suggested that *Mtnoot1* mutant roots are thinner than wild-type roots. To quantify this, cross sections on *Mtnoot1* mutant line *tnk507* were made on the middle parts of zone 1 to zone 4 and the size of the cross-sectional

Continued

DAG when compared to primary roots of wild-type medicago seedlings (WT). **c** The RAM of medicago *Mtnoot1* *tnk507* seedlings is larger at 6 DAG when compared to the RAM of primary roots of wild-type medicago seedlings. The data represent means + SD of three independent experiments, each experiment contains 16-20 roots. **d** The cortical cell size at the proximal part of the RAM is not affected in the root of the medicago *Mtnoot1* *tnk507* mutant seedlings. Given is the average cell size of cortical cells at the proximal part of the RAM of wild-type and *Mtnoot1* mutant roots. The data represent means + SD of two independent experiments, each experiment contains 16-20 roots. Student *t*-test was performed to assess significant differences (****: $P < 0.0001$, ns: not significant). A representation of the RAM of wild-type (**e**) and *Mtnoot1* mutant seedling (**f**) primary roots at 6 DAG. White dotted line marks the quiescent center/stem cell niche region, arrowhead marks the boundary between the RAM and the EDZ of the second layer of cortical cells. Scale bar: 100 μ m.

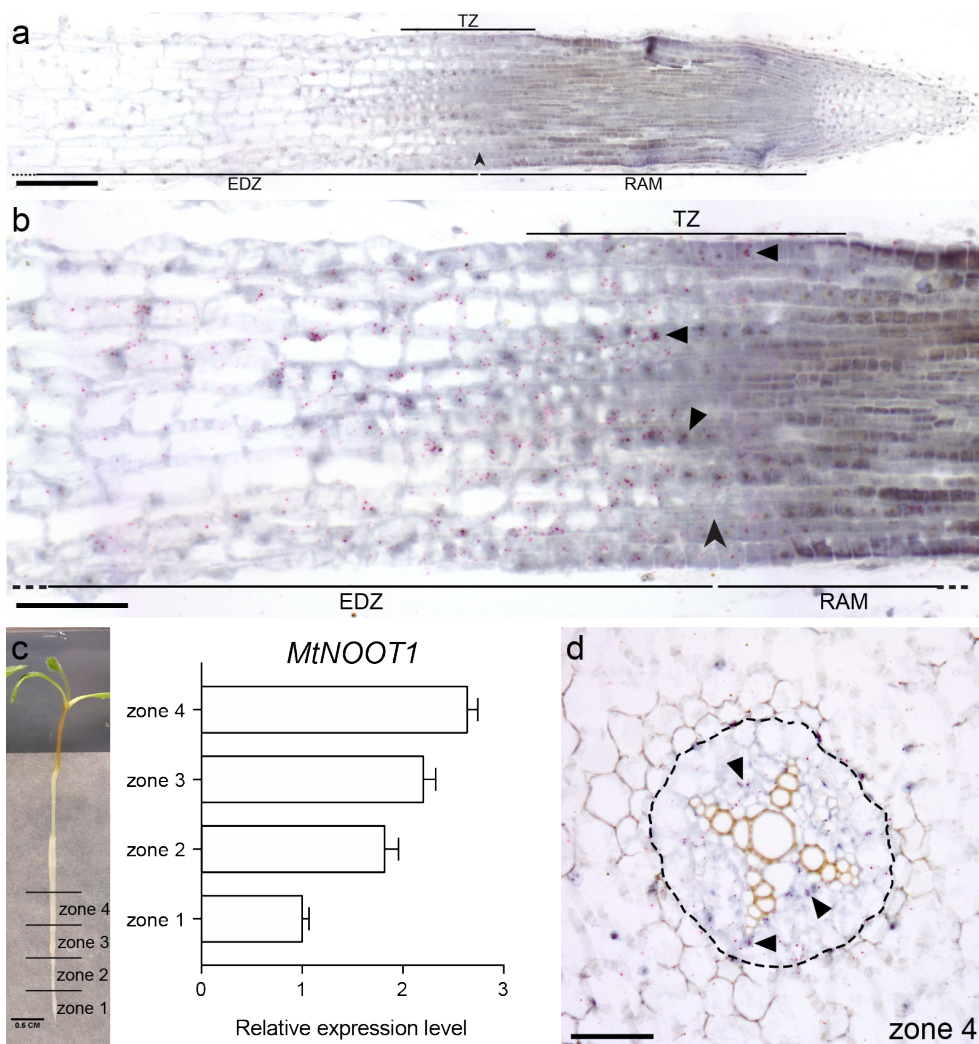


Figure 2. *MtNOOT1* Spatial Expression Pattern in Medicago Wild-type Primary Root. **a, b** Longitudinal section of root tip. *MtNOOT1* expression pattern in root tip determined by *in situ* hybridization. *MtNOOT1* is mainly expressed in the TZ and distal part of the EDZ. **b** A close-up of (a), visualizing abundance of *MtNOOT1* mRNA (red dots) in epidermal and cortical cells in the TZ. Arrowhead indicates the boundary between the RAM and the EDZ of the second layer of cortical cells. **c** The expression pattern of *MtNOOT1* in different zones of root determined by qRT-PCR. Left panel: the primary root of a wild-type medicago seedling at 6 DAG is divided into four zones of 5 mm each. Right panel: *MtNOOT1* expression as determined by qRT-PCR reveals increased expression in older regions of the root. The data represent means + SEM of three independent experiments. **d** Cross section of zone 4. *MtNOOT1* expression pattern in zone 4 determined by *in situ* hybridization. *MtNOOT1* is mainly expressed in the procambium cells of the root vascular bundle. Black dotted line circles the pericycle of vascular bundle. Triangles indicate the *MtNOOT1* mRNA signals. Scale bar: 100 μ m (a), 50 μ m (b, d).

area was determined. This showed that in zone 2 to zone 4 the cross-sectional area of the *Mtnoot1* mutant roots is significantly smaller when compared to the counterparts of wild-type roots. The root cross-sectional area sizes of zone 3 and zone 4 of the *Mtnoot1* mutants were more comparable to those of zone 2 and zone 3 in wild-type, respectively (Fig. 3a). A similar reduction in root cross-sectional area size was also observed in the *Mtnoot1* mutant line NF2717 (Supplementary Figure 3b). Further, the cross-sectional area sizes of the vasculature also showed that this is significantly smaller in *Mtnoot1* (tnk507) root zone 2 to zone 4 when compared to wild-type roots. This suggests that the *Mtnoot1* mutants have a delayed pattern of root radial growth, which correlates with the growth defects in its vasculature.

Vascular bundles are mainly built up of xylem and phloem cells, in medicago roots in a four-arch constitution (Fig. 3c, e). During the development of the root, vascular metaxylem cells differentiate and become lignified (Schuetz et al., 2013). Upon toluidine blue staining, lignified metaxylem cells gain a lighter blue colouration than non-lignified cells (Lars Hennig and Köhler, 2010). Upon toluidine blue staining of wild-type and *Mtnoot1* tnk507 roots, we found that 32% (19/60) of wild-type zone 3 showed lignified central metaxylem cells, in contrast to only 2% (1/60) of *Mtnoot1* zone 3 showed lignification of central metaxylem cells. Furthermore, central metaxylem cells are lignified in 68% (41/60) of wild-type zone 4, but only in 27% (16/60) of *Mtnoot1* zone 4, which is more similar to the lignification level of wild-type zone 3 (Fig. 4). A similar result was obtained by analysing the *Mtnoot1* NF2717 mutant allele (Supplementary Figure 3c-g). These observations demonstrate that in *Mtnoot1* mutants the lignification level of vascular metaxylem cells in zone 3 and zone 4 is lower when compared with wild-type, suggesting that the differentiation of *Mtnoot1* root vasculature is delayed. This is consistent with the observation that the cross-sectional area sizes of *Mtnoot1* root vasculature in zone 2 to zone 4 are significantly smaller when compared to wild-type (Fig. 3b).

The Expression of Genes Involved in Xylem Cell Differentiation Is Delayed in *Mtnoot1* Mutant Roots

In arabidopsis, secondary cell wall formation and subsequent programmed cell death (PCD) are two critical steps in the maturation of proto-/metaxylem and fibre cells (Schuetz et al., 2013). Secondary cell wall biosynthesis is initiated by the master regulators VASCULAR-RELATED NAC-DOMAIN 7 (AtVND7) for

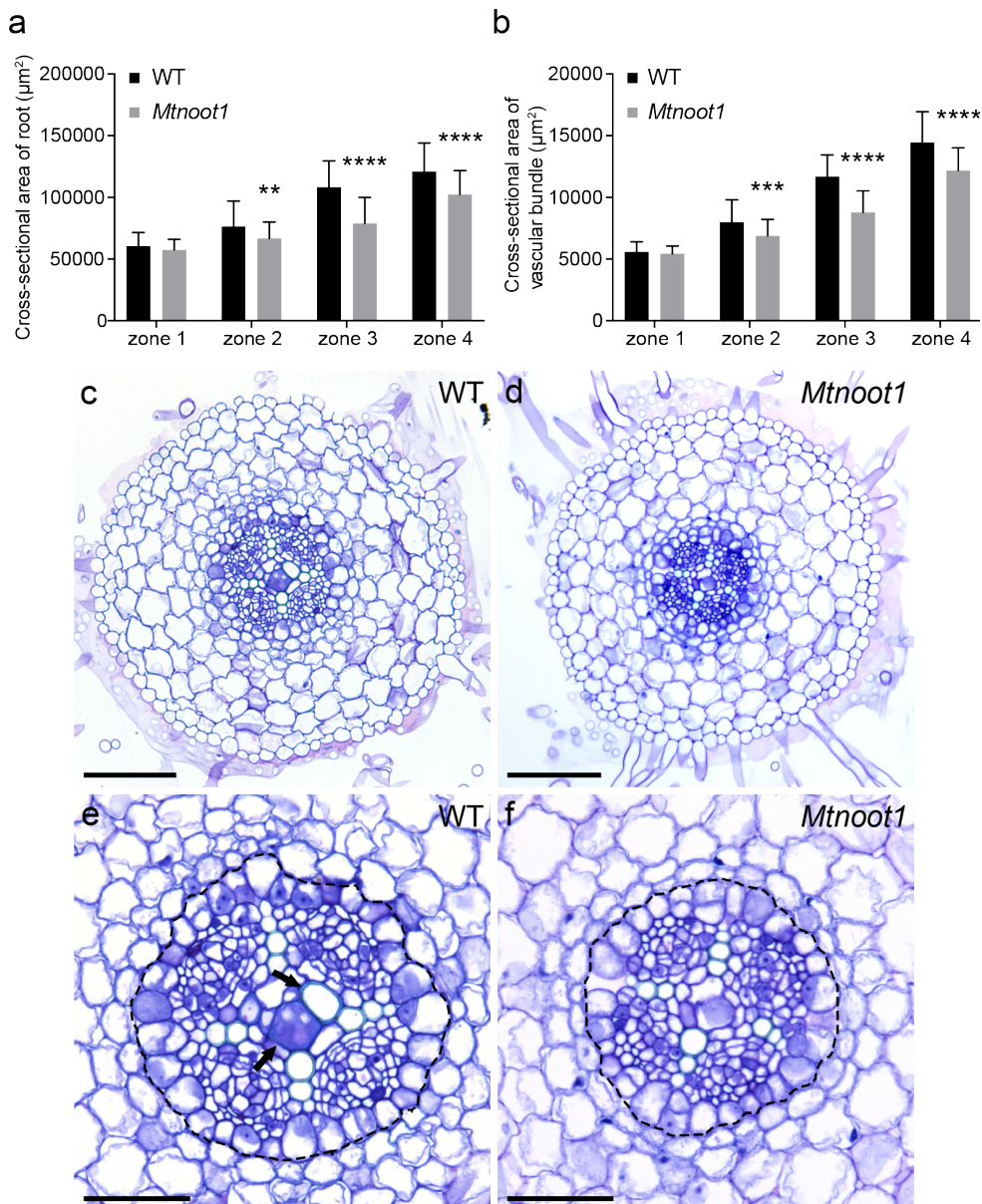


Figure 3. Medicago *Mtnoot1* Mutant Seedlings Have a Thinner Primary Root at 6 DAG. The size of the cross-sectional area of (a) primary root and (b) vascular bundle of the medicago *Mtnoot1* *tnk507* mutant at zone 2, 3 and 4 are significantly smaller when compared to wild-type medicago roots. The data represent means + SD of three independent experiments, each experiment contains 18-20 roots. Student *t*-test was performed to assess significant differences (**: $P < 0.01$, ***: $P < 0.001$, ****: $P < 0.0001$). Representative root cross sections of wild-type (c) and *Mtnoot1* (d) roots, and wild-type (e) and *Mtnoot1* (f) vascular bundle at zone

Continued on next page

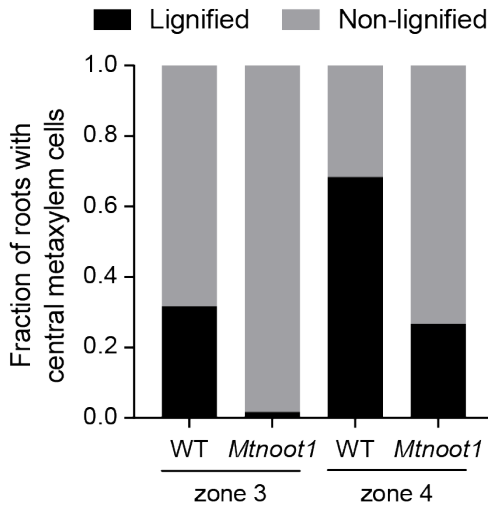


Figure 4. Vascular Xylem Differentiation Is Delayed in the Primary Root of *Mtnoot1* at 6 DAG.

The fraction of roots with lignified central metaxylem cells in zone 3 and zone 4 is decreased in the *Mtnoot1* *tnk507* mutant when compared with wild-type seedlings. The lignification level of the central metaxylem cells in zone 4 of the *Mtnoot1* mutant is similar to that of wild-type medicago zone 3, indicating that the differentiation of vascular xylem cells is delayed in the *Mtnoot1* mutant. The presented data combines three independent experiments, each experiment contains 20 roots.

protoxylem, *AtVND6* for metaxylem and SECONDARY WALL-ASSOCIATED NAC DOMAIN PROTEIN 1 (*AtSND1*) for fibre differentiation (Schuetz et al., 2013). These master regulators control secondary cell wall biosynthesis via a network of genes, which include the transcription factors *AtMYB46*, *AtMYB58*, *AtMYB63*, *AtMYB83* and *AtMYB85* that ultimately control lignin biosynthesis genes, and the peptidase encoding gene *XYLEM CYSTEINE PEPTIDASE 1* (*AtXCP1*) involved in the PCD during xylem cell development (Zhong et al., 2008; Ohashi-Ito et al., 2010; Zhong et al., 2010; Schuetz et al., 2013). To find molecular support for the observation of the delayed vasculature development in the *Mtnoot1* mutant, we aimed to analyse the transcript levels of the putative medicago orthologues of the above-mentioned genes. To identify such medicago orthologues we used phylogenetic reconstruction (Supplementary Figures 4-9). Subsequent qRT-PCR expression studies on medicago root zone 3 and zone 4 revealed that both *MtVND6* and *MtVND7*, but not *MtSND1* are slightly lower expressed in zone 3 of *Mtnoot1* mutant root (Supplementary Figure 10), while the putative downstream targets *MtMYB46-1*, *MtMYB46-2*, *MtMYB83*, *MtMYB58/63*, and *MtMYB85* and *MtXCP1* are markedly lower expressed in the *Mtnoot1* root (Fig. 5a). In zone 4 of the *Mtnoot1* mutant root, the expression of all these genes was restored to the wild-type level (Fig. 5a), indicating a delayed transcriptional regulation of genes controlling secondary cell wall biosynthesis in

Continued

4. Black dotted line circles the pericycle of vascular bundle. Black arrow marks differentiated/lignified metaxylem cells, which are not found in the *Mtnoot1* mutant. Scale bar: 100 μ m (c, d), 50 μ m (e, f).

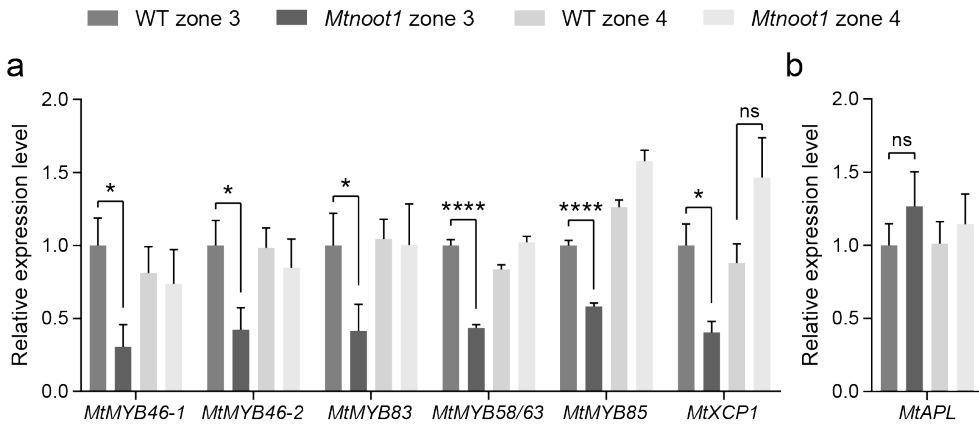


Figure 5. Genes Putatively Involved in Xylem Cell Differentiation Display Reduced Expression in *Mtnoot1* roots. a, b Expression level of various genes putatively involved in xylem and phloem cell differentiation in zone 3 and zone 4 of wild-type and *Mtnoot1* tnk507 roots determined by qRT-PCR. a The MYB-type transcription factors *MtMYB46-1*, *MtMYB46-2*, *MtMYB83* and *MtMYB85*, and the XYLYME CYSTEINE PEPTIDASE 1 putative ortholog *MtXCP1* are lower expressed in zone 3 of *Mtnoot1* mutant roots when compared to wild-type. c The expression level of phloem marker gene *MtAPL* is not affected in *Mtnoot1* mutant roots. The data represent means + SEM of two (*MtXCP1* and *MtAPL*) or three (*MtMYBs*) independent experiments. Student *t*-test was performed to assess significant differences (*: $P < 0.05$, ****: $P < 0.0001$, ns: not significant).

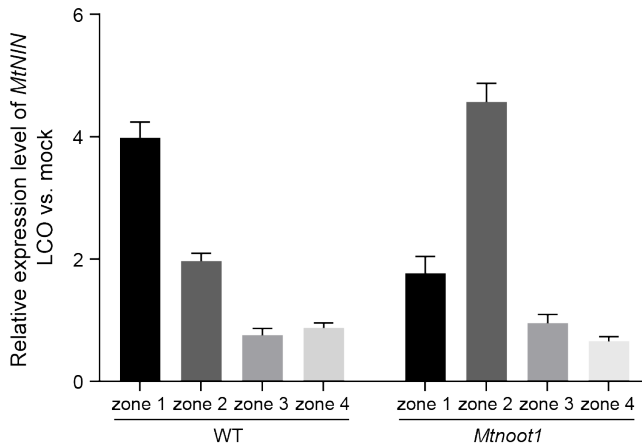


Figure 6. Rhizobium LCO-induced *MtNIN* Expression Is Spatially Different in the Medicago *Mtnoot1* Roots in Comparison with Wild-type Roots. *MtNIN* expression is quantified using qRT-PCR in four root zones at three hours post application of 10^{-9} M *S. meliloti* LCOs. The data represent means + SEM of two independent experiments using the *Mtnoot1* tnk507 mutant.

the apical-basal direction in the *Mtnoot1* mutant roots. In contrast, the expression level of a phloem marker gene, *ALTERED PHLOEM DEVELOPMENT* (*MtAPL*) (Bonke et al., 2003), is not affected in *Mtnoot1* (Fig. 5b), suggesting that phloem cell development is not disturbed. Taken together, these results support our observation that xylem cell differentiation in the *Mtnoot1* mutant is delayed.

The LCO Susceptible Zone of *Mtnoot1* Mutant Roots Is Shifted Basipetally

In medicago, the site where the interaction with rhizobia occurs is tightly linked to the developmental status of the root tissue. At the start of the differentiation zone, where young elongating root hairs can be found is called the susceptible zone, and it is here where rhizobium LCOs can trigger expression of symbiotic genes such as *MtNIN* (Yano et al., 2008; Vernié et al., 2015; Van Zeijl et al., 2015). The delayed root differentiation observed in the medicago *Mtnoot1* mutant led us to question whether this may also affect the susceptibility of the root to rhizobium. To investigate this, we studied the expression of *MtNIN* in the four root zones upon application of $\sim 10^{-9}$ M *Sinorhizobium meliloti* 2011 LCOs (dissolved in 1% DMSO) or mock (1% DMSO). qRT-PCR expression analysis showed that in wild-type roots the strongest induction of *MtNIN* occurred in zone 1 and a lower induction in zone 2. This indicates that the LCO susceptible zone of wild-type predominately locates in zone 1 (Fig. 6). In contrast, in the medicago *Mtnoot1* mutant, the strongest *MtNIN* expression is observed in zone 2 (Fig. 6), implying that the *Mtnoot1* mutation caused the LCO susceptible zone to shift to zone 2. This is consistent with the delayed differentiation of the *Mtnoot1* root, which affects the LCO response by basipetally shifting the LCO susceptible zone.

DISCUSSION

Here, we demonstrate that *MtNOOT1* is required for coordinated development of the primary root of medicago along the apical-basal axis. A knockout mutation in the *MtNOOT1* gene causes two root developmental affects; (1) the primary root growth is faster due to a larger RAM, meaning more dividing cells, and (2) the primary root is thinner with delayed root differentiation. This demonstrates that in roots *MtNOOT1* not only functions as a homeotic gene in nodule development, but also coordinates root development.

In situ hybridization revealed that *MtNOOT1* is expressed in the transition zone,

which is located between the RAM and the elongation/differentiation zone. A larger RAM due to an increased number of meristematic cells indicates that the transition zone is positioned more distal from the stem cell niche. This suggests that MtNOOT1 controls the size of the RAM by defining the position of the boundary region (i.e. the transition zone) between the RAM and the elongation//differentiation zone. This is consistent with the aerial function of its orthologs in arabidopsis, where AtBOP1 and AtBOP2 promote the boundary specification between groups of cells with different fates (Aida and Tasaka, 2006; Žádníková and Simon, 2014; Khan et al., 2014; Hepworth and Pautot, 2015). In contrast to what we report for medicago *Mtnoot1*, a root growth and differentiation phenotype has not been reported in the arabidopsis *Atbop1;Atbop2* double mutant (Woerlen et al., 2017). The recruitment of NBCL family by legumes to maintain nodule symbiotic organ identity by defining nodule territories may have required adaptations in protein regulation and functioning (Couzigou et al., 2012). Such adaptations could be causal for the difference in root functioning of MtNOOT1 in medicago and AtBOP1 and AtBOP2 in arabidopsis. Further, it has been proposed that arabidopsis has a closed RAM organization with distinct initial cells, while legumes have a RAM with a basic-open organization. In the latter case, the identity of cell files seems disorganized and cannot be predicted (Rost, 2011). This deviation in structure of the RAM may explain the different functioning of BOP1/NOOT1 in arabidopsis and legume roots.

We also noted a basipetal shift of the root zone that is susceptible for rhizobium LCO signal molecules in the medicago *Mtnoot1* mutant. Such shift of susceptibility to rhizobium can be explained by the delayed differentiation of root cells. In medicago, susceptibility to LCO signalling can only occur in defined window of development. By elongating the RAM, the differentiation zone gets shifted basipetally. As a result, the susceptible zone shifts basipetally as well.

In the arabidopsis root the transition zone is determined by the antagonistic interaction between auxin and cytokinin. A well-defined auxin minimum is established in the boundary region, which is mediated by an active cytokinin signalling in the transition zone (Kong et al., 2018). Activation of auxin signalling or inhibition of cytokinin signalling can lead to accelerated primary root elongation and a larger RAM with increased number of meristematic cells, which are similar to the phenotype of *Mtnoot1* roots (Dello iolo et al., 2007; iolo et al., 2008). Auxin and cytokinin are also involved in root vasculature development (Reviewed in (Campbell and Turner, 2017; Ruonala et al., 2017)). For example, mutations in cytokinin biosynthetic genes lead to abolished cambium formation and reduced

thickening of the arabidopsis root (Matsumoto-Kitano et al., 2008), and auxin signalling is required for xylem differentiation and the organizer identity of vascular cambium cells in arabidopsis root (Smetana et al., 2019). In legumes, auxin and cytokinin participate in the LCO response and nodule organogenesis (Reviewed in (Boivin et al., 2016; Gamas et al., 2017; Kohlen et al., 2018)). For example, a mutation in cytokinin perception severely weakens the LCO response and perturbs nodule organogenesis (Gonzalez-Rizzo et al., 2006; Van Zeijl et al., 2015), whereas LCOs trigger auxin biosynthesis in the epidermis, leading to a rapid accumulation of auxin locally (Nadzieja et al., 2018). Recent findings suggest that in *Mtnoot1* nodules the interplay between auxin and cytokinin is imbalanced (Magne et al., 2018a). In line with that, we speculate that the auxin/cytokinin signalling pathway is affected during the primary growth of *Mtnoot1* roots, which will be targeted in future research.

We also showed that the lignification of xylem cells is delayed in *Mtnoot1* primary roots, which correlates with a delayed induction of a cascade of transcription factors involved in xylem cell differentiation. This can be explained by the extended RAM, leading to delayed cell differentiation in the basal region of primary root. However, the expression of *MtNOOT1* in the procambium cells by *in situ* hybridization suggests that MtNOOT1 can positively regulate vascular cell differentiation in a cell-autonomous manner. This is in line with the function of arabidopsis AtBOP1 and AtBOP2 in stem vasculature, where they can induce lignin deposition in vascular cells by promoting the expression of lignin biosynthetic genes. Ectopic expression of *AtBOP1/AtBOP2* in stem tissue leads to an expanded pattern of lignification (Khan et al., 2012). Therefore, we hypothesize that MtNOOT1 promotes root vasculature differentiation by activating a cascade of genes involved in xylem cell differentiation.

CONCLUSIONS

Here, we showed that *MtNOOT1* controls two aspects of root development; (1) the positioning of the transition zone, and (2) vasculature development by transcriptionally activating of a cascade of genes involved in xylem cell differentiation at a controlled distance from the root tip. Knockout of the *MtNOOT1* gene not only leads to a delayed differentiation of the root, but also shift the root region susceptible to LCOs. Taken together, this demonstrates that *MtNOOT1* not only maintains nodule identity, but also coordinates the primary root development along the apical-basal axis.

METHODS

Plant Materials and Growth Conditions

Medicago truncatula wild-type accession R108-1 plants and *Mtnoot1* mutant lines tnk507 and NF2717 were used in this study (Couzigou et al., 2012; Magne et al., 2018a). R108-1 was acquired from Toan Hanh Trinh (Hoffmann et al., 1997). tnk507 and NF2717 were acquired from Pascal Ratet (IPS2, CNRS, Gif-sur-Yvette, France), they were identified by a forward genetics screen of Tnt1 insertion lines (Institut des Sciences du Végétal, France; Noble Foundation, Ardmore, USA). The surface-sterilization and germination of medicago seeds were performed as previously described by (Limpens et al., 2004). Note that medicago seeds germinated at room temperature for one day, before growing on Fahraeus agar medium (Fahraeus, 1957) (including 0.75 mM $\text{Ca}(\text{NO}_3)_2$) in square petri dish (9 cm x 9 cm) and exposed to light for another five days. Plants were grown in an environmentally controlled growth chamber at 21 °C with a 16-h light/8-h dark.

Microscopy and Imaging

For microscopy studies, root segments were all collected at 6 DAG. For measuring the length of the RAM, ~5 mm root tips were cut and immersed in chloral hydrate solution at 4 °C overnight, analysed under Axio Imager A1 microscope (Zeiss) with Nomarski optics. For measuring cross-sectional areas, root segments were fixed with 4% paraformaldehyde (w/v), 5% glutaraldehyde (v/v) in 0.05 M sodium phosphate buffer (pH 7.2) at 4 °C overnight. The fixed material was dehydrated in an ethanol series and subsequently embedded in Technovit 7100 (Heraeus Kulzer) according to the manufacturer's protocol. Sections (5 µm) were made with a RJ2035 microtome (Leica Microsystems) stained 1.5 min in 0.05% toluidine blue O. For phloroglucinol-HCl staining, root segments were fixed as abovementioned. The fixed material was washed with 1 x PBS (sodium phosphate buffer), and directly embedded in 6% low melting agarose dissolved in 1 x PBS. Sections (50 µm) were made with a VT1000 S vibratome (Leica Microsystems), stained with 2% phloroglucinol (in 95% ethanol) for 2 min and applied with a few drops of 37% HCl. Sections were all analysed by using a DM5500B microscope equipped with a DFC425C camera (Leica Microsystems).

***In situ* Hybridization**

Hybridization was performed twice on root segments at 6 DAG by using Invitrogen ViewRNA ISH Tissue 1-Plex assay kit (Thermo Fisher Scientific), as previously described by (Kulikova et al., 2018; Liu et al., 2019). For user manual, visit https://assets.thermofisher.com/TFS-Assets/LSG/manuals/MAN0018633_viewRNA_ISH_UG.pdf. The probe sets for *MtNOOT1* (catalogue number: VF1-16434, information is available on request) were designed and synthesized by Thermo Fisher Scientific. *MtNOOT1* probe sets cover the region 2-913 nucleotide (nt) of the coding sequence (1449 nt, Medtr7g090020.1). A typical probe set contains ~20 oligonucleotide pairs of probes that hybridize to specific regions across the target mRNA. Each probe covers 20 nt, only a pair of two adjacent probes, which can target 40 nt, can form a site for signal amplification. By this principle, control probes are not needed (Katsushima et al., 2016; Osteen et al., 2016; Roux et al., 2014; Kulikova et al., 2018; Liu et al., 2019). Sections were imaged as mentioned above.

Phylogenetic Tree Construction

The protein sequences of different orthogroups were obtained from (van Velzen et al., 2018). For phylogenetic reconstruction, full length (predicted) protein sequences of at least two closely related orthogroups were aligned using MAFFT v7.017 (Kato, 2002), implemented in Geneious R6 (Biomatters, Auckland, New Zealand), using default parameter settings. After manual inspection, alignments were used for tree building by using W-IQ-TREE (Trifinopoulos et al., 2016) with best-fit substitution model (Kalyaanamoorthy et al., 2017). Branch support was assessed by using Ultrafast Bootstrap Approximation based on 1000 replicates (Minh et al., 2013).

RNA Isolation and qRT-PCR Analysis

RNA was isolated from root segments at 6 DAG using the EZNA Plant RNA mini kit (Omega), following the supplier's manual. 1 µg total RNA was used to synthesize cDNA using iScript cDNA synthesis kit (Bio-Rad). Equal amounts of cDNA were used for qPCR using SYBR Green Super-mix (Bio-Rad) in a Bio-Rad CFX connect real-time system qPCR machine. The gene expression was normalized using *MtACT2* as reference gene. Three technical replicates per biological replicate. All primers used in this study are listed in Supplementary

Table 1.

ACKNOWLEDGMENTS

We thank Pascal Ratet for providing the *Mtnoot1* seeds (tnk507 and NF2717) and thank Huchen Li and Kévin Magne for their comments on the manuscript.

AUTHOR CONTRIBUTIONS

RG and TB supervised this research. DS designed and performed most of the experiments with help from KG and WK. OK and DS performed the *in situ* hybridization. DS drafted the manuscript with input from HF. RG contributed to writing and revising the manuscript. All authors read and approved the final manuscript.

REFERENCES

- Aida, M. and Tasaka, M.** (2006). Genetic control of shoot organ boundaries. *Curr. Opin. Plant Biol.* **9**: 72–77.
- Bell, E.M., Lin, W. -c., Husbands, A.Y., Yu, L., Jaganatha, V., Jablonska, B., Mangeon, A., Neff, M.M., Girke, T., and Springer, P.S.** (2012). *Arabidopsis* LATERAL ORGAN BOUNDARIES negatively regulates brassinosteroid accumulation to limit growth in organ boundaries. *Proc. Natl. Acad. Sci.* **109**: 21146–21151.
- Benedito, V.A. et al.** (2008). A gene expression atlas of the model legume *Medicago truncatula*. *Plant J.* **55**: 504–513.
- Boivin, S., Fonouni-Farde, C., and Frugier, F.** (2016). How Auxin and Cytokinin Phytohormones Modulate Root Microbe Interactions. *Front. Plant Sci.* **7**: 1–12.
- Bonke, M., Thitamadee, S., Mähönen, A.P., Hauser, M.T., and Helariutta, Y.** (2003). APL regulates vascular tissue identity in *Arabidopsis*. *Nature* **426**: 181–186.
- Campbell, L. and Turner, S.** (2017). Regulation of vascular cell division. *J. Exp. Bot.* **68**: 27–43.
- Couzigou, J.-M.J. et al.** (2012). *NODULE ROOT* and *COCHLEATA* Maintain Nodule Development and Are Legume Orthologs of *Arabidopsis* *BLADE-ON-PETIOLE* Genes. *Plant Cell* **24**: 4498–4510.
- Couzigou, J.M., Magne, K., Mondy, S., Cosson, V., Clements, J., and Ratet, P.** (2016). The legume *NOOT-BOP-COCH-LIKE* (*NBCL*) genes are conserved regulators of abscission, a major agronomical trait in cultivated crops. *New Phytol.* **209**: 228–240.
- Desbrosses, G.J. and Stougaard, J.** (2011). Root nodulation: A paradigm for how plant-microbe symbiosis influences host developmental pathways. *Cell Host*

- Microbe **10**: 348–358.
- Fahraeus, G.** (1957). The infection of clover root hairs by nodule bacteria studied by a simple glass slide technique. *J. Gen. Microbiol.* **16**: 374–81.
- Gamas, P., Brault, M., Jardinaud, M.F., and Frugier, F.** (2017). Cytokinins in Symbiotic Nodulation: When, Where, What For? *Trends Plant Sci.* **22**: 792–802.
- Gonzalez-Rizzo, S., Crespi, M., and Frugier, F.** (2006). The *Medicago truncatula* CRE1 cytokinin receptor regulates lateral root development and early symbiotic interaction with *Sinorhizobium meliloti*. *Plant Cell* **18**: 2680–93.
- Ha, C.M., Jun, J.H., Nam, H.G., and Fletcher, J.C.** (2007). *BLADE-ON-PETIOLE1* and 2 Control *Arabidopsis* Lateral Organ Fate through Regulation of LOB Domain and Adaxial-Abaxial Polarity Genes. *Plant Cell* **19**: 1809–25.
- Ha, C.M., Kim, G.-T., Kim, B.C., Jun, J.H., Soh, M.S., Ueno, Y., Machida, Y., Tsukaya, H., and Nam, H.G.** (2003). The *BLADE-ON-PETIOLE 1* gene controls leaf pattern formation through the modulation of meristematic activity in *Arabidopsis*. *Development* **130**: 161–72.
- He, J., Benedito, V.A., Wang, M., Murray, J.D., Zhao, P.X., Tang, Y., and Udvardi, M.K.** (2009). The *Medicago truncatula* gene expression atlas web server. *BMC Bioinformatics* **10**: 441.
- Hepworth, S.R. and Pautot, V.A.** (2015). Beyond the Divide: Boundaries for Patterning and Stem Cell Regulation in Plants. *Front. Plant Sci.* **6**: 1052.
- Hoffmann, B., Trinh, T.H., Leung, J., Kondorosi, A., and Kondorosi, E.** (1997). A new *Medicago truncatula* line with superior in vitro regeneration, transformation, and symbiotic properties isolated through cell culture selection. *Mol. Plant-Microbe Interact.* **10**: 307–315.
- Holmes, P., Goffard, N., Weiller, G.F., Rolfe, B.G., and Imin, N.** (2008). Transcriptional profiling of *Medicago truncatula* meristematic root cells. *BMC Plant Biol.* **8**: 21.
- Ichihashi, Y., Kawade, K., Usami, T., Horiguchi, G., Takahashi, T., and Tsukaya, H.** (2011). Key Proliferative Activity in the Junction between the Leaf Blade and Leaf Petiole of *Arabidopsis*. *Plant Physiol.* **157**: 1151–1162.
- Dello Iorio, R., Linhares, F.S., Scacchi, E., Casamitjana-Martinez, E., Heidstra, R., Costantino, P., and Sabatini, S.** (2007). Cytokinins Determine *Arabidopsis* Root-Meristem Size by Controlling Cell Differentiation. *Curr. Biol.* **17**: 678–682.
- Ioio, R.D., Nakamura, K., Moubayidin, L., Perilli, S., Taniguchi, M., Morita, M.T., Aoyama, T., Costantino, P., and Sabatini, S.** (2008). A Genetic Framework for the Control of Cell Division and Differentiation in the Root Meristem. *Science* **322**: 1380–1384.
- Jun, J.H., Ha, C.M., and Fletcher, J.C.** (2010). *BLADE-ON-PETIOLE1* Coordinates Organ Determinacy and Axial Polarity in *Arabidopsis* by Directly Activating *ASYMMETRIC LEAVES2*. *Plant Cell* **22**: 62–76.
- Kalyaanamoorthy, S., Minh, B.Q., Wong, T.K.F., Von Haeseler, A., and Jermini, L.S.** (2017). ModelFinder: Fast model selection for accurate phylogenetic estimates. *Nat. Methods* **14**: 587–589.
- Katoh, K.** (2002). MAFFT: a novel method for rapid multiple sequence alignment based on fast Fourier transform. *Nucleic Acids Res.* **30**: 3059–3066.
- Katsushima, K. et al.** (2016). Targeting the Notch-regulated non-coding RNA TUG1

for glioma treatment. *Nat. Commun.* **7**: 1–14.

Khan, M., Xu, H., and Hepworth, S.R. (2014). BLADE-ON-PETIOLE genes: Setting boundaries in development and defense. *Plant Sci.* **215–216**: 157–171.

Khan, M., Xu, M., Murmu, J., Tabb, P., Liu, Y., Storey, K., McKim, S.M., Douglas, C.J., and Hepworth, S.R. (2012). Antagonistic interaction of BLADE-ON-PETIOLE1 and 2 with BREVIPEDICELLUS and PENNYWISE regulates *Arabidopsis* inflorescence architecture. *Plant Physiol.* **158**: 946–60.

Kohlen, W., Ng, J.L.P., Deinum, E.E., and Mathesius, U. (2018). Auxin transport, metabolism, and signalling during nodule initiation: Indeterminate and determinate nodules. *J. Exp. Bot.* **69**: 229–244.

Kong, X., Liu, G., Liu, J., and Ding, Z. (2018). The Root Transition Zone: A Hot Spot for Signal Crosstalk. *Trends Plant Sci.* **23**: 403–409.

Kulikova, O., Franken, C., and Bisseling, T. (2018). In situ hybridization method for localization of mRNA molecules in medicago tissue sections. In *Methods in Molecular Biology* (Humana Press, New York, NY), pp. 145–159.

Lars Hennig and Köhler, C. (2010). *Plant Developmental Biology Methods and Protocols*.

Liebsch, D., Sunaryo, W., Holmlund, M., Norberg, M., Zhang, J., Hall, H.C., Helizon, H., Jin, X., Helariutta, Y., Nilsson, O., Polle, A., and Fischer, U. (2014a). Class I KNOX transcription factors promote differentiation of cambial derivatives into xylem fibers in the *Arabidopsis* hypocotyl. *Development* **141**: 4311–4319.

Liebsch, D., Sunaryo, W., Holmlund, M., Norberg, M., Zhang, J., Hall, H.C., Helizon, H., Jin, X., Helariutta, Y., Nilsson, O., Polle, A., and Fischer, U. (2014b). Class I KNOX transcription factors promote differentiation of cambial derivatives into xylem fibers in the *Arabidopsis* hypocotyl. *Development* **141**: 4311–4319.

Limpens, E., Ramos, J., Franken, C., Raz, V., Compaa, B., Franssen, H., Bisseling, T., and Geurts, R. (2004). RNA interference in *Agrobacterium rhizogenes*-transformed roots of *Arabidopsis* and *Medicago truncatula*. *J. Exp. Bot.* **55**: 983–992.

Liu, J., Rutten, L., Limpens, E., van der Molen, T., van Velzen, R., Chen, R., Chen, Y., Geurts, R., Kohlen, W., Kulikova, O., and Bisseling, T. (2019). A Remote *cis*-Regulatory Region Is Required for *NIN* Expression in the Pericycle to Initiate Nodule Primordium Formation in *Medicago truncatula*. *Plant Cell* **31**: 68–83.

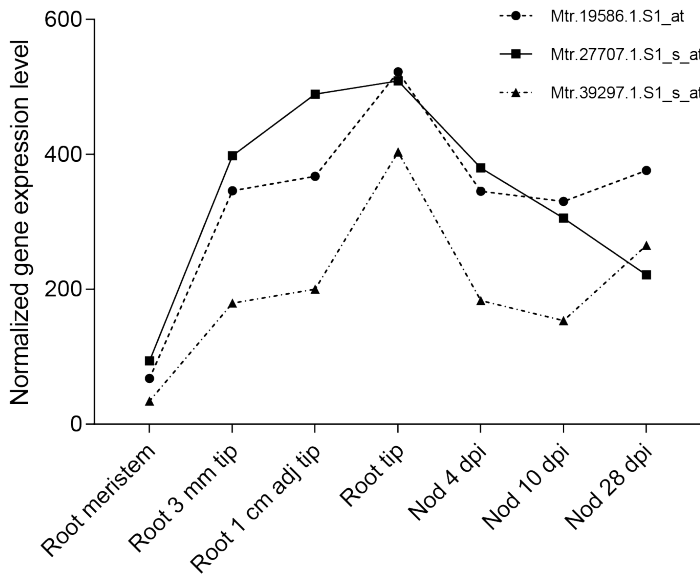
Magne, K. et al. (2018a). MtNODULE ROOT1 and MtNODULE ROOT2 Are Essential for Indeterminate Nodule Identity. *Plant Physiol.* **178**: 295–316.

Magne, K., George, J., Berbel Tornero, A., Broquet, B., Madueño, F., Andersen, S.U., and Ratet, P. (2018b). *Lotus japonicus* NOOT-BOP-COCH-LIKE1 is essential for nodule, nectary, leaf and flower development. *Plant J.* **94**: 880–894.

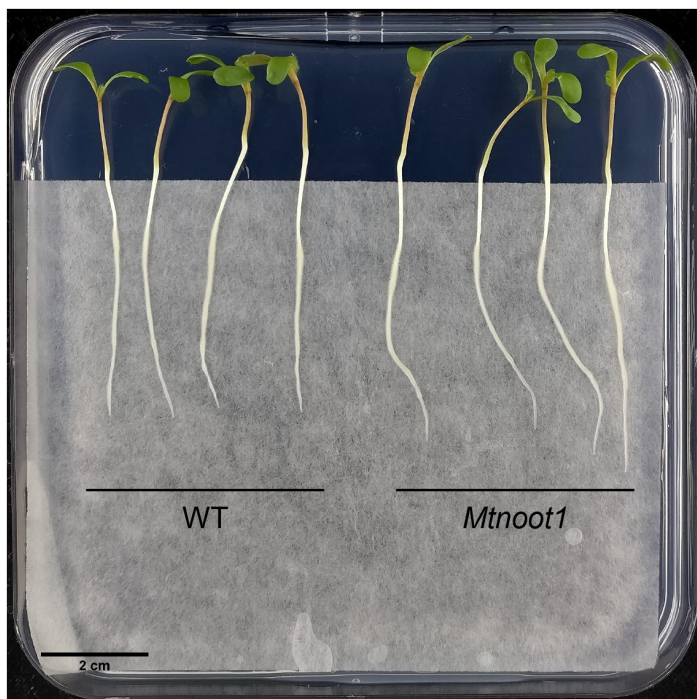
Marsh, J.F., Rakocevic, A., Mitra, R.M., Brocard, L., Sun, J., Eschstruth, A., Long, S.R., Schultze, M., Ratet, P., and Oldroyd, G.E.D. (2007). *Medicago truncatula* NIN Is Essential for Rhizobial-Independent Nodule Organogenesis Induced by Autoactive Calcium/Calmodulin-Dependent Protein Kinase. *Plant Physiol.* **144**: 324–335.

- Matsumoto-Kitano, M., Kusumoto, T., Tarkowski, P., Kinoshita-Tsujimura, K., Vaclavikova, K., Miyawaki, K., and Kakimoto, T.** (2008). Cytokinins are central regulators of cambial activity. *Proc. Natl. Acad. Sci.* **105**: 20027–20031.
- McKim, S.M., Stenvik, G.-E., Butenko, M.A., Kristiansen, W., Cho, S.K., Hepworth, S.R., Aalen, R.B., and Haughn, G.W.** (2008). The *BLADE-ON-PETIOLE* genes are essential for abscission zone formation in *Arabidopsis*. *Development* **135**: 1537–1546.
- Minh, B.Q., Nguyen, M.A.T., and Von Haeseler, A.** (2013). Ultrafast approximation for phylogenetic bootstrap. *Mol. Biol. Evol.* **30**: 1188–1195.
- Nadzieja, M., Kelly, S., Stougaard, J., and Reid, D.** (2018). Epidermal auxin biosynthesis facilitates rhizobial infection in *Lotus japonicus*. *Plant J.* **95**: 101–111.
- Ohashi-Ito, K., Oda, Y., and Fukuda, H.** (2010). *Arabidopsis* VASCULAR-RELATED NAC-DOMAIN6 Directly Regulates the Genes That Govern Programmed Cell Death and Secondary Wall Formation during Xylem Differentiation. *Plant Cell* **22**: 3461–3473.
- Osteen, J.D. et al.** (2016). Selective spider toxins reveal a role for the Nav1.1 channel in mechanical pain. *Nature* **534**: 494–499.
- Rost, T.L.** (2011). The organization of roots of dicotyledonous plants and the positions of control points. *Ann. Bot.* **107**: 1213–1222.
- Roux, B. et al.** (2014). An integrated analysis of plant and bacterial gene expression in symbiotic root nodules using laser-capture microdissection coupled to RNA sequencing. *Plant J.* **77**: 817–837.
- Ruonala, R., Ko, D., and Helariutta, Y.** (2017). Genetic Networks in Plant Vascular Development. *Annu. Rev. Genet.* **51**: 335–359.
- Schauser, L., Roussis, A., Stiller, J., and Stougaard, J.** (1999). A plant regulator controlling development of symbiotic root nodules. *Nature* **402**: 191–195.
- Schuetz, M., Smith, R., and Ellis, B.** (2013). Xylem tissue specification, patterning, and differentiation mechanisms. *J. Exp. Bot.* **64**: 11–31.
- Smetana, O. et al.** (2019). High levels of auxin signalling define the stem-cell organizer of the vascular cambium. *Nature* **565**: 485–489.
- Soyano, T., Kouchi, H., Hirota, A., and Hayashi, M.** (2013). NODULE INCEPTION Directly Targets *NF-Y* Subunit Genes to Regulate Essential Processes of Root Nodule Development in *Lotus japonicus*. *PLoS Genet.* **9**: e1003352.
- Trifinopoulos, J., Nguyen, L.T., von Haeseler, A., and Minh, B.Q.** (2016). W-IQ-TREE: a fast online phylogenetic tool for maximum likelihood analysis. *Nucleic Acids Res.* **44**: W232–W235.
- van Velzen, R. et al.** (2018). Comparative genomics of the nonlegume *Parasponia* reveals insights into evolution of nitrogen-fixing rhizobium symbioses. *Proc. Natl. Acad. Sci. U. S. A.* **115**: E4700–E4709.
- Vernié, T., Kim, J., Frances, L., Ding, Y., Sun, J., Guan, D., Niebel, A., Gifford, M.L., de Carvalho-Niebel, F., and Oldroyd, G.E.D.** (2015). The NIN Transcription Factor Coordinates Diverse Nodulation Programs in Different Tissues of the *Medicago truncatula* Root. *Plant Cell* **27**: 3410–3424.
- Wang, Q., Hasson, A., Rossmann, S., and Theres, K.** (2016). *Divide et impera*: Boundaries shape the plant body and initiate new meristems. *New Phytol.* **209**: 485–498.

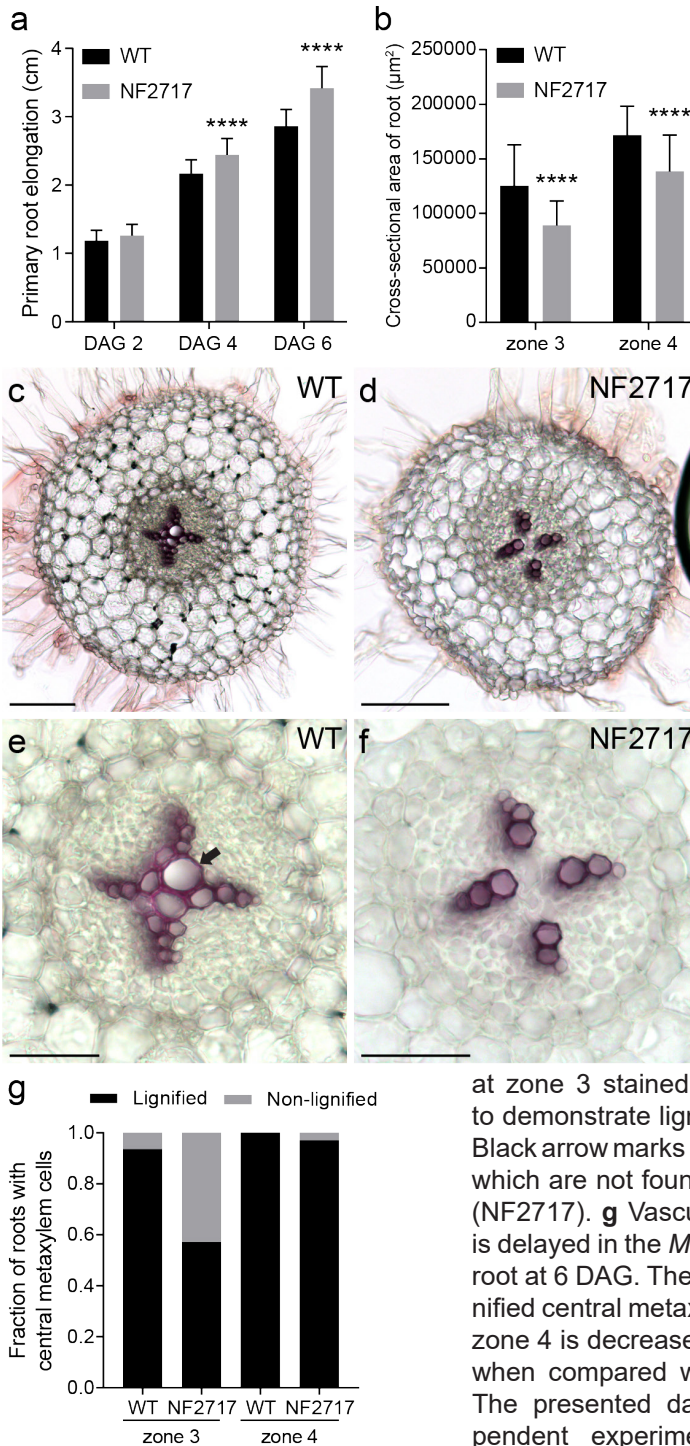
- Woerlen, N., Allam, G., Popescu, A., Corrigan, L., Pautot, V., and Hepworth, S.R.** (2017). Repression of *BLADE-ON-PETIOLE* genes by KNOX homeodomain protein BREVIPEDICELLUS is essential for differentiation of secondary xylem in *Arabidopsis* root. *Planta* **245**: 1079–1090.
- Xiao, T.T., Schilderink, S., Moling, S., Deinum, E.E., Kondorosi, E., Franssen, H., Kulikova, O., Niebel, A., and Bisseling, T.** (2014). Fate map of *Medicago truncatula* root nodules. *Development* **141**: 3517–3528.
- Yano, K. et al.** (2008). CYCLOPS, a mediator of symbiotic intracellular accommodation. *Proc. Natl. Acad. Sci. U. S. A.* **105**: 20540–20545.
- Žádníková, P. and Simon, R.** (2014). How boundaries control plant development. *Curr. Opin. Plant Biol.* **17**: 116–125.
- Van Zeijl, A., Op Den Camp, R.H.M., Deinum, E.E., Charnikhova, T., Franssen, H., Op Den Camp, H.J.M., Bouwmeester, H., Kohlen, W., Bisseling, T., and Geurts, R.** (2015). Rhizobium Lipo-chitooligosaccharide Signaling Triggers Accumulation of Cytokinins in *Medicago truncatula* Roots. *Mol. Plant* **8**: 1213–1226.
- Zhong, R., Lee, C., and Ye, Z.-H.** (2010). Global analysis of direct targets of secondary wall NAC master switches in *Arabidopsis*. *Mol. Plant* **3**: 1087–103.
- Zhong, R., Lee, C., Zhou, J., McCarthy, R.L., and Ye, Z.-H.** (2008). A Battery of Transcription Factors Involved in the Regulation of Secondary Cell Wall Biosynthesis in *Arabidopsis*. *Plant Cell Online* **20**: 2763–2782.



Supplementary Figure 1. *Medicago MtNOOT1* is expressed in the root tip. Expression profiles are derived from the *Medicago truncatula* Gene Expression Atlas (He et al., 2009). *MtNOOT1* is targeted by the probe-sets Mtr.19586.1.S1_at, Mtr.27707.1.S1_s_at, and Mtr.39297.1.S1_s_at. Root 3 mm tip: 3 mm root tip (Holmes et al., 2008); adj tip: 1 cm root segment adjacent to 3 mm root tip (Holmes et al., 2008); Nod: nodules, all nodule samples are derived from (Benedito et al., 2008); dpi: days post inoculation.

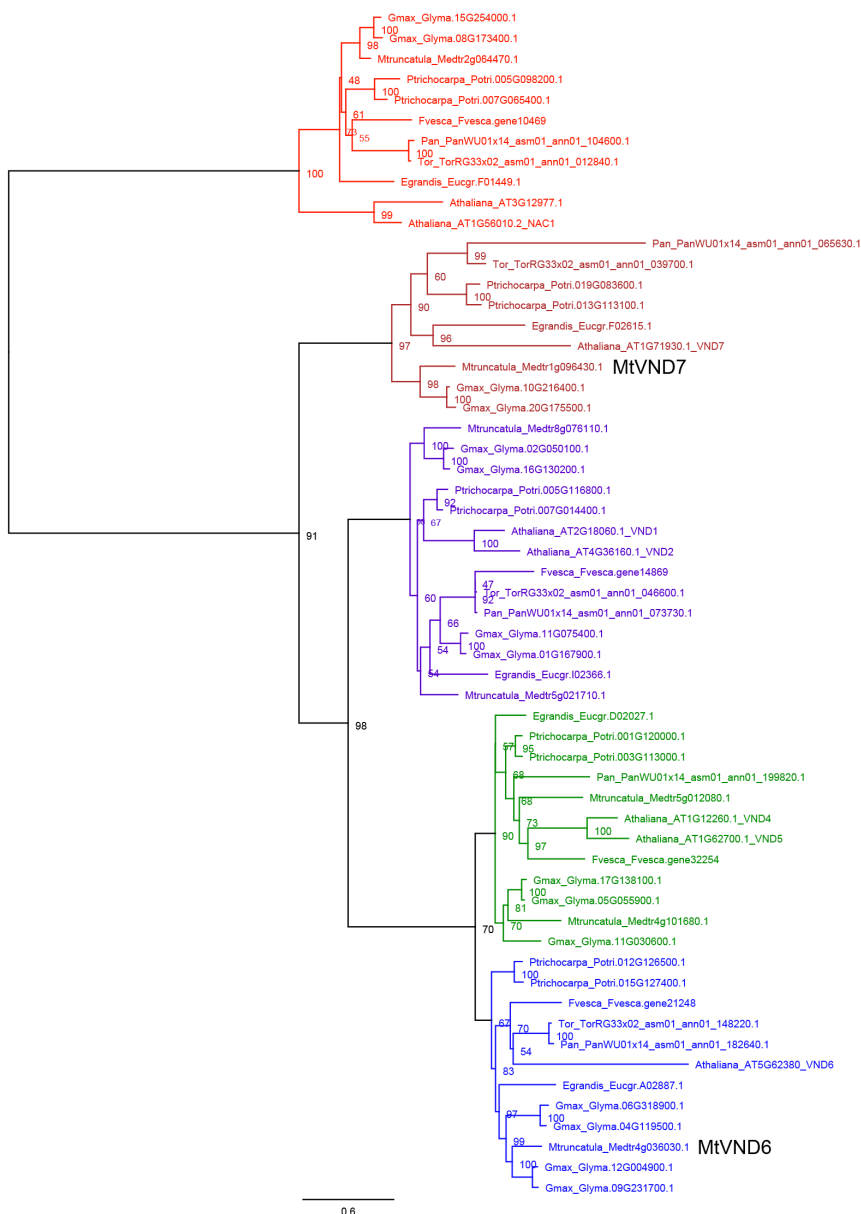


Supplementary Figure 2. The primary root *Mtnoot1* *tnk507* mutant is longer than wild-type. Representative seedlings at 6 DAG are presented.

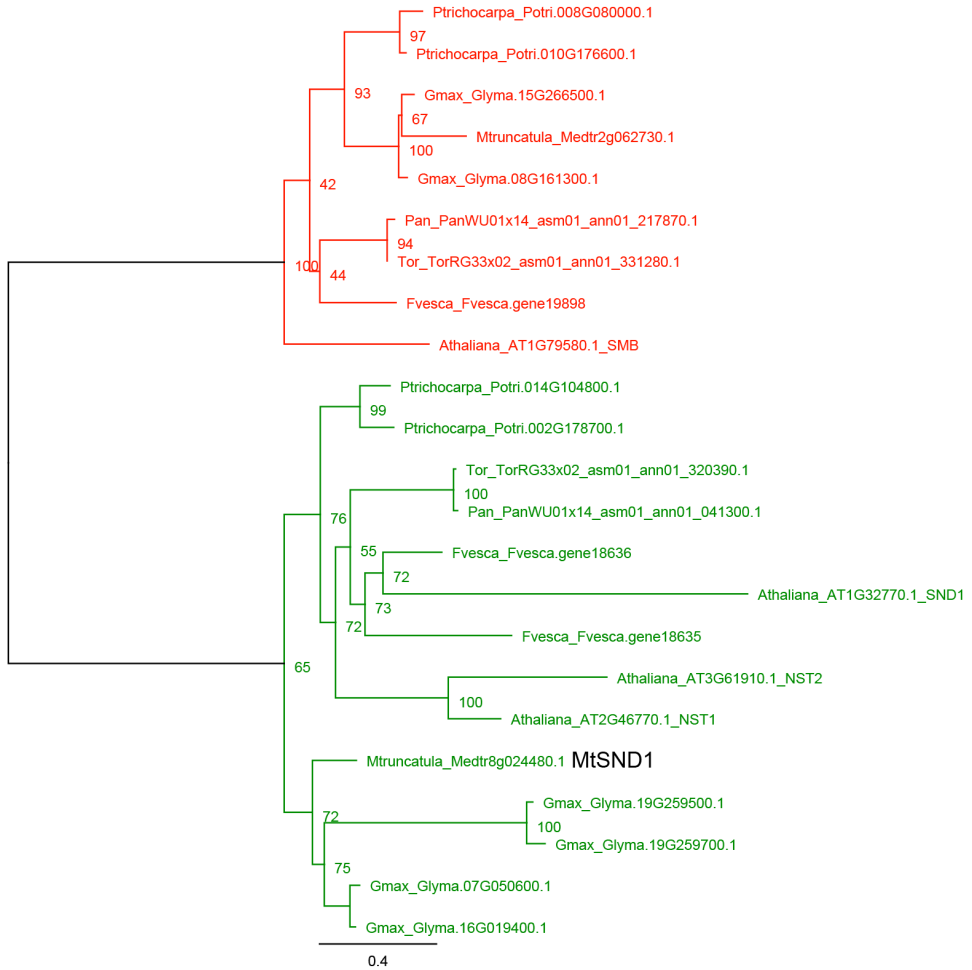


Supplementary Figure 3. The *Mtnoot1* NF2717 mutant allele shows a similar phenotype as the *Mtnoot1* tnk507 allele. **a** Root length of the medicago *Mtnoot1* mutant (NF2717) is markedly longer at 4 DAG and 6 DAG when compared to primary roots of wild-type medicago seedlings (WT). **b** The cross-sectional area is significantly reduced in the medicago *Mtnoot1* mutant (NF2717) at zone 3 and zone 4. The data represent means + SD of two independent experiments, each experiment contains 15-20 roots. Student *t*-test was performed to assess significant differences (****: $P < 0.0001$). Representative root cross sections of wild-type (**c**, **e**) and *Mtnoot1* (NF2717) (**d**, **f**) vascular bundle

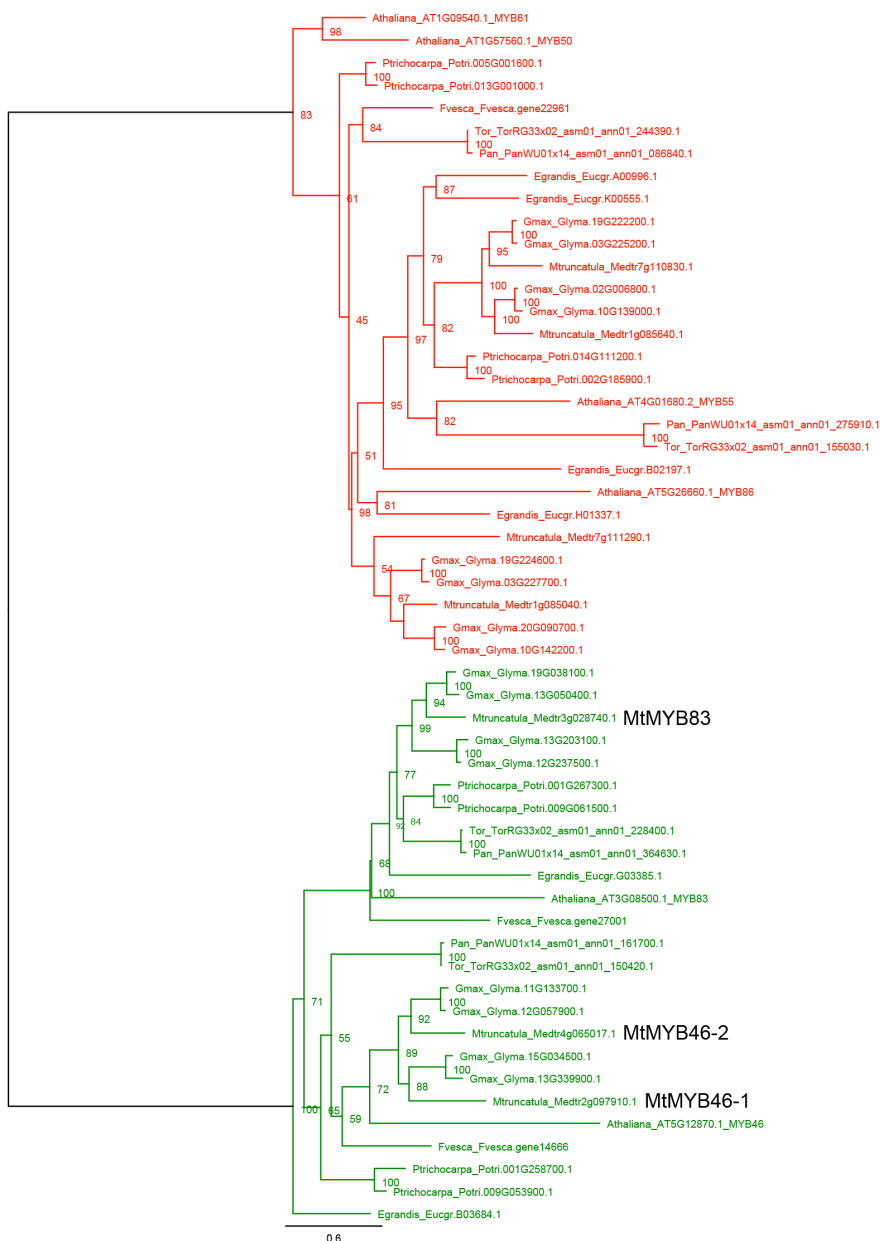
at zone 3 stained with phloroglucinol-HCl to demonstrate lignin deposition at 6 DAG. Black arrow marks lignified metaxylem cells, which are not found in the *Mtnoot1* mutant (NF2717). **g** Vascular xylem differentiation is delayed in the *Mtnoot1* (NF2717) primary root at 6 DAG. The fraction of roots with lignified central metaxylem cells in zone 3 and zone 4 is decreased in the *Mtnoot1* mutant when compared with wild-type seedlings. The presented data combines two independent experiments, each experiment contains 15-18 roots. Scale bar: 50 μm (**c**, **d**), 100 μm (**e**, **f**).



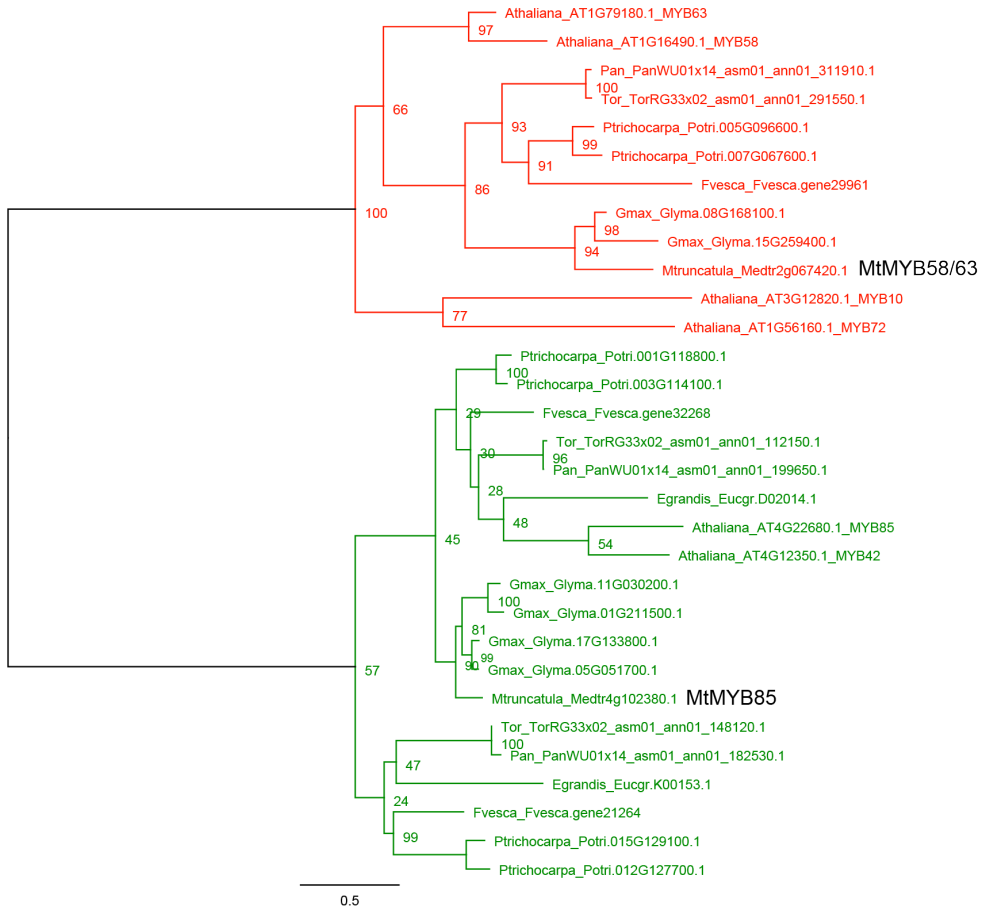
Supplementary Figure 4. Maximum likelihood tree of VND6, VND7 and related proteins. The protein sequences of OG0006787 (red), OG0009959 (dark red), OG0004118 (purple), OG0001465 (green and blue) are obtained from van Velzen et. al (2018), except VND6, which was not included in OG0001465. Species include *arabidopsis* (*Athaliana*), *Eucalyptus grandis* (*Egrandis*), *Fragaria vesca* (*Fvesca*), *Glycine max* (*Gmax*), *medicago* (*Mtruncatula*), *Populus trichocarpa* (*Trichocarpa*), *Parasponia andersonii* (*Pan*) and *Trema orientalis* (*Tor*). Numbers at the branches indicate support from 1000 ultrafast bootstrap replicates. OG0006787 including NAC1 was used as outgroup.



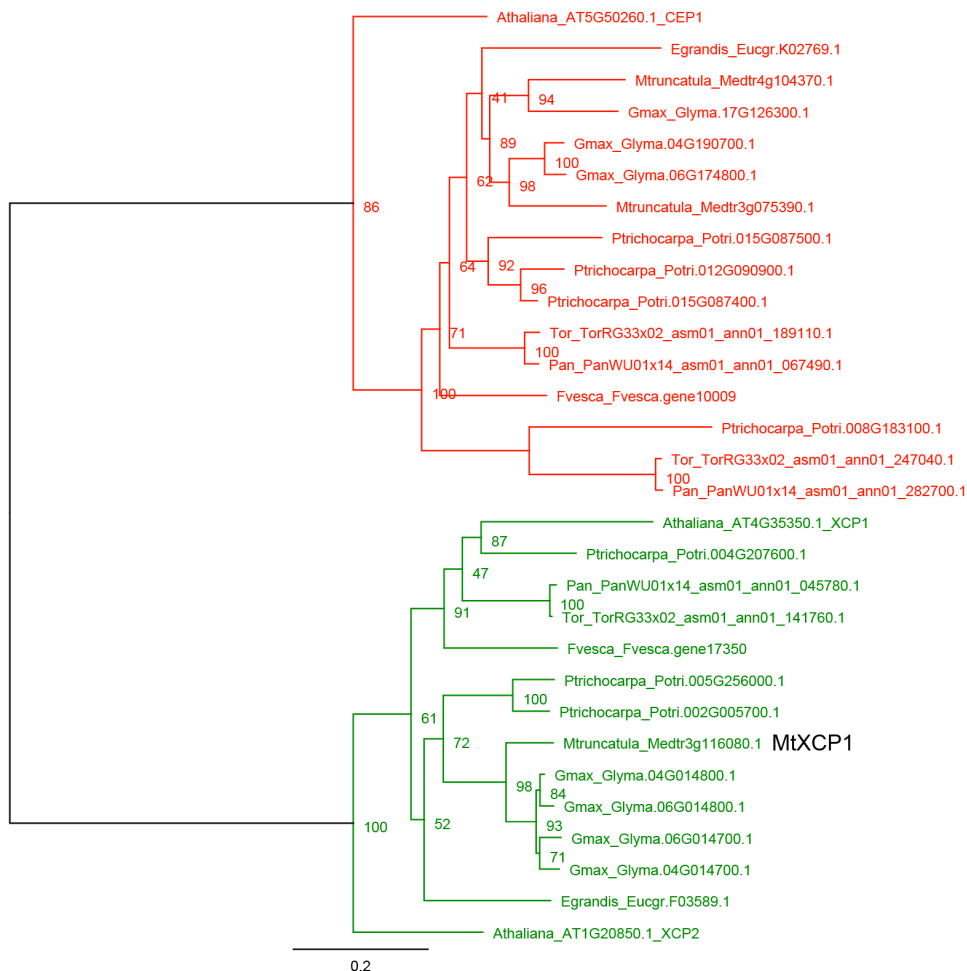
Supplementary Figure 5. Maximum likelihood tree of SND1 and related proteins. The protein sequences of OG0009898 (red) and OG0001875 (green) are obtained from van Velzen et. al (2018). Species include *arabidopsis* (*Athaliana*), *Eucalyptus grandis* (*Egrandis*), *Fragaria vesca* (*Fvesca*), *Glycine max* (*Gmax*), *medicago* (*Mtruncatula*), *Populus trichocarpa* (*P. trichocarpa*), *Parasponia andersonii* (*Pan*) and *Trema orientalis* (*Tor*). Numbers at to the branches indicate support from 1000 ultrafast bootstrap replicates. OG0009898 containing SMB was used as outgroup.



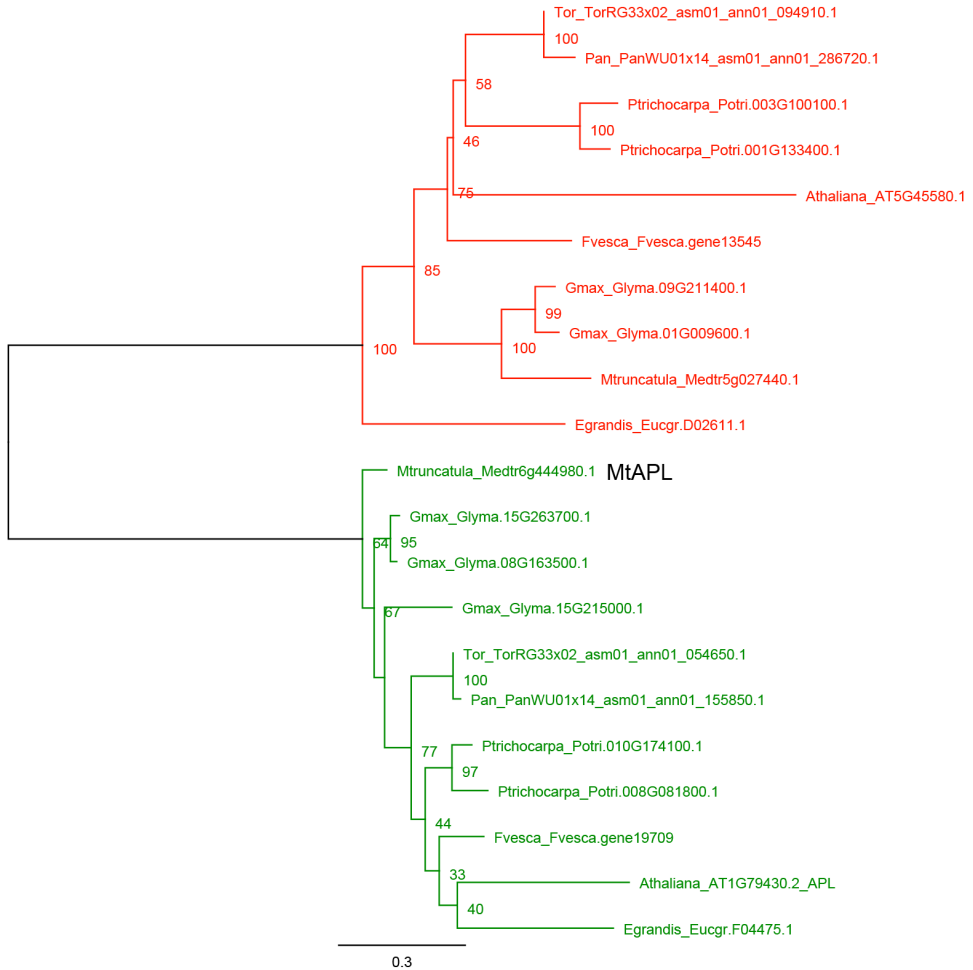
Supplementary Figure 6. Maximum likelihood tree of MYB46, MYB83 and related proteins. The protein sequences of OG0000857 (red) and OG0001270 (green) are obtained from van Velzen et. al (2018). Species include arabidopsis (*Athaliana*), *Eucalyptus grandis* (*Egrandis*), *Fragaria vesca* (*Fvesca*), *Glycine max* (*Gmax*), medicago (*Mtruncatula*), *Populus trichocarpa* (*Ptrichocarpa*), *Parasponia andersonii* (*Pan*) and *Trema orientalis* (*Tor*). Numbers at the branches indicate support from 1000 ultrafast bootstrap replicates. OG0000857 containing MYB50 was used as outgroup.



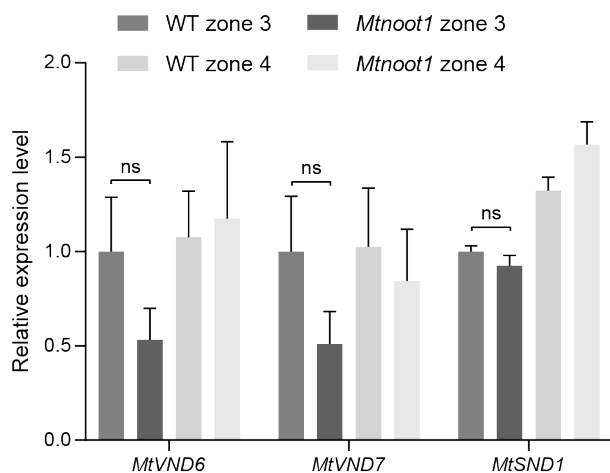
Supplementary Figure 7. Maximum likelihood tree of MYB58, MYB63 and MYB85 proteins. The protein sequences of OG0005384 (red) and OG0002420 (green) are obtained from van Velzen et. al (2018). Species include *arabidopsis* (*Athaliana*), *Eucalyptus grandis* (*Egrandis*), *Fragaria vesca* (*Fvesca*), *Glycine max* (*Gmax*), *medicago* (*Mtruncatula*), *Populus trichocarpa* (*Ptrichocarpa*), *Parasponia andersonii* (*Pan*) and *Trema orientalis* (*Tor*). Numbers at the branches indicate support from 1000 ultrafast bootstrap replicates. OG0005384 containing MYB58 and MYB63 was used as outgroup.



Supplementary Figure 8. Maximum likelihood tree of XCP1 and related proteins. The protein sequences of OG0003401 (red) and OG0003952 (green) are obtained from van Velzen et. al (2018). Species include *arabidopsis* (*Athaliana*), *Eucalyptus grandis* (*Egrandis*), *Fragaria vesca* (*Fvesca*), *Glycine max* (*Gmax*), *medicago* (*Mtruncatula*), *Populus trichocarpa* (*Ptrichocarpa*), *Parasponia andersonii* (*Pan*) and *Trema orientalis* (*Tor*). Numbers at the branches indicate support from 1000 ultrafast bootstrap replicates. OG0003401 containing CEP1 was used as outgroup.



Supplementary Figure 9. Maximum likelihood tree of APL and related proteins. The protein sequences of OG0009526 (red) and OG0006786 (green) are obtained from van Velzen et. al (2018). Species include arabidopsis (*Athaliana*), *Eucalyptus grandis* (*Egrandis*), *Fragaria vesca* (*Fvesca*), *Glycine max* (*Gmax*), medicago (*Mtruncatula*), *Populus trichocarpa* (*Ptrichocarpa*), *Parasponia andersonii* (*Pan*) and *Trema orientalis* (*Tor*). Numbers at the branches indicate support from 1000 ultrafast bootstrap replicates. OG0009526 containing sequences highly homologous to MtAPL was used as outgroup.



Supplementary Figure 10. The NAC domain transcription factors *MtVND6* and *MtVND7*, but not *MtSND1*, are lower expressed in zone 3 of *Mtnoot1* *tnk507* roots when compared to wild-type. The data represent means + SEM of three independent experiments. Student *t*-test was performed to assess significant differences (ns: not significant).

Supplementary Table 1. qRT-PCR primers used in this study.

Name	Gene ID	Sequence
MtACT2-F	Medtr2g008050	CAGATGTGGATCTCCAAGGGTGA
MtACT2-R		TGACTGAAATATGGCACAAGACTGAGA
MtAPL-F	Medtr6g444980	ACTTGAAAGACCTTCACCAAGA
MtAPL-R		GAACCTCTACCTTGTGCCATAG
MtMYB46-1-F	Medtr2g097910	ACTTCATCATCAACATCTCCATCA
MtMYB46-1-R		ACTATGATCCATCACAGGCAAC
MtMYB46-2-F	Medtr4g065017	ACAACCTGCAATGTTGTTAGTAAGAG
MtMYB46-2-R		CTTCCAAATTCCAATCTCCAACAG
MtMYB58/63-F	Medtr2g067420	TCAATCAAATGTTGGTGAAGAGAC
MtMYB58/63-R		CACCTACTACTCCAAACTCATTCT
MtMYB83-F	Medtr3g028740	AAAGCCATAACAACCACTTCAA
MtMYB83-R		TCTCCTTGCCCATGATTTC
MtMYB85-F	Medtr4g102380	GATAGCATTTGCAGTGACGATTC
MtMYB85-R		CTGCTATAGGTGTAGTGTCATT
MtNOOT1-F	Medtr7g090020	GTTTAGTCCACGCACACAGA
MtNOOT1-R		CAGAAACTGAAGCATCAACAAGAA
MtSND1-F	Medtr8g024480	CAACACACGCCAGAACTACTA
MtSND1-R		AGAAGACGACAACAAGGATGAA
MtVND6-F	Medtr4g036030	GTTGCTTCACAACTTAGTCAAGAT
MtVND6-R		GGCACCATTTCTTGTCTCTCC
MtVND7-F	Medtr1g096430	AGCATGCCATTGATGATACCT
MtVND7-R		TGAATCAGGAAAGCAACCTAAGA
MtXCP1-F	Medtr3g116080	CAGGCAGAGATTTCAGTTCTA
MtXCP1-R		CCAAACCCTTTGATGTACCATATC

CHAPTER 3

A Homeotic Mutation Changes Legume Nodule Ontogeny into Actinorhizal-type Ontogeny

Defeng Shen^{1,#}, Ting Ting Xiao^{1,4,#}, Robin van Velzen^{1,2}, Olga Kulikova¹, Xiaoyun Gong^{3,5}, René Geurts¹, Katharina Pawlowski³, and Ton Bisseling^{1,*}

¹Laboratory of Molecular Biology, Department of Plant Sciences, Wageningen University, 6708 PB Wageningen, The Netherlands.

²Biosystematics Group, Department of Plant Sciences, Wageningen University, 6708 PB Wageningen, The Netherlands.

³Department of Ecology, Environment and Plant Sciences, Stockholm University, 106 91 Stockholm, Sweden.

⁴Present address: King Abdullah University of Science and Technology (KAUST), Biological and Environmental Sciences and Engineering (BESE), Thuwal, 23955-6900, Saudi Arabia.

⁵Present address: Faculty of Biology, Genetics, LMU Munich, Großhaderner Strasse 2-4, 82152 Martinsried, Germany.

[#]These authors contributed equally to this work.

^{*}Corresponding author: ton.bisseling@wur.nl.



ABSTRACT

Some plants can fix atmospheric nitrogen by hosting symbiotic diazotrophic rhizobia or *Frankia* bacteria in root organs, known as nodules. Such nodule symbiosis occurs in ten lineages in four taxonomic orders; Fabales, Fagales, Cucurbitales and Rosales, which collectively are known as the nitrogen-fixing clade (NFC). Based on differences in ontogeny and histology, nodules have been divided into two types: legume-type and actinorhizal-type nodules. The evolutionary relationship between these nodule types has been a long-standing enigma for molecular and evolutionary biologists. Recent phylogenomic studies on nodulating and non-nodulating species in the NFC indicated a shared evolutionary origin of the nodulation trait in all ten lineages. However, this hypothesis faces a conundrum that legume-type and actinorhizal-type nodules have been regarded as fundamentally different. Here, we analysed the actinorhizal-type nodules formed by *Parasponia andersonii* (Rosales) and *Alnus glutinosa* (Fagales), and found that their ontogeny is more similar to that of legume-type nodules (Fabales) than generally assumed. We also show that in *Medicago truncatula* a homeotic mutation in the co-transcriptional regulator encoding gene *NODULE ROOT1* (*MtNOOT1*) converts a legume-type nodule into actinorhizal type. These experimental findings suggest that the two nodule types have a shared evolutionary origin.

INTRODUCTION

Nitrogen-fixing root nodule symbiosis represents the most efficient biological process by which atmospheric nitrogen is transferred into ammonium and becomes a nitrogen source for plants. Nodules are specialised novel root organs whose formation is triggered by diazotrophic *Frankia* or rhizobium bacteria (reviewed in Sprent et al., 1987; Pawlowski and Bisseling, 1996; Huss-Danell, 1997; Franche et al., 2009; Pawlowski and Demchenko, 2012; Santi et al., 2013; Imanishi et al., 2014; Ibáñez et al., 2017).

Nitrogen-fixing root nodule symbioses occur in ten paraphyletic lineages in the so-called nitrogen-fixing clade (NFC), which is represented by the orders Fabales, Fagales, Cucurbitales and Rosales (Soltis et al., 1995) (Supplementary Figure 1). Species of the Fabaceae (order Fabales) and the genus *Parasponia* (Cannabaceae, order Rosales) form nodules with rhizobia, whereas eight lineages of actinorhizal plant species (in the orders Fagales, Cucurbitales and

Rosales) do so with *Frankia*. Nodulation is common in the Fabaceae of order Fabales, but rare in the other three orders that also represent many lineages of non-nodulating species. Recent phylogenomic studies showed that non-nodulating species within the NFC lost some genes that are essential and specific for nodulation (van Velzen et al., 2018; Griesmann et al., 2018). Therefore, it has been hypothesised that the nodulation trait evolved in the common ancestor of the NFC, and that this trait has been lost in many descendant lineages (van Velzen et al., 2019). However, this hypothesis does not readily explain differences in the ontogeny and histology of legume and actinorhizal nodule types, which are considered fundamental and suggestive of independent origins (Doyle, 2011; Parniske, 2018). To overcome this discrepancy, it has been suggested that the common ancestor of the NFC evolved only the capacity to accommodate intracellular infection of bacteria in root cortical cells; thereafter nodule formation evolved several times independently (Parniske, 2018).

To be able to compare developmental programs leading to nodule formation in the different lineages fate maps are indispensable. A detailed fate map has been made for the model legume *Medicago truncatula* (Medicago) (Xiao et al., 2014). This showed that cell division is first induced in the root pericycle and then extends to endodermis and inner cortical cells by which a nodule primordium is formed. After a few rounds of divisions, the pericycle- and endodermis-derived cells lose their mitotic activity and form about eight layers of cells that are not infected by rhizobia. The cells derived from the inner cortex are penetrated by infection threads that originate in the epidermis and grow towards these cells. At this stage a non-infected meristem is formed from the middle cortical cell layer. Rhizobia are released from the infection threads into the cells derived from the inner cortex. Once inside, the bacteria divide and differentiate, leading to a situation where ultimately infected plant cells contain hundreds of nitrogen-fixing rhizobia. These cells will form the infected central tissue that grows by cells that are added by the apical meristem. Vascular bundles are formed at the periphery of the nodule primordium and originate from cells derived from the dividing inner cortical cells and subsequently their growth is controlled by the apical meristem (Xiao et al., 2014). A characteristic of all studied legume nodules is that the infected central tissue is formed from the mitotically activated cortical cells. Further, the vascular bundles are located at the periphery and are also formed from cortex-derived cells (and not from the pericycle).

Actinorhizal-type nodules, including those nodules induced by rhizobium on *Parasponia* spp., have been described as coralloid organs consisting of

multiple lobes with a central vascular system. These lobes are considered to be formed by a modified lateral root developmental program and have a pericycle origin (Pawlowski and Bisseling, 1996; Huss-Danell, 1997; Pawlowski and Demchenko, 2012; Svistoonoff et al., 2014; Ibáñez et al., 2017) and in some actinorhizal plants nodules can even have a root growing out of the lobe apex (Pawlowski and Bisseling, 1996; Franche et al., 2009). It is concluded that the cortical cells of these “modified lateral roots” are infected without first being mitotically activated (Pawlowski and Bisseling, 1996; Santi et al., 2013). Studies on the initial stages of actinorhizal-type nodule formation in Fagales species have shown that a group of root cortical cells can be mitotically activated and become infected. These so-called prenodules are considered to be important for infection, but do not develop into an integral part of the actinorhizal-type nodule (Pawlowski and Bisseling, 1996; Franche et al., 2009; Pawlowski and Demchenko, 2012; Santi et al., 2013; Svistoonoff et al., 2014). In contrast to legumes, however, a detailed developmental fate map of actinorhizal-type nodules is lacking and our current view on the ontogeny of actinorhizal-type nodules might be incorrect.

Novel organs generally originate through the modification of existing developmental programs (Carroll, 2000; Shubin et al., 2009). Homeotic genes are key players in determining the identity and loss-of-function mutation in such homeotic genes can result in a switch to the ancestral developmental program. A classic example in *Drosophila* species is the switch from halter to wing development by mutations in the *Ultrabithorax* gene (Lewis, 1963). In plants, the developmental program of flower organs can (partially) switch to that of (vegetative) leaves by mutating a few homeotic genes (Ditta et al., 2004). In case of root nodules, a mutation in a homeotic gene may uncover the evolutionary relationship of root lateral organs, including both nodule types. One such gene has been described previously, namely the *NOOT-BOP-COCH-LIKE* (*NBCL*) gene encoding a co-transcriptional regulator. Mutations in this gene (named *NODULE ROOT1* (*MtNOOT1*) in *Medicago*, *COCHLEATIA1* (*PsCOCH1*) in *Pisum sativum* (pea) and *LjNBCL1* in *Lotus japonicus*) can cause outgrowth of roots from nodules, suggesting that this gene functions in maintenance of nodule identity (Couzigou et al. 2012; Magne et al. 2018a).

Here, we describe detailed fate maps for actinorhizal-type nodules formed by *Parasponia andersonii* (*Parasponia*) and *Alnus glutinosa* (*Alnus*). This shows that their ontogeny is markedly more similar to that of legume nodules than generally assumed. Further, we show that a mutation in the *Medicago MtNOOT1* converts

the ontogeny of legume-type nodules into that of actinorhizal-type nodules. We hypothesize that these two nodule types could have a common evolutionary origin and that legume-type nodules evolved from an actinorhizal-type nodule.

RESULTS

Infected Cells in Actinorhizal-type Nodules Are Derived from the Root Cortex

Actinorhizal-type nodules have been described as composed of “modified lateral roots” (Pawlowski and Bisseling, 1996; Pawlowski and Demchenko, 2012; Ibáñez et al., 2017). To obtain insight to what extent the nodule developmental program is distinct from the lateral root developmental program, we aimed to generate fate maps of two representative species; *Parasponia* and *Alnus*. These two species were selected because they can grow on plates allowing spot inoculation of rhizobia/*Frankia*. This is essential to obtain young nodule primordia for ontogenetic analysis.

First we analysed the ontogeny of lateral roots of *Parasponia* and *Alnus*. Sectioning of roots of both species revealed that lateral root primordia are derived from the pericycle and endodermis, similarly as in other plant species (*Convolvulus arvensis* (Bonnett, 1969), *Daucus carota* (Lloret et al., 1989), *Allium cepa* (Casero et al., 1996)). During lateral root formation 4-6 pericycle cells and their adjacent endodermis cells were mitotically activated (Supplementary Figures 2A and 3A). Endodermis cells only divided anticlinally (Supplementary Figures 2C, 2D and 3B) and formed the outermost layer of the lateral root primordium and later became part of the root cap/columella (Figure 1A and 1D; Supplementary Figures 2F and 3C). In the lateral root primordium, epidermis, cortex and a vasculature surrounded by a newly formed endodermis can be discerned (Figure 1A and 1D; Supplementary Figures 2F and 3C).

Next, we studied nodule primordium formation, by applying a compatible symbiont (*Bradyrhizobium elkanii* WUR3 for *Parasponia* and *Frankia alni* ACN14a for *Alnus*) on *in vitro* grown plants (see METHODS). At an early stage of nodule primordium formation, cell divisions occurred in the root cortex and pericycle of both species (Supplementary Figures 4A, 4B, 5A and 5B). In *Parasponia*, cell divisions were also induced in the epidermis (Supplementary Figure 4A). At subsequent stages, divisions continued in the cortex, and anticlinal divisions were induced in endodermis cells. In contrast to legume nodule primordium

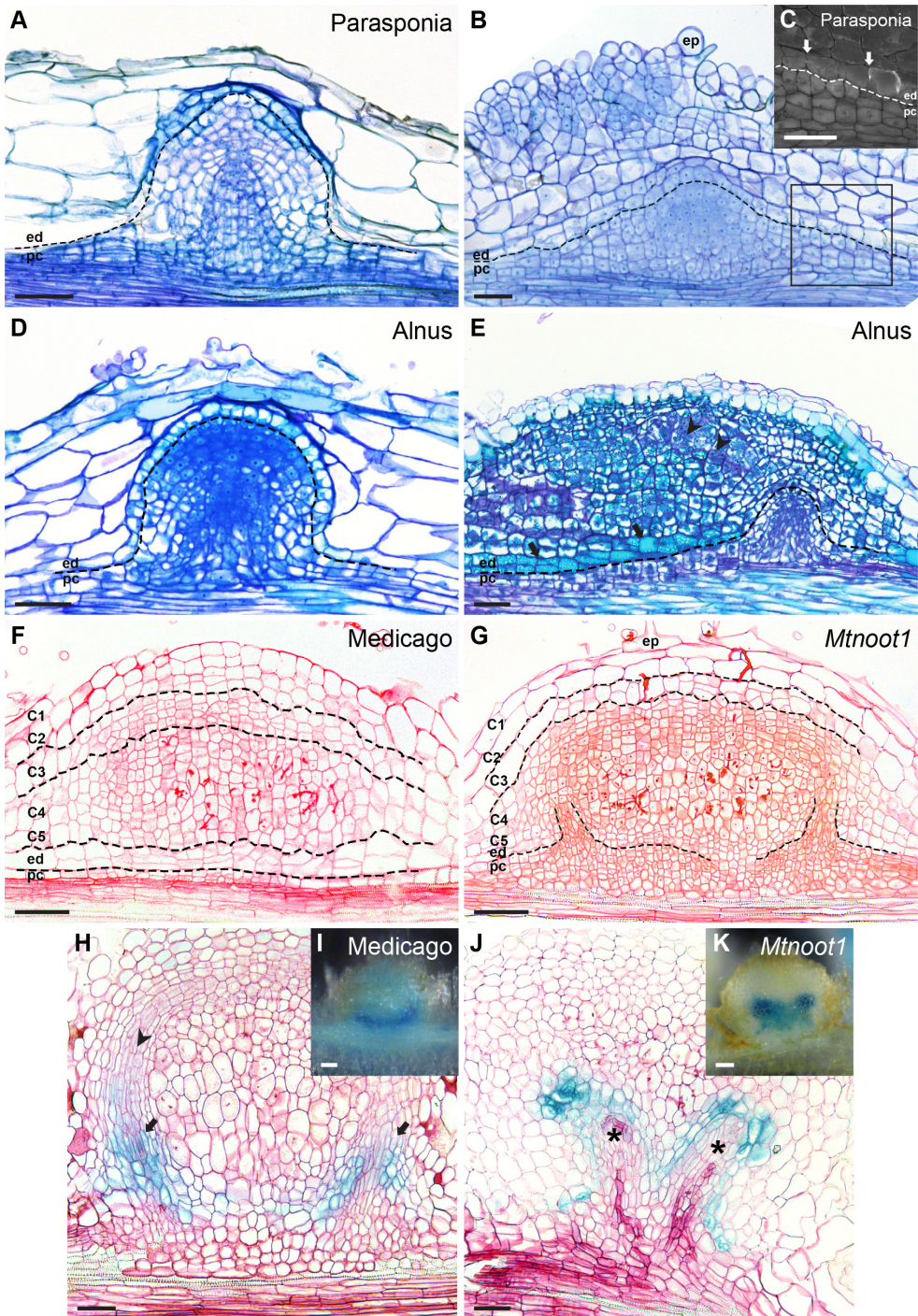


Figure 1. The Ontogeny of Actinorhizal-type Nodules Is Similar to that of *Medicago Mtnoot1* Mutant.

Lateral root primordium (**A, D**) and nodule primordium (**B, E**) of *Parasponia andersonii* (*Parasponia*) (**A, B**) and *Alnus glutinosa* (*Alnus*) (**D, E**).

(**A, D**) Pericycle- and endodermis-derived cells form the lateral root primordium in *Parasponia* (**A**) and *Alnus* (**D**). Endodermis-derived cells form the outermost layer of the lateral root primordium and later become part of the root cap/columella.

(**B, E**) Pericycle-derived cells form the nodule vasculature in *Parasponia* (**B**) and *Alnus* (**E**). (**B**) The root endodermis cells have divided anticlinally in *Parasponia* nodule primordia. At early stages they lose the Casparian strips (see also Supplementary Figure 4H) and these are reformed at the stage shown in (**B**). (**C**) UV light image of the endodermis region as indicated by the box in the section shown in (**B**). Casparian strips are reformed at the peripheral region of root endodermis-derived cells (arrows). (**E**) In *Alnus* nodule development, root endodermis-derived cells also lose the Casparian strips at the primordium stage (see also Supplementary Figure 5I); these cells display a light blue coloration when stained by toluidine blue (arrows). Cortex-derived cells are infected by bacteria (arrowheads) (see also Supplementary Figure 5F). Nodule primordium of *Medicago truncatula* (*Medicago*) wild-type (**F**), compared with similar developmental stage of *Mtnoot1* (**G**). Pericycle- and endodermis-derived cells stop dividing in the wild-type (**F**), but remain mitotically active in *Mtnoot1* where they have formed more cell layers consisting of markedly smaller cells (**G**). Dotted lines mark the border between different cell types. ep, epidermis; C1-C5, the five cortical cell layers; ed, endodermis; pc, pericycle.

Longitudinal sections of transgenic nodules (14 dpi) expressing *ProAtCASP1:GUS* in *Medicago* wild-type (**H, I**) and *Mtnoot1* (**J, K**). (**H, I**) In wild-type nodules, *ProAtCASP1:GUS* is mainly expressed in the newly formed endodermis cells of the nodule vascular bundles (arrows). These cells develop from root cortex-derived cells. Young developing vascular cells have an elongated shape (arrowhead). (**J, K**) In *Mtnoot1*, GUS activity occurs in the most distal cells of the developing nodule vascular bundles (*). These cells are derived from the root endodermis. At the proximal part of the nodule vasculature a new endodermis is formed in which *AtCASP1* is expressed. (**I, K**) are whole-mount views of the nodules of which sections are shown in (**H**) and (**J**), respectively. (**H-K**) are representative results from three independent experiments. Scale bar: 50 μ m (**A-H, J**), 100 μ m (**I, K**).

formation, in *Parasponia* and *Alnus* cell division in the pericycle persisted and led to the formation of a dome-shaped structure (Supplementary Figures 4F and 5D). At a subsequent stage, the pericycle-derived dome formed vascular tissue, and was flanked by cells derived from mitotically activated (parental) root endodermis cells. These cells had lost their Casparian strips and formed a new nodule vascular endodermis. In *Parasponia*, these latter nodule vascular endodermis cells regained identity at an early stage by forming new Casparian strips (Supplementary Figure 4I), whereas in *Alnus* such a nodule vascular endodermis was formed at a later stage of development (Supplementary Figure 6). So, in both species the nodular structure that was formed from the pericycle, was a vasculature flanked by a newly formed endodermis and not a modified lateral root (Figure 1B and 1E; Supplementary Figures 4F and 5E). This implies that the pericycle-derived nodular structure does not have a cortex, so it lacks cells that can be infected by bacteria. Cells that become infected by bacteria are derived from the dividing root cortical cells, which will form the infected tissue of the nodule (Figure 1B and 1E; Supplementary Figures 4F and 5E). At the apex of the pericycle-derived vasculature, endodermis-derived cells remained mitotically active (Supplementary Figures 4I and 5J). Together with dividing inner cortex- and pericycle-derived cells, they appeared to form a nodule meristem at the tip of the vasculature. The nodule meristem supported the growth of nodule vascular bundle and added cells to the cortex-derived infected cells (Supplementary Figures 4K and 5G).

Taken together, this shows that in *Parasponia* as well as *Alnus*, cells derived from the root cortex form the infected tissue and the prenodule becomes part of the mature nodule. The fact that mitotically activated root cortex cells form the infected tissue is similar to legume nodule formation. In contrast to legume-type nodules, where the nodule vasculature is formed by cortex-derived cells, in actinorhizal-type nodules of *Alnus* and *Parasponia* nodule vasculature is derived from pericycle cells. So, a key difference between legume and *Alnus*/*Parasponia* nodules is the origin of the vasculature: from the cortex in legumes, and from the pericycle in actinorhizal-type nodules.

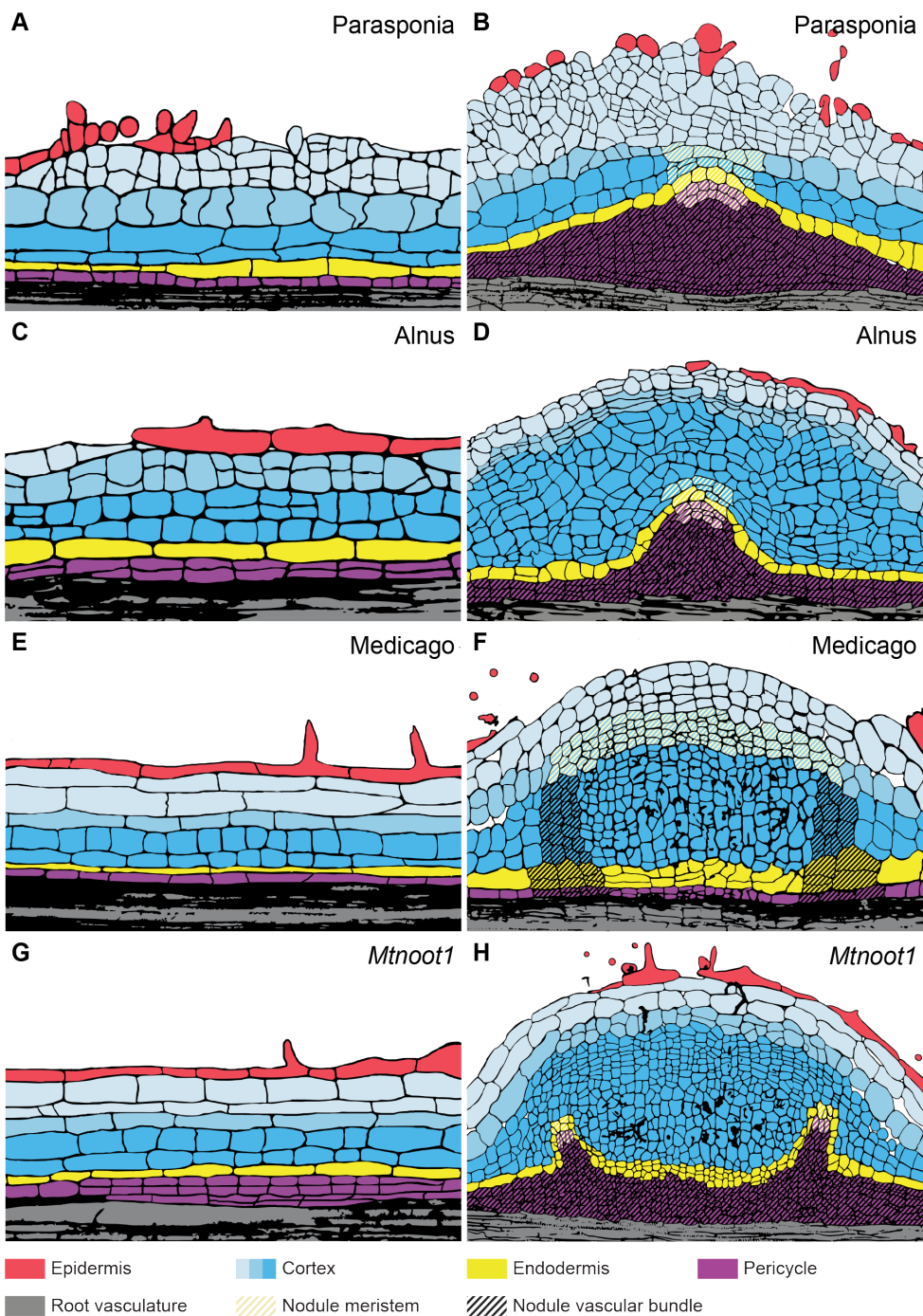
To see whether the nodule ontogeny as observed in *Alnus* and *Parasponia* also holds for nodules of other actinorhizal plant species, we carefully re-interpreted published data (Torrey, 1976; Callaham and Torrey, 1977; Torrey and Callaham, 1979; Newcomb and Pankhurst, 1982; Hafeez et al., 1984; Lancelle and Torrey, 1984; Miller and Baker, 1985; Lancelle and Torrey, 1985; Burgess and Peterson, 1987; Racette and Torrey, 1989; Liu and Berry, 1991; Valverde and

Wall, 1999; Berg et al., 1999; Fournier et al., 2018). In none of these studies the developmental fate of root endodermis cells was traced. Consequently, it could not be determined whether pericycle-derived cells solely contribute to the formation of nodule vasculature and do not form a cortical tissue that can be infected by the nitrogen-fixing microbe. Therefore, we conclude that none of the published studies provided direct support for the assumption that actinorhizal-type nodules are composed of “modified lateral roots”, which would mean the formation of a functional nodule exclusively from dividing pericycle cells.

In the order Fagales, besides *Alnus*, *Comptonia peregrina*, *Myrica gale* and *Casuarina cunninghamiana* have been studied and reported to form infected prenodules derived from root cortical cells (Torrey, 1976; Callaham and Torrey, 1977; Torrey and Callaham, 1979). This opens the possibility that the *Alnus*/Parasponia nodule ontogeny is a common trait in this order. In Rosales, in addition to Parasponia, cortical cell divisions were also observed in *Ceanothus arboreus*, however, infection of these cells was not reported (Liu and Berry, 1991). It has not been investigated whether in Cucurbitales species cell divisions are induced in root cortical cells (Newcomb and Pankhurst, 1982; Hafeez et al., 1984; Berg et al., 1999). Nevertheless, the occurrence of the *Alnus*/Parasponia nodule type in a wide range of Fagales species and in two Rosales species is most consistent with the idea that their common ancestor, so also the ancestor of Cucurbitales species, formed this actinorhizal nodule type. A common feature of actinorhizal-type nodule development is that pericycle-derived cells form the nodule vasculature (Figure 2B and 2D). This is a main difference with legume-type nodules where the nodule vasculature is derived from the root cortex (Figure 2F). As the nodule vasculature of actinorhizal-type nodules most probably has an identity that is closer to that of a lateral root, this might be the reason that the apical meristems of lobes of some actinorhizal-type nodules have the ability to spontaneously start forming roots at the apex of nodule lobes (Pawlowski and Bisseling, 1996; Franche et al., 2009).

Medicago *MtNOOT1* Functions as a Homeotic Gene Controlling Legume-type Nodule Ontogeny

The fact that actinorhizal-type and legume-type nodules share that their infected tissue is derived from mitotically activated root cortical cells suggests that they could have a common evolutionary origin. To study this, we first searched for a legume mutant having the ability to form roots at the apex of nodules. We



Continued on next page

selected a legume mutant in the *NOOT/NBCL* gene, which can form functional nodules and like some of the actinorhizal-type nodules can form a root at their apex (Couzigou et al. 2012; Magne et al. 2018a). To determine if in a *noot/nbcl* mutant nodule the vascular bundles have a similar ontogeny as observed in actinorhizal-type nodules, we studied nodule development in the Medicago *Mtnoot1* knockout mutant.

Mtnoot1 nodule primordia were compared with wild-type primordia of which inner cortical cells (C4 and C5) were at similar developmental stages. We first analysed *Mtnoot1* nodule primordia when C4 and C5 started to divide. In *Mtnoot1*, pericycle-derived cells formed two cell layers, compared with one layer in wild-type nodule primordia (Supplementary Figure 7A and 7B). In the *Mtnoot1* nodule primordia with approximately eight cell layers derived from C4 and C5, there were approximately 6-8 cell layers derived from endodermis and pericycle; whereas only 4-6 of such cell layers occurred in wild-type nodule primordia (Supplementary Figure 7C and 7D). At subsequent stages of *Mtnoot1* nodule primordium development, the difference became larger because in wild-type nodule primordia, pericycle- and endodermis-derived cells stopped dividing, whereas they remained mitotically active in the *Mtnoot1* mutant (Figure 1F and 1G; Supplementary Figure 7E and 7F).

In Medicago wild-type nodules, the vascular bundles are formed from primordium cells derived from the inner cortex, which grow by the activity of the nodule meristem (Xiao et al., 2014). To trace endodermis-derived cells at later stages of development, we introduced the *ProAtCASP1:GUS* reporter into *Mtnoot1* and wild-type roots by *Agrobacterium rhizogenes*-mediated transformation. *AtCASP1* is an *Arabidopsis thaliana* (Arabidopsis) gene that is specifically expressed in the root endodermis (Roppolo et al., 2011). The *ProAtCASP1:GUS* reporter is also specifically expressed in the Medicago root endodermis, and during nodule primordium formation it remains, for some time, expressed in endodermis-derived cells by which these can be traced (Xiao et al., 2014). In *Mtnoot1*, *ProAtCASP1:GUS* was expressed in 1-2 cell layers surrounding the

Continued

Figure 2. Actinorhizal-type Nodules and *Mtnoot1* Nodule Fate Maps. (A-H) Two nodule primordium stages of Parasponia (A, B), Alnus (C, D), Medicago wild-type (E, F), and *Mtnoot1* (G, H). (B, D, F, H) In all cases, cortex-derived cells are colonized by infection threads containing bacteria. These infected cells become part of the mature nodule. (B, D, H) The ontogeny of the nodule vascular bundle is similar in actinorhizal-type nodules (B, D) and in *Mtnoot1* (H).

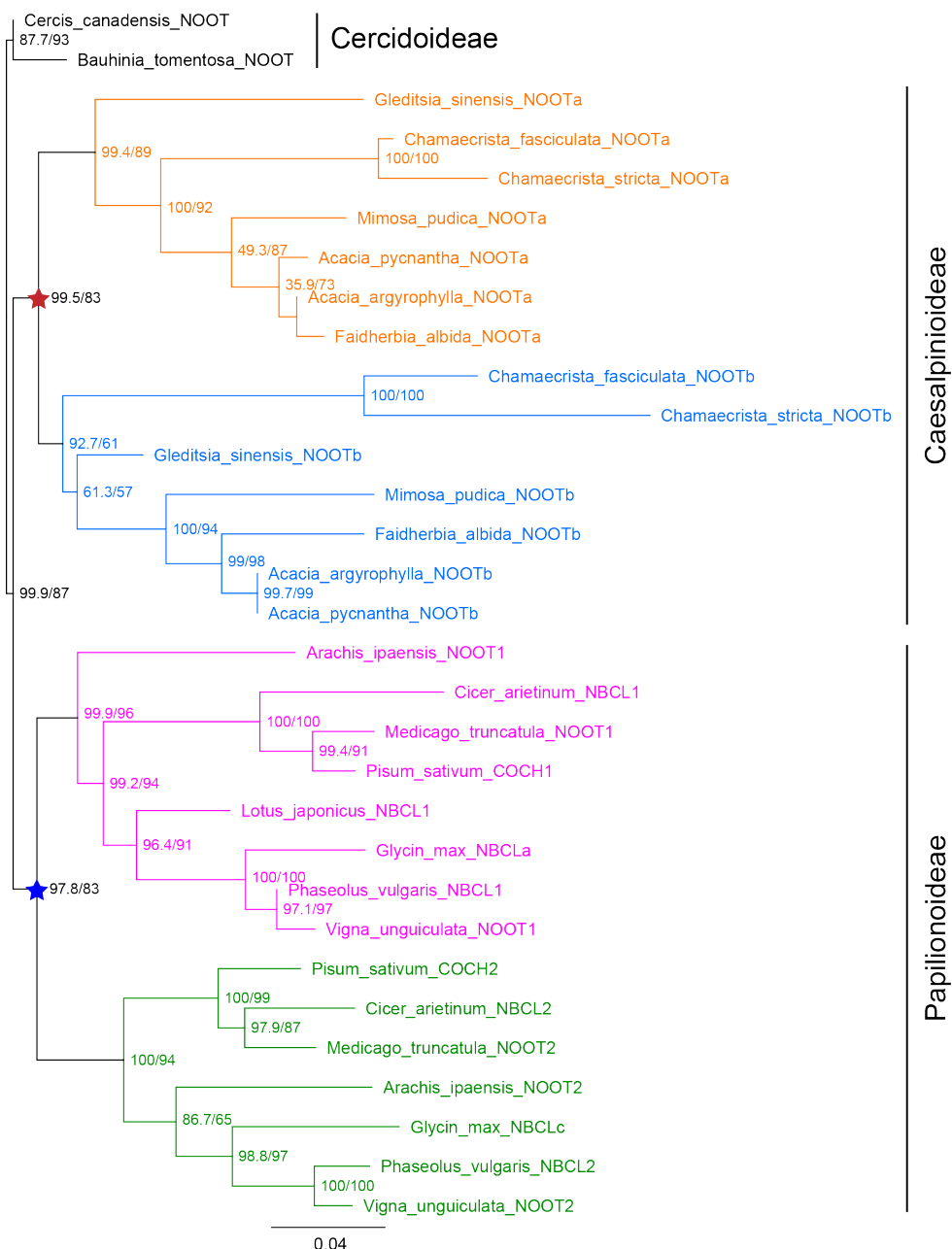


Figure 3. Maximum Likelihood Tree of Legume NOOT/NBCL Proteins. The NOOT/NBCL proteins are present in three legume subfamilies, of which Cercidoideae is the most basal one. The Cercidoideae of which sequence data are available, *Cercis canadensis* and *Bauhinia tomentosa*, do not form nodules and have a single NOOT/NBCL gene. Except *Lotus japonicus* and *Glycine max*, all other legumes (subfamilies Papilionoideae and Caesalpinioideae) of which sequence data are

Continued on next page

tip of the developing nodule vascular bundles (Figure 1J), implying that these cells were derived from the root endodermis and that the vascular bundles developed from pericycle-derived cells. Therefore, the ontogeny of the *Mtnoot1* nodule vasculature is different from that of wild-type and more similar to that of actinorhizal-type nodules. Mutations in the *MtNOOT1* orthologues of pea (*Pscoch1*) and *L. japonicus* (*Ljnbcl1*) can also cause root outgrowth from nodules (Couzigou et al. 2012; Magne et al. 2018a). Therefore, we assume that also in these legume mutants, the ontogeny of the nodule vasculature is actinorhizal-like. In actinorhizal-type nodules (e.g. *M. gale* and *Datisca glomerata*), which can form so-called nodule roots, the apical meristems of lobes have the potential to switch to root production (Pawlowski and Bisseling, 1996; Franche et al., 2009). Therefore, it seems probable that the potential of legume *noot1/nbcl1* mutant nodules to form nodule roots is caused by their similarity with actinorhizal-type nodules regarding vasculature ontogeny.

Legume *NOOT/NBCL* Experienced Ancestral Duplications in Two Legume Subfamilies

A loss of function in homeotic genes tends to lead to an ancestral phenotype (Garcia-Bellido, 1977; Wellmer et al., 2014). In line with this, we hypothesize that the actinorhizal-type nodules are ancestral, and that legume-type nodules evolved from these. Legume-specific neofunctionalization of *MtNOOT1*-*PsCOCH1*-*LjNBCL1* could have contributed to this switch. Therefore, we studied whether this hypothesis may find support in the evolutionary trajectory of this gene.

Continued

available have two *NOOT/NBCL* genes that group into four major clades, of which two clustered clades contain Papilionoideae *NOOT/NBCL* genes (indicated in pink and green) while the other two clustered clades contain Caesalpinioideae *NOOT/NBCL* genes (indicated in orange and blue). This suggests that the *NOOT/NBCL* gene was independently duplicated in the common ancestor of Papilionoideae (blue star) and in that of Caesalpinioideae (red star). Numbers at the nodes indicate Approximate Bayes support (%) / Ultrafast Bootstrap support (%). Ultrafast Bootstrap Approximation based on 5000 replicates. Protein sequences used in this analysis were summarised in Supplementary Table 1. For convenience, previously unnamed *NOOT/NBCL* proteins were all named as *NOOT* in this analysis. *Glycine max* *NBCLb* (Glyma19g131000.1) is a truncated protein, therefore, was not included. *C. canadensis* and *B. tomentosa* from Cercidoideae subfamily are the two most basal legumes in the analysis, therefore, *C. canadensis* *NOOT* and *B. tomentosa* *NOOT* were used as outgroup.

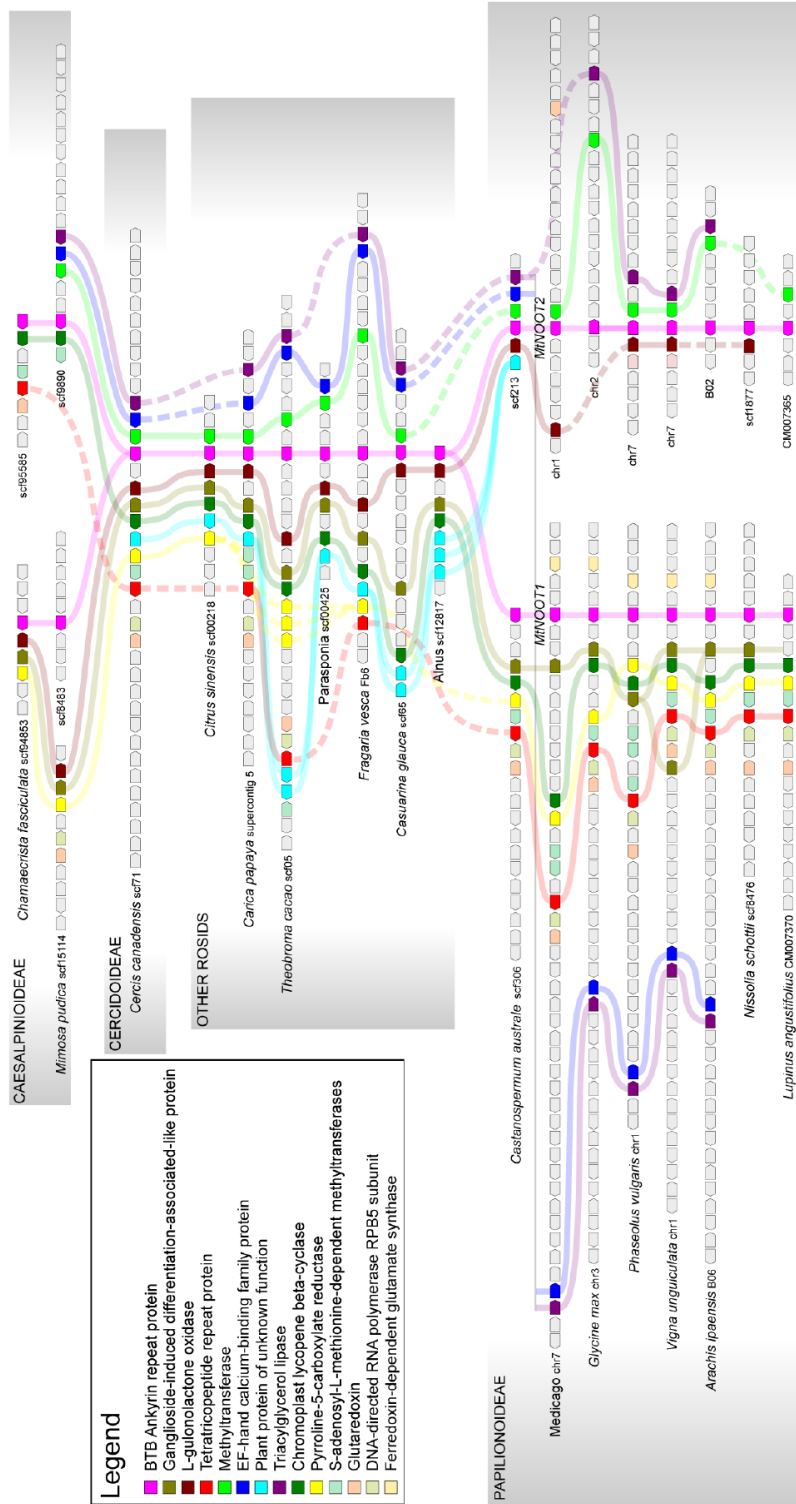


Figure 4. Independent Duplication of *NOOT/NBCL* Genomic Region in Legumes. *NOOT/NBCL* gene (pink block) is part of a block of microsynteny (different colored blocks) across rosids shown here, including *Citrus sinensis* (Sapindales), *Carica papaya* (Brassicales), *Theobroma cacao* (Malvales), *Parasponia* (Rosales), *Fragaria vesca* (Rosales), *Casuarina glauca* (Fagales, actinorhizal plant) and *Alnus* (Fagales). These species were selected because they have only a single *NOOT/NBCL* gene, which seems to represent the ancestral microsyntenic block of *NOOT/NBCL* genes. In the basal legume subfamily Cercidoideae, the microsyntenic block of the *Cercis canadensis* *NOOT/NBCL* gene is conserved as in the other rosids. In other legumes (subfamilies Papilionoideae and Caesalpinioideae), this entire block was duplicated, giving rise to *NOOT1/NBCL1* and *NOOT2/NBCL2* paralogs. In Papilionoideae (*Castanospermum australe*, Medicago, *Glycine max*, *Phaseolus vulgaris*, *Vigna unguiculata*, *Arachis ipaensis*, *Nissolia schottii*, *Lupinus angustifolius*), the gene context of *NOOT1/NBCL1* and *NOOT2/NBCL2* (including *C. australe*, a sister species to all other Papilionoideae species) shows similarity with that of rosids with one copy of *NOOT/NBCL* gene. However, the gene context of the two Papilionoideae *NOOT/NBCL* genes is clearly different. For example, the Methyltransferase (in light green), the L-gulonolactone oxidase (in dark red) and the Plant protein of unknown function (in cyan) are lost in all case around the gene locus of Papilionoideae *NOOT1/NBCL1*. Around the gene locus of Papilionoideae *NOOT2/NBCL2* the Ganglioside-induced differentiation-associated-like protein (in tan colour), the Chromoplast lycopene beta-cyclase (in green), and the Pyrroline-5-carboxylate reductase (in yellow) are absent. Most likely this is the result of independent loss of different surrounding genes after the duplication of the *NOOT/NBCL* genomic region in the common ancestor of Papilionoideae, after which the gene composition was maintained. The gene context of the two Caesalpinioideae (*Chamaecrista fasciculata* and *Mimosa pudica*) also shows similarity with that of rosids with a single *NOOT/NBCL* gene. However, the gene context of the two Caesalpinioideae *NOOT/NBCL* genes is different from that of Papilionoideae *NOOT/NBCL* genes; different genes were lost around the gene locus of the two Caesalpinioideae *NOOT/NBCL* genes. Together with the phylogenetic analysis, the microsynteny analysis suggests that the *NOOT/NBCL* genomic region was duplicated independently in the common ancestor of Papilionoideae and that of Caesalpinioideae. *Pisum sativum* *COCH1* (*PsCOCH1*), *PsCOCH2* and *Lotus japonicus* *NBCL1* (*LjNBCL1*) were not included in the microsynteny analysis, because the *P. sativum* genome is not yet well annotated and three loci of the *LjNBCL1* gene with identical nucleotide sequence are present in *L. japonicus* genome. Gene functions of colored blocks are indicated in the inserted legend.

Recently it was shown that species of the legume Papilionoideae subfamily generally have two *NOOT/NBCL* genes that group in two distinct subclades; NBCL1 and NBCL2 subclades (Magne et al. 2018b). *Medicago MtNOOT1*, pea *PsCOCH1* and *L. japonicus LjNBCL1* are orthologous and group in the NBCL1 subclade (Magne et al. 2018b). Mutant analysis in *Medicago* demonstrated that only *Mtnoot1* mutant nodules form nodule roots, whereas a mutation in the *Medicago MtNOOT2* gene, of the NBCL2 subclade, does not cause nodules with nodule roots (Magne et al. 2018b). Therefore, the NBCL1 subclade might have contributed to the evolution of the legume nodule type and its evolution might have been driven by an ancestral duplication in the *NOOT/NBCL* orthogroup. To study this, we analysed the phylogeny of *NOOT/NBCL* genes within three legume subfamilies, of which sequence data of some species are available. The subfamily Cercidoideae is sister to the two other subfamilies Papilionoideae and Caesalpinioideae (LPWG, 2017). The two species of Cercidoideae, *Cercis canadensis* and *Bauhinia tomentosa*, do not form nodules and have a single *NOOT/NBCL* gene. Almost all other legumes (subfamilies Papilionoideae and Caesalpinioideae) have two such genes that group into four major clades, of which two represent NBCL subclades of Papilionoideae species (e.g. *Medicago* and pea), while two other clades represent the *NOOT/NBCL* genes of Caesalpinioideae species (Figure 3). This suggests that independent ancestral duplications have occurred in the root of both legume subfamilies. To confirm this, we conducted a microsynteny analysis of legume *NOOT/NBCL* genes, and compared these with several other rosids species. We selected species with a single *NOOT/NBCL* gene because these could have a rather conserved microsyntenic block, whereas duplication tends to lead to loss of genes (Panchy et al., 2016). Indeed, the microsyntenic block surrounding the *NOOT/NBCL* locus across rosids with a single *NOOT/NBCL* gene, including *C. canadensis* of Cercidoideae subfamily, is conserved (Figure 4). The syntenic context of *NOOT/NBCL* genes of Papilionoideae species (including that from *Castanospermum australe*, a basal species in this subfamily) shows similarity with that of rosids with a single *NOOT/NBCL* gene. However, there are some clear differences between the syntenic context of the two Papilionoideae *NOOT/NBCL* genes (Figure 4). For example, the gene cluster around Papilionoideae *NOOT1/NBCL1* lacks in all cases the Methyltransferase (in light green), the L-gulonolactone oxidase (in dark red) and the Plant protein of unknown function (in cyan). In the Papilionoideae *NOOT2/NBCL2* cluster, other genes are missing in all species; namely, the Ganglioside-induced differentiation-associated-like protein (in tan color), the Chromoplast lycopene beta-cyclase (in green), and

the Pyrroline-5-carboxylate reductase (in yellow), etc. (Figure 4). This suggests that these genes were rapidly lost after the duplication of *NOOT/NBCL* region. Subsequently, small changes occurred by which the clusters become a little bit different. For example, the Triacylglycerol lipase (in purple) and the EF-hand calcium-binding family protein (in blue) were lost around the gene locus of some Papilionoideae *NOOT1/NBCL1* (e.g. *Lupinus angustifolius NOOT1/NBCL1*) (Figure 4). The syntenic context of the two *NOOT/NBCL* genes of Caesalpinioideae species shows a similar pattern of synteny and gene loss. However, their syntenic context is different from that of the Papilionoideae *NOOT/NBCL* regions (Figure 4). This, together with the phylogenetic analysis, led us to conclude that the ancestral duplication of *NOOT/NBCL* has occurred independently in two nodulating legume subfamilies; the Caesalpinioideae and Papilionoideae, respectively.

Medicago *MtNOOT1* Is Differentially Regulated in Nodule Pericycle Cells, Compared with *MtNOOT2* and Parasponia *PanNOOT1*

We have shown that in *Medicago MtNOOT1* is required to suppress cell division in pericycle-derived cells at an early stage of nodule primordium development, whereas such repression does not occur in species that make actinorhizal-type nodules. In line with this, we hypothesize that *MtNOOT1* obtained the ability to be expressed in the pericycle-derived cells in *Medicago* nodule primordia to suppress cell division, whereas in actinorhizal-type nodule primordia *NOOT/NBCL* is not expressed in the pericycle-derived cells during nodule formation. We studied the expression pattern of *NOOT* genes by *in situ* hybridization in *Medicago* and *Parasponia* nodule primordia, since no functional promoters (that can complement *Mtnoot1* phenotype) could be obtained for GUS reporter studies (tested up to 5 kb upstream region before the start codon of *MtNOOT1*). The hybridization probe sets contained ~20 adjacent oligonucleotide pairs of 20 nt long probes that hybridize to specific regions within the target mRNA (see METHODS). In *Medicago* nodule primordia, *MtNOOT1* and *MtNOOT2* were expressed in the nodule meristem and (young) infected cells. Further, *MtNOOT1* was expressed in the pericycle-derived cells, whereas *MtNOOT2* was not (Figure 5A-5D). *Parasponia PanNOOT1* transcripts were detected in the nodule meristem and infected cells of primordia, similar to *MtNOOT1* and *MtNOOT2*, but not in the dividing pericycle cells (Figure 5E). This suggests that in *Medicago* the *cis*-regulatory elements of *MtNOOT1* and *MtNOOT2* diverged and that *MtNOOT1* has (neo)functionalized to allow expression in the pericycle-

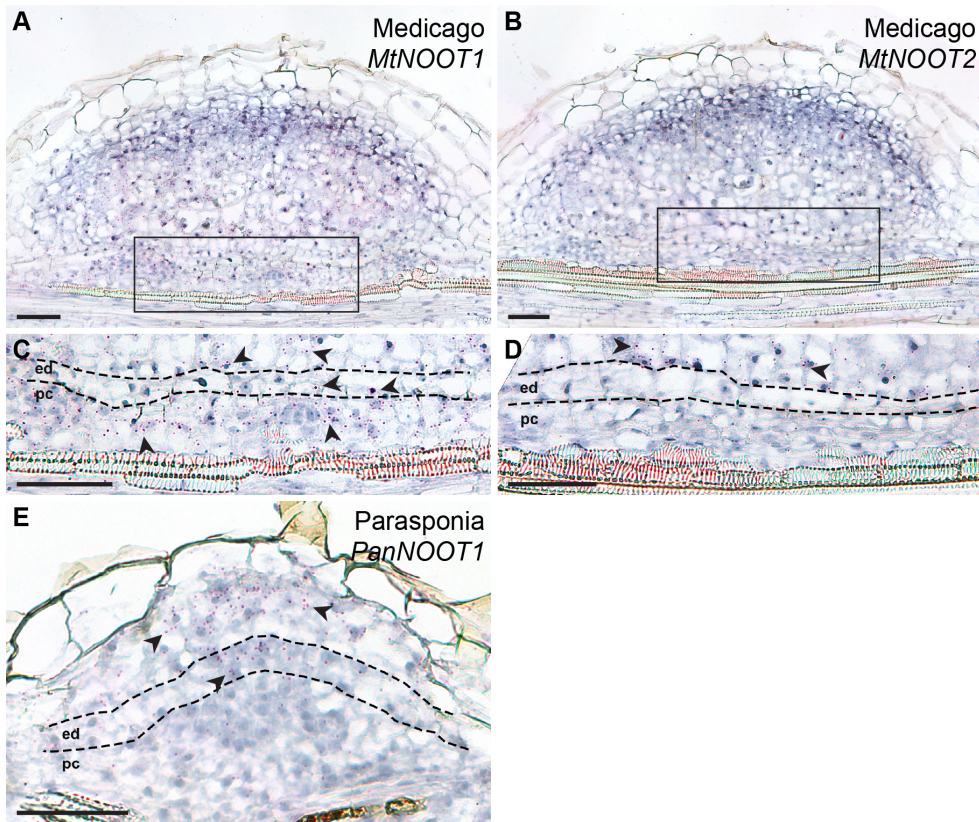


Figure 5. The Expression Patterns of *MtNOOT1*, *MtNOOT2* and *PanNOOT1* in Nodule Primordia. (A, C) *MtNOOT1* is expressed in the pericycle- and endodermis-derived cells in nodule primordia. *MtNOOT1* is also expressed in the developing nodule meristem and infected cells. (C) The boxed region in the section shown in (A). (B, D) *MtNOOT2* is expressed in the developing nodule meristem and infected cells, but not in the pericycle- or endodermis-derived cells in nodule primordia. (D) The boxed region in the section shown in (B). Note that sections shown in (A) and (B) are adjacent sections of a single *Medicago* nodule primordium. (E) *PanNOOT1* is expressed in the infected cells and developing nodule meristem, but not in the pericycle-derived cells in nodule primordia. Red dots represent mRNA transcripts, and some are indicated by arrowheads. Dotted line marks the border between different cell types. ed, endodermis; pc, pericycle. Scale bars: 50 μ m.

derived cells in nodule primordia. Such expression is essential to suppress the development of actinorhizal-type nodules in this legume species, suggesting that actinorhizal-type nodules are ancestral and legume-type legumes are derived.

DISCUSSION

Actinorhizal-type nodules have been described as modified lateral roots and originating from the root pericycle, like lateral roots (Pawlowski and Bisseling, 1996; Huss-Danell, 1997; Pawlowski and Demchenko, 2012; Svistoonoff et al., 2014; Ibáñez et al., 2017). However, we showed that during actinorhizal-type nodule formation the cells derived from the (parental) root cortex specifically form the tissue containing the intracellularly hosted nitrogen-fixing microsymbionts. This is very similar to legume nodule formation in which case the infected central tissue is also derived from mitotically activated root cortex cells (Xiao et al., 2014). This led us to conclude that the legume and actinorhizal-type nodule ontogeny is markedly more similar than previously proposed. Further, we show that legume-type nodules can be (partially) converted to actinorhizal-type nodules by knocking out a *NOOT/NBCL* gene, i.e. *MtNOOT1* in *Medicago*, suggesting that legume-type nodules could have evolved from actinorhizal-type nodules. This supports the hypothesis that nodulation evolved only once in a common ancestor of the NFC. Furthermore, our study provides circumstantial evidence that the actinorhizal nodule type is ancestral.

Nodule formation involves processes co-opted from the more ancient arbuscular mycorrhizal (AM) symbiosis. For example, in both legume and actinorhizal plants the signalling pathway that is essential for nodule formation is (in part) shared with that activated by AM fungi (reviewed in Markmann and Parniske, 2009; Oldroyd et al., 2011; Geurts et al., 2012). Further, in *Medicago* it has been shown that the same exocytosis pathway is used for the intracellular hosting of rhizobia as well as AM fungi (Ivanov et al., 2012). Here, we revealed an additional commonality, because in both nodule and AM symbiosis exclusively the root cortex (-derived tissue) is used to host the microsymbiont. A difference between these two symbioses is that bacterial infection involves mitotically activated cortical cells while AM fungi enter “existing” cortical cells. However, recently it was suggested that cell-division-related processes also occur in the cortical cells during the accommodation of AM fungi (Russo et al., 2019).

A major difference between legume-type and actinorhizal-type nodules is the ontogeny and position of the nodular vascular bundles (Figure 2). In actinorhizal-type nodules they are pericycle derived, whereas in legume-type nodules they are derived from cortical cells. Further, the vasculature has a central position in actinorhizal-type nodules, whereas they are located at the periphery of legume-type nodules. Loss-of-function mutation in *Medicago MtNOOT1* causes a switch from legume to actinorhizal-type ontogeny of the nodule vasculature (Figure 2).

Previously, we showed that nodule primordia formed by the *Medicago lin* (*lumpy infections*) mutant can form small vasculature derived from pericycle cells (Xiao et al., 2014). It has been shown that *MtLIN* gene encodes a predicted E3 ubiquitin ligase, required for infection thread formation. *Mtlin* mutants only form small nodule primordia with a very few cortex-derived cells (Kuppusamy et al., 2004; Kiss et al., 2009; Guan et al., 2013; Liu et al., 2019a). However, the number of cell layers derived from pericycle is higher than in wild-type primordia. So the formation of vasculature from pericycle cells correlates with increased mitotic activity in these cells, like in the *Mtnoot1* mutant. The *Mtnoot1* phenotype exhibits a stronger shift toward the actinorhizal-type nodules than *Mtlin* phenotype, as *Mtnoot1* mutant nodules are larger, contain fully infected cells and roots can grow out at their apex. The *Mtnoot1* mutation did not result in a central position of the vasculature. However, vasculatures can originate from a central position in the mutant but still “migrate” to the periphery of the nodule (Figure 1J). In actinorhizal-type nodules the vasculature obtains a position in between clusters of dividing cells. We hypothesize that the cortical cell divisions during legume nodule primordium formation are more organised by which only a single cluster of cells is formed and the vasculature can only obtain a peripheral position.

Medicago MtNOOT1, *MtNOOT2* and *Parasponia PanNOOT1* are orthologous to the Arabidopsis paralogous genes *BLADE-ON-PETIOLE1* (*AtBOP1*) and *AtBOP2*. These Arabidopsis genes are involved in the formation of boundaries between the shoot apical meristem and lateral organs by suppressing cell division (reviewed in Aida and Tasaka, 2006; Žádníková and Simon, 2014; Khan et al., 2014; Hepworth and Pautot, 2015; Wang et al., 2016). Knockout of *AtBOP1* and *AtBOP2* disrupts organ boundary patterning, causing loss of leave abscission, leafy petioles, fused inflorescence, etc. (Ha et al., 2003, 2004; Hepworth et al., 2005; McKim et al., 2008). The general function of *AtBOP1* and *AtBOP2* is to suppress cell division to form a boundary between two groups of cells with different fates (the shoot apical meristem vs. lateral organs). This is

consistent with the function of *MtNOOT1* in *Medicago* nodule primordia, where it suppresses the mitotic activity of the pericycle- and endodermis-derived cells. By this, a boundary is formed between the infected tissue and the root vasculature. In contrast to its paralog *MtNOOT2* and the single-copy ortholog *PanNOOT1*, *MtNOOT1* is expressed in the pericycle-derived cells of nodule primordia. This suggests that the *cis*-regulatory elements of *MtNOOT1* have neofunctionalized to allow expression of *MtNOOT1* in these cells, thereby suppressing the development of actinorhizal-type nodule vasculature.

We also showed that *NOOT/NBCL* genes duplicated most likely independently in the root of Papilionoideae subfamily and that of Caesalpinioideae subfamily. Papilionoideae as well as Caesalpinioideae species form legume-type nodules (Elliott et al., 2007; Santos et al., 2017). One of the most important outcomes of gene duplication is the origin of novel functions (Zhang, 2003). Therefore, the evolutionary trajectory of *NOOT/NBCL* in legumes suggests that such altered *cis*-regulatory elements of *MtNOOT1*, controlling expression in pericycle derived cells, could widely occur in legumes. The evolution of regulatory sequences is often the basis for the evolution of form (Carroll, 2005). Therefore, the proposed neofunctionalization of the *cis*-regulatory elements of legume *NOOT/NBCL* could represent a significant evolutionary step towards the evolution of the legume nodule type. Since the duplication of *NOOT/NBCL* in Papilionoideae could be independent from the one in Caesalpinioideae, it seems probable that the evolution of legume-type nodule is to some extent independent in Caesalpinioideae. To prove this, functional analysis of Caesalpinioideae *NOOT/NBCL* genes will be targeted in further research.

METHODS

Plant Materials and Growth Conditions

Parasponia andersonii line WU1-14 tissue culture plants were generated as previously described (Op den Camp et al., 2011). Plantlets were spot inoculated on the root tip region with *Bradyrhizobium elkanii* WUR3 (Op den Camp et al., 2012) after two weeks grown on EKM medium with low nitrate (0.02 mM NH_4NO_3) on plates (Becking, 1983). After inoculation the position of root tip was marked, only the root segments (about 0.5 cm) above the mark were sampled. Root segments were harvested 7, 10, 18 and 20 days post inoculation. Root segments containing lateral root primordia were harvested from plantlets of 2

weeks on EKM without inoculation.

Alnus glutinosa seeds were obtained from Svenska Skogsplanter AB (Lagan, Sweden). For surface sterilization, seeds were first washed with 0.2% SDS in a 2 mL Eppendorf tube for 10 minutes in a water sonicator, and then incubated with 70% ethanol for 5 minutes before proceeding with a concentrated H_2SO_4 treatment for 3 to 4 minutes. Then, *A. glutinosa* seeds were rinsed with sterile dd H_2O two times before sterilizing with 7% NaClO in 0.1% SDS for 30 minutes on a rotary shaker at 150 rpm at room temperature. At last, the seeds were washed five times with sterile dd H_2O . *A. glutinosa* seedlings were grown either on plates or in sand with 1/4 strength Hoagland's (Hoagland and Arnon, 1939). Seedlings on plates were spot inoculated on the root tip region with *Frankia alni* ACN14a (Goltzman et al., 2006) grown in BAP medium (Benoist et al., 1992). After inoculation the position of root tip was marked, and only the root segments (about 0.5 cm) above the mark were sampled. Root segments were harvested at 10, 12, and 21 days post inoculation. Seedlings in sand were inoculated with *Frankia alni* ACN14a grown in BAP medium and root segments were harvested at 17 and 28 days post inoculation. Root segments contain lateral root primordia were harvested from sand without inoculation.

Medicago truncatula *noot1* mutant line *tnk507* (Couzigou et al., 2012) and wild-type accession R108 plants were grown on BNM medium (supplemented with 1 mM amino ethoxyvinylglycine) to study *Medicago* nodule development. They were also used to generate *ProAtCASP1:GUS Agrobacterium rhizogenes* (strain MSU440) mediated transgenic roots as previously described (Xiao et al., 2014; Limpens et al., 2004). The *ProAtCASP1:GUS* construct is derived from (Roppolo et al., 2011). The *AtCASP1* promoter region is 1207 bp before the start codon of *AtCASP1* (AT2G36100). Transgenic GUS material was grown in perlite saturated with nitrogen-free Färhaeus solution. *Sinorhizobium meliloti* Rm41 (Szende and Ördögh, 1960) carrying a pHc60-GFP construct was used to induce *Medicago* nodule formation. The surface-sterilization and germination of *Medicago* seeds were performed as previously described (Limpens et al., 2004).

Microscopy and Imaging

Root segments and nodules were fixed at 4 °C overnight with 4% paraformaldehyde (w/v), 5% glutaraldehyde (v/v) in 0.05 M sodium phosphate buffer (pH 7.2). The fixed material was dehydrated in an ethanol series and subsequently embedded

in Technovit 7100 (Heraeus Kulzer) according to the manufacturer's protocol. Sections (7-12 µm) were made with a RJ2035 microtome (Leica Microsystems, Rijswijk, The Netherlands), stained 1.5 minutes in 0.05% toluidine blue O for lateral root and nodule development analysis, or 10 minutes in 0.1% ruthenium red for transgenic GUS material. Sections were analysed by using a DM5500B microscope equipped with a DFC425C camera (Leica Microsystems, Wetzlar, Germany). For observing Casparian strips, sections were analysed by using a SP8 confocal microscope (Leica, Germany) or a LSM 710 confocal laser scanning microscope (Zeiss, Germany).

Microsynteny Analysis

To assess microsyntenic context of *NOOT/NBCL* within rosids, we selected the following genomes from the legume family, irrespective of *NOOT/NBCL* copy number. From Cercidoideae: *Cercis canadensis* (doi:10.5524/101044); from Caesalpinioideae: *Chamaecrista fasciculata* (doi:10.5524/101045) and *Mimosa pudica* (doi:10.5524/101049); from Papilionoideae: *Castanospermum australe* (kindly provided by Henk Hilhorst), *Arachis ipaensis* (peanutbase.org), *Nissolia schottii* (doi:10.5524/101050), *Lupinus angustifolius* (ncbi: GCA_001865875.1), *Medicago truncatula*, *Glycine max*, *Phaseolus vulgaris* and *Vigna unguiculata*. We selected the following genomes from other rosids based on the fact that they contain a single putative *NOOT/NBCL* ortholog and therefore are likely to retain an ancestral microsyntenic pattern. From Malvids: *Theobroma cacao*, *Carica papaya* and *Citrus sinensis*; from Fabids: *Fragaria vesca*, *Alnus glutinosa* (doi:10.5524/101042), *Casuarina glauca* (doi:10.5524/101051) and *Parasponia andersonii* (parasponia.org). Genomes were downloaded from Phytozome v12 except when indicated otherwise. Putative orthologous genes were identified based on phylogenetic analysis of aligned predicted proteins, using MAFFT v7.388 (Katoh, 2002) with default parameter settings (Auto algorithm; Scoring matrix: BLOSUM62; Gap opening penalty: 1.53; Offset value: 0.123), and FastTree 2.1.5 (Price et al., 2010) with default parameter settings (Rates categories of sites: 20), implemented in Geneious R8 (Biomatters, Auckland, New Zealand).

Phylogenetic Analysis

The information of the protein sequences used for phylogenetic analysis were summarized in Supplementary Table 1. For phylogenetic analysis, full length

or partial (predicted) protein sequences were aligned by using MAFFT v7.429 (<https://mafft.cbrc.jp/alignment/server/>) (Katoh, 2002; Katoh et al., 2017), with default parameter settings (Auto algorithm; Scoring matrix: BLOSUM62; Gap opening penalty: 1.53; Offset value: 0). The alignment was curated by using trimAl v1.4.1 (<https://ngphylogeny.fr/tools/tool/284/form>) (Capella-Gutiérrez et al., 2009), with default parameter settings (Gap threshold: automatic; Similarity threshold: automatic; Consistency threshold: automatic) (Supplementary File). Curated alignment was used for tree building by using W-IQ-TREE (Trifinopoulos et al., 2016) with best-fit substitution model (Kalyaanamoorthy et al., 2017). Branch support analysis was performed by using Ultrafast Bootstrap Approximation based on 5000 replicates (Minh et al., 2013) and Approximate Bayes Test (Anisimova et al., 2011). The tree was rooted on *Cercis canadensis* NOOT and *Bauhinia tomentosa* NOOT, as *C. canadensis* and *B. tomentosa* are the two most basal legume species in the analysis.

***In situ* Hybridization**

For sample preparation, *M. truncatula* R108 plants were grown as abovementioned, nodule primordia were collected at 5 days post inoculation; *P. andersonii* tissue culture plants were grown for 10 days in perlet with EKM solution, inoculated with *Mesorhizobium plurifarum* BOR2 as previously described (van Zeijl 2018). Hybridization were performed by using Invitrogen ViewRNA ISH Tissue 1-Plex Assay kits (Thermo Fisher Scientific), as previously described (Liu et al., 2019b). For user manual, visit https://assets.thermofisher.com/TFS-Assets/LSG/manuals/MAN0018633_viewRNA_ISH_UG.pdf. Modifications: section thickness is 6 µm; silane-prep slides (Sigma-Aldrich) were used to increase the adhesion of the sections with the slides. The probe sets for *MtNOOT1* (catalogue number: VF1-16434), *MtNOOT2* (catalogue number: VF1-6001055) and *PanNOOT1* (catalogue number: VF1-6000669) were designed and synthesized by request at Thermo Fisher Scientific. *MtNOOT1* probe sets cover the region 2-913 nt of the coding sequence (1449 nt, Medtr7g090020.1); *MtNOOT2* probe sets cover the region 1024-2221 nt of the full-length mRNA (2537 nt, XM_013611955); *PanNOOT1* probe sets cover the region 281-1146 nt of the coding sequence (1512 nt, PanWU01x14_292800.1). A typical probe set contains ~20 oligonucleotide pairs of probes that hybridize to specific regions across the target mRNA. Each probe covers 20 nucleotides (nt), only a pair of two adjacent probes, which targets 40 nt long sequence, can form a site for signal amplification. By this principle, background is reduced, control probes are

not needed. Sections were imaged as abovementioned.

Accession Numbers

Sequence data from this article are listed in Supplementary Table 1.

Supplementary Data

Supplementary Figure 1. Nitrogen-fixing clade.

Supplementary Figure 2. *Parasponia* lateral root developmental stages.

Supplementary Figure 3. *Alnus* lateral root developmental stages.

Supplementary Figure 4. *Parasponia* root nodule developmental stages.

Supplementary Figure 5. *Alnus* root nodule developmental stages.

Supplementary Figure 6. The Casparian strips of *Alnus* nodule vascular endodermis cells are formed at a later stage of development.

Supplementary Figure 7. Pericycle- and endodermis-derived cells in *Mtnoot1* nodule primordia remain mitotically active.

Supplementary Table 1. Protein sequences used in the phylogenetic analysis.

Supplementary File 1. Curated alignment of legume NOOT/NBCL protein sequences.

ACKNOWLEDGMENTS

We thank Pascal Ratet for providing *Mtnoot1* seeds, and Niko Geldner for providing the *AtCASP1* promoter GUS fusion vector. We also thank Henk Hilhorst for providing the access to the unpublished genome of *Castanospermum australe*, and Wouter Kohlen for the access to the unpublished transcriptome of *Chamaecrista stricta*.

AUTHOR CONTRIBUTIONS

TB conceived the project. TB and KP designed the experiments. DS and TTX performed most of the experiments with help from XG. RvV performed the microsynteny analysis. OK and DS performed *in situ* hybridization. DS and TB wrote the manuscript with input from RvV, RG and KP.

REFERENCES

- Aida, M. and Tasaka, M.** (2006). Genetic control of shoot organ boundaries. *Curr. Opin. Plant Biol.* **9**: 72–77.
- Anisimova, M., Gil, M., Dufayard, J.-F., Dessimoz, C., and Gascuel, O.** (2011). Survey of Branch Support Methods Demonstrates Accuracy, Power, and Robustness of Fast Likelihood-based Approximation Schemes. *Syst. Biol.* **60**: 685–699.
- Becking, J.H.** (1983). The *Parasponia parviflora*-Rhizobium symbiosis. Host specificity, growth and nitrogen fixation under various conditions. *Plant Soil* **75**: 309–342.
- Benoist, P., Muller, A., Hoang Gia Diem, and Schwencke, J.** (1992). High-molecular-mass multicatalytic proteinase complexes produced by the nitrogen-fixing actinomycete *Frankia* strain BR. *J. Bacteriol.* **174**: 1495–1504.
- Berg, R.H., Langenstein, B., and Silvester, W.B.** (1999). Development in the *Datisca-Coriaria* nodule type. *Can. J. Bot.* **77**: 1334–1350.
- Bonnett, H.T.** (1969). Cortical cell death during lateral root formation. *J. Cell Biol.* **40**: 144–159.
- Burgess, D. and Peterson, R.L.** (1987). Development of *Alnus japonica* root nodules after inoculation with *Frankia* strain HFPA13. *Can. J. Bot.* **65**: 1647–1657.
- Callaham, D. and Torrey, J.G.** (1977). Prenodule formation and primary nodule development in roots of *Comptonia* (Myricaceae). *Can. J. Bot.* **55**: 2306–2318.
- Capella-Gutiérrez, S., Silla-Martínez, J.M., and Gabaldón, T.** (2009). trimAl: A tool for automated alignment trimming in large-scale phylogenetic analyses. *Bioinformatics* **25**: 1972–1973.
- Carroll, S.B.** (2000). Endless forms: The evolution of gene regulation and morphological diversity. *Cell* **101**: 577–580.
- Carroll, S.B.** (2005). Evolution at Two Levels: On Genes and Form. *PLoS Biol.* **3**: e245.
- Casero, P.J., Casimiro, I., and Lloret, P.G.** (1996). Pericycle proliferation pattern during the lateral root initiation in adventitious roots of *Allium cepa*. *Protoplasma* **191**: 136–147.
- Chang, Y. et al.** (2019). The draft genomes of five agriculturally important African orphan crops. *Gigascience* **8**.
- Couzigou, J.-M.J. et al.** (2012). *NODULE ROOT* and *COCHLEATA* Maintain Nodule Development and Are Legume Orthologs of *Arabidopsis* *BLADE-ON-*

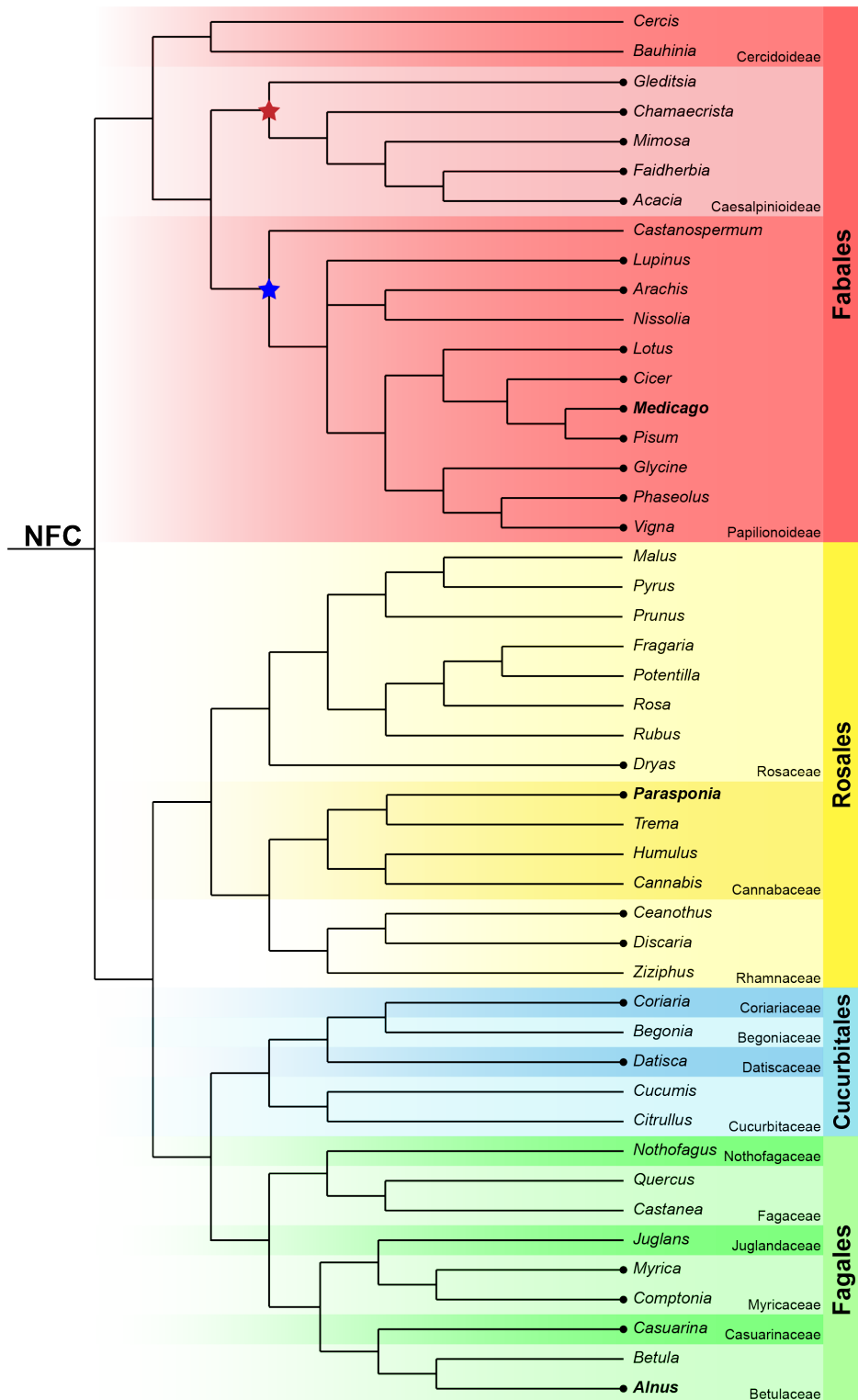
- PETIOLE* Genes. *Plant Cell* **24**: 4498–4510.
- Ditta, G., Pinyopich, A., Robles, P., Pelaz, S., and Yanofsky, M.F.** (2004). The *SEP4* Gene of *Arabidopsis thaliana* Functions in Floral Organ and Meristem Identity. *Curr. Biol.* **14**: 1935–1940.
- Doyle, J.J.** (2011). Phylogenetic Perspectives on the Origins of Nodulation. *Mol. Plant-Microbe Interact.* **24**: 1289–1295.
- Elliott, G.N. et al.** (2007). *Burkholderia phymatum* is a highly effective nitrogen-fixing symbiont of *Mimosa* spp. and fixes nitrogen *ex planta*. *New Phytol.* **173**: 168–180.
- Fournier, J. et al.** (2018). Cell remodeling and subtilase gene expression in the actinorhizal plant *Discaria trinervis* highlight host orchestration of intercellular *Frankia* colonization. *New Phytol.* **219**: 1018–1030.
- Franche, C., Lindström, K., and Elmerich, C.** (2009). Nitrogen-fixing bacteria associated with leguminous and non-leguminous plants. *Plant Soil* **321**: 35–59.
- Garcia-Bellido, A.** (1977). Homoeotic and atavistic mutations in insects. *Am. Zool.* **17**: 613–629.
- Geurts, R., Lillo, A., and Bisseling, T.** (2012). Exploiting an ancient signalling machinery to enjoy a nitrogen fixing symbiosis. *Curr. Opin. Plant Biol.* **15**: 438–443.
- Goltsman, E. et al.** (2006). Genome characteristics of facultatively symbiotic *Frankia* sp. strains reflect host range and host plant biogeography. *Genome Res.* **17**: 7–15.
- Griesmann, M. et al.** (2018). Phylogenomics reveals multiple losses of nitrogen-fixing root nodule symbiosis. *Science* **361**: eaat1743.
- Guan, D. et al.** (2013). Rhizobial Infection Is Associated with the Development of Peripheral Vasculature in Nodules of *Medicago truncatula*. *Plant Physiol.* **162**: 107–115.
- Ha, C.M., Jun, J.H., Nam, H.G., and Fletcher, J.C.** (2004). *BLADE-ON-PETIOLE1* Encodes a BTB/POZ Domain Protein Required for Leaf Morphogenesis in *Arabidopsis thaliana*. *Plant Cell Physiol.* **45**: 1361–1370.
- Ha, C.M., Kim, G.-T., Kim, B.C., Jun, J.H., Soh, M.S., Ueno, Y., Machida, Y., Tsukaya, H., and Nam, H.G.** (2003). The *BLADE-ON-PETIOLE 1* gene controls leaf pattern formation through the modulation of meristematic activity in *Arabidopsis*. *Development* **130**: 161–72.
- Hafeez, F., Akkermans, A.D.L., and Chaudhary, A.H.** (1984). Observations on the ultrastructure of *Frankia* sp. in root nodules of *Datisca cannabina* L. *Plant Soil* **79**: 383–402.
- Hepworth, S.R. and Pautot, V.A.** (2015). Beyond the Divide: Boundaries for Patterning and Stem Cell Regulation in Plants. *Front. Plant Sci.* **6**: 1052.
- Hepworth, S.R., Zhang, Y., McKim, S., Li, X., and Haughn, G.W.** (2005). *BLADE-ON-PETIOLE*-dependent signaling controls leaf and floral patterning in *Arabidopsis*. *Plant Cell* **17**: 1434–48.
- Hoagland, D.R. and Arnon, D.I.** (1939). The water-culture method for growing plants without soil. *Calif. Agric. Exp. Stn. Circ.* **347**: 1–32.
- Huss-Danell, K.** (1997). Actinorhizal symbioses and their N₂ fixation. *New Phytol.* **136**: 375–405.
- Ibáñez, F., Wall, L., and Fabra, A.** (2017). Starting points in plant-bacteria nitrogen-

- fixing symbioses: Intercellular invasion of the roots. *J. Exp. Bot.* **68**: 1905–1918.
- Imanishi, L., Perrine-Walker, F.M., Ndour, A., Vayssières, A., Conejero, G., Lucas, M., Champion, A., Laplaze, L., Wall, L., and Svistoonoff, S.** (2014). Role of auxin during intercellular infection of *Discaria trinervis* by *Frankia*. *Front. Plant Sci.* **5**: 1–9.
- Ivanov, S., Fedorova, E.E., Limpens, E., De Mita, S., Genre, A., Bonfante, P., and Bisseling, T.** (2012). *Rhizobium*-legume symbiosis shares an exocytotic pathway required for arbuscule formation. *Proc. Natl. Acad. Sci.* **109**: 8316–8321.
- Kalyaanamoorthy, S., Minh, B.Q., Wong, T.K.F., Von Haeseler, A., and Jermini, L.S.** (2017). ModelFinder: Fast model selection for accurate phylogenetic estimates. *Nat. Methods* **14**: 587–589.
- Katoh, K.** (2002). MAFFT: a novel method for rapid multiple sequence alignment based on fast Fourier transform. *Nucleic Acids Res.* **30**: 3059–3066.
- Katoh, K., Rozewicki, J., and Yamada, K.D.** (2017). MAFFT online service: multiple sequence alignment, interactive sequence choice and visualization. *Brief. Bioinform.* **bbx108**.
- Khan, M., Xu, H., and Hepworth, S.R.** (2014). BLADE-ON-PETIOLE genes: Setting boundaries in development and defense. *Plant Sci.* **215–216**: 157–171.
- Kiss, E., Olah, B., Kalo, P., Morales, M., Heckmann, A.B., Borbola, A., Lozsa, A., Kontar, K., Middleton, P., Downie, J.A., Oldroyd, G.E.D., and Endre, G.** (2009). LIN, a Novel Type of U-Box/WD40 Protein, Controls Early Infection by Rhizobia in Legumes. *Plant Physiol.* **151**: 1239–1249.
- Kuppusamy, K.T., Endre, G., Prabhu, R., Penmetsa, R.V., Veereshlingam, H., Cook, D.R., Dickstein, R., and Vandenbosch, K.A.** (2004). *LIN*, a *Medicago truncatula* gene required for nodule differentiation and persistence of rhizobial infections. *Plant Physiol.* **136**: 3682–91.
- Lancelle, S.A. and Torrey, J.G.** (1984). Early Development of *Rhizobium*-Induced Root-Nodules of *Parasponia rigida*. I. Infection and Early Nodule Initiation. *Protoplasma* **123**: 26–37.
- Lancelle, S.A. and Torrey, J.G.** (1985). Early development of *Rhizobium*-induced root nodules of *Parasponia rigida*. II. Nodule morphogenesis and symbiotic development. *Can. J. Bot.* **63**: 25–35.
- Lewis, E.B.** (1963). Genes and Developmental Pathways. *Am. Zoology* **3**: 33–56.
- Limpens, E., Ramos, J., Franken, C., Raz, V., Compaan, B., Franssen, H., Bisseling, T., and Geurts, R.** (2004). RNA interference in *Agrobacterium rhizogenes*-transformed roots of *Arabidopsis* and *Medicago truncatula*. *J. Exp. Bot.* **55**: 983–992.
- Liu, C.-W. et al.** (2019a). A protein complex required for polar growth of rhizobial infection threads. *Nat. Commun.* **10**: 2848.
- Liu, J., Rutten, L., Limpens, E., van der Molen, T., van Velzen, R., Chen, R., Chen, Y., Geurts, R., Kohlen, W., Kulikova, O., and Bisseling, T.** (2019b). A Remote *cis*-Regulatory Region Is Required for *NIN* Expression in the Pericycle to Initiate Nodule Primordium Formation in *Medicago truncatula*. *Plant Cell* **31**: 68–83.
- Liu, Q.Q. and Berry, A.M.** (1991). The infection process and nodule initiation in the *Frankia-Ceanothus* root nodule symbiosis - A structural and histochemical

- study. *Protoplasma* **163**: 82–92.
- Lloret, P.G., Casero, P.J., Pulgarini, A., and Navascues, J.** (1989). The Behaviour of Two Cell Populations in the Pericycle of *Allium cepa*, *Pisum sativum*, and *Daucus carota* During Early Lateral Root Development. *Ann. Bot.* **63**: 465–475.
- LPWG** (2017). A new subfamily classification of the Leguminosae based on a taxonomically comprehensive phylogeny. *Taxon* **66**: 44–77.
- Magne, K. et al.** (2018a). MtNODULE ROOT1 and MtNODULE ROOT2 Are Essential for Indeterminate Nodule Identity. *Plant Physiol.* **178**: 295–316.
- Magne, K., George, J., Berbel Tornero, A., Broquet, B., Madueño, F., Andersen, S.U., and Ratet, P.** (2018b). *Lotus japonicus* NOOT-BOP-COCH-LIKE1 is essential for nodule, nectary, leaf and flower development. *Plant J.* **94**: 880–894.
- Markmann, K. and Parniske, M.** (2009). Evolution of root endosymbiosis with bacteria: how novel are nodules? *Trends Plant Sci.* **14**: 77–86.
- McKim, S.M., Stenvik, G.-E., Butenko, M.A., Kristiansen, W., Cho, S.K., Hepworth, S.R., Aalen, R.B., and Haughn, G.W.** (2008). The *BLADE-ON-PETIOLE* genes are essential for abscission zone formation in *Arabidopsis*. *Development* **135**: 1537–1546.
- Miller, I.M. and Baker, D.D.** (1985). The initiation, development and structure of root nodules in *Elaeagnus angustifolia* L. (*Elaeagnaceae*). *Protoplasma* **128**: 107–119.
- Minh, B.Q., Nguyen, M.A.T., and Von Haeseler, A.** (2013). Ultrafast approximation for phylogenetic bootstrap. *Mol. Biol. Evol.* **30**: 1188–1195.
- Newcomb, W. and Pankhurst, C.E.** (1982). Fine structure of actinorhizal root nodules of *Coriaria arborea* (Coriariaceae). *New Zeal. J. Bot.* **20**: 93–103.
- Oldroyd, G.E.D., Murray, J.D., Poole, P.S., and Downie, J.A.** (2011). The rules of engagement in the legume-rhizobial symbiosis. *Annu. Rev. Genet.* **45**: 119–44.
- Op den Camp, R., Streng, A., De Mita, S., Cao, Q., Polone, E., Liu, W., Ammiraju, J.S.S., Kudrna, D., Wing, R., Untergasser, A., Bisseling, T., and Geurts, R.** (2011). LysM-type mycorrhizal receptor recruited for rhizobium symbiosis in nonlegume *Parasponia*. *Science* **331**: 909–912.
- Op den Camp, R.H.M., Polone, E., Fedorova, E., Roelofsen, W., Squartini, A., Op den Camp, H.J.M., Bisseling, T., and Geurts, R.** (2012). Nonlegume *Parasponia andersonii* Deploys a Broad Rhizobium Host Range Strategy Resulting in Largely Variable Symbiotic Effectiveness. *Mol. Plant-Microbe Interact.* **25**: 954–963.
- Panchy, N., Lehti-Shiu, M.D., and Shiu, S.-H.** (2016). Evolution of gene duplication in plants. *Plant Physiol.* **171**: pp.00523.2016.
- Parniske, M.** (2018). Uptake of bacteria into living plant cells, the unifying and distinct feature of the nitrogen-fixing root nodule symbiosis. *Curr. Opin. Plant Biol.* **44**: 164–174.
- Pawlowski, K. and Bisseling, T.** (1996). Rhizobial and Actinorhizal Symbioses: What Are the Shared Features? *Plant Cell* **8**: 1899–1913.
- Pawlowski, K. and Demchenko, K.N.** (2012). The diversity of actinorhizal symbiosis. *Protoplasma* **249**: 967–979.
- Price, M.N., Dehal, P.S., and Arkin, A.P.** (2010). FastTree 2 - Approximately maximum-likelihood trees for large alignments. *PLoS One* **5**: e9490.

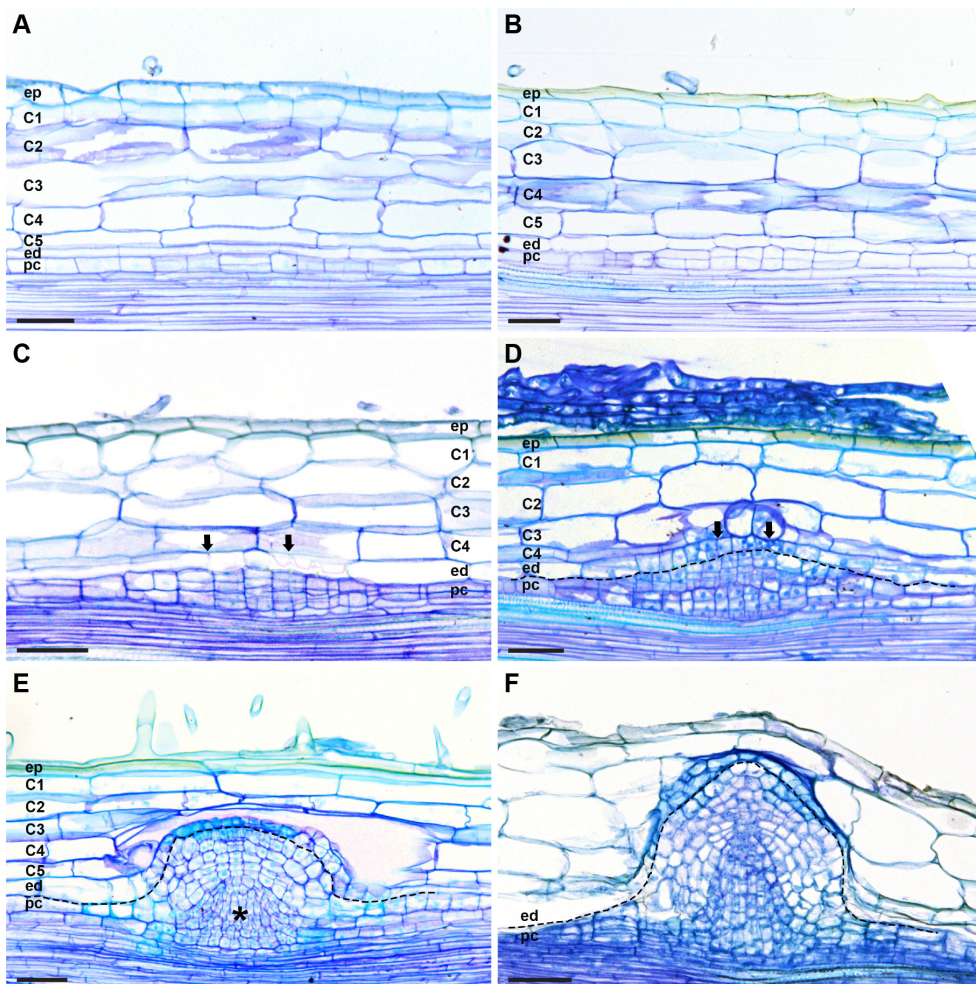
- Racette, S. and Torrey, J.G.** (1989). Root nodule initiation in *Gymnostoma* (Casuarinaceae) and *Shepherdia* (Elaeagnaceae) induced by *Frankia* strain HFPGp11. *Can. J. Bot.* **67**: 2873–2879.
- Roppolo, D., De Rybel, B., Tendon, V.D., Pfister, A., Alassimone, J., Vermeer, J.E.M., Yamazaki, M., Stierhof, Y.-D., Beeckman, T., and Geldner, N.** (2011). A novel protein family mediates Casparian strip formation in the endodermis. *Nature* **473**: 380–383.
- Russo, G., Carotenuto, G., Fiorilli, V., Volpe, V., Chiapello, M., Van Damme, D., and Genre, A.** (2019). Ectopic activation of cortical cell division during the accommodation of arbuscular mycorrhizal fungi. *New Phytol.* **221**: 1036–1048.
- Santi, C., Bogusz, D., and Franche, C.** (2013). Biological nitrogen fixation in non-legume plants. *Ann. Bot.* **111**: 743–67.
- Santos, J.M.F. dos, Casaes Alves, P.A., Silva, V.C., Kruschewsky Rhem, M.F., James, E.K., and Gross, E.** (2017). Diverse genotypes of *Bradyrhizobium* nodulate herbaceous *Chamaecrista* (Moench) (Fabaceae, Caesalpinioideae) species in Brazil. *Syst. Appl. Microbiol.* **40**: 69–79.
- Shubin, N., Tabin, C., and Carroll, S.** (2009). Deep homology and the origins of evolutionary novelty. *Nature* **457**: 818–823.
- Soltis, D.E., Soltis, P.S., Morgan, D.R., Swensen, S.M., Mullin, B.C., Dowd, J.M., and Martin, P.G.** (1995). Chloroplast gene sequence data suggest a single origin of the predisposition for symbiotic nitrogen fixation in angiosperms. *Proc. Natl. Acad. Sci. U. S. A.* **92**: 2647–2651.
- Sprent, J.I., Sutherland, J.M., de Faria, S.M., Dilworth, M.J., Corby, H.D.L., Becking, J.H., Materon, L.A., and Drozd, J.W.** (1987). Some Aspects of the Biology of Nitrogen-Fixing Organisms [and Discussion]. *Philos. Trans. R. Soc. B Biol. Sci.* **317**: 111–129.
- Swistonoff, S., Hoher, V., and Gherbi, H.** (2014). Actinorhizal root nodule symbioses: What is signalling telling on the origins of nodulation? *Curr. Opin. Plant Biol.* **20**: 11–18.
- Szende, K. and Ördögh, F.** (1960). Die Lysogenie von *Rhizobium meliloti*. *Naturwissenschaften* **47**: 404–405.
- Tedersoo, L., Laanisto, L., Rahimlou, S., Toussaint, A., Hallikma, T., and Pärtel, M.** (2018). Global database of plants with root-symbiotic nitrogen fixation: NodDB. *J. Veg. Sci.* **29**: 560–568.
- Torrey, J.G.** (1976). Initiation and development of root nodules of Casuarina (Casuarinaceae). *Am. J. Bot.* **63**: 335–344.
- Torrey, J.G. and Callaham, D.** (1979). Early nodule development in *Myrica gale*. *Bot. Gaz.* **140**: S10–S14.
- Trifinopoulos, J., Nguyen, L.T., von Haeseler, A., and Minh, B.Q.** (2016). W-IQ-TREE: a fast online phylogenetic tool for maximum likelihood analysis. *Nucleic Acids Res.* **44**: W232–W235.
- Valverde, C. and Wall, L.G.** (1999). Time course of nodule development in the *Discaria trinervis* (Rhamnaceae) - *Frankia* symbiosis. *New Phytol.* **141**: 345–354.
- van Velzen, R. et al.** (2018). Comparative genomics of the nonlegume *Parasponia* reveals insights into evolution of nitrogen-fixing rhizobium symbioses. *Proc. Natl. Acad. Sci. U. S. A.* **115**: E4700–E4709.

- van Velzen, R., Doyle, J.J., and Geurts, R.** (2019). A Resurrected Scenario: Single Gain and Massive Loss of Nitrogen-Fixing Nodulation. *Trends Plant Sci.* **24**: 49–57.
- Wang, Q., Hasson, A., Rossmann, S., and Theres, K.** (2016). *Divide et impera*: Boundaries shape the plant body and initiate new meristems. *New Phytol.* **209**: 485–498.
- Wellmer, F., Graciet, E., and Riechmann, J.L.** (2014). Specification of floral organs in *Arabidopsis*. *J. Exp. Bot.* **65**: 1–9.
- Xiao, T.T., Schilderink, S., Moling, S., Deinum, E.E., Kondorosi, E., Franssen, H., Kulikova, O., Niebel, A., and Bisseling, T.** (2014). Fate map of *Medicago truncatula* root nodules. *Development* **141**: 3517–3528.
- Žádníková, P. and Simon, R.** (2014). How boundaries control plant development. *Curr. Opin. Plant Biol.* **17**: 116–125.
- Zhang, J.** (2003). Evolution by gene duplication: An update. *Trends Ecol. Evol.* **18**: 292–298.



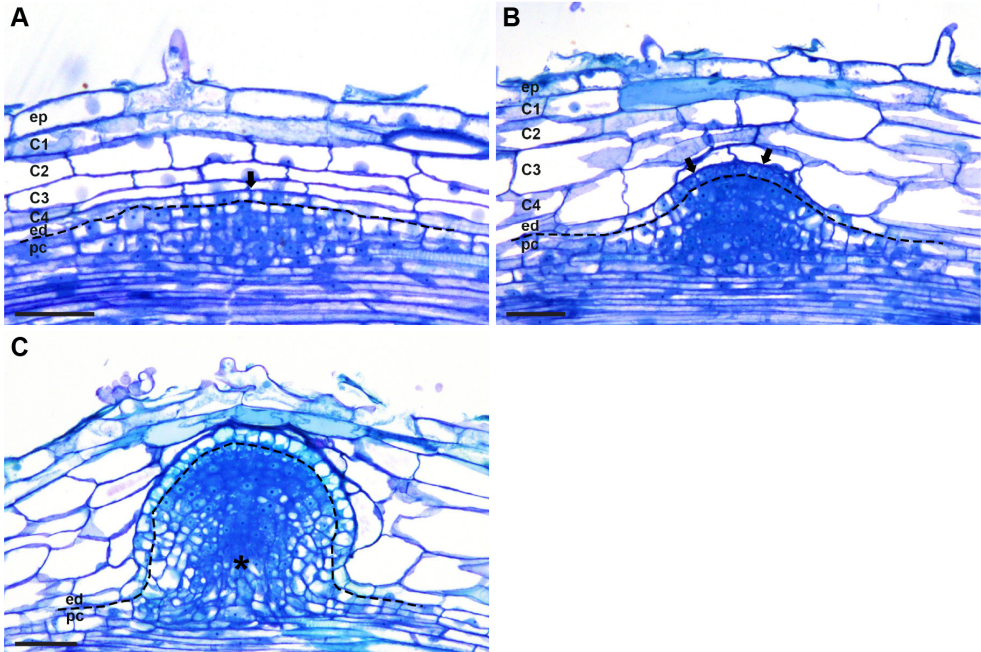
Supplementary Figure 1. Nitrogen-fixing clade.

All nodulating plant species belong to the nitrogen-fixing clade (NFC), which is composed of four orders: Fabales, Fagales, Cucurbitales and Rosales (Soltis et al. 1995). Legumes (Fabaceae, order Fabales) and the non-legume genus *Parasponia* (Cannabaceae, order Rosales) form nodules with rhizobia, whereas actinorhizal plants (orders Rosales, Cucurbitales and Fagales) form nodules with *Frankia* bacteria. Represented here are genera, of which species were mentioned in this study, or genome sequence data of species belonging to those genera are available. The shown genera of the legume family belong to three subfamilies: Cercidoioideae, Caesalpinioideae and Papilionoideae. Genus names in bold print indicate that nodule ontogeny was examined in the species belonging to those genera in this study. Black dots at the branch tips indicate that nodulating species occur in those genera. This shows that nodulation is common in the Fabaceae of order Fabales, but rare in the other three orders. Red and blue asterisks indicate the independent duplication of *NOOT/NBCL* gene in the common ancestor of Caesalpinioideae and that of Papilionoideae, respectively. Phylogenetic tree of the NFC based on LPWG, 2017 and Tedersoo et al., 2018, distribution of nodulating plants based on Tedersoo et al., 2018.



Supplementary Figure 2. *Parasponia* lateral root developmental stages.

(A) Lateral root formation starts with anticlinal divisions in pericycle. (B) Periclinal divisions are induced in pericycle and this results in the formation of two cell layers. (C, D) Cell divisions continue in pericycle-derived cells and lead to the formation of a multi-layered primordium. Divisions are also induced in the endodermis (arrows). (E) Pericycle-derived primordium cells continue to divide and endodermis-derived cells form the outermost cell layer of the primordium. The primordium is a dome-shaped structure and the vascular bundle starts to be formed (*). (F) Different root tissues of lateral root primordium begin to be formed. Endodermis-derived cells become part of the root cap/columella. Supplementary Figure 2F is identical to Figure 1A. Dotted lines mark the border between endodermis- and pericycle-derived cells. ep, epidermis; C1-C5, five cortical cell layers numbered from outside (C1) to inside (C5); ed, endodermis; pc, pericycle. Scale bars: 50 μ m.

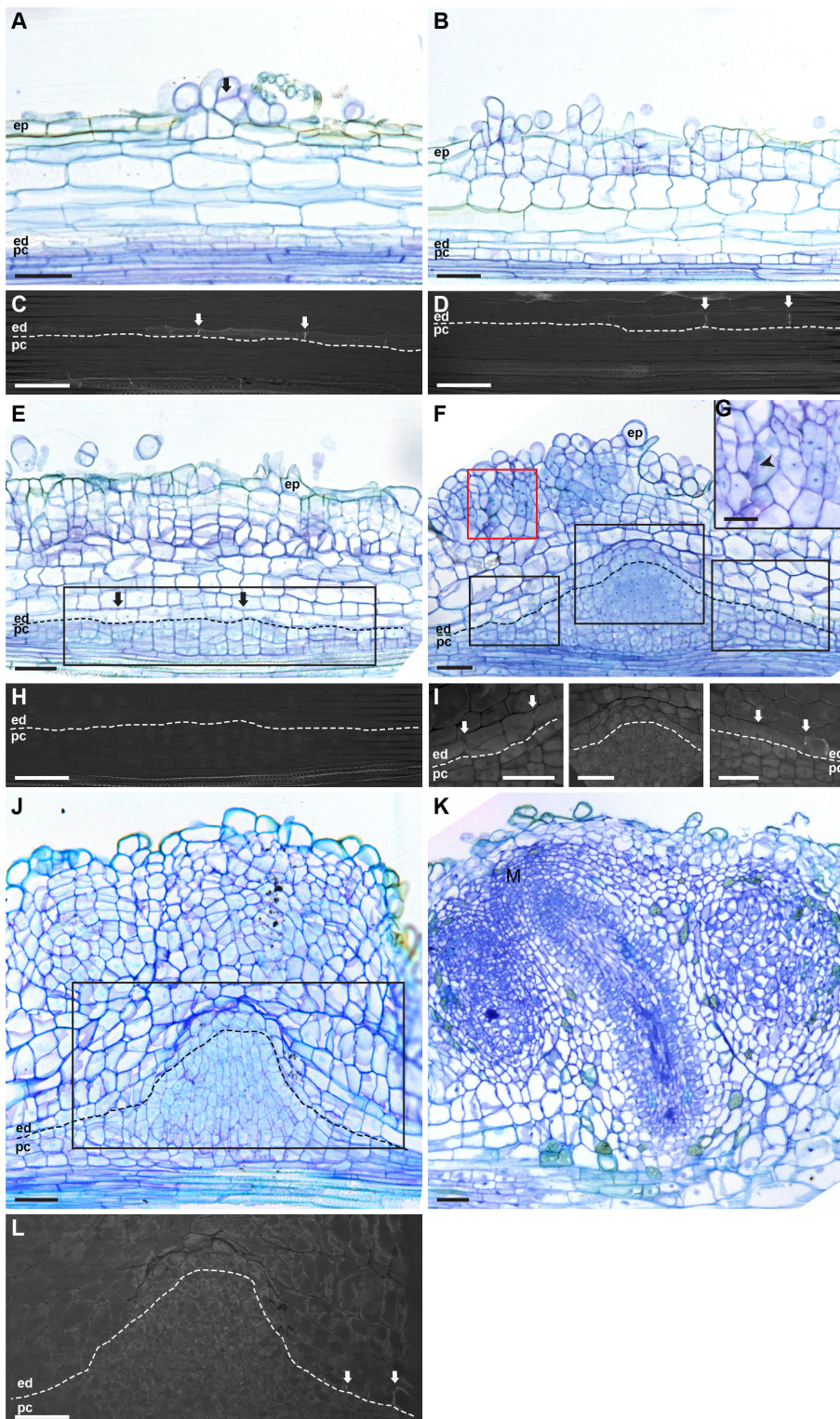


Supplementary Figure 3. *Alnus* lateral root developmental stages.

(A) Lateral root formation starts with cell divisions in pericycle. After a few rounds of cell division in the pericycle cells, endodermis cells divide anticlinally (arrow).

(B) Pericycle-derived cells continue dividing and form a dome-shape structure. Endodermis cells only divide anticlinally (arrows), forming one cell layer.

(C) Lateral root primordium starts to form different root tissues, including root vasculature (*) and cortex, which are derived from root pericycle cells. Endodermis-derived cells form the outermost layer of the lateral root primordium and later become part of the root cap/columella. Root cortical cells do not divide during lateral root formation. Supplementary Figure 3C is identical to Figure 1D. Dotted lines mark the border between endodermis- and pericycle-derived cells. ep, epidermis; C1-C4, four cortical cell layers numbered from outside (C1) to inside (C4); ed, endodermis; pc, pericycle. Scale bars: 50 μ m.



Supplementary Figure 4. *Parasponia* root nodule developmental stages.

(A) Nodule formation starts with cell divisions in epidermis (arrow).

(B) Cell divisions are induced in the outer cortical cell layers and pericycle, divisions continue in epidermis.

(C, D) UV light images of the endodermis regions of the sections shown in **(A)** and **(B)**, respectively to visualize fluorescence of Casparian strips. At place of nodule primordium formation the Casparian strips of endodermis cells are visible (arrows).

(E) Cell divisions occur in all cortical cell layers, pericycle and in the endodermis (arrows).

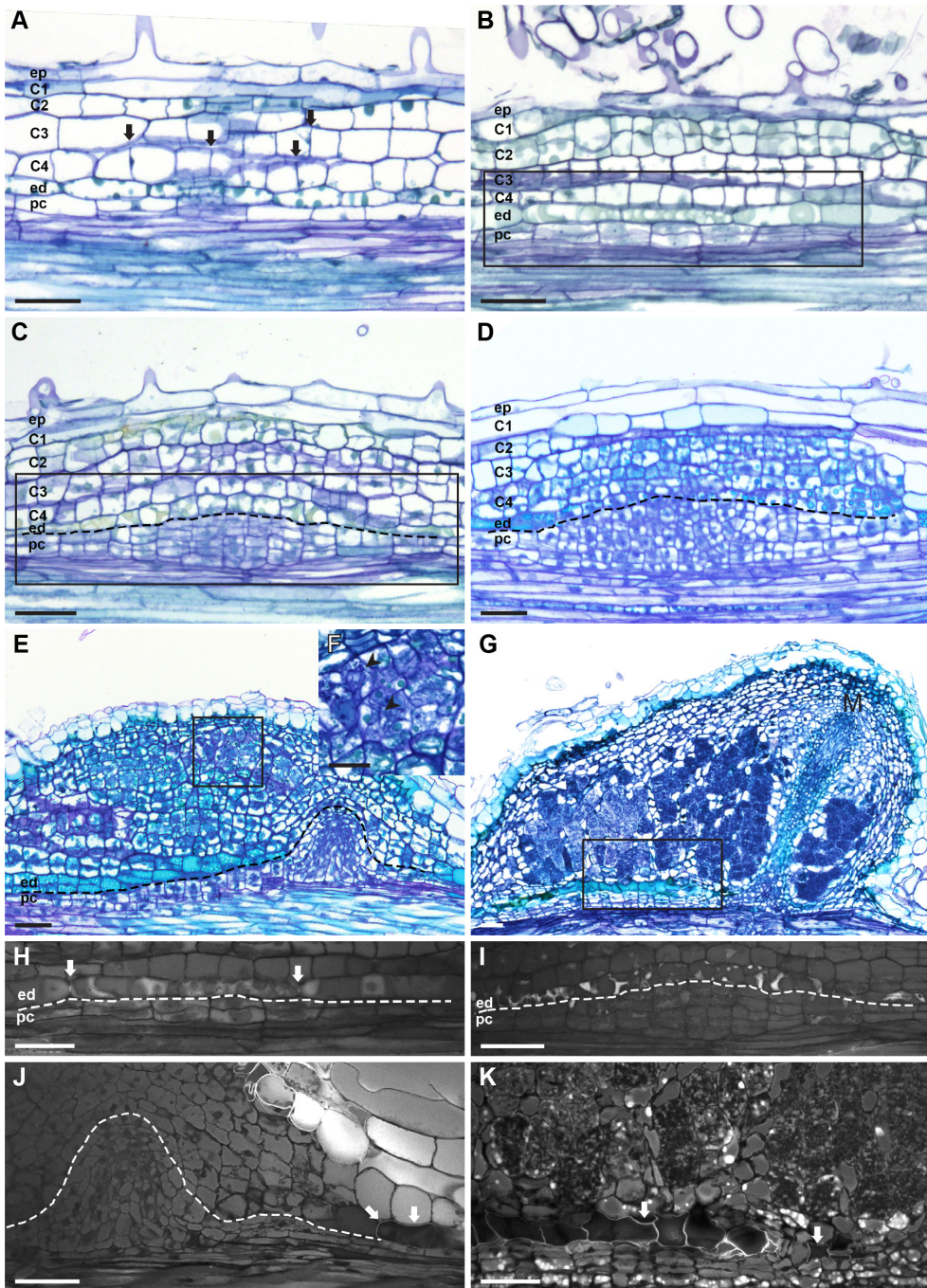
(F, G) Cortex-derived cells contain rhizobium-induced infection threads (see arrowhead in **(G)** and the red boxed region in **(F)**). Pericycle-derived cells form a dome-shaped structure flanked by root endodermis-derived cells. Supplementary Figure 4F and 4I (right panel) is identical to Figure 1B and 1C, respectively.

(H, I) UV light images of the root endodermis regions as indicated by the black boxes in the sections shown in **(E)** and **(F)**, respectively. **(H)** Mitotically activated root endodermis cells have lost their Casparian strips. **(I)** Casparian strips are reformed in the peripheral region (arrows), but still absent in the central region of root endodermis-derived cells.

(J) Cell divisions continue in the outer cortical cells. The pericycle-derived dome-shaped structure starts to elongate and forms the vascular tissues. At the apex of the pericycle-derived vasculature a nodule meristem is formed from cells derived from pericycle, endodermis and inner cortex.

(K) The outer cortex-derived cells become part of the mature nodule. A nodule meristem (M) at the apex of the nodule vasculature supports the growth of the nodule vasculature and adds cells to the infected tissue.

(L) UV light image of the root endodermis region of the section shown in **(J)**. Root endodermis-derived cells flanking the pericycle cells, have formed Casparian strips (arrows). This is the newly formed endodermis that surrounds the nodule vasculature. Endodermis-derived cells remain undifferentiated at the apex of the pericycle-derived vasculature. Dotted lines mark the border between endodermis- and pericycle-derived cells. ed, endodermis; pc, pericycle. Scale bars: 50 μm (**A-F**, **H-L**), 25 μm (**G**).



Supplementary Figure 5. *Alnus* root nodule developmental stages.

(A) Nodule formation starts with anticlinal divisions in cortex.

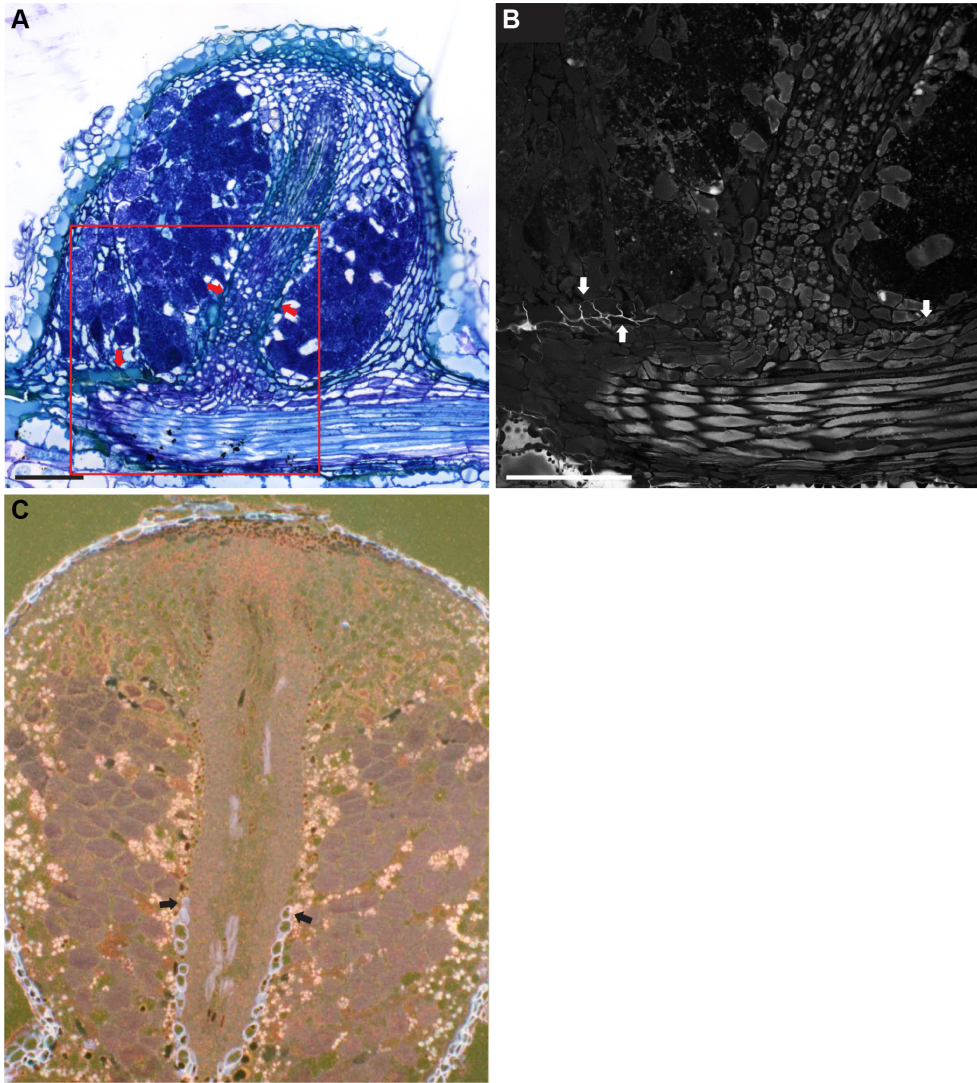
(B, H) Subsequently, divisions are induced in pericycle and continue in cortex. (H) UV light image of endodermis region of the section shown in (B). Not yet divided endodermis cells still have Casparian strips (arrows).

(C, I) Anticlinal divisions are induced in endodermis. (I) UV light image of endodermis region as indicated by the black box in the section shown in (C). Mitotically active endodermis cells lost Casparian strips.

(D, E) Cell divisions continue in inner cortical cells (C3-C4) forming multiple cell layers, and pericycle-derived cells form a dome-shaped structure. (E, F) Pericycle-derived cells start to form nodule vascular tissues. Root endodermis-derived cells, showing a light blue coloration after toluidine blue staining, flank the pericycle-derived nodule vasculature. At the apex of the vascular bundle, root endodermis-derived cells remain undifferentiated (without Casparian strips, see Supplementary Figure 5J). They form the nodule lobe meristem together with cells derived from pericycle and inner cortex. Cells derived from C3-C4 are infected by *Frankia*, see arrowheads in (F), the black boxed region in (E). Supplementary Figure 5E is identical to Figure 1E.

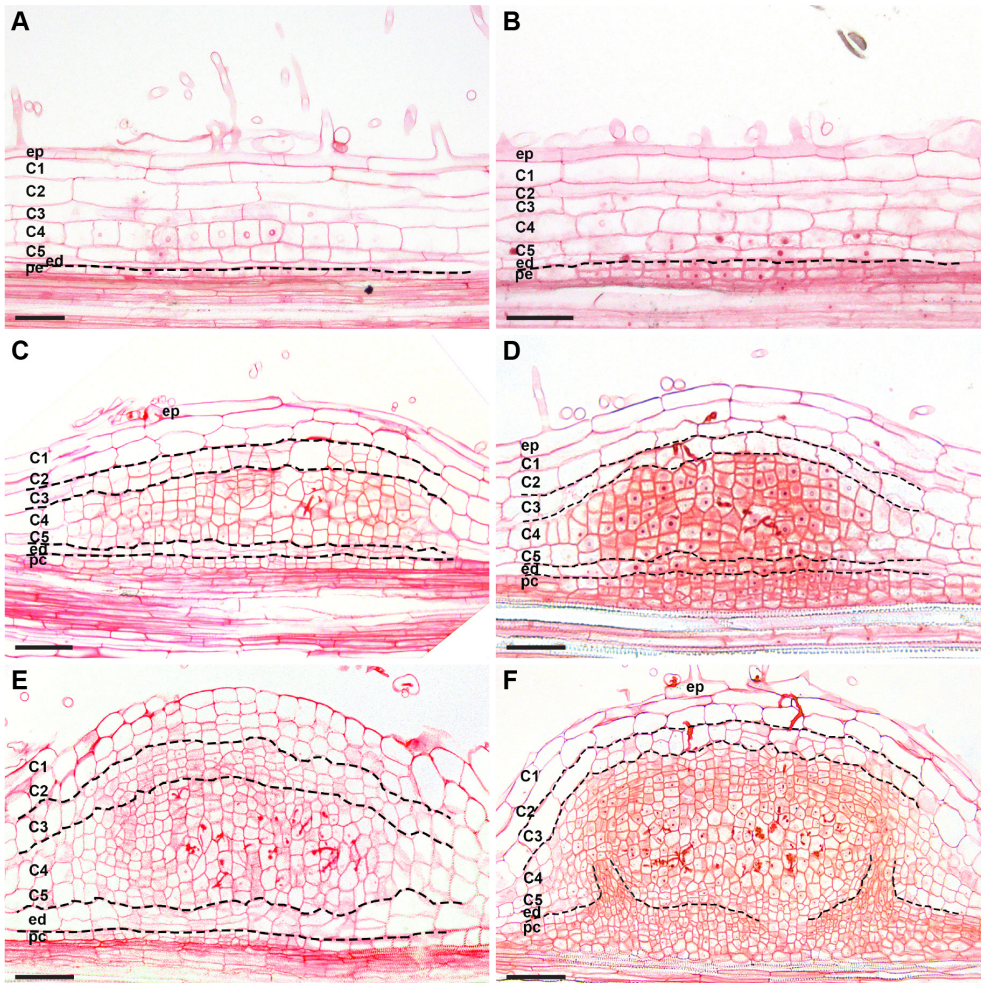
(G) Infected cortical cells become part of the mature nodule lobe. Nodule lobe meristem is indicated (M).

(J, K) UV light images of root endodermis regions of the nodules shown in (E) and of the black boxed region shown in (G), respectively. Root endodermis-derived cells at the apex of the nodule vasculature remain undifferentiated. Root endodermis cells in the peripheral region of the nodule vasculature have lignified cell walls, as indicated by arrows in (J) and (K). Dotted line marks the border between endodermis- and pericycle-derived cells. ep, epidermis; C1-C4, four cortical cell layers; ed, endodermis; pc, pericycle. Scale bars: 50 μm (A-E, G-K), 25 μm (F).



Supplementary Figure 6. The Casparian strips of *Alnus* nodule vascular endodermis cells are formed at a later stage of development.

(A-C) Longitudinal sections of *Alnus* mature nodules. (A) The endodermis cells of the root and nodule vasculature and root display a lighter blue coloration when stained by toluidine blue (arrows). (B) UV light image of the endodermis region as indicated by the box in the section shown in (A). The nodule vascular endodermis cells have not formed Casparian strips yet, only the endodermis cells at the junction of nodule vasculature and root vasculature are lignified (arrows). (C) UV light image of a more developed *Alnus* nodule than the one shown in (A). The nodule vascular endodermis cells are only lignified at the basal region of nodule vasculature (arrows), suggesting that the Casparian strips of nodule vasculature are formed at a later stage of development in *Alnus*. Scale bars: 100 μ m (A and B).



Supplementary Figure 7. Pericycle- and endodermis-derived cells in *Mtnoot1* nodule primordia remain mitotically active.

(A-F) Three subsequent stages of *Medicago* wild-type nodule primordia (A, C, E), compared with similar developmental stages of *Mtnoot1* nodule primordia (B, D, F), respectively. (A, B) The mitotic activity of pericycle-derived cells is more active in *Mtnoot1* (B). (C, D) Pericycle- and endodermis-derived cells form 4-6 cell layers in wild-type (C), and 6-8 cell layers in *Mtnoot1* nodule primordia (D). The number of periclinal divisions is markedly higher in *Mtnoot1* (D). (E, F) Pericycle- and endodermis-derived cells stop dividing in wild-type nodule primordia (E); however, they maintain their mitotic activity in *Mtnoot1* (F). Supplementary Figure 7E and 7F is identical to Figure 1F and 1G, respectively. Dotted lines mark the border between different cell types. ep, epidermis; C1-C5, five cortical cell layers; ed, endodermis; pc, pericycle. Scale bars: 50 μ m.

Supplementary Table 1. Protein sequences used in the phylogenetic analysis.

Name	Accession number	Reference
Acacia_argyrophylla_NOOTa	ZCDJ_scaffold_2091482	1kp project
Acacia_argyrophylla_NOOTb	ZCDJ_scaffold_2016325	1kp project
Acacia_pycnantha_NOOTa	ATQZ_scaffold_2091091	1kp project
Acacia_pycnantha_NOOTb	ATQZ_scaffold_2105894	1kp project
Arachis_ipaensis_NOOT1	LOC107645552	NCBI
Arachis_ipaensis_NOOT2	LOC107625400	NCBI
Bauhinia_tomentosa_NOOT	JETM_scaffold_2094600	1kp project
Cercis_canadensis_NOOT	Cerca71S10679	Griesmann et al., 2018
Chamaecrista_fasciculata_NOOTa	scaffold95585_cov211	Griesmann et al., 2018
Chamaecrista_fasciculata_NOOTb	scaffold94853_cov194	Griesmann et al., 2018
Chamaecrista_stricta_NOOTa	CHAST_transcripts_0012196	Wouter Kohlen
Chamaecrista_stricta_NOOTb	CHAST_transcripts_0012201	Wouter Kohlen
Cicer_arietinum_NBCL1	XP_004493408	NCBI
Cicer_arietinum_NBCL2	XP_004514968	NCBI
Faidherbia_albida_NOOTa	Faial01199g0126.1	Chang et al., 2019
Faidherbia_albida_NOOTb	Faial00941g0041.1	Chang et al., 2019
Gleditsia_sinensis_NOOTa	VHZV_scaffold_2080920	1kp project
Gleditsia_sinensis_NOOTb	VHZV_scaffold_2022360	1kp project
Glycin_max_NBCLa	Glyma.03G128600.1	Phytozome
Glycin_max_NBCLc	Glyma.02G188700.1	Phytozome
Lotus_japonicus_NBCL1	AEM62768	NCBI
Medicago_truncatula_NOOT1	Medtr7g090020.1	Phytozome
Medicago_truncatula_NOOT2	Medtr1g051025.1	Phytozome
Mimosa_pudica_NOOTa	Mimosa pu9890S28934	Griesmann et al., 2018
Mimosa_pudica_NOOTb	Mimosa pu9483S28675	Griesmann et al., 2018
Phaseolus_vulgaris_NBCL1	Phvul.001G124100.1	Phytozome
Phaseolus_vulgaris_NBCL2	Phvul.007G248000.1	Phytozome
Pisum_sativum_COCH1	AET34790	NCBI
Pisum_sativum_COCH2	ASV72503	NCBI
Vigna_unguiculata_NOOT1	Vigun01g107500.1	Phytozome
Vigna_unguiculata_NOOT2	Vigun07g038300.1	Phytozome

CHAPTER 4

Conserved Functions of *NODULE ROOT1* Genes in Actinorhizal-type and Legume-type Nodules Formed by *Parasponia andersonii* and *Medicago truncatula*

Defeng Shen¹, Olga Kulikova¹, Elena E. Fedorova², Fengjiao Bu¹, Huchen Li^{1,3}, René Geurts¹, and Ton Bisseling^{1,*}

¹Laboratory of Molecular Biology, Department of Plant Sciences, Wageningen University, Droevendaalsesteeg 1, 6708 PB Wageningen, The Netherlands.

²K. A. Timiryazev Institute of Plant Physiology RAS, Botanicheskaya 35, Moscow 127276, Russia.

³Beijing Advanced Innovation Center for Tree Breeding by Molecular Design, Beijing University of Agriculture, China.

*Corresponding author: ton.bisseling@wur.nl.

ABSTRACT

The maintenance of legume nodule identity requires *NOOT1* genes (*Medicago truncatula* (*Medicago*) *NODULE ROOT1* (*MtNOOT1*), *Pisum sativum* *COCHLEATA1*, *Lotus japonicus* *NOOT-BOP-COCH-LIKE1*). Knockout of *NOOT1* genes in legumes results in the formation of nodule roots at the nodule apex. Earlier studies have suggested that *Medicago MtNOOT1* maintains nodule identity of the nodule vascular meristem in a cell autonomous manner. However, we previously showed that in *Medicago Mtnoot1* mutant nodules, nodule vasculature is derived from the pericycle cells, similar to the ontogeny of actinorhizal-type nodule vasculature. Some actinorhizal species can also form nodules with nodule roots. Therefore, *Medicago MtNOOT1* might indirectly maintain nodule identity of the vascular meristem by repressing the formation of actinorhizal-type vasculature. So whether *Medicago MtNOOT1* has a direct effect on the maintenance of nodule identity of the vascular meristem remains unclear. To investigate this, we selected *Parasponia andersonii* (*Parasponia*), which forms actinorhizal-type nodules, and generated CRISPR/Cas9 mutants on the gene orthologous to *Medicago MtNOOT1*, named *PanNOOT1*. We show that nodule roots also occur in the *Parasponia Pannoot1* mutants. By *in situ* hybridization it is shown that *Medicago MtNOOT1* and *Parasponia PanNOOT1* are expressed in the vascular meristem and so they could maintain nodule identity of the vascular meristem in a cell autonomous manner. We further show that *Medicago MtNOOT1* and *Parasponia PanNOOT1* share conserved functions in regulating nodule meristem development and intracellular colonization of bacteria in the host cells. The analysis of *Parasponia PanNOOT1* could bring insight into the ancestral symbiotic functions of *NOOT1*.

INTRODUCTION

Nitrogen-fixing root nodule symbiosis occurs in four plant orders that together form the nitrogen-fixing clade (NFC) (Soltis et al., 1995). The formation of root nodules is induced by a group of Gram-negative bacteria that are collectively named rhizobia. They especially form nodules with species of the legume family (Fabaceae, order Fabales). Further, the Gram-positive *Frankia* bacteria form nodules with some plant species belonging to the orders Rosales, Fagales and Cucurbitales. These, so-called actinorhizal plants, form actinorhizal-type nodules whose ontogeny and histology are markedly different from those of

legume nodules (Pawlowski and Bisseling, 1996; Pawlowski and Demchenko, 2012). Outside the legume family there is one genus that can also form nodules with rhizobium. This is *Parasponia* (order Rosales) and it forms actinorhizal-type nodule (Lancelle and Torrey, 1984, 1985). Although the development of actinorhizal-type and legume-type nodules is different, in both cases they seem to have evolved (in part) from the root developmental program. This hypothesis is supported by the fact that nodule roots can grow out at the apex of both nodule types, and the vasculature of the nodule roots is connected with the nodule vasculature. This homeotic switch of the vascular meristem to root identity can occur in a few (wild-type) actinorhizal species (Pawlowski and Bisseling, 1996), whereas in legumes it is induced by loss-of-function mutation in the *NOOT1* genes (*Medicago truncatula* (Medicago) *NODULE ROOT1* (*MtNOOT1*), *Pisum sativum* (pea) *COCHLEATA1* (*PsCOCH1*), *Lotus japonicus* (Lotus) *NOOT-BOP-COCH-LIKE1* (*LjNBCL1*)) (Ferguson and Reid, 2005; Couzigou et al., 2012; Magne et al., 2018b). The latter suggests that in legumes *NOOT1* is involved in the maintenance of nodule identity of the vascular meristem in a cell autonomous manner. However, we showed that in the *Medicago noot1* mutant the nodule vasculature is formed from mitotically activated pericycle cells, not from the cortex. In this aspect *Mtnoot1* mutant nodules are similar to actinorhizal-type nodules (CHAPTER 3). Therefore, we hypothesize that *Medicago MtNOOT1* might repress a switch from nodule vascular meristem to root identity in two different ways: 1) Actinorhizal-type nodule vasculature in *Medicago Mtnoot1* mutants is primed to switch to root development, and *MtNOOT1* might indirectly maintain nodule identity of the vascular meristem by suppressing cell division in the pericycle; 2) *MtNOOT1* maintains nodule identity of the vascular meristem in a cell autonomous manner in addition to its function in suppressing pericycle mitotic activity. To determine whether *MtNOOT1* has a direct function in maintaining nodule identity of the vascular meristem, we made use of *Parasponia* as it makes actinorhizal-type nodules and it expresses a gene orthologous to *MtNOOT1* during nodule formation (Lancelle and Torrey, 1984, 1985; van Velzen et al., 2018).

Legume-type nodules have peripheral vascular bundles and a central infected tissue; both tissues are formed from mitotically activated cortical cells. Recently, we showed that in actinorhizal-type nodules of *Parasponia andersonii* and *Alnus glutinosa*, also the mitotically activated root cortical cells form the infected tissue, similar to legume nodules. Further, the central vasculature in these actinorhizal-type nodules is formed from the mitotically activated root pericycle

cells. This is the only structure formed from the pericycle and not a root-like organ as was previously reported. Therefore, the main difference between the two nodule types is the origin of nodule vasculature; cortical cells in the legume-type, pericycle cells in the actinorhizal-type (CHAPTER 3).

Recent studies have revealed that *MtNOOT1* and its orthologous genes (*PsCOCH1* and *LjNBCL1*) are required for the maintenance of nodule identity in legumes. Knockout of these genes results in the occurrence of nodule roots at the nodule apex. Such nodule root vasculature is connected with the nodule vasculature, suggesting the nodule vascular meristem can switch to root development (Ferguson and Reid, 2005; Couzigou et al., 2012; Magne et al., 2018b). It has been shown that *Medicago MtNOOT1* is expressed at the tip of nodule vasculatures, suggesting that *MtNOOT1* maintains nodule identity of the vascular meristem in a cell autonomous way (Couzigou et al., 2012; Magne et al., 2018a). We previously showed that in *Medicago Mtnoot1* mutants, nodule vasculature is formed by the pericycle-derived cells, instead of the cortical cells. This is similar to the ontogeny of actinorhizal-type nodule vasculature (CHAPTER 3). Nodule roots can also occur in several plant species forming actinorhizal-type nodules (Pawlowski and Bisseling, 1996). This suggests that in these actinorhizal plants the nodule vascular meristem is primed to switch to root identity. Therefore this might also be the case for the “actinorhizal-like” nodule vasculatures in *Medicago Mtnoot1* mutant nodules. In this case *Medicago MtNOOT1* indirectly maintains nodule identity of the vascular meristem by repressing an actinorhizal-type ontogeny of nodule vasculature. Therefore, it remains unclear how *MtNOOT1* maintains nodule identity of the vascular meristem; directly or indirectly?

To distinguish between these two scenarios, we made use of *Parasponia*, which forms actinorhizal-type nodules. In *Parasponia* nodules, host cells are intracellularly infected by infection threads, from which rhizobia are not released. Infection threads undergo a transition to fixation threads, which have a much thinner cell wall, but still contain a plant-derived membrane (Lancelle and Torrey, 1984, 1985). We previously revealed that there is a single *Medicago MtNOOT1* orthologous gene in the *P. andersonii* (*Parasponia*) genome, namely *PanNOOT1*. Its expression is induced during nodule organogenesis (van Velzen et al., 2018; CHAPTER 3), suggesting a symbiotic function. The ontogeny of *Parasponia* nodule vasculature is similar to that of *Medicago Mtnoot1* nodule vasculature. If *PanNOOT1* has a direct effect on the maintenance of nodule identity of the vascular meristem, then knocking out of *PanNOOT1* would also

cause an increased switch of nodule vascular meristem to root development. The availability of efficient and fast CRISPR/Cas9-mediated mutagenesis (van Zeijl et al., 2018) makes *Parasponia* an ideal tool to examine whether *PanNOOT1* has a direct effect on maintaining nodule identity of the vascular meristem.

Here, we generated *Parasponia Pannoot1* knockout mutants using CRISPR/Cas9. We found that *Pannoot1* nodules can form nodule roots at the nodule apex. By *in situ* hybridization, it was revealed that *Parasponia PanNOOT1* and *Medicago MtNOOT1* share a broad expression pattern at the nodule apex, including nodule meristem (that adds cells to be infected), vascular meristem and infected cells. The expression of *PanNOOT1* and *MtNOOT1* in the nodule vascular meristem suggests that NOOT1 in these two species maintains nodule identity of the vascular meristem in a cell autonomous manner. The shared broad expression domain of *PanNOOT1* and *MtNOOT1* genes suggests that additional function(s) besides maintaining nodule identity of the vascular meristem could be conserved between *Parasponia* and *Medicago*. We showed that these additional conserved functions are related to nodule meristem formation/maintenance and intracellular hosting of the microbes.

RESULTS

Knockout of *PanNOOT1* Leads to Formation of Nodules with Nodule Roots in *Parasponia*

To study whether the actinorhizal-type ontogeny of nodule vasculature in *Medicago Mtnoot1* nodules causes the switch of nodule vasculature to root development, we studied whether *NOOT1* has a function in maintaining nodule vasculature identity in actinorhizal-type nodules of *Parasponia*. Four independent *Parasponia Pannoot1* knockout lines (A5, A10, A16 and A29) were generated by using CRISPR/Cas9 (van Zeijl et al., 2018; Wardhani et al., 2019). They all have a deletion in the first exon and in all four cases this leads to early translation stoppage (Supplementary Figure 1). *Parasponia* plants inoculated with *Mesorhizobium plurifarium* BOR2 did not form nodule roots under our growth conditions. Therefore, we could test whether knockout of *Parasponia PanNOOT1* can cause a switch from nodule to root identity. All four *Parasponia Pannoot1* mutant lines inoculated with *M. plurifarium* BOR2 showed nodule roots at the nodule apex, similar to legume *noot1*, and nodule roots were never found in the transgenic control line mutants (Figure 1A-D; Supplementary Figure 2) (Table

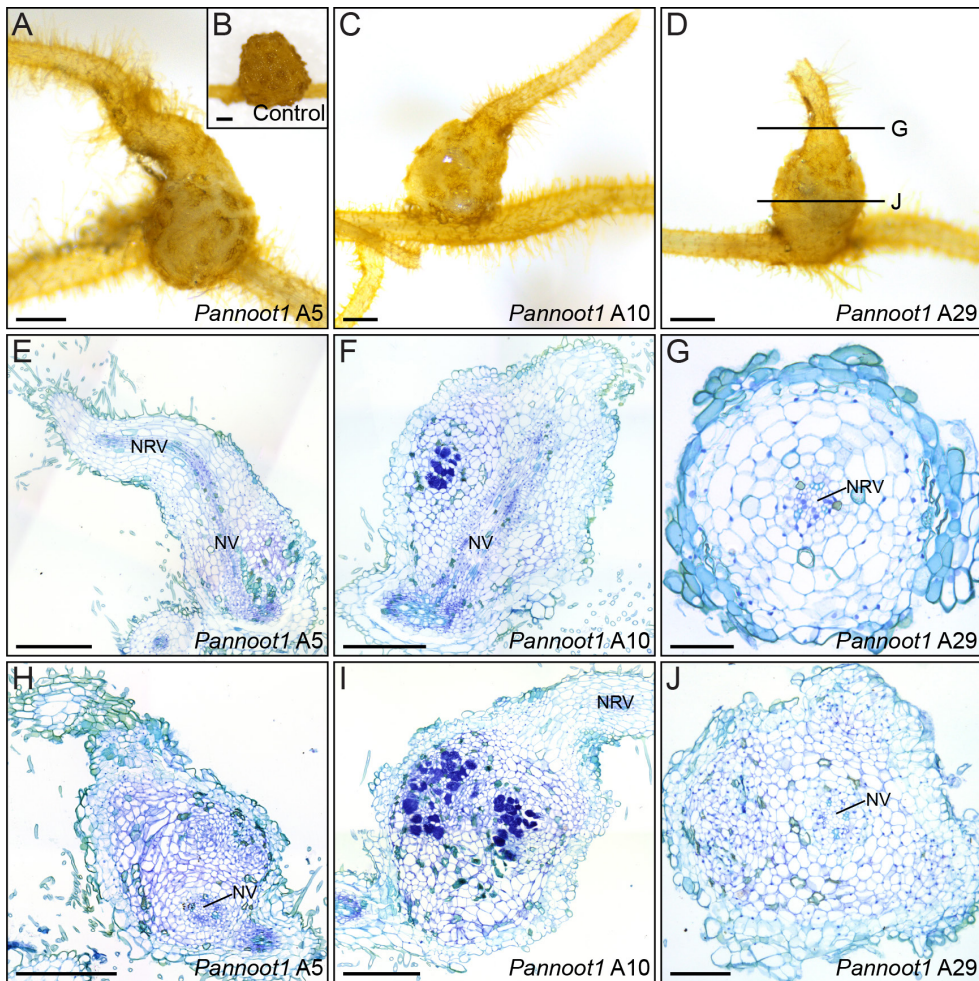


Figure 1. *Parasponia Pannoot1* Mutant Nodules Form Nodule Roots. Shown here are three independent *Parasponia Pannoot1* mutant lines A5 (A, E, H), A10 (C, F, I) and A29 (D, G, J) show nodule roots at the nodule apex, which were never observed in transgenic control line (B). (E, H) and (F, I) are two sequential longitudinal sections of the nodules shown in (A) and (C), respectively. (G, J) are two sequential cross sections of the nodule shown in (D). The approximate position of the cross sections is indicated in (D). These sections on *Pannoot1* mutant nodules show that the vasculature of nodule root (NRV) is connected with the nodule vasculature (NV), indicating that the vasculature meristem of *Pannoot1* mutant nodules can convert to root development. Scale bars: 250 μ m (A-F, H, I), 50 μ m (G), 100 μ m (J).

Table 1. Frequencies of Nodules with Nodule Root.

Time point	3 wpi		6 wpi	
Genotype	Fraction of nodules with nodule root	No. of plants	Fraction of nodules with nodule root	No. of plants
Control	0/98	8	0/269	7
<i>Pannoot1</i> A5	2/84 (2%)	6	25/288 (9%)	6
<i>Pannoot1</i> A10	2/81 (2%)	7	22/179 (12%)	6

Note that nodule roots were not observed in transgenic control line nodules in at least three independent experiments, of which two were statistically analysed. wpi: weeks post-inoculation.

1). Longitudinal sections of *Pannoot1* nodule roots showed that the vasculature of nodule roots was connected with the nodule vasculature (Figure 1E-F, H-I). This indicates that the developmental program of *Pannoot1* mutant nodule vasculature can switch to root identity, and *Parasponia PanNOOT1* is required to maintain the nodule identity of vasculature. Further, the nodule vasculature ontogeny was not affected in the *Parasponia Pannoot1* mutants, with a central nodule vasculature derived from the root pericycle (Supplementary Figure 3A-C). Therefore, in *Parasponia PanNOOT1* has a function in maintaining identity of the nodule vascular bundle. This also suggests that the actinorhizal-type ontogeny of the *Medicago Mtnoot1* nodule vasculatures is not sufficient to cause the switch of nodule to root identity and an additional function of *MtNOOT1* could be required to maintain the nodule identity.

***PanNOOT1* Is Expressed in a Broad Region at the *Parasponia* Nodule Apex Including Vascular Meristem, Nodule Tissue Meristem and Infection Zone**

To determine whether *Parasponia PanNOOT1* can control the nodule identity in a cell autonomous way, we investigated its expression pattern in nodules at two developmental stages by *in situ* hybridization. In young and mature *Parasponia* nodules, *PanNOOT1* mRNA occurred in the vascular meristem (Figure 2). This suggests that *PanNOOT1* controls nodule identity of the vasculature in a cell autonomous manner. The expression pattern of *PanNOOT1* was markedly broader than the vascular meristem as it was also expressed in the part of the meristem that adds cells to the infected tissue (nodule tissue meristem) as well

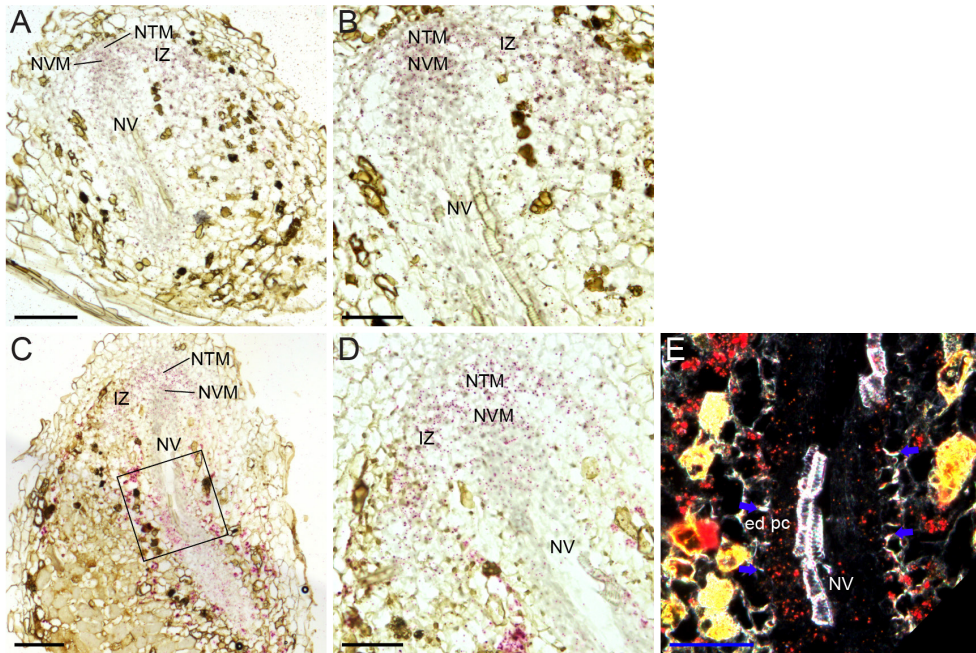


Figure 2. Parasponia *PanNOOT1* Expression Pattern in Two Stages of Nodules by *in situ* Hybridization. Longitudinal sections of young nodule (A, B) and mature nodule (C-E). (A-D) In young (3 wpi) and mature nodules (4 wpi), *PanNOOT1* mRNA occurs in a broad region, including nodule tissue meristem (NTM), vascular meristem (NVM), infection zone (IZ) and nodule vasculature (NV). (B) and (D) are close-up views of the sections shown in (A) and (C), respectively. (E) *PanNOOT1* mRNA also occurs in the pericycle cells of nodule vasculature. (E) is a dark field picture of the boxed region in (C). Blue arrows indicate Casparian strips. ed, endodermis of nodule vasculature; pc, pericycle of nodule vasculature. Scale bars: 100 μ m (A, C), 50 μ m (B, D, E),

as in the young infection zone. We further found that *PanNOOT1* transcripts occurred in the nodule vasculature, especially in the pericycle cells (Figure 2E). Therefore, it seems probable that, in addition to maintaining nodule identity, *PanNOOT1* has other functions in Parasponia nodule development.

We expected that the mechanism by which NOOT1 maintains nodule identity of the vasculature is similar in Parasponia and Medicago, and hypothesised that also in Medicago nodules *MtNOOT1* is expressed in the nodule vascular meristem.

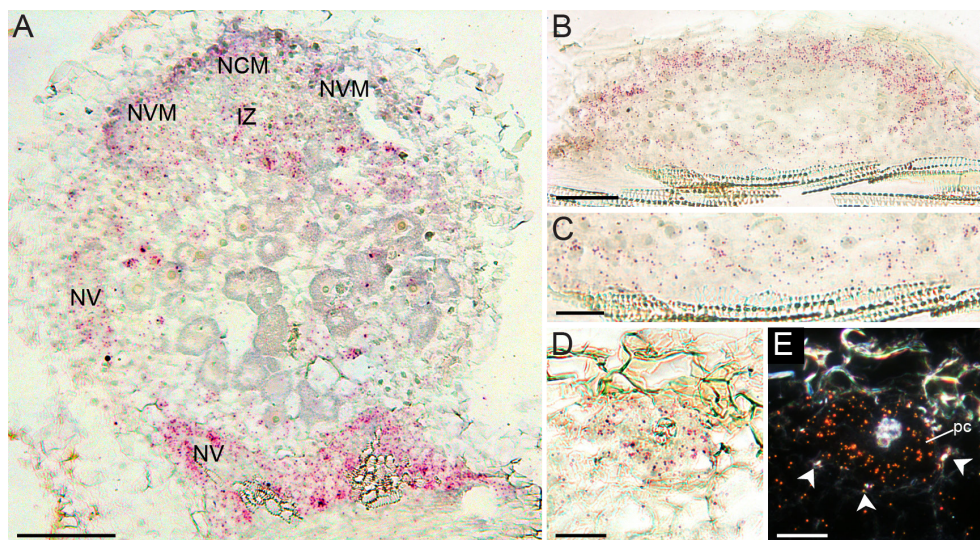


Figure 3. Medicago *MtNOOT1* Expression Pattern in Nodule Primordium and Mature Nodule by *in situ* Hybridization. Longitudinal sections of mature nodule (A) and stage V nodule primordium (B, C). Cross sections of mature nodule (D, E). (A) In mature nodule, *MtNOOT1* mRNA occurs in the nodule central meristem (NCM), nodule vascular meristem (NVM), and infection zone (IZ). (A, D, E) *MtNOOT1* mRNA also occurs in the pericycle (pc) and central tissues of nodule vascular bundle. (E) is a dark field picture of (D). (B) At stage V primordium, *MtNOOT1* mRNA occurs in the future nodule meristem, developing nodule vascular bundles, endodermis and pericycle-derived cells. (C) is a close-up of the basal region of (B). Red dots represent *MtNOOT1* transcripts, revealed by *MtNOOT1* probe set 1. Arrowheads indicate Casparian strips of endodermis cells. Scale bars: 100 μm (A), 50 μm (B), 25 μm (C), 25 μm (D, E).

***MtNOOT1* Is Expressed in Medicago Nodule Vascular and Central Meristem and Infection Zone**

To determine whether *MtNOOT1* is expressed in the nodule vascular meristem, we investigated the expression pattern of *MtNOOT1* in nodules. Previously, it has been shown that *MtNOOT1* is expressed in the distal part of the nodule vascular bundles by using a promoter::GUS construct (Couzigou et al., 2012; Magne et al., 2018a). However, we could not complement the *Mtnoot1* nodule phenotype by using 5 kb promoter upstream region (including the region used in the published promoter::GUS studies). Further, an *in situ* hybridization study was only performed on 28-day-old nodules, in which nodule meristem was hardly present in the shown sections (Magne et al., 2018a). Therefore, we

4 studied *MtNOOT1* expression by *in situ* hybridization in primordia at the stage when the meristem is formed (stage V according to Xiao et al., 2014) as well as in mature nodules. In stage V nodule primordia the cells of C3 have divided and they form the nodule meristem. We found that *MtNOOT1* mRNA occurred in these C3-derived cells (Figure 3B). Further, *MtNOOT1* was also expressed in the pericycle- and endodermis-derived cells as we previously described and there it plays a role in suppressing cell division (CHAPTER 3) (Figure 3B-C). To determine whether the expression of *MtNOOT1* in meristem is maintained in the mature nodules, we used median longitudinal sections of 2 weeks post inoculation (wpi) nodules for *in situ* hybridization. *MtNOOT1* was expressed in the nodule central meristem as well as the adjacent nodule vascular meristems. *MtNOOT1* mRNA was further detected in the infection zone, and in the pericycle cells of nodule vascular bundle (Figure 3A, 3D-E). We also used another set of 20 nt long *MtNOOT1* probes (see METHODS), which targeted different regions of *MtNOOT1* mRNA. Both probe sets for *MtNOOT1* were gene-specific and resulted in a similar expression pattern (Supplementary Figure 4). These results show that Medicago *MtNOOT1* is expressed in the nodule vascular meristem, so like *PanNOOT1*, it might control the maintenance of nodule identity in a cell autonomous manner.

***PanNOOT1* Is Required for the Maintenance of Mitotic Activity of Parasponia Nodule Meristem**

MtNOOT1 has a very similar broad expression pattern as *PanNOOT1* in the nodule apex, and functions in addition to maintenance of nodule identity might be conserved between Medicago *MtNOOT1* and Parasponia *PanNOOT1*. To identify such additional functions, we first analysed the *Pannoot1* mutants. In addition to the nodule roots, a striking phenotype of *Pannoot1* mutants was that they formed smaller nodules compared with nodules formed by the transgenic control line. To quantify this difference, we measured the nodule size of two *Pannoot1* mutant lines (A5 and A10) and the control line at 6 wpi. This showed that the nodule size of *Pannoot1* mutants was markedly reduced (~70% reduction in A5 line, ~60% reduction in A10 line) (Figure 4). Nodule size is largely determined by the activity of nodule meristem, therefore, we postulated that this defect could be due to the formation of a smaller meristem or reduced ability to maintain the activity of *Pannoot1* nodule meristems. To investigate this, we studied the histology of *Pannoot1* nodules. At young nodule stage (3 wpi), the tissue organization of *Pannoot1* mutant nodules was similar to that of the control

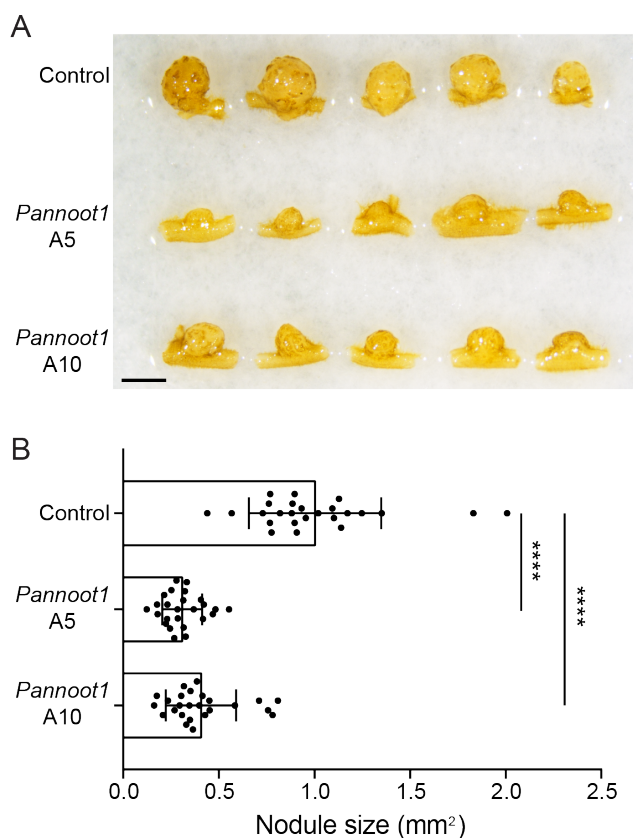


Figure 4. The Size of *Parasponia Pannoot1* Mutant Nodules Is Remarkably Reduced. (A) A comparison of nodules formed by the transgenic control line and two independent *Pannoot1* mutant lines A5 and A10 nodules at 4 wpi. (B) The nodule size is significantly reduced in *Pannoot1* mutant A5 (n=25) and A10 lines (n=25) compared with control line (n=25). Each dot represents the size of a single nodule at 4 wpi. Data are mean \pm SD. Student *t*-test was performed to assess significant differences (****: $P < 0.0001$). Scale bar: 1 mm.

line. In both cases, cell divisions occurred in the cortical cells, which were infected by rhizobia, the central vasculature starts to be formed (Supplementary Figure 3A-C). To examine the activity of nodule meristem, vascular meristem activity was used as a proxy. During the growth of nodule vasculature, cells derived from the vascular meristem differentiate, including endodermis cells. We used Casparian strips as marker because they are formed in the fully differentiated endodermal cells of nodule vasculature. We found that in most of the nodules formed by *Pannoot1* (A5: 65%, 13/20; A10: 69%, 11/13) and the control line (87.5%, 12/14), Casparian strips were only formed in the endodermis cells at a certain distance from the vascular meristem (Figure 5G; Supplementary Figure 3E-F). This indicates that new cells are added to the developing vasculature and that after some time/several cell layers they are fully differentiated. This implies that at 3 wpi the meristem in the control line and *Pannoot1* mutants is active. However, at a later stage (6 wpi) most of the *Pannoot1* nodules (A5: 80%, 20/25; A10: 63%, 12/19) showed differentiated endodermal cells with Casparian strips at the tip of nodule vasculature, which only occurred in a minority of control line

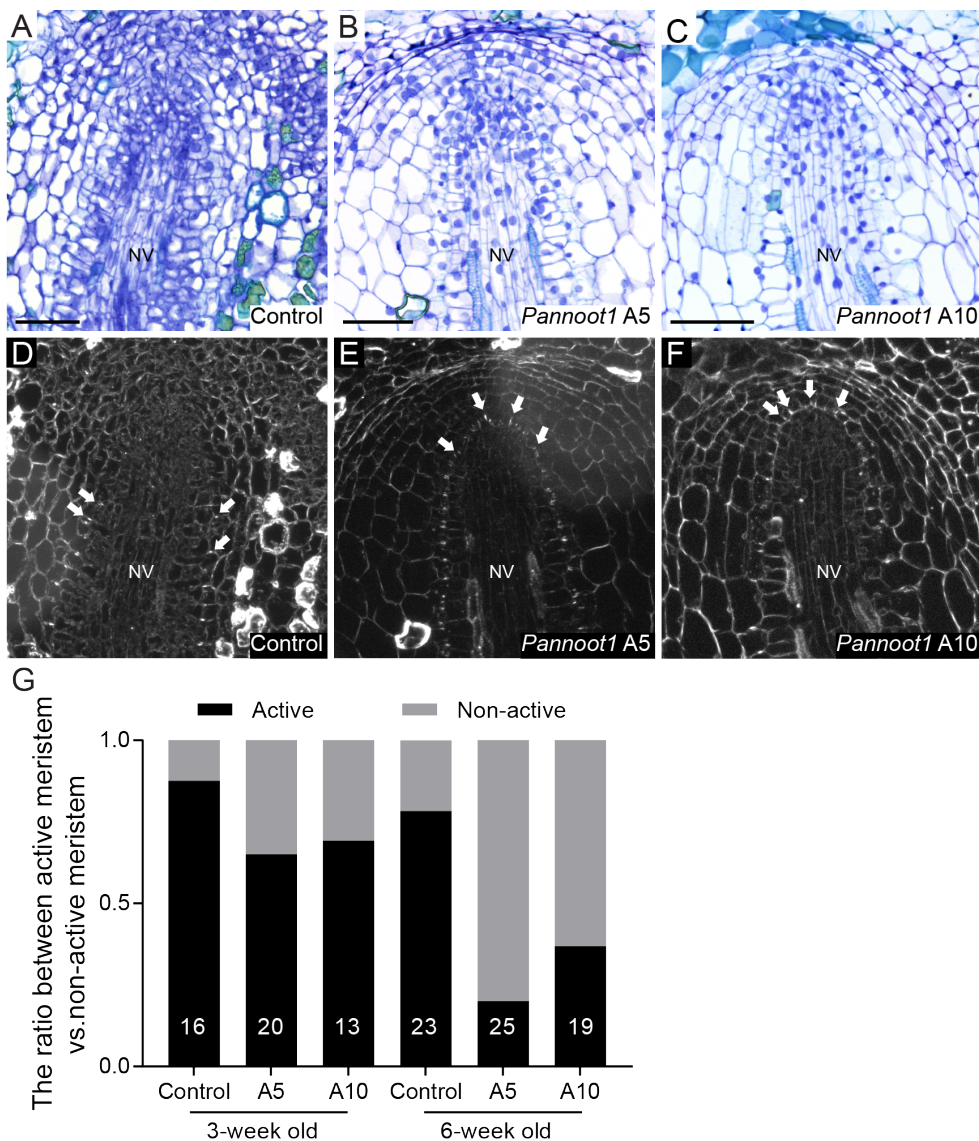


Figure 5. The Nodule Meristem Activity Is Reduced in *Parasponia Pannoot1* Mutants. (A-F) Longitudinal sections of nodule meristem regions of control line (A, D) and two independent *Pannoot1* mutant lines A5 (B, E) and A10 (C, F) at 6 wpi. (D-F) are dark field images of the sections shown in (A-C), respectively. This is to visualize Casparian strips in the endodermis cells of nodule vasculature (NV). (D-F) Casparian strips (arrows) are not formed at the differentiated endodermis cells at the tip of nodule vasculature in control nodules (D), but formed in the majority of *Pannoot1* mutant nodules (E, F). (G) The ratio of nodules with active meristem and non-active meristem at 3 wpi and 6 wpi. The number of nodules analysed is indicated on the bar. Scale bars: 50 μ m.

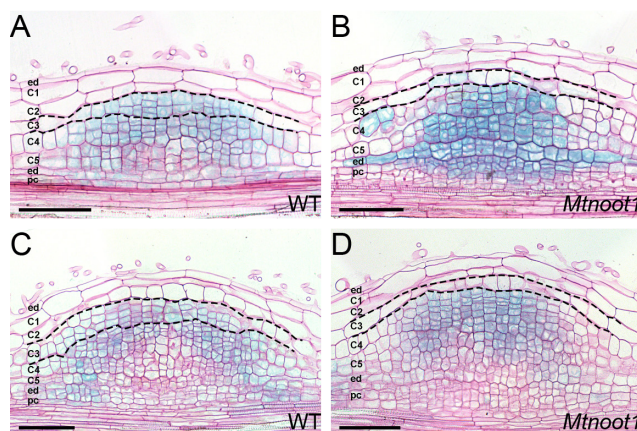


Figure 6. The Expression of *AtCYCB1;1::GUS* Is Absent from the C3-derived Cells in Medicago *Mtnoot1* Nodule Primordia. (A–D) Longitudinal sections of transgenic nodule primordia expressing *AtCYCB1;1::GUS* in Medicago wild-type (A, C) and *Mtnoot1* (B, D) at two sequential stages. (A, C) In wild-type nodule primordia, *AtCYCB1;1::GUS* is expressed in the C3-derived cells, which are actively dividing. (B, D) In *Mtnoot1* nodule primordia, the expression of *AtCYCB1;1::GUS* mainly occurs in C4-derived cells, absent from the C3-derived cells, of which mitotic activity is low compared with wild-type primordia (A, C). Dotted lines outline the cells derived from C3. Scale bars: 100 μ m.

nodules (22%, 5/23) (Figure 5G). This indicates that nodule vascular meristem does not add new cells to the vasculature in *Pannoot1* nodules, suggesting that the maintenance of nodule meristem activity is reduced in the *Pannoot1* mutants at this stage of development. This finding is consistent with the smaller *Pannoot1* nodule size (Figure 4). These results suggest that *PanNOOT1* is required for maintenance of nodule meristem activity.

***MtNOOT1* Is Required for the Formation of Medicago Nodule Meristem**

The reduced ability to maintain the activity of *Pannoot1* nodule meristem prompted us to investigate whether the nodule meristem activity is also affected in Medicago *Mtnoot1* mutants. Therefore, we first analysed the *Mtnoot1* primordia stage when the meristem is formed. This showed that in *Mtnoot1*, the mitotic activity of the middle cortical layer (C3), which forms nodule meristem in wild-type nodules, was markedly reduced. In wild-type nodule primordia with approximately eight cell layers derived from the inner cortex, there were 2–3 cell layers derived from C3. Whereas in *Mtnoot1* nodule primordia with similar number of cells derived from the inner cortex, there was only a few anticlinal

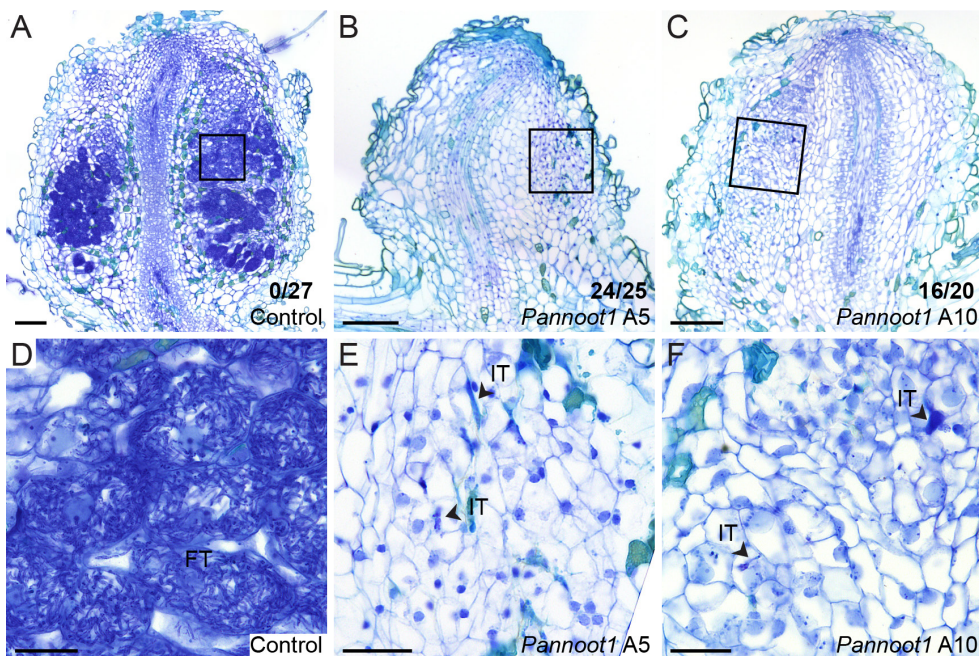


Figure 7. The Intracellular Colonization of Rhizobia Is Disturbed in *Parasponia Pannoot1* Mutant Nodules. Longitudinal sections of nodules formed by transgenic control line (A, D) and two independent *Pannoot1* mutant lines A5 (B, E) and A10 (C, F) at 6 wpi. (A, D) Control nodules are well infected, filled with fixation threads (FT) (B, C, E, F) The intracellular colonization of rhizobia is disturbed in *Pannoot1*. Infection threads are indicated with arrowheads. (D-F) are close-up views of the boxed region in (A-C), respectively. The number of nodules showing a defect in intracellular colonization is indicated at the right bottom of each image. Scale bars: 100 μ m (A-C), 25 μ m (D-F).

divisions in the C3 layer (Supplementary Figure 5A-B). At subsequent stage of *Mtnoot1* nodule primordium development, the difference became larger as in wild-type nodule primordia, C3-derived cells continued dividing, forming a multi-layered nodule meristem (Supplementary Figure 5C); whereas C3-derived cells divided less frequently in *Mtnoot1*, only forming 2-3 layers of cells (Supplementary Figure 5D). This shows that the mitotic activity of C3-derived cells is reduced in *Medicago Mtnoot1* mutant nodules. To confirm this, we introduced the *AtCyclin B1* (*AtCYCB1*);1::*GUS* reporter into *Mtnoot1* and wild-type roots by *Agrobacterium rhizogenes*-mediated transformation. *AtCYCB1*;1 is specifically expressed in mitotically active cells (Colón-Carmona et al., 1999). In wild-type nodule primordia (stage IV), *AtCYCB1*;1::*GUS* was expressed in actively dividing cortical cells, including the C3-derived cells (Figure 6A). In

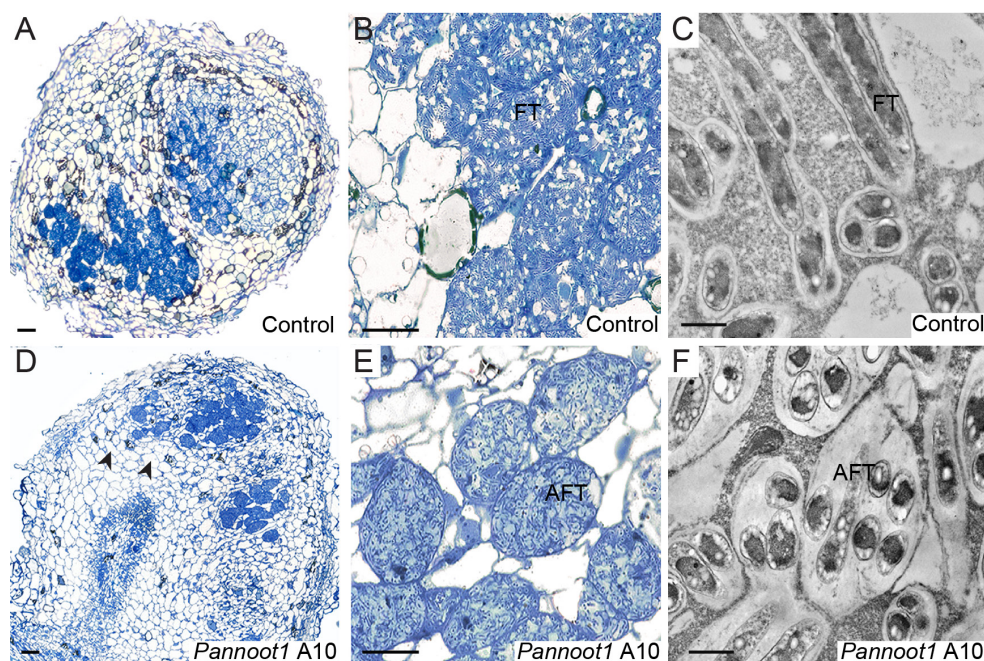


Figure 8. Fixation Thread Formation Is Disturbed in *Parasponia Pannoot1* Mutant Nodules. (A, B, D, E) Longitudinal sections (0.6 μm thickness) of nodules formed by the transgenic control line (A, B) and *Pannoot1* A10 line (D, E) at 4 wpi. (A) A mature nodule with infected cells filled with fixation threads. (B) A close-up view of infected cells, fixation threads contain 2-3 fila of rhizobia. (D) Infected cells are filled with aberrant fixation threads. The host cell's cytoplasm has been lysed and within 2-3 cell layers the cells contain no host cytoplasm (arrowheads). (E) A close-up view of infected cells; aberrant fixation threads (AFT) are embedded in dense matrix. (C, F) Transmission electron microscope images of infected cells in the control nodule (C) and *Pannoot1* A10 nodule (F). (C) Fixation threads (FT) filled with 2-3 fila of rhizobia. (F) Fusing aberrant fixation threads (AFT) with more than 4 fila of rhizobia. The cytoplasm of bacteroids is of a high electron density, some of the bacteroids display sight of lysis. Scale bars: 100 μm (A, D), 50 μm (B, E), 1 μm (C, F).

Mtnoot1 nodule primordia with similar number of cells derived from the inner cortex, *AtCYCB1;1::GUS* was expressed in the dividing inner cortex (C4 and C5) and endodermis- and pericycle-derived cells, but not in the C3-derived cells (Figure 6B). At the subsequent stage of wild-type nodule primordia, *AtCYCB1;1::GUS* remained active in the C3-derived cells, which have already formed a multiple layers of cells (future meristem) (Figure 6C). In *Mtnoot1* nodule primordia, *AtCYCB1;1::GUS* was mainly expressed in the C4-derived cells (Figure 6D). This implies that the mitotic activity of C3-derived cells is indeed reduced in *Medicago Mtnoot1* mutants, in line with the histological analysis.

Taken together, these results suggest that the formation of nodule meristem is disturbed in *Medicago Mtnoot1* mutants, and *MtNOOT1* is required for the formation of *Medicago* nodule meristem.

Knockout of *PanNOOT1* Affects Intracellular Colonization of Rhizobia in Parasponia

It has been shown that intracellular colonization of rhizobia can be affected in *Medicago Mtnoot1* nodules and this is more severely affected in the *Mtnoot1Mtnoot2* double mutants (Magne et al., 2018a). Since both of *Parasponia PanNOOT1* and *Medicago MtNOOT1* are expressed in the infection zone of nodule, we therefore investigated whether also *PanNOOT1* plays a role in intracellular colonization. In *Parasponia* nodules, infection threads, containing dividing rhizobia, enter the host cell cytoplasm and then they continue to grow as fixation threads that are characterized by a thinner cell wall, 2-3 fila of bacteria and the induction of the nitrogen fixation (*nif*) genes. The fixation threads can occupy a major part of the cytoplasm (Lancelle and Torrey, 1984, 1985; Op den Camp et al., 2011, 2012) (Figures 7A and D, Figure 8C). Surprisingly, this intracellular colonization was hampered in the *Pannoot1* mutants. Infection threads could enter the host cells in the majority of *Pannoot1* nodules (A5: 96%, 24/25; A10: 80%, 16/20). However, the fixation threads failed to fill up the host cells (Figure 7B, C, E and F). This indicates that the colonization of host cells by fixation threads is disturbed in *Pannoot1*. Such defect was not observed in nodules formed by the control line (0/23). In rare cases (A5: 4%, 1/25; A10: 20%, 4/20), aberrant fixation threads were formed, containing bacteria, but the amount of matrix was markedly increased. The host cell's cytoplasm started to be lysed (Figure 8D) and within 2-3 cell layers the cells were completely dead, containing no host cytoplasm (Figure 8C). This indicates that early senescence occurred in the *Parasponia Pannoot1* nodules. Taken together, these results indicate that *Parasponia PanNOOT1* is required for colonization of host cells and fixation thread formation.

DISCUSSION

Here we show that a loss-of-function mutation of *PanNOOT1* can cause a switch from nodule to root identity of the nodule vascular meristem in *Parasponia* nodules. The identity maintenance of vascular meristem is most likely controlled

by PanNOOT1 in a cell autonomous manner. This indicates that also in Medicago MtNOOT1 can directly be involved in maintaining nodule identity in this part of meristem and the actinorhizal nature of *Mtnoot1* nodule vasculatures is most likely not the (only) cause of the identity switch. In Parasponia as well as Medicago, *NOOT1* is further expressed in the nodule meristem and infection zone where it has a function in nodule meristem development and intracellular colonization of bacteria.

We previously showed that the vasculature of Medicago *Mtnoot1* nodules is derived from root pericycle, which is similar to the ontogeny of vascular bundles in actinorhizal-type nodules (CHAPTER 3). As some actinorhizal-type nodules can form nodule roots, we hypothesised that this altered ontogeny of the vasculature in *Mtnoot1* nodules is the cause of the switch from nodule to root identity. However, here we show that knockout mutation in Parasponia *PanNOOT1* can also cause a switch from nodule to root identity. The percentage of the nodules in which this switch occurs is markedly lower than in Medicago (6-12% in *Pannoot1* vs 50% in *Mtnoot1*) (Couzigou et al., 2012; Magne et al., 2018a). However, also in Lotus *Ljnbcl1* mutants the fraction of nodules with nodule root is relatively low (4-5%) (Magne et al., 2018b). So our data show that PanNOOT1 also contributes to the maintenance of nodule identity of the vascular meristem in the actinorhizal-type nodules of Parasponia. Whether this is also the case in other actinorhizal plants remains to be studied, but an indication might be obtained by comparing *NOOT* expression in species that do form nodule roots with species that do not. As in Medicago *Mtnoot1* mutant nodules root outgrowth is correlated with an actinorhizal ontogeny of the vasculature, it cannot be excluded that this ontogeny contributes to the switch in identity, although by itself it seems not sufficient. We showed that *MtNOOT2* is not expressed in the pericycle- and endodermis-derived cells in Medicago nodule primordia (CHAPTER 3). This suggests that MtNOOT2 is not involved in repressing the actinorhizal-type ontogeny of nodule vasculature. In line with this, a loss-of-function mutation in Medicago *MtNOOT2* does not result in nodule roots (Magne et al., 2018a). However, it has been shown that the frequency of nodule-to-root switch is increased (to 90%) in Medicago *Mtnoot1Mtnoot2* double mutants, and *MtNOOT2* is expressed in the nodule vascular meristem (Magne et al., 2018a). This suggests that Medicago MtNOOT1 and MtNOOT2 plays a redundant role in maintaining nodule identity of vascular meristem in a cell autonomous manner.

In Parasponia nodules, the addition of cells to be infected at the periphery and

the growth of the central nodule vasculature are coordinated and governed by nodule meristem, of which vascular meristem supports the nodule vasculature development. Casparian strips are formed in differentiated vascular endodermis cells. We showed that Casparian strips can be a good proxy to examine the activity of nodule meristem. At an early stage of development (3 wpi), Casparian strips were only formed in the differentiated endodermis cells at a certain distance from the vasculature meristem in most of *Pannoot1* mutant and control line nodules. This suggests that the nodule vascular meristem is formed to add cells to the nodule vasculature in *Pannoot1* mutants and the control line. In line with this, at this stage (3 wpi) *Pannoot1* mutant nodules appear to have a similar size as the nodules formed by the control line. However, at a later stage (6 wpi) in most of *Pannoot1* nodules the Casparian strips were detectable in differentiated endodermal cells at the tip of nodule vasculature. This suggests that the formation of the meristem is not affected in *Pannoot1* nodules whereas the maintenance of its activity is reduced at earlier stages of development. In agreement with this, the nodule size was drastically reduced in the *Parasponia Pannoot1* mutants, due to the maintenance of nodule meristem activity is reduced.

In contrast to *Parasponia Pannoot1* mutants, the formation of nodule meristem is disturbed in *Medicago Mtnoot1* mutants. In *Mtnoot1* nodule primordia the mitotic activity of middle cortical cell layer, from which the nodule meristem is formed, is lower compared with wild-type. This indicates that in *Medicago* the formation of nodule meristem requires MtNOOT1. In *Parasponia*, nodule meristem is possibly derived from a group of cells consisting of cortex, endodermis and pericycle cells (CHAPTER 3). The nodule meristem is responsible for adding cells to the peripheral infection zones and to the central vasculature. The part of meristem that adds cells to infected tissue (nodule tissue meristem) seems to be located above the vascular meristem. In *Medicago*, nodule meristem is derived from the middle cortical cells. The nodule central meristem adds cells to the central infected tissue, the nodule vascular meristems are located at the periphery of the central meristem, supporting the growth of the peripheral nodule vasculatures. The different function of NOOT1 in nodule meristem between *Parasponia* and *Medicago* can be explained by the different origin and characteristics of the nodule meristem in those two species. Further, the fact that *MtNOOT1* is expressed in the nodule (central) meristem in mature nodule suggests that MtNOOT1 is involved in the maintenance of *Medicago* nodule meristem activity. In mature *Medicago* nodules, approximately eight layers of

infected cells at the basal region are derived from the root cortex (Xiao et al., 2014). As some *Mtnoot1* nodules with nodule roots can grow bigger, with more than eight layers of infected cells (not published data; Magne et al., 2018a), this suggests that a (temporal) nodule meristem is formed to add cells to be infected. Given the observation that the C4-derived cells of *Mtnoot1* nodule primordia show high mitotic activity (*AtCYCB1;1::GUS* expression), we propose that these cells can form the (temporal) nodule meristem in Medicago *Mtnoot1* nodules.

The disturbed intracellular colonization of fixation thread in *Parasponia Pannoot1* nodules is reminiscent of Medicago *Mtnoot1* and *Mtnoot1Mtnoot2* mutants. In *Mtnoot1* nodules with nodule roots the rhizobial infection is hampered, resulting in low rhizobial colonization and early senescence. Such phenotype becomes severe in *Mtnoot1Mtnoot2* double mutants, which completely lose nitrogen-fixing ability (Magne et al., 2018a). These findings indicate that *PanNOOT1* and Medicago *NOOT* genes share a conserved role in regulating intracellular colonization of rhizobia in the host cells. In Medicago nodules, mutations in several genes associated with repressing host defence responses (e.g. *MtNAD1*, *MtDNF2*, *MtSymCRK*) lead to different degree of disturbed colonization of bacteria and an early senescence phenotype (Bourcy et al., 2013; Berrabah et al., 2014; Wang et al., 2016), similar to Medicago *Mtnoot1* and *Mtnoot1Mtnoot2* mutant nodules (Magne et al., 2018a). Therefore, the disturbed intracellular colonization in *Parasponia Pannoot1* and Medicago *Mtnoot1* and *Mtnoot1Mtnoot2* mutants could be a secondary effect of induced defence responses. In line with this, several defence response genes are upregulated in Medicago *Mtnoot1* and *Mtnoot1Mtnoot2* mutants (Magne et al., 2018a). This suggests that *Parasponia PanNOOT1* and Medicago *NOOT* genes could be involved in repressing defence responses. It would be interesting to test whether genes associated with repressing defence responses are differentially expressed in *Parasponia Pannoot1* and Medicago *Mtnoot1*, *Mtnoot1Mtnoot2* mutant nodules.

We previously proposed that legume-type and actinorhizal-type nodules share a common evolutionary origin, and the nodules formed by the common ancestor of the NFC were actinorhizal type. Thereafter, legume-type nodules evolved from actinorhizal type, and neofunctionalization of legume *NOOT1* contributed to this process (CHAPTER 3). Here, we show that *PanNOOT1* and *MtNOOT1* function similarly in several processes in these two nodule types. This would suggest that *NOOT* gene was already recruited by the common ancestor of the NFC to have symbiotic functions: maintaining nodule identity of the vascular

meristem, sustaining nodule meristem activity, and regulating intracellular colonization of bacteria. In legumes NOOT1 was neofunctionalized to allow expression in pericycle-derived cells in nodule primordia. By this cell divisions in those cells are suppressed.

METHODS

Plant Materials and Growth Conditions

Pannoot1 CRISPR/Cas9 mutants were generated from *P. andersonii* WU1-14 as previously described (van Zeijl et al., 2018; Wardhani et al., 2019). Three single guide RNA (sgRNA) target sites were designed for *PanNOOT1* locus (Supplementary Figure 1). Primers used to generate sgRNAs and mutant genotyping are listed in Supplementary Table 1. Ctr44 was used as transgenic control line (van Zeijl et al., 2018). Tissue culture and nodulation assay were performed as previously described (van Zeijl et al., 2018; Wardhani et al., 2019).

Medicago truncatula noot1 mutant line tnk507 (Couzigou et al., 2012) and wild-type accession R108 plants were grown on BNM medium (supplemented with 1 mM amino ethoxyvinylglycine (AVG)) for *in situ* hybridization. They were also used to generate *AtCYCB1;1::GUS Agrobacterium rhizogenes* (strain MSU440) mediated transgenic roots as previously described (Limpens et al., 2004). Transgenic GUS material was grown on BNM medium (supplemented with 1 mM AVG). *Sinorhizobium meliloti* Rm41 carrying a pHc60-GFP construct was used to induce *Medicago* nodule formation. The surface-sterilization and germination of *Medicago* seeds were performed as previously described (Limpens et al., 2004).

Sequence Alignment

PanNOOT1 (PanWU01x14_292800) genomic sequence is available at <http://www.bioinformatics.nl/parasponia/>. Sequence alignment was performed using MAFFT v7.017 (Kato, 2002), implemented in Geneious R6 (Biomatters), using default parameter settings. The figure of gene model and sequence alignment was exported from Geneious R6 and edited using Adobe Illustrator CC (Adobe Systems).

Microscopy and Imaging

For semi-thin (0.6 μm) light microscopy (Figure 8A, B, D, E) and transmission electron microscopy, nodules were fixed with 3% of glutaraldehyde, postfixed with 2% of OsO_4 , embedded in LR white resin, as described by Wang et al., 2010. For other light microscopy, nodules were fixed with 4% paraformaldehyde (w/v), 5% glutaraldehyde (v/v) in 0.05 M sodium phosphate buffer (pH 7.2) at 4 °C overnight. Then fixed materials were washed with 1 x PBS, dehydrated by an ethanol series and subsequently embedded in Technovit 7100 (Heraeus Kulzer) according to the manufacturer's protocol. Section thickness was 5 μm . Sections were made with a RJ2035 microtome (Leica Microsystems), and stained for 1.5 min in 0.05% toluidine blue O. Sections were imaged by using a DM5500B microscope equipped with a DFC425C camera (Leica Microsystems).

In situ Hybridization

Hybridization was performed twice on wild-type *P. andersonii* (WU1-14) young (3 wpi) and mature (4 wpi) nodules, and on wild-type *Medicago truncatula* (accession R108) nodule primordia (5 days post-inoculation) and mature nodules (2 wpi). Invitrogen ViewRNA ISH Tissue 1-Plex Assay kits (Thermo Fisher Scientific) were used for hybridization, as previously described (Liu et al., 2019). The *PanNOOT1* probe set (catalogue number: VF1-6000669), *MtNOOT1* probe set 1 (catalogue number: VF1-16434), and *MtNOOT1* probe set 2 (catalogue number: VF1-6001168) were designed and synthesized by Thermo Fisher Scientific. *PanNOOT1* probe set covers the region 281-1146 nt of the coding sequence (1512 nt, PanWU01x14_292800.1). *MtNOOT1* probe set 1 covers the region 2-913 nt of the coding sequence (1449 nt, Medtr7g090020.1); *MtNOOT1* probe set 2 covers the regions 2-227 nt and 1184-1936 nt of the full-length mRNA (1981 nt, XM_003624964). A typical probe set contains ~20 adjacent oligonucleotide pairs of probes that hybridize to specific regions across the target mRNA. Each probe covers 20 nucleotides, only a pair of two adjacent probes can form a site for signal amplification. By this principle, background is reduced. Sections were imaged using a DM5500B microscope equipped with a DFC425C camera (Leica Microsystems).

ACKNOWLEDGMENTS

We thank Arjan van Zeijl for the help in designing the CRISPR/Cas9 single guide RNAs, and the provision of Ctr44 transgenic control line. We thank Pascal Ratet for providing the *Mtnoot1* seeds (tnk507).

AUTHOR CONTRIBUTIONS

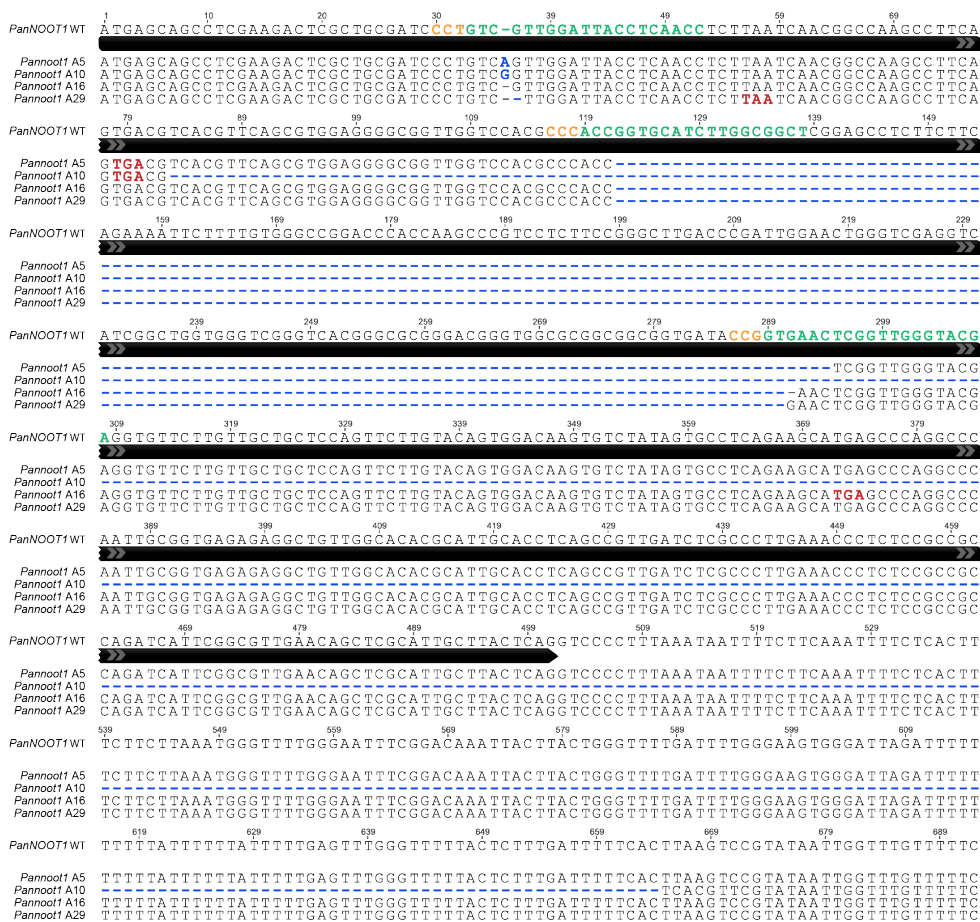
TB and RG conceived and supervised this research. DS designed and performed most of the experiments with help from FB. OK and DS performed the *in situ* hybridization. EF performed the semi-thin (0.6 μ m) light microscopy and transmission electron microscopy. DS analysed the results and drafted the manuscript with input from TB and HL. TB revised the manuscript.

REFERENCES

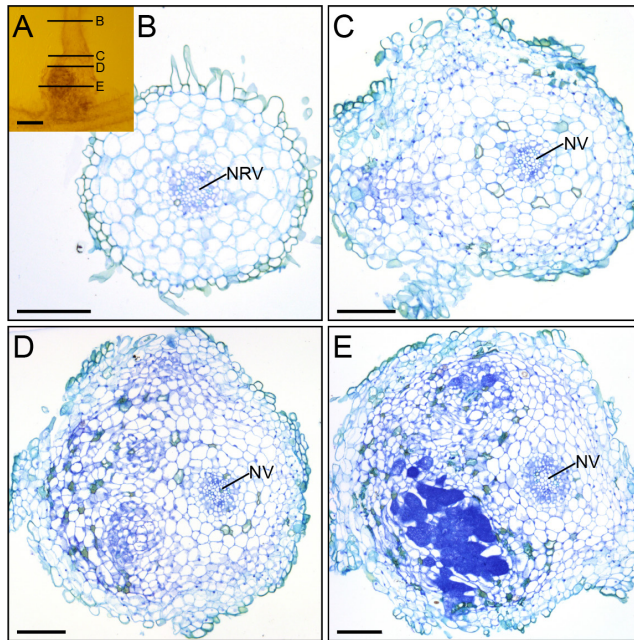
- Berrabah, F., Bourcy, M., Eschstruth, A., Cayrel, A., Guefrachi, I., Mergaert, P., Wen, J., Jean, V., Mysore, K.S., Gourion, B., and Ratet, P.** (2014). A nonRD receptor-like kinase prevents nodule early senescence and defense-like reactions during symbiosis. *New Phytol.* **203**: 1305–1314.
- Bourcy, M., Brocard, L., Pislariu, C.I., Cosson, V., Mergaert, P., Tadege, M., Mysore, K.S., Udvardi, M.K., Gourion, B., and Ratet, P.** (2013). *Medicago truncatula* DNF2 is a PI-PLC-XD-containing protein required for bacteroid persistence and prevention of nodule early senescence and defense-like reactions. *New Phytol.* **197**: 1250–1261.
- Colón-Carmona, A., You, R., Haimovitch-Gal, T., and Doerner, P.** (1999). Spatio-temporal analysis of mitotic activity with a labile cyclin-GUS fusion protein. *Plant J.* **20**: 503–508.
- Couzigou, J.-M.J. et al.** (2012). *NODULE ROOT* and *COCHLEATA* Maintain Nodule Development and Are Legume Orthologs of *Arabidopsis* *BLADE-ON-PETIOLE* Genes. *Plant Cell* **24**: 4498–4510.
- Ferguson, B.J. and Reid, J.B.** (2005). *Cochleata*: Getting to the root of legume nodules. *Plant Cell Physiol.* **46**: 1583–1589.
- Katoh, K.** (2002). MAFFT: a novel method for rapid multiple sequence alignment based on fast Fourier transform. *Nucleic Acids Res.* **30**: 3059–3066.
- Lancelle, S.A. and Torrey, J.G.** (1984). Early Development of *Rhizobium*-Induced Root-Nodules of *Parasponia rigida*. I. Infection and Early Nodule Initiation. *Protoplasma* **123**: 26–37.
- Lancelle, S.A. and Torrey, J.G.** (1985). Early development of *Rhizobium*-induced root nodules of *Parasponia rigida*. II. Nodule morphogenesis and symbiotic development. *Can. J. Bot. Can. Bot.* **63**: 25–35.
- Limpens, E., Ramos, J., Franken, C., Raz, V., Compaan, B., Franssen, H., Bisseling, T., and Geurts, R.** (2004). RNA interference in *Agrobacterium*

- rhizogenes*-transformed roots of *Arabidopsis* and *Medicago truncatula*. J. Exp. Bot. **55**: 983–992.
- Liu, J., Rutten, L., Limpens, E., van der Molen, T., van Velzen, R., Chen, R., Chen, Y., Geurts, R., Kohlen, W., Kulikova, O., and Bisseling, T. (2019). A Remote *cis*-Regulatory Region Is Required for *NIN* Expression in the Pericycle to Initiate Nodule Primordium Formation in *Medicago truncatula*. Plant Cell **31**: 68–83.
- Magne, K. et al. (2018a). *MtNODULE ROOT1* and *MtNODULE ROOT2* Are Essential for Indeterminate Nodule Identity. Plant Physiol. **178**: 295–316.
- Magne, K., George, J., Berbel Tornero, A., Broquet, B., Madueño, F., Andersen, S.U., and Ratet, P. (2018b). *Lotus japonicus* NOOT-BOP-COCH-LIKE1 is essential for nodule, nectary, leaf and flower development. Plant J. **94**: 880–894.
- Op den Camp, R., Streng, A., De Mita, S., Cao, Q., Polone, E., Liu, W., Ammiraju, J.S.S., Kudrna, D., Wing, R., Untergasser, A., Bisseling, T., and Geurts, R. (2011). LysM-type mycorrhizal receptor recruited for rhizobium symbiosis in nonlegume *Parasponia*. Science **331**: 909–912.
- Op den Camp, R.H.M., Polone, E., Fedorova, E., Roelofsen, W., Squartini, A., Op den Camp, H.J.M., Bisseling, T., and Geurts, R. (2012). Nonlegume *Parasponia andersonii* Deploys a Broad Rhizobium Host Range Strategy Resulting in Largely Variable Symbiotic Effectiveness. Mol. Plant-Microbe Interact. **25**: 954–963.
- Pawlowski, K. and Bisseling, T. (1996). Rhizobial and Actinorhizal Symbioses: What Are the Shared Features? Plant Cell **8**: 1899–1913.
- Pawlowski, K. and Demchenko, K.N. (2012). The diversity of actinorhizal symbiosis. Protoplasma **249**: 967–979.
- Soltis, D.E., Soltis, P.S., Morgan, D.R., Swensen, S.M., Mullin, B.C., Dowd, J.M., and Martin, P.G. (1995). Chloroplast gene sequence data suggest a single origin of the predisposition for symbiotic nitrogen fixation in angiosperms. Proc. Natl. Acad. Sci. U. S. A. **92**: 2647–2651.
- van Velzen, R. et al. (2018). Comparative genomics of the nonlegume *Parasponia* reveals insights into evolution of nitrogen-fixing rhizobium symbioses. Proc. Natl. Acad. Sci. U. S. A. **115**: E4700–E4709.
- Wang, C. et al. (2016). *NODULES WITH ACTIVATED DEFENSE 1* is required for maintenance of rhizobial endosymbiosis in *Medicago truncatula*. New Phytol. **212**: 176–191.
- Wang, D., Griffiths, J., Starker, C., Fedorova, E., Limpens, E., Ivanov, S., Bisseling, T., and Long, S. (2010). A nodule-specific protein secretory pathway required for nitrogen-fixing symbiosis. Science **327**: 1126–1129.
- Wardhani, T.A., Purwana Roswanjaya, Y., Dupin, S., Li, H., Linders, S., Hartog, M., Geurts, R., and van Zeijl, A. (2019). Genome Editing and Phenotyping the Nitrogen-fixing Tropical Cannabaceae Tree *Parasponia andersonii*. J. Vis. Exp: 59971.
- Xiao, T.T., Schilderink, S., Moling, S., Deinum, E.E., Kondorosi, E., Franssen, H., Kulikova, O., Niebel, A., and Bisseling, T. (2014). Fate map of *Medicago truncatula* root nodules. Development **141**: 3517–3528.
- van Zeijl, A., Wardhani, T.A.K., Seifi Kalhor, M., Rutten, L., Bu, F., Hartog, M.,

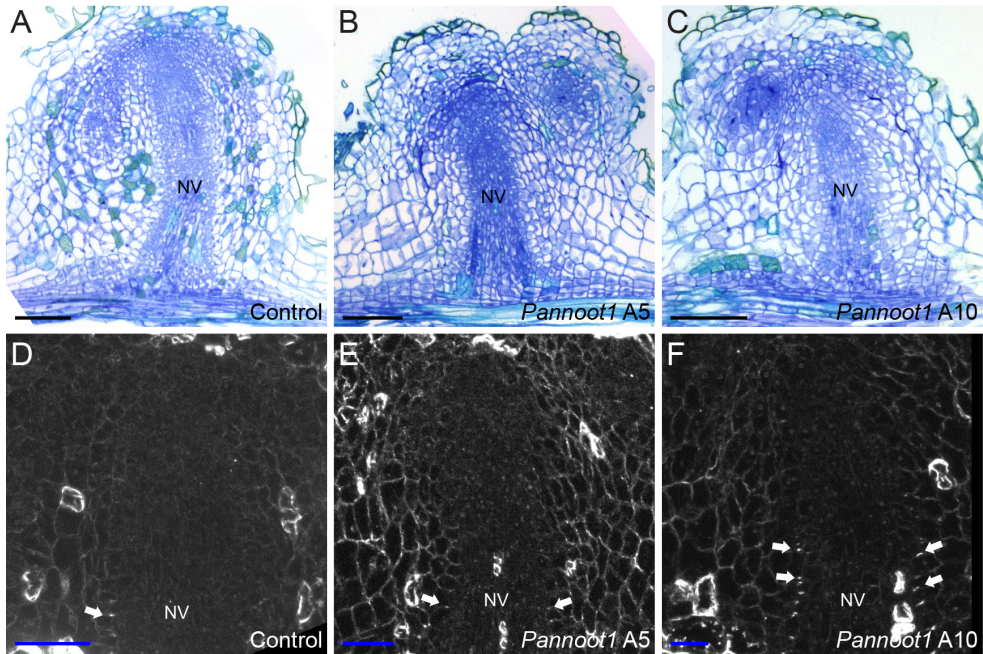
Linders, S., Fedorova, E.E., Bisseling, T., Kohlen, W., and Geurts, R. (2018). CRISPR/Cas9-Mediated Mutagenesis of Four Putative Symbiosis Genes of the Tropical Tree *Parasponia andersonii* Reveals Novel Phenotypes. *Front. Plant Sci.* **9**: 1–14.



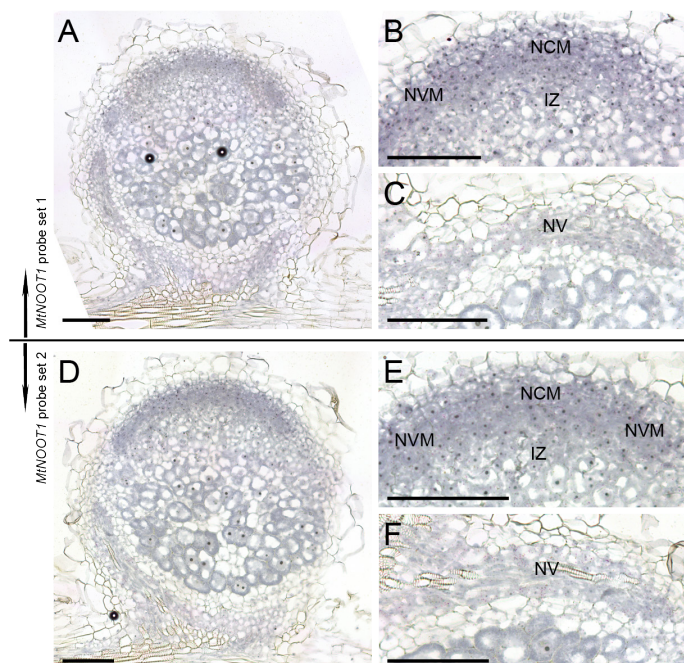
Supplementary Figure 1. Sequence alignment of *PanNOOT1* in wild-type and *Pannoot1* mutant lines. A part of the *PanNOOT1* genomic sequence (including the first exon and part of the intron) is used as the alignment reference, the black arrow indicates the first exon. Numbers above the *PanNOOT1* genomic sequence indicate nucleotide position starting from ATG. The sgRNA target sites and PAM (protospacer adjacent motif) sequences are highlighted in green and orange, respectively. The inserted nucleotides or deleted sequences in the *Pannoot1* mutant lines are highlighted in blue. Premature stop codons are highlighted in red, indicating that the *Pannoot1* mutant lines cannot produce functional PanNOOT1 protein.



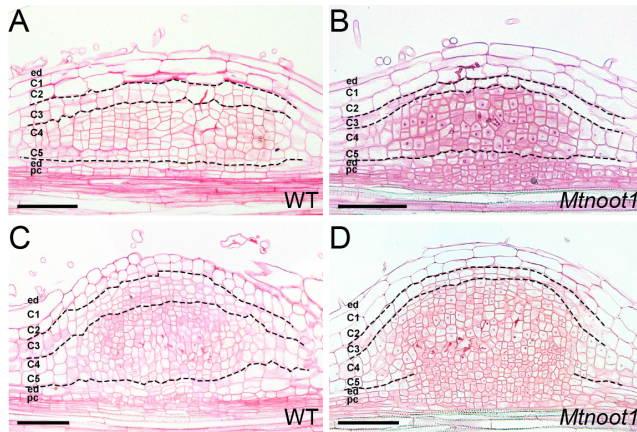
Supplementary Figure 2. Cross section of a nodule with nodule root formed by *Pannoot1* A16 line. **(A)** A overview of a nodule with nodule root formed by *Pannoot1* A16 line. **(B-E)** Four sequential cross sections of the nodule shown in **(A)**. This shows that the nodule root vasculature (NRV) is connected with the nodule vasculature (NV). The positions of the cross sections shown in **(B-E)** are indicated in **(A)**. Scale bars: 250 μm (A), 100 μm (B-E).



Supplementary Figure 3. A majority of *Pannoot1* nodules have an active meristem at 3 wpi. (A-F) Longitudinal sections of nodule meristem regions of control line (A, D) and two independent *Pannoot1* mutant lines A5 (B, E) and A10 (C, F) at 3 wpi. (D-F) are dark field images of the sections shown in (A-C), respectively. This is to visualize Casparian strips in the endodermis cells of nodule vasculature (NV). (D-F) Casparian strips (arrows) are not formed at the differentiated endodermis cells at the tip of nodule vasculature in the majority of control nodules (D) and *Pannoot1* mutants (E, F). Scale bars: 100 μ m (A-C), 50 μ m (D-F).



Supplementary Figure 4. Similar *MtNOOT1* expression pattern revealed by two sets of probes in mature nodule. (A-F) Longitudinal sections of a wild-type mature nodule at 2 wpi. Two sets of *MtNOOT1* probes were designed and targeted to different regions of *MtNOOT1* mRNA. *MtNOOT1* probe set 1 (A-C) and set 2 (D-F) were hybridized on sequential sections of a single nodule. (B) and (D) are close-up views of the nodule apex region shown in (A) and (D), respectively. (C) and (E) are close-up views of the nodule vasculature (NV) shown in (A) and (D), respectively. In both cases, *MtNOOT1* is expressed in nodule central meristem (NCM) and nodule vascular meristem (NVM). *MtNOOT1* mRNA also occurs in infection zone (IZ) and nodule vasculature (NV). This reveals a similar expression of *MtNOOT1* in mature nodule, corroborating the validity of *MtNOOT1* expression pattern. Scale bars: 100 μ m.



Supplementary Figure 5. The mitotic activity of C3-derived cells is reduced in *Mtnoot1* nodule primordia. Longitudinal sections of nodule primordia formed by wild-type (**A, C**) and *Mtnoot1* (**B, D**) at two sequential stages. (**A**) In wild-type nodule primordia with approximately eight cell layers derived from the inner cortex, there are 2-3 cell layers derived from C3, in contrast to only one layer of C3 in *Mtnoot1* nodule primordia (**B**). (**C**) At subsequent stage of wild-type nodule primordia, C3-derived cells continue dividing, forming a multi-layered nodule meristem. (**D**) C3-derived cells divide less frequently in *Mtnoot1*, only forming 2-3 layers of cells. This shows that the mitotic activity of C3-derived cells is reduced in *Mtnoot1*. Dotted lines mark the border between different cell types. ep, epidermis; C1-C5, five cortical cell layers; ed, endodermis; pc, pericycle. Scale bars: 100 μ m.

CHAPTER 5

PanNODULE ROOT1* Is a *BLADE-ON-PETIOLE* Gene that Regulates Branching, Stipule Formation and Leaf Patterning in the Tropical Cannabaceae Tree *Parasponia andersonii

Defeng Shen¹, Kévin Magne¹, Olga Kulikova¹, Fengjiao Bu¹, Yuanyuan Zhang², Jing Wang¹, Ton Bisseling¹, Wouter Kohlen¹, René Geurts^{1,*}

¹Laboratory of Molecular Biology, Department of Plant Sciences, Wageningen University, Droevendaalsesteeg 1, 6708 PB Wageningen, The Netherlands.

²Laboratory of Plant Physiology, Department of Plant Science, Wageningen University, Droevendaalsesteeg 1, 6708 PB Wageningen, The Netherlands.

*Corresponding author: rene.geurts@wur.nl.

ABSTRACT

Plant architecture is modified by the development of axillary branches. The hormonal and genetic regulatory network that controls branching has been mainly described in herbaceous model systems, whereas the molecular basis of branching in woody species remains unclear. *Arabidopsis thaliana* BLADE-ON-PETIOLE1 (AtBOP1) and AtBOP2, and their orthologs in several herbaceous species are co-transcriptional factors involved in leaf patterning. Recent studies revealed that a BOP ortholog also functions in branching in barley (*Hordeum vulgare*) and maize (*Zea mays*), however, their functioning remains unclear in trees. Here, we studied the functioning of the *BOP* gene (*PanNOOT1*) in a tropical tree *Parasponia andersonii* (Cannabaceae) by analysing CRISPR/Cas9-mediated *Pannoot1* knockout mutants. We show that plant architecture is modified in the *Pannoot1* mutant plants, due to the delayed axillary bud emergence and outgrowth. Also, the *Pannoot1* mutants display disturbed stipule formation and organ fusion between the stem and the petiole. We further show that in the *Pannoot1* mutants the proximal-distal patterning and adaxial-abaxial patterning of leaves are affected; petioles are shorter with downwardly curled vasculature and additional abaxialized vasculatures. To our knowledge, this is the first report on the functioning of a *BOP* gene in a tree. Our data demonstrate that *PanNOOT1* is a *BOP* gene, required for axillary branch development, stipule formation and leaf patterning along the proximal-distal and adaxial-abaxial axes in the tropical tree *P. andersonii*.

INTRODUCTION

Plants modulate growth and development throughout their life cycle to cope with changing and unpredictable conditions. To fulfil the indeterminate and open development, shoot and root apical meristems generate aerial and underground parts, respectively. The activities of the shoot apical meristem and the axillary meristems at the leaf axils together shape the shoot architecture. During the growth period, the shoot apical meristem remains active, while axillary meristem develops into a bud that stays dormant or grows out to form branch (Bennett and Leyser, 2006; Wang et al., 2018).

The activity of axillary buds is regulated by the antagonistic interaction between auxin and cytokinin. Auxin can repress the outgrowth of axillary buds by dampening the biosynthesis of cytokinin, which promotes bud outgrowth by

repressing the expression of *BRANCHED1/TEOSINTE BRANCHED1 (BRC1/TB1)* (Teichmann and Muhr, 2015). In *Arabidopsis (Arabidopsis thaliana)*, pea (*Pisum sativum*) and rice (*Oryza sativa*), mutation in *BRC1/TB1* lead to enhanced branching. Further, *BRC1/TB1* expression is enhanced by strigolactones (SLs). In *Arabidopsis* and pea, the expression of *AtBRC1/PsBRC1* is downregulated in SL deficiency mutants, which show increased branching, indicating that SLs regulate *BRC1* transcriptionally (Aguilar-Martínez et al., 2007). There are also evidences supporting a role for SLs and *BRC1/TB1* on branching in trees. Synthetic SL analog GR24 can suppress the outgrowth of grey poplar (*Populus x canescens*) buds and willow (*Salix* spp.) basal buds (Ward et al., 2013; Muhr et al., 2016). In grey poplar, knockdown of a SL biosynthesis gene exhibits increased branching pattern and *PcBRC1* is downregulated (Muhr et al., 2016). Further, *Pcbrc1-1* mutants exhibit strongly enhanced bud outgrowth (Muhr et al., 2018). Therefore, it appears a conservation of major regulatory mechanisms in controlling bud outgrowth between the herbaceous model system *Arabidopsis* and the poplar trees.

Recent findings unveiled a new player in regulating axillary branch development. In barley (*Hordeum vulgare*) *Uniculm4 (HvCul4)* encodes a BTB/POZ and ankyrin domain-containing protein orthologous to *Arabidopsis* BLADE-ON-PETIOLE1 (*AtBOP1*) and *AtBOP2*. *Hvcul4* mutants show reduced tillering, deregulated number of axillary buds in an axil. Consistent with these findings, *HvCul4* is expressed at the leaf axil boundary, prior to the formation of axillary meristem and later more diffusely in the axillary buds (Tavakol et al., 2015). *tassels replace upper ears1 (tru1)*, the orthologue of *AtBOPs* in maize (*Zea mays*), also plays a role in regulating axillary branching. *Zmtru1* mutants show enhanced axillary branching, an opposite phenotype of *Hvcul4* mutants. In the axillary meristem, the expression of *Zmtru1* is directly activated by *ZmTB1* (Dong et al., 2017). Despite different function in axillary branching, the orthologues of *AtBOP1/AtBOP2* in barley and maize are expressed in axillary buds and regulate axillary branch development. The connection between *BOP* and the key branching regulator *BRC1/TB1* makes *BOP* an important player in axillary branch development. The orthologues of *AtBOP1/AtBOP2* are also expressed in the axillary buds of several *Populus* species (Sjödin et al., 2009; Howe et al., 2015; Wang et al., 2019), however no functional studies have yet been conducted in tree species.

Studies in *Arabidopsis* have revealed also a role of *AtBOP1* and *AtBOP2* on leaf patterning along the proximal-distal axis. During leaf differentiation, proximal

(nearer to the stem) -distal (away from the stem) and adaxial (upper surface of a leaf) -abaxial (lower surface of a leaf) axes are established (Du et al., 2018). Knockout mutations in *AtBOP1/AtBOP2* lead to ectopic outgrowths of blade tissue along the petioles of cotyledons and leaves (Ha et al., 2003, 2004). Further, *AtBOP1*, *AtBOP2* and their orthologous genes in legumes (Medicago (*Medicago truncatula*): *NODULE ROOT1* (*MtNOOT1*), pea: *COCHLEATA1* (*PsCOCH1*), and Lotus (*Lotus japonicus*): *NOOT-BOP-COCH-LIKE1* (*LjNBCL1*)) play a conserved role in modifying the proximal region of the leaf (McKim et al., 2008; Ichihashi et al., 2011; Couzigou et al., 2012; Magne et al., 2018). Arabidopsis *Atbop1;Atbop2* double mutants do not form stipules (McKim et al., 2008; Ichihashi et al., 2011), which are also simplified or reduced in the Medicago *Mtnoot1* mutant or at early nodes of the pea *Pscoch1* mutant, respectively (Couzigou et al., 2012). In Lotus *Ljnbcl1* mutant nectary glands, which are proposed to be modified stipules, are completely absent (Magne et al., 2018). In barley and rice, *HvCul4* and *OsBOP1*, *OsBOP2*, *OsBOP3* are indispensable for the development of ligule, which separates the distal blade and proximal sheath of leaf (Tavakol et al., 2015; Toriba et al., 2019). Knockout of three *OsBOP* genes completely abolishes sheath development, only blade is formed (Toriba et al., 2019). These findings indicate that *BOP* genes are also involved in proximal-distal patterning in grass species. In addition, Arabidopsis *AtBOP1* and *AtBOP2* are involved in the adaxial-abaxial patterning of the leaf (Ha et al., 2007). *AtBOP1* and *AtBOP2* promote the adaxial cell fate by activating the expression of *AtASYMMETRIC LEAVES2* (*AtAS2*) at the adaxial base of the leaf (Jun et al., 2010). *AtAS2* is one of the factors promoting the adaxial cell fates (reviewed in Du et al., 2018). Mutation in *AtAS2* gene leads to downwardly curled leaves (Iwakawa et al., 2007). In Arabidopsis *Atbop1;Atbop2* mutants abaxialized vasculature is formed in the leaf petiole, and this vascular patterning defect is greatly enhanced in the *Atbop1;Atbop2;Atas2* leaf petioles (Ha et al., 2007).

The role of *BOP* in plant architecture and leaf patterning has only been described in herbaceous model species. Here, we created a *bop* mutant in a tree aiming to determine to what extent its functioning is conserved in trees. For this we used *Parasponia andersonii*, as a fast and efficient transformation protocol has been established (van Zeijl et al., 2018; Wardhani et al., 2019). *Parasponia* spp. are fast-growing tropical trees, capable of covering nitrogen-poor eroded soils in a relatively short time span (Becking, 1992). What makes *Parasponia* intriguing is that it is the only non-legume genus which can form nitrogen-fixing root nodules.

The genome of *P. andersonii* contains only one putative *BOP* gene, *PanNODULE ROOT1* (*PanNOOT1*) (van Velzen et al., 2018). We generated CRISPR/Cas9 knockout mutants of *PanNOOT1*, to our knowledge, the first *bop* gene mutant in a tree. The functions of *PanNOOT1* in branching and leaf patterning were characterized. We show that in the *Pannoot1* mutants the axillary branch growth is reduced, and the leaf patterning along the proximal-distal and adaxial-abaxial axes is affected. Further, we show that the stipule formation is disturbed and organ fusion between the stem and petiole occurs in the *Pannoot1* mutants.

RESULTS

Pannoot1 Mutants Show Reduced Axillary Branch Growth

To investigate the function of *PanNOOT1* in *Parasponia* (*P. andersonii*) shoot branching, we generated two independent CRISPR/Cas9 *Pannoot1* mutant lines, named A5 and A10 (Supplementary Figure 1). Both lines were grown in soil for 10 weeks and phenotypically compared to a wild-type (*P. andersonii* WU1-14) and a transgenic control line (Ctr44) containing the CRISPR/Cas9 cassette and kanamycin resistance genes but no guide RNA. We observed that both *Pannoot1* mutant lines formed shorter axillary branches than wild-type or the transgenic control line (Figure 1A-H). To quantify this difference, we measured the lengths of all visible branches in all four lines; wild-type, transgenic control line, and two *Pannoot1* mutant lines. This revealed that branches formed on the two *Pannoot1* mutant lines were markedly shorter, compared with wild-type or transgenic control line (Figure 1I). This indicates that knockout of *PanNOOT1* negatively affects axillary branch length. Next, we compared branch length at a specific node position. As our plants are derived from tissue culture, it is difficult to synchronize the developmental status of the plant. For this reason, we monitored the internode length and determined that, from the top-down, the last internode that is shorter than the next internode is the last elongating internode. We determined at which position of the plant this internode is found and designated the basal node belonging to this internode as N0 (see an example in Supplementary Figure 2A). From this point we numbered all consecutive nodes downwards. We selected five nodes (N1-N5) per plant and for each node, the length of its axillary branch was determined. This revealed that the branch length per node was significantly reduced in both *Pannoot1* mutant lines (Figure 1J, Supplementary Figure 2B). These results indicate that the axillary branch growth is drastically reduced in both *Pannoot1* mutant lines.

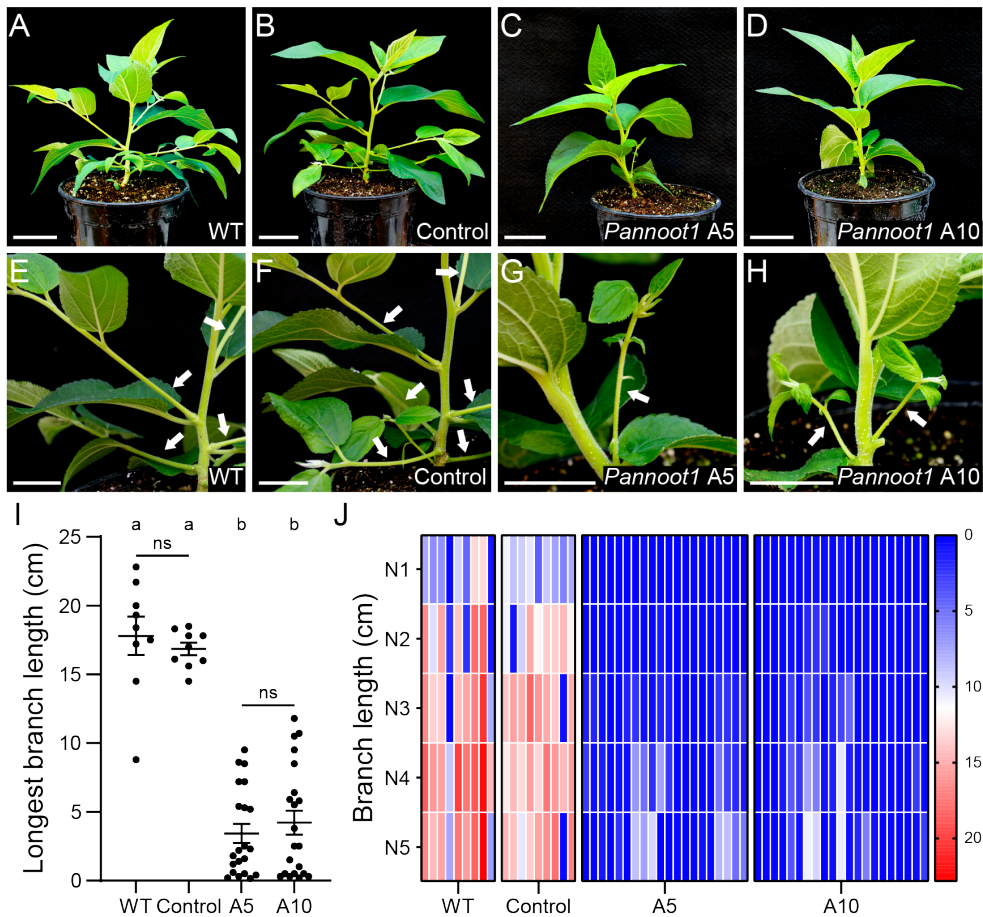


Figure 1. *Pannoot1* Mutants Show Reduced Axillary Branch Growth. (A-H) Representative plants of wild-type (A, E), transgenic control line (B, F), and two independent *Pannoot1* mutant lines A5 (C, G) and A10 (D, H) grown in soil for 10 weeks. (E-H) A close-up view of the basal region of the plants shown in (A-D), respectively. Arrows indicate axillary branches, which are shorter in the two *Pannoot1* mutant lines A5 (G) and A10 (H), compared with wild-type (E) and control line (F). (I) The longest branch formed by each plant is significantly reduced in the two *Pannoot1* mutant lines A5 (n=21) and A10 (n=21), compared with wild-type (n=9) and control line (n=9). Each dot represents the length of the longest branch formed in a single plant. Data are mean \pm SD. One-way ANOVA with Tukey's multiple comparisons test was performed to assess significant differences. Lowercase letters indicate statistically different groups ($P < 0.0001$, ns: not significant). (J) The lengths of branches formed at each node are visualized in a heatmap image according to the color scale shown in the right-hand panel. The heat map shows that the overall branch lengths are reduced in the two *Pannoot1* mutant lines A5 (n=20) and A10 (n=21), compared with wild-type (n=9) and control line (n=9). Each column represents a single plant. See Supplementary Figure 2A for an example of node numbering. Scale bars: 5 cm (A-D), 2.5 cm (E-H).

Interestingly, many of the *Pannoot1* axillary branches at the apical nodes (N1&N2) remained at a bud-like stage (<0.5 cm), in contrast to the elongating branches in the control lines (Figure 1J, Supplementary Figure 2B). Nevertheless, those *Pannoot1* axillary buds elongated at the basal nodes (N4&N5) (Figure 1J, Supplementary Figure 2B), suggesting that the outgrowth of axillary buds is delayed in the *Pannoot1* mutants.

***Pannoot1* Mutants Show Delayed Axillary Bud Development**

To investigate whether the reduced axillary branch growth in *Parasponia Pannoot1* mutants is due to a delay in axillary bud development, we longitudinally sectioned the shoot apex region and compared the position of the first visible axillary bud between *Pannoot1* and the transgenic control line by using confocal microscopy. Since both *Pannoot1* mutant lines (A5 and A10) showed similar phenotypes regarding axillary branch development, we chose to focus our analysis on a single line in this comparison; namely A5 line. In the transgenic control line, the first visible axillary buds usually occurred in the leaf axil of P5 (Figure 2A-B). In contrast, in the *Pannoot1* A5 line the first visible axillary buds were usually found in the axil of P7 (Figure 2E-F, 2K). We also noticed that the first visible axillary buds in the control line were usually relatively bigger than the ones in the *Pannoot1* mutant line. This suggests that axillary buds of the control line can be already formed in the axils before P5. Therefore, we further performed cross sections on the shoot apex of the control line to determine the position of the first visible axillary buds. This revealed that the first visible axillary buds usually occurred in the leaf axil of P3 (Figure 2I-J, 2K). These results indicate that the axillary bud emergence in the *Pannoot1* mutants is delayed. Moreover, we found that the axillary buds of the transgenic control line rapidly elongate after their emergence (Figure 2B-D). In contrast, *Pannoot1* axillary buds develop slowly and remained small at the subsequent stages (Figure 2F-H). The difference in the outgrowth of axillary bud between the control line and *Pannoot1* mutant is consistent with the difference in branch length observed at the basal part of plants (Figure 1J, Supplementary Figure 2B). This suggests that the not only axillary bud emergence is delayed in the *Pannoot1* mutants, but also their outgrowth.

In addition to a change in the temporal bud emergence and outgrowth, we also found that the position of axillary buds in the *Pannoot1* mutants was shifted towards the petiole. In wild-type and the transgenic control line buds were

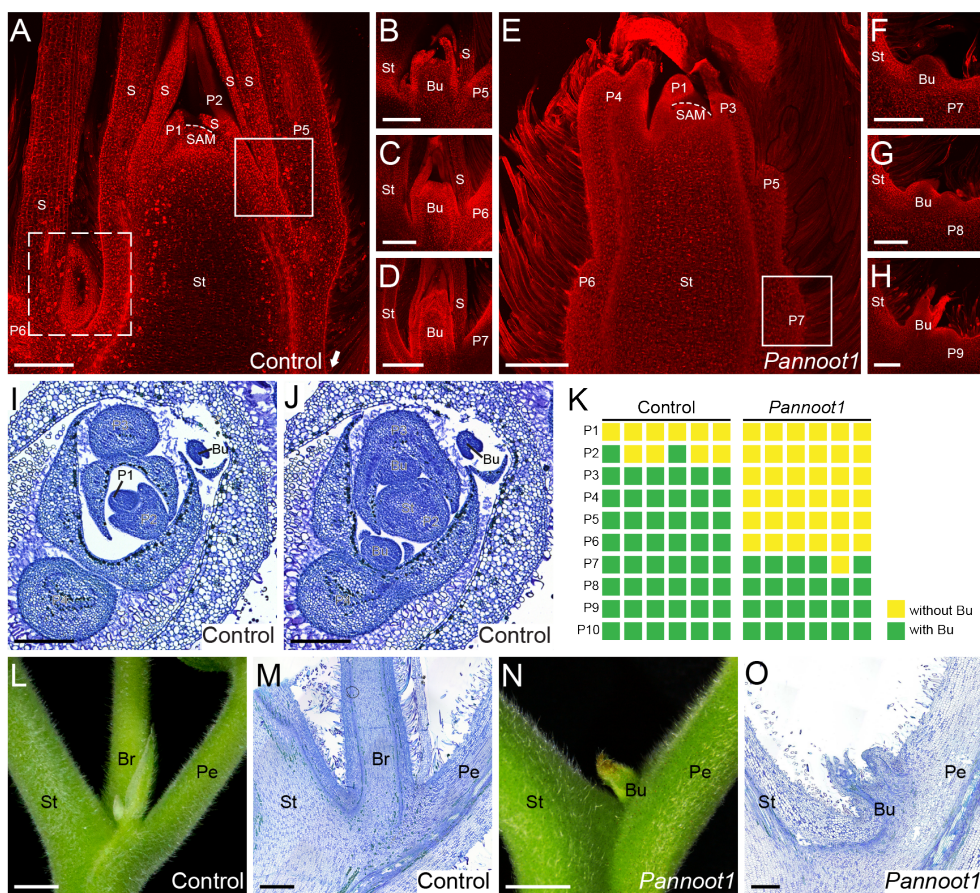


Figure 2. The Axillary Buds of the *Pannoot1* Mutants Show Developmental Defects. (A-H) Representative confocal image of longitudinal section of the shoot apical region in the transgenic control line (A-D) and *Pannoot1* mutant A5 line (E-H). This shows that the emergence and outgrowth of axillary buds are delayed in the *Pannoot1* mutants. (B-D) The first (B), second (C) and third (D) visible axillary bud (Bu) of a single control line plant, which is indicated by white line box, white dotted line box and arrow, respectively in (A). Note that the axillary bud of the control line is first observed in the axil of P5, and drastically grows at the subsequent stages. (F-H) The first (F), second (G) and third (H) visible axillary bud (Bu) of a single *Pannoot1* mutant plant shown in (E). Note that the first visible axillary bud of the *Pannoot1* mutant is formed in the axil of P7 (the white line boxed region in (E)), and remain small at the subsequent stages. (I, J) Two sequential cross sections of the shoot apex of a single control line plant, showing that axillary bud is first formed in the axil of P3. Leaf primordium numbering in (A-J) was based on a series of sections. (K) Schematic representation of axillary bud emergence in leaf axils of the control line (n=6), and the *Pannoot1* mutant A5 line (n=6) grown in soil for 8 weeks. This shows that the axillary bud emergence is delayed in the *Pannoot1* mutants. Each column represents a single plant, and each square within a column

Continued on next page

formed at the axil between the petiole and the stem (Figure 2B-D). However, in the *Pannoot1* mutants we found that the axillary buds have shifted towards the proximal region of petioles (Figure 2F-H). Consistently, the majority of *Pannoot1* mutant branches (including buds (<0.5 cm)) are positioned at the proximal region of petioles (Figure 2N). To confirm this displacement, we made longitudinal sections of nodes from position N2. This showed that in the transgenic control line axillary branches are positioned between the petiole and the stem, confirming that the axillary branch is formed at the leaf axil (Figure 2L). However, in the *Pannoot1* mutants the axillary buds are often located on the petioles (Figure 2O). Taken together, these results indicate that the position of axillary bud formation is shifted in the *Pannoot1* mutants.

Based on these observations we concluded that *PanNOOT1* is involved in the emergence, outgrowth and positioning of axillary buds.

***Pannoot1* Mutants Show Defects in Stipule Formation**

Previous studies have shown that *AtBOPs* and their orthologs in Arabidopsis, pea, Medicago and Lotus are essential for stipule development (McKim et al., 2008; Ichihashi et al., 2011; Couzigou et al., 2012; Magne et al., 2018). This prompted us to examine if this process is also affected in the *Pannoot1* mutant trees. In wild-type and the transgenic control line, stipules are formed at the adaxial side of all leaves examined (Figure 3A-D). However, in *Pannoot1* most of leaf axils do not form any visible stipules (Figure 3E). The absence of stipules

Continued

indicates an individual leaf (primordium) axil. The top row represents the axils of the first visible leaf primordia (P1), with positions of progressively to older leaf primordia (P2 to P10) below it. Yellow denotes the absence of a visible axillary bud and green denotes the presence of a visible axillary bud in any particular leaf axil. (L-O) Representative overview (L, N) and longitudinal section (M, O) of the axillary branch (Br) /bud formed at N2. (L) The formation of axillary branches is between the petiole and the stem in the control line (105/105, n=9), which is consistent with the placement of axillary buds shown in (B-D). Similar phenotype was observed in wild-type (103/103, n=9). (N) The position of axillary buds is shifted towards the proximal region of petioles in the *Pannoot1* mutants (A5: 118/159, n=20; A10: 126/180, n=21), which is consistent with the shifted position of axillary buds shown in (F-H). The position of axillary branch/bud in the control line and *Pannoot1* mutants is confirmed by the section shown in (M) and (O), respectively. White dotted line outlines the shoot apical meristem (SAM); P, leaf primordium; S, stipule primordium; St, stem; Pe, petiole. Scale bars: 250 µm (A-J), 2.5 mm (L, N) 500 µm (M, O).



Continued on next page

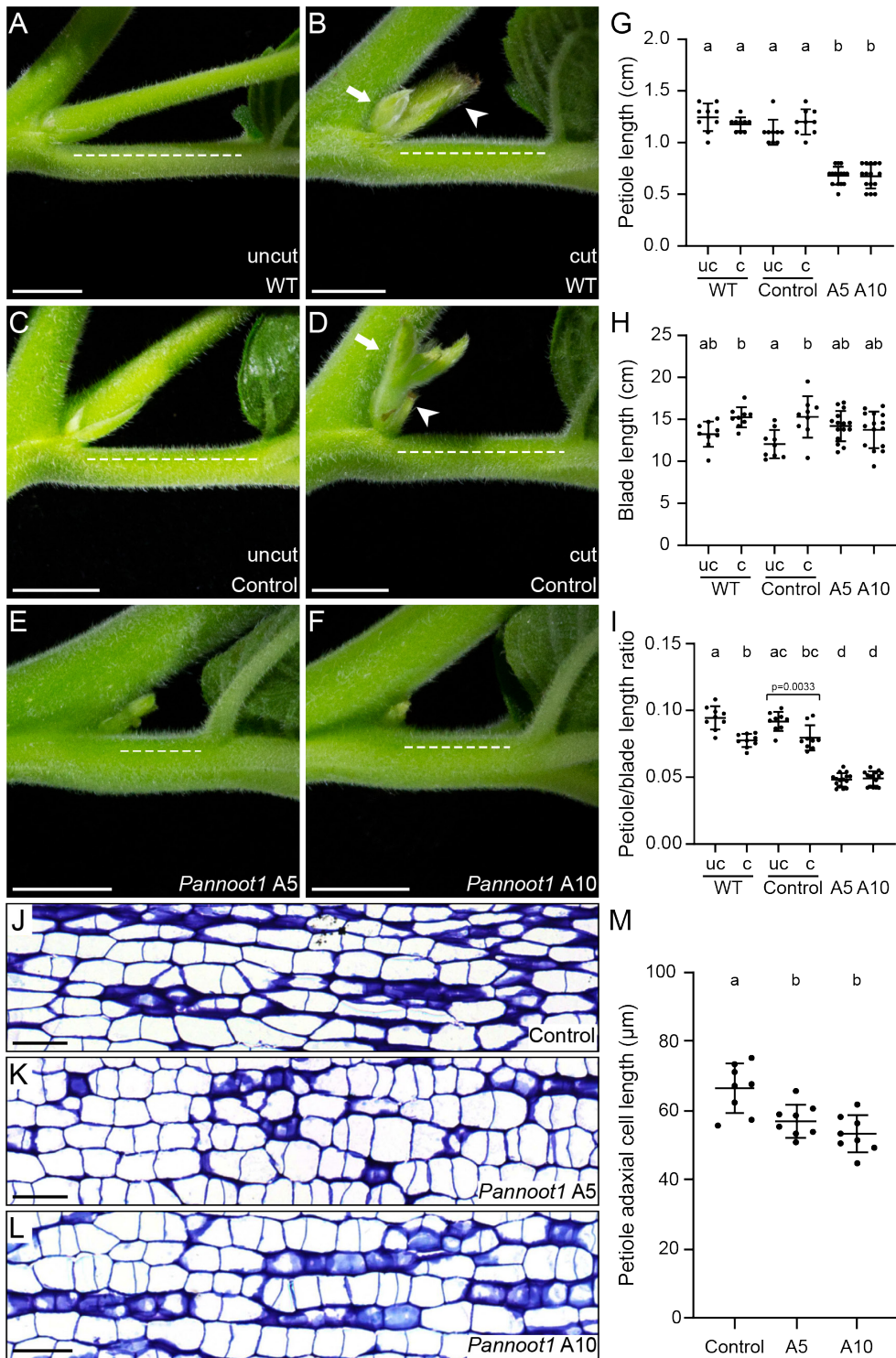
was confirmed by analysing longitudinal sections of the petiole axils (Figure 3H-I). Interestingly, in some of the *Pannoot1* mutants leafy tissues were formed on the petiole next to the branches (Figure 3F-G). These structures do not resemble the stipules formed on wild-type or the transgenic control line (Figure 3A-D). To identify the origin of stipules in *Parasponia* we investigated the leaf primordium stage in the control line. We found that stipules are formed at the adaxial side of leaf primordia already at P2 (Figure 3J). Together with leaf primordia, stipules drastically enlarge and elongate at the subsequent stages (Figure 3J). However, in the *Pannoot1* mutants stipules are not formed (Figure 3K-L). This indicates that stipule formation is disturbed in the *Pannoot1* mutants.

***Pannoot1* Mutants Show Shorter Leaf Petiole**

Leaf architecture is often drastically modified in *bop* mutants of several plant species (Ha et al., 2003; Couzigou et al., 2012; Tavakol et al., 2015; Magne et al., 2018; Toriba et al., 2019). Therefore, we investigated whether the leaf architecture of *Parasponia Pannoot1* mutants is also affected. This revealed that the petiole length of the *Pannoot1* mutants is shorter compared with wild-type and transgenic control line (Figure 4A-B, 4E-F). To quantify the difference,

Continued

Figure 3. The Formation of Stipules Is Disturbed in the *Pannoot1* Mutants. (A-D) Stipules are formed at the adaxial side of petioles in wild-type (A) (105/105, n=9) and the transgenic control line (B-D) (103/103, n=9). (C) A view of the adaxial side of a petiole (abaxial side of axillary branch), showing two pieces of stipules. Note that the petiole was removed to visualize stipules. (D) Two pieces of stipules separated from an axillary branch. (E) A majority of the *Pannoot1* mutants (A5: 35/46, n=20; A10: 39/56, n=21) do not form stipules at the adaxial side of petioles). (F, G) Leafy tissues occur at the adaxial side of some petioles (abaxial side of axillary branch) in the *Pannoot1* mutants (A5: 11/46, n=20, A10: 17/56, n=21). (G) An abaxial view of the branch in (F). (H, I) Representative longitudinal sections of the basal part of branches in the control line (H) and the *Pannoot1* mutants (I), showing the absence of stipule in the *Pannoot1* mutants. (J-L) Representative confocal images of longitudinal sections of the shoot apical region in the control line (J) and the *Pannoot1* mutant A5 line (K, L). (J) Stipules are formed at the adaxial side of leaf primordium at P2 stage. (K, L) Two sequential sections of a single plant, showing the absence of stipule formation in the *Pannoot1* mutants. Yellow dotted lines outline the leaf primordia, cyan dotted lines outline the stipule primordia. Arrows indicate stipules, arrowheads indicate the absence of stipules, double arrowheads indicate leafy tissues. St, stem; Pe, petiole; Br, axillary branch; P, leaf primordium; S, stipule primordium. Scale bars: 0.5 cm (A, B, E, F), 0.25 cm (C, D, G), 500 µm (H, I), 250 µm (J-L).



we measured the length of petiole and blade formed at N1, N2 and N3. We found that the length of petiole and the ratio between the petiole and blade length are significantly reduced in the *Pannoot1* mutants (~50% reduction in both parameters), compared with wild-type and transgenic control line, irrespectively of the node position (Figure 4G-I, Supplementary Figure 3). To rule out the possibility that this could be a secondary consequence of shorter axillary branches formed by the *Pannoot1* mutants, we included an additional control experiment, in which emerging axillary branches of wild-type and transgenic control line were cut since plantlet stage (Figure 4B, 4D). In this way, shoot architecture of wild-type and transgenic control line resembles that of the *Pannoot1* mutants. This revealed that the petiole length and the ratio between the petiole and blade length of these cut wild-type and transgenic control line are markedly longer than those of the *Pannoot1* mutants, irrespectively of the node position (Figure 4G-I, Supplementary Figure 3). This indicates that the shorter petioles formed by the *Pannoot1* mutants is not a secondary effect of the arrested axillary shoot growth. Further, the reduced ratio between the petiole and blade length in the *Pannoot1* mutants indicates that the proximal (petiole)-distal (blade) patterning of leaf architecture is affected.

Next, we investigated whether the shorter petiole of *Pannoot1* is caused by reduced cell size in the petiole. We therefore performed longitudinal sections on *Pannoot1* petioles and measured the cell length of collenchymatous cells

Continued

Figure 4. The Petiole Length of the *Pannoot1* Mutants Is Remarkably Reduced. (A-F) Representative petioles formed at N2 in wild-type (A, B), transgenic control line (C, D), and two *Pannoot1* mutant lines A5 (E) and A10 (F). Branches were uncut in (A, C, E and F); cut in (B and D). White dotted lines indicate the petiole length. Arrowheads indicate cut branches, arrows indicate elongated collateral buds. (G-I) The petiole length (G) and the ratio between the petiole and blade length (I) are significantly reduced in the two *Pannoot1* mutant lines, but the blade length (H) is not affected. Each dot represents the length of petiole (G), the length of blade (H) and the ratio between the lengths of petiole and blade (I) formed at N1 of a single plant (uncut wild-type: n=9, cut wild-type: n=9, uncut control: n=9, cut control: n=9, A5: n=15, A10: n=15). (J-L) Representative longitudinal sections of the adaxial side of petioles formed at N1 in the control line (J) and two *Pannoot1* mutant lines A5 (K) and A10 (L). (M) The length of collenchymatous cells was significantly reduced in the two *Pannoot1* mutant lines (control: n=8, A5: n=8, A10: n=8). Data are mean \pm SD. One-way ANOVA with Tukey's multiple comparisons test was performed to assess significant differences. Lowercase letters indicate statistically different groups ($P < 0.0001$ in (G), $P < 0.01$ in (H), $P < 0.001$ in (I), $P < 0.05$ in (M), ns: not significant). uc, uncut; c: cut. Scale bars: 0.5 cm (A-F), 100 μ m (J-L).

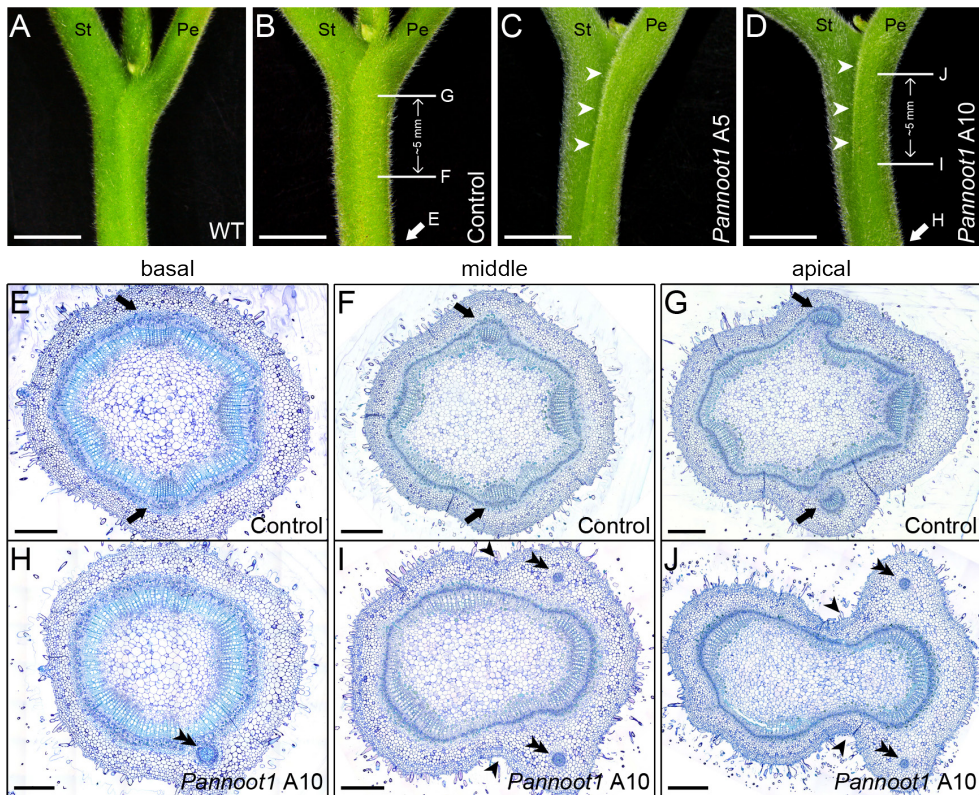


Figure 5. Organ Fusion Occurs in the *Pannoot1* Mutants. (A-D) Overview of the internode below N1 in wild-type (A), transgenic control line (B), and two *Pannoot1* mutant lines A5 (C) and A10 (D). (C, D) Grooves occur on the internode in the *Pannoot1* mutants, as indicated by arrowheads. (E-J) Cross sections of the internode below N1 of the control line (E-G) and *Pannoot1* A10 line (H-J) at the positions as indicated in (B) and (D), respectively. Arrows indicate the petiole-connected vasculatures have merged (E, F) or are merging (G) with the stem vasculature in the control line. Double arrowheads indicate the petiole-derived vasculatures are already deviating (H) or deviated (I, J) from the stem vasculature in the *Pannoot1* mutants. The tissues surrounding the petiole-connected vasculatures in the *Pannoot1* mutants form the grooves shown in (C) and (D). St, stem; Pe, petiole. Scale bars: 0.5 cm (A-D), 500 μ m (E-J).

(Figure 4J-L), which are the main constitute of the petiole besides vasculature. We found that the length of collenchymatous cells was significantly reduced (~10% reduction) in the *Pannoot1* mutants, compared with transgenic control line (Figure 4M). This suggests that the reduced length of collenchymatous cells contributes to the shorter petiole phenotype observed in the *Pannoot1* mutants.

***Pannoot1* Mutants Show Organ Fusion**

It appears that the reduced petiole cell length (~10% reduction) cannot fully explain the shorter petiole phenotype (~50% reduction) of *Parasponia Pannoot1* mutants. Thus, other defect(s) could also contribute to this phenotype. It has been shown that mutation in *BOP* genes in *Arabidopsis* and tomato (*Solanum lycopersicum*), organ fusion could occur (Hepworth et al., 2005; Xu et al., 2016). Therefore, the shorter petiole length in the *Pannoot1* mutants could be associated with organ fusion between the petiole and the stem. To investigate this, we compared the region where petiole attaches to the stem and found that in the *Pannoot1* mutants grooves are formed on the stem at the basal region of the petiole, suggestive of organ fusion between the petiole and the stem (Figure 5C-D). Such grooves were not observed in the region where petiole attaches to the stem in wild-type or transgenic control line (Figure 5A-B). To obtain further insight into the organ fusion, we performed cross section at three positions (basal, middle and apical) on the internode, and compared the vascular system between the *Pannoot1* mutants and the transgenic control line. We found that in the transgenic control line at the basal and middle position of internode, the vasculatures connecting the petiole vascular system are fully merged with stem vascular system (Figure 5E-F). Only at the apical position, the petiole vascular system starts to deviate from the stem vasculature (Figure 5G). However, in the *Pannoot1* mutants petiole-connected vasculature is already deviating from the stem vascular system at the basal position of internode (Figure 5H). Further, at the middle and apical positions of the *Pannoot1* internode, abaxialized vasculatures (phloem cells surrounding xylem cells), which connect petiole vasculature, are already at the peripheral region of the main vascular system (Figure 5I-J). This indicates that at the apical and middle positions of the *Pannoot1* internode, the petiole vascular system is already partially disconnected with the stem vasculature, and the disconnected vasculatures and the surrounding cells form the grooves along the region where petiole attaches to the stem. These results demonstrate that organ fusion between the petiole and the stem indeed occurs in the *Pannoot1* mutants, and suggest that the defect in separating these two

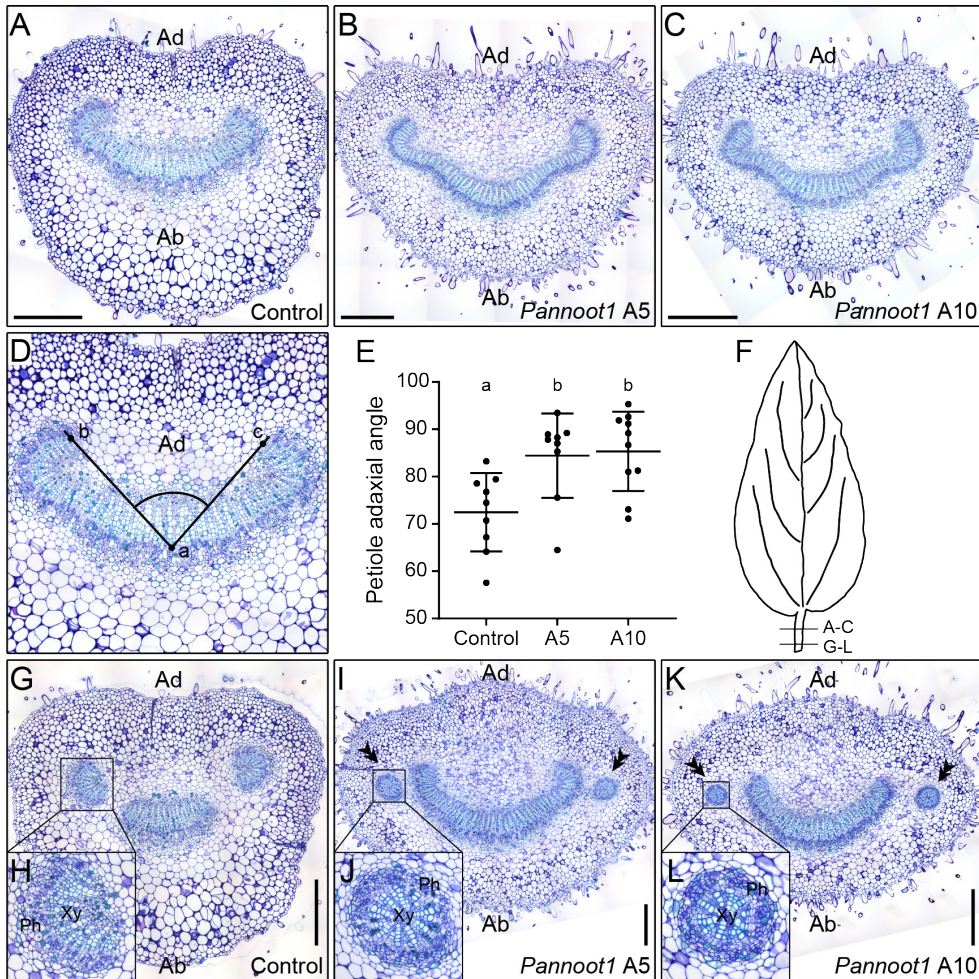


Figure 6. The Petioles of the *Pannoot1* Mutants Are Downwardly Curled and Abaxialized. (A–C) Representative cross sections of the distal part of petioles formed at N1 in the transgenic control line (A) and two *Pannoot1* mutant lines A5 (B) and A10 (C). These sections show that polarized vasculatures occur in the petioles of control and mutant lines, with xylem cells at the adaxial side and phloem cells at the abaxial side. (D) Illustration of how the adaxial angle of petiole vasculature was determined. The middle position (indicated by lowercase letter a) is in the middle region of cambium cells. The two peripheral positions (indicated by lowercase letters b and c) are at the edges of xylem cell files. (E) The adaxial angle of petiole vasculature is significantly increased in the *Pannoot1* mutants, compared with control line, showing a downwardly curled patterning. Each dot represents the adaxial angle of petiole vasculature of a single plant (control: n=9, A5: n=9, A10: n=10). Data are mean \pm SD. One-way ANOVA with Tukey's multiple comparisons test was performed to assess significant differences. Lowercase letters indicate statistically different groups ($P < 0.05$). (F) Illustration of the position of sections shown in (A–

Continued on next page

organs could be associated with the *Pannoot1* shorter petiole phenotype.

***Pannoot1* Mutants Show Abaxialized Leaf Petiole**

The petiole-connected abaxialized vasculature in the *Parasponia Pannoot1* mutant stems is reminiscent of the structure of *Arabidopsis Atbop1;Atbop2* mutant petiole vasculatures, suggesting the vascular system in the *Pannoot1* petioles is also affected. We therefore analysed the internal morphology of *Pannoot1* petioles by cross sections. The petioles of the transgenic control line contain polarized vascular bundles consisting of xylem on the adaxial side and phloem on the abaxial side. A similar composition was also observed in the *Pannoot1* mutants (Figure 6A-C). However, we found that the tissue organization of the *Pannoot1* petioles become more downwardly curled, as the adaxial angle of petiole vasculature is significantly increased in the two mutant lines (Figure 6D-E). Interestingly, at the proximal position of leaf petioles nearly half of the *Pannoot1* mutant petioles (A5: 12/27, A10: 18/30) displayed additional abaxialized vasculature(s) at the peripheral region of the central petiole vasculature (Figure 6I-L, Supplementary Figure 4B-C). Such abaxialized vasculature was not seen in control petioles (Figure 6G-H, Supplementary Figure 4A). This is in line with the structure of petiole-connected vasculatures observed in the *Pannoot1* mutant stems (Figure 5H-J), corroborating that those abaxialized vasculatures present in the *Pannoot1* stems connect with the vascular system in the petioles. A similar phenotype of downwardly curled leaf and abaxialized vasculature has been reported in *Arabidopsis* mutated in genes promoting leaf adaxial cell fate (Ha et al., 2007; Jun et al., 2010). Therefore, we conclude that the adaxial-abaxial patterning of leaf architecture is affected in the *Pannoot1* mutants.

Continued

C, G-L) on the petiole. **(G-L)** Representative cross sections of the proximal part of petioles formed at N1 in the control line **(G, H)** and two *Pannoot1* mutant lines A5 **(I, J)** and A10 **(K, L)**. *Pannoot1* mutants form abaxialized vasculatures, in which xylem cells are surrounded by phloem cells. Such abaxialized vasculatures are not present in the control line, which have vasculatures of a half-moon shape at the periphery. **(H, J, L)** A close-up view of the boxed region in **(G, I, K)**, respectively. Ad, adaxial side; Ab, abaxial side; Xy, xylem; Ph, phloem. Scale bars: 500 µm.

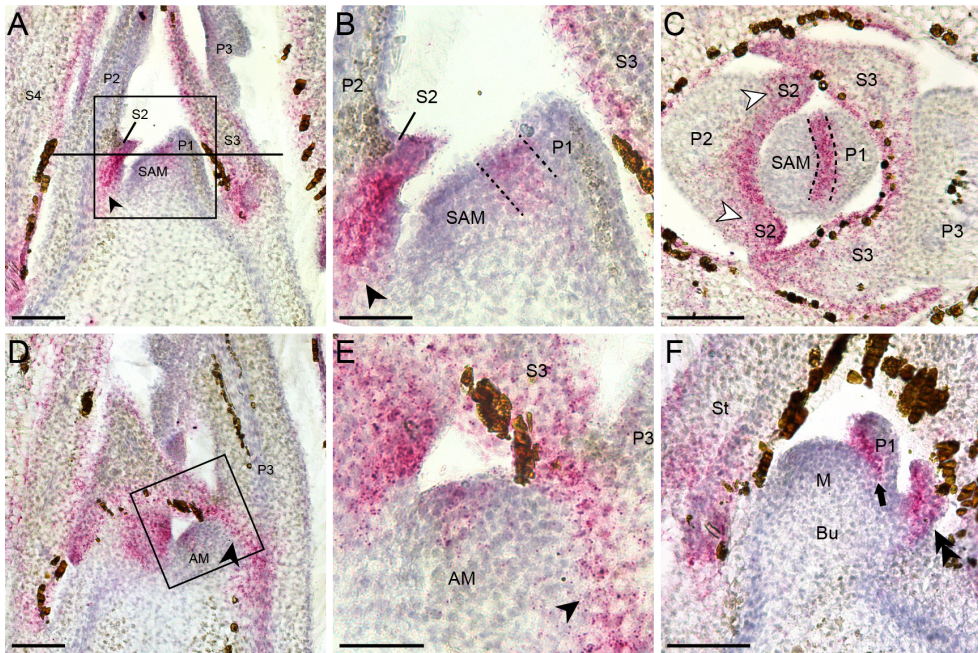


Figure 7. *PanNOOT1* Expression Pattern in the Shoot Apical Region by *in situ* Hybridization. Longitudinal sections (**A**, **B**, **D-F**) and cross section (**C**) of the shoot apical region in wild-type. (**A-C**) *PanNOOT1* is expressed in the boundary region between the shoot apical meristem and P1, and in the developing stipule primordia (S2 and S3). Further, *PanNOOT1* transcripts occur at the base of P2 on the adaxial side, indicated by black arrowhead. (**B**) A close-up view the boxed region in (**A**). Dotted lines mark the boundary region between the SAM and P1. White arrowheads in (**C**) indicate the base of S2. (**D**) A sequential section of the shoot apical region shown in (**A**). *PanNOOT1* is expressed in the axillary meristem, and at the adaxial base of P3, indicated by arrowhead. (**E**) A close-up view of the boxed region in (**D**). (**F**) In the axillary bud, *PanNOOT1* is expressed in the boundary region between the axillary bud meristem and P1, indicated by arrow. *PanNOOT1* is also expressed in the leaf primordia at later stage, indicated by double arrowheads. Red dots represent mRNA molecules. SAM, shoot apical meristem; P, leaf primordium; S, stipule primordium; AM, axillary meristem; Bu, axillary bud; M, axillary bud meristem; St, stipule. Scale bars: 100 μ m (**A**, **C**, **D**, **F**), 50 μ m (**B**, **E**).

The Expression Pattern of *PanNOOT1* by *in situ* Hybridization

To determine whether the observed phenotypes could be controlled by *PanNOOT1* in a cell autonomous fashion, we performed *in situ* hybridization in the shoot apical region. We found that *PanNOOT1* is expressed in the boundary region between the SAM and P1 (Figure 7A-C), suggesting that *PanNOOT1* is involved in the boundary formation. At the later leaf primordium stages (P2 and P3), *PanNOOT1* transcript was dominantly detected at the base of the leaf primordium on the adaxial side adjacent to SAM (Figure 7A-B, D). Also, *PanNOOT1* mRNA occurs in the developing stipules (S2 and S3) (Figure 7A-B). This is consistent with the disturbed formation of stipules observed in *Pannoot1*. *PanNOOT1* is also expressed in the axillary meristem prior to the axillary bud emergence (Figure 7E). In the emerging axillary buds, *PanNOOT1* transcripts occurs in boundary region between the axillary bud meristem and P1, and in the more developed leaf primordia (Figure 7F). These results indicate that *PanNOOT1* is expressed in the tissues, of which development is affected in the *Pannoot1* mutants, suggesting that *PanNOOT1* acts in a cell autonomous manner.

DISCUSSION

In this study, we have shown that a knockout of *PanNOOT1* gene in *Parasponia* causes three major developmental defects: (1) axillary branch growth is drastically reduced due to delayed axillary bud emergence and outgrowth; (2) stipules formation is disturbed; and (3) leaf patterning is disturbed along the proximal-distal and adaxial-abaxial axes. These phenotypes are comparable to those reported *bop* mutants in several species, including *Arabidopsis*, pea, *Medicago*, rice and barley. This demonstrates that *Parasponia PanNOOT1* is a *BOP* gene, required for axillary branch development, stipule formation, and leaf patterning.

PanNOOT1 Regulates Axillary Branch Development

We showed that the emergence and outgrowth of axillary buds are delayed in the *Pannoot1* mutants, compared with wild-type and transgenic control line. These defects result in reduced axillary branch growth. This is consistent with the role of *BOP* gene (*HvCul4*) in barley, in which *Hvcul4* mutants also show reduced axillary branching (Tavakol et al., 2015). Further, the expression pattern

of *PanNOOT1* is axillary meristem and axillary buds is similar to *HvCul4*. To our knowledge, this is the first time the function of *BOP* genes in branching has been characterized in a dicot. This suggests that the role of *BOP* genes in promoting axillary branch development is well-conserved between monocots and dicots.

Axillary meristems are formed in the centre of the boundary zone at the adaxial side of leaf axils (Teichmann and Muhr, 2015). We show that the positioning of axillary buds is shifted towards the petiole in *Parasponia Pannoot1* mutants, suggesting the boundary formation is disturbed. This is in line with the reported function of *BOP* genes in the specification of boundary region (reviewed in Žádníková and Simon, 2014; Hepworth and Pautot, 2015; Wang et al., 2016). In *Arabidopsis*, *AtBOP1* and *AtBOP2* can promote expression of *LATERAL ORGAN BOUNDARIES (LOB)* genes to repress brassinosteroid signalling, leading to the repression of cell growth and division in the boundary region between the SAM and leaf primordium (Ha et al., 2007; Bell et al., 2012). Loss-of-function *Arabidopsis Atlob* mutants exhibit organ fusions between the axillary branch and leaf tissues, and expanded expression pattern of boundary markers *AtLATERAL ORGAN FUSION1* and *AtORGAN BOUNDARY1* into the fused region. This implies that *Atlob* mutants have an expansion of the boundary resulting in organ separation defects (Bell et al., 2012). Further, inactivation of *Arabidopsis AtBOP1* and *AtBOP2* genes leads to fused flower organs (Hepworth et al., 2005), which also occur in tomato *Slbop2* and *Slbop3* mutants (Xu et al., 2016). Similar to *Atbop1;Atbop2*, *Slbop2/3*, and *Atlob* mutants, organ fusion also occurs in the *Pannoot1* mutants: the stem and the petiole are fused. This suggests that in the *Pannoot1* mutants the boundary region is between the stem and petiole expanded, leading to the shifted positioning of axillary buds. In line with this study, silencing of three tomato *SIBOP* genes also shifts the position of axillary meristem from the leaf axil to the proximal region of petioles (Izhaki et al., 2018). Together with the expression of *PanNOOT1* at the boundary between the SAM and P1, it demonstrates that *PanNOOT1* is involved in the formation of the SAM-petiole boundary, which is a prerequisite for the correct positioning of axillary buds.

We hypothesize that *PanNOOT1* regulates axillary branch development in three ways: (1) specifying the boundary formation between the stem and the petiole to ensure the correct positioning of axillary buds; (2) inducing axillary bud emergence; and (3) promoting axillary bud outgrowth.

***PanNOOT1* Regulates Stipule Formation and Leaf Patterning**

The disturbed stipule formation in *Parasponia Pannoot1* mutants is reminiscent of the mutation in *BOP* genes in several other plant species (*Arabidopsis Atbop1;Atbop2*, *Medicago Mtnoot1*, pea *Pscoch1*, and *Lotus Ljncbl1*), in which the stipules/nectary glands are absent or reduced (McKim et al., 2008; Ichihashi et al., 2011; Couzigou et al., 2012; Magne et al., 2018). Further, in *Parasponia PanNOOT1* is expressed in the stipule primordia, which is similar to the expression pattern of the *BOP* gene *PsCOCH1* in pea (Couzigou et al., 2012). These findings support that *PanNOOT1* is indeed a *BOP* gene, and the functions in modifying the proximal region of the leaf in *Parasponia*.

We also showed that the proximal-distal patterning and adaxial-abaxial patterning are affected in *Parasponia Pannoot1* mutants. In *Arabidopsis Atbop1;Atbop2* mutants, the leaf proximal-distal patterning is also disturbed; blade tissues develop along the petiole, resulting in the loss of distinct proximal and distal zones in the leaf (Hepworth et al., 2005). Ichihashi et al. revealed that in *Arabidopsis* a proliferative zone is established at the leaf blade-petiole junction shortly after leaf primordia initiation. It has been suggested that *AtBOPs* are required for the correct positioning of this proliferative zone, regulating the proximal-distal patterning of the leaf petiole and blade (Ichihashi et al., 2011). Similarly, in barley *Hvcu4* and rice *Osbop* mutants, the proximal-distal patterning is also affected (Tavakol et al., 2015; Toriba et al., 2019). Especially in rice *Osbop1;Osbop2;Osbop3* triple mutants, the proximal sheath differentiation is abolished, indicating that *OsBOP* genes promote the proximal sheath development (Toriba et al., 2019). Combining with the shorter petiole phenotype and reduced ratio between the (proximal) petiole and (distal) blade length in the *Pannoot1* mutants, it appears that *PanNOOT1* coordinates the proximal-distal patterning of leaves by promoting the growth of petioles.

The occurrence of abaxialized vasculature (xylem cells surrounded by phloem cells) in the *Pannoot1* petioles is similar with the defect observed in *Atbop1;Atbop2* mutants (Ha et al., 2007). The downwardly curled petiole of *Pannoot1* mutants is reminiscent of the knockout mutant in *AtAS2* gene, which promotes adaxial cell fate (Jun et al., 2010). Therefore, the vascular patterning defect and downwardly curled petioles observed in the *Pannoot1* petioles imply that the adaxial cell fate is suppressed. Further, *PanNOOT1* is expressed at the base of leaf primordia on the adaxial side. This is consistent with the expression pattern of *AtBOP1* and *AtBOP2* in leaf primordia, where they induce the specific

activation of *AtAS2* in the proximal, adaxial region of the leaf (Jun et al., 2010). This suggests that similar to *AtBOP1* and *AtBOP2*, *PanNOOT1* modulates the leaf patterning along the adaxial-abaxial axis by promoting adaxial cell fate. Therefore, in *Parasponia* *PanNOOT1* appears to regulate leaf architecture in three ways: (1) inducing stipule formation at the proximal region of leaf; (2) modulating proximal-distal patterning by regulating the petiole length; (3) modulating adaxial-abaxial patterning by promoting adaxial cell fate of leaf petiole.

METHODS

Plant Materials and Growth Conditions

Pannoot1 CRISPR/Cas9 mutants were generated from *P. andersonii* WU1-14 as previously described (van Zeijl et al., 2018). Three single guide RNA (sgRNA) target sites were designed for the *PanNOOT1* locus (Supplementary Figure 1). Primers used for generating sgRNAs and mutant genotyping are listed in Supplementary Table 1. *P. andersonii* WU1-14 was used as the wild-type line, Ctr44 was used as the transgenic control line (van Zeijl et al., 2018). Tissue culture was performed as previously described (van Zeijl et al., 2018). After rooting, tissue-cultured plantlets were transferred to soil, three plantlets were grown per pot, supplemented with 100 mL of 10 mM NH_4NO_3 (pH=5.8) weekly. Axillary branches were removed from plantlet stage if applicable.

Sequence Alignment

PanNOOT1 (PanWU01x14_292800) genomic sequence is available at <http://www.bioinformatics.nl/parasponia/>. Sequence alignment was performed using MAFFT v7.017 (Kato, 2002), implemented in Geneious R6 (Biomatters), using default parameter settings. The figure of gene model and sequence alignment was exported from Geneious R6 and edited using Adobe Illustrator CC (Adobe Systems).

Phenotyping

For stipule formation scoring, only the node positions bearing axillary branch length ≥ 0.5 cm were considered. For axillary branch length measurement, the distance from the branch basal part till the furthest blade tip was measured

for each branch. For petiole length measurement, the distance between the base of axillary branch and the proximal edge of the blade was measured at the adaxial side of petiole. For cell length measurement, at the adaxial side of petioles formed at N1, five cell files from the peripheral region and from the middle region of each petiole were randomly selected and measured, each cell file contains 8-10 collenchymatous cells. To calculate the average cell length, the total length of five cell files was divided by the total measured cell number. To measure the petiole vasculature adaxial angle (formed at N1; Figure 6D), three positions (one middle, two peripheral) were selected. The middle position represents the middle region of cambium cells (letter a, Figure 6D), and the two peripheral positions represent the two ends of xylem cell files (letter b and c, Figure 6D).

Microscopy and Imaging

For confocal images, shoot tips (approx. 1 cm) were collected from 8-week-old transgenic control line and *Pannoot1* A5 line plants. The materials were fixed with 4% paraformaldehyde (w/v), 5% glutaraldehyde (v/v) in 0.05 M sodium phosphate buffer (pH 7.2) at 4 °C overnight. Then fixed materials were washed with 1 x PBS, and embedded in 6% low melting agarose dissolved in 1 x PBS. Longitudinal sections (90 µm) were made with a VT1000 S vibratome (Leica Microsystems), stained with propidium iodide (200 x diluted saturated solution). The sections were imaged using an SP8 microscope (Leica Microsystems), using an excitation wavelength of 543 nm for propidium iodide. Leaf primordium numbering was based on a series of sections. For other microscopy images, materials were fixed as above-mentioned. Fixed materials (except the shoot tips for cross sections) was dehydrated by an ethanol series and subsequently embedded in Technovit 7100 (Heraeus Kulzer) according to the manufacturer's protocol. For cross sections of shoot tips, fixed materials were embedded in paraffin (Paraplast X-tra, McCormick Scientific). Sections were made with a RJ2035 microtome (Leica Microsystems), and stained for 1.5 min in 0.05% toluidine blue O. Section thickness was 5 µm, except cross sections of shoot tips (10 µm). Sections were imaged by using a DM5500B microscope equipped with a DFC425C camera (Leica Microsystems).

In situ Hybridization

Hybridization was performed twice on 10 week-old wild-type *P. andersonii* plants using Invitrogen ViewRNA ISH Tissue 1-Plex Assay kits (Thermo Fisher Scientific), as previously described (Liu et al., 2019), with minor modifications. Modifications: section thickness was 20 μm ; silane-prep slides (Sigma-Aldrich) with section ribbons were baked at 42 °C overnight to increase the adhesion of the sections with the slides. The *PanNOOT1* probe set (catalogue number: VF1-6000669) was designed and synthesized by Thermo Fisher Scientific, it covers the region 281–1146 nt of the coding sequence (1512 nt). A typical probe set contains ~20 adjacent oligonucleotide pairs of probes that hybridize to specific regions across the target mRNA. Each probe covers 20 nucleotides, only a pair of two adjacent probes can form a site for signal amplification. By this principle, background is reduced. Sections were imaged using a DM5500B microscope equipped with a DFC425C camera (Leica Microsystems).

ACKNOWLEDGMENTS

We thank Arjan van Zeijl for the help in designing the CRISPR/Cas9 single guide RNAs, and the provision of *P. andersonii* WU1-14 as wild-type line and Ctr44 transgenic control line. We also thank Henk Franssen for the critical comments on the draft manuscript.

AUTHOR CONTRIBUTIONS

RG and TB supervised this research. DS designed and performed most of the experiments with help from KM, FB, YZ and JW. OK and DS performed the *in situ* hybridization. DS analysed the results and drafted the manuscript with input from WK. RG and KM revised the manuscript.

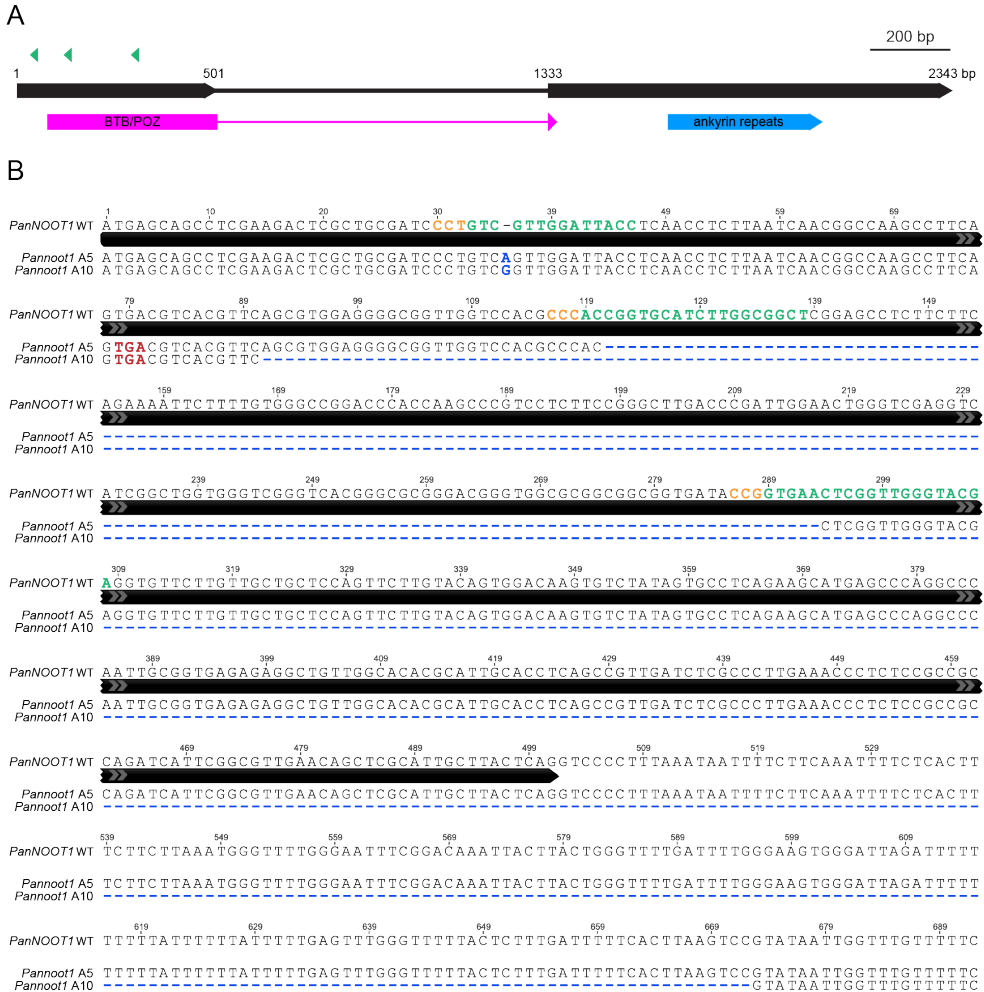
REFERENCES

- Aguilar-Martínez, J.A., Poza-Carrión, C., and Cubas, P.** (2007). *Arabidopsis BRANCHED1* acts as an integrator of branching signals within axillary buds. *Plant Cell* **19**: 458–72.
- Becking, J. H.** (1992). "The Rhizobium symbiosis of the nonlegume *Parasponia*," in *Biological Nitrogen Fixation*, eds G. S. Stacey, H. J. Evans, and R. H. Burris (New York, NY: Routledge), 497–559.

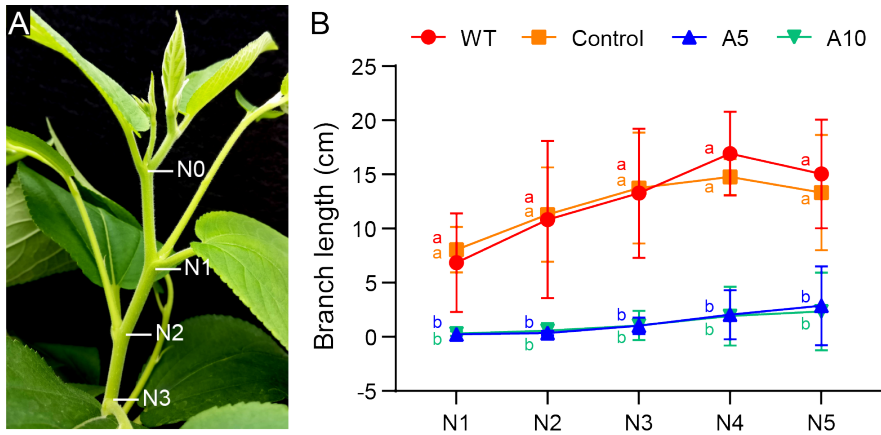
- Bell, E.M., Lin, W. -c., Husbands, A.Y., Yu, L., Jaganatha, V., Jablonska, B., Mangeon, A., Neff, M.M., Girke, T., and Springer, P.S.** (2012). *Arabidopsis* LATERAL ORGAN BOUNDARIES negatively regulates brassinosteroid accumulation to limit growth in organ boundaries. *Proc. Natl. Acad. Sci.* **109**: 21146–21151.
- Bennett, T. and Leyser, O.** (2006). Something on the Side: Axillary Meristems and Plant Development. *Plant Mol. Biol.* **60**: 843–854.
- Couzigou, J.-M.J. et al.** (2012). *NODULE ROOT* and *COCHLEATA* Maintain Nodule Development and Are Legume Orthologs of *Arabidopsis* *BLADE-ON-PETIOLE* Genes. *Plant Cell* **24**: 4498–4510.
- Dong, Z., Li, W., Unger-Wallace, E., Yang, J., Vollbrecht, E., and Chuck, G.** (2017). Ideal crop plant architecture is mediated by *tassels replace upper ears1*, a BTB/POZ ankyrin repeat gene directly targeted by TEOSINTE BRANCHED1. *Proc. Natl. Acad. Sci.*: 201714960.
- Du, F., Guan, C., and Jiao, Y.** (2018). Molecular Mechanisms of Leaf Morphogenesis. *Mol. Plant* **11**: 1117–1134.
- Ha, C.M., Jun, J.H., Nam, H.G., and Fletcher, J.C.** (2007). *BLADE-ON-PETIOLE1* and 2 Control *Arabidopsis* Lateral Organ Fate through Regulation of LOB Domain and Adaxial-Abaxial Polarity Genes. *Plant Cell* **19**: 1809–25.
- Ha, C.M., Jun, J.H., Nam, H.G., and Fletcher, J.C.** (2004). *BLADE-ON-PETIOLE1* Encodes a BTB/POZ Domain Protein Required for Leaf Morphogenesis in *Arabidopsis thaliana*. *Plant Cell Physiol.* **45**: 1361–1370.
- Ha, C.M., Kim, G.-T., Kim, B.C., Jun, J.H., Soh, M.S., Ueno, Y., Machida, Y., Tsukaya, H., and Nam, H.G.** (2003). The *BLADE-ON-PETIOLE 1* gene controls leaf pattern formation through the modulation of meristematic activity in *Arabidopsis*. *Development* **130**: 161–72.
- Hepworth, S.R. and Pautot, V.A.** (2015). Beyond the Divide: Boundaries for Patterning and Stem Cell Regulation in Plants. *Front. Plant Sci.* **6**: 1052.
- Hepworth, S.R., Zhang, Y., McKim, S., Li, X., and Haughn, G.W.** (2005). *BLADE-ON-PETIOLE*-dependent signaling controls leaf and floral patterning in *Arabidopsis*. *Plant Cell* **17**: 1434–48.
- Howe, G.T., Horvath, D.P., Dharmawardhana, P., Priest, H.D., Mockler, T.C., and Strauss, S.H.** (2015). Extensive Transcriptome Changes During Natural Onset and Release of Vegetative Bud Dormancy in *Populus*. *Front. Plant Sci.* **6**: 989.
- Ichihashi, Y., Kawade, K., Usami, T., Horiguchi, G., Takahashi, T., and Tsukaya, H.** (2011). Key Proliferative Activity in the Junction between the Leaf Blade and Leaf Petiole of *Arabidopsis*. *Plant Physiol.* **157**: 1151–1162.
- Iwakawa, H., Iwasaki, M., Kojima, S., Ueno, Y., Soma, T., Tanaka, H., Semiarti, E., Machida, Y., and Machida, C.** (2007). Expression of the *ASYMMETRIC LEAVES2* gene in the adaxial domain of *Arabidopsis* leaves represses cell proliferation in this domain and is critical for the development of properly expanded leaves. *Plant J.* **51**: 173–184.
- Izhaki, A., Alvarez, J.P., Cinnamon, Y., Genin, O., Liberman-Aloni, R., and Eyal, Y.** (2018). The Tomato *BLADE ON PETIOLE* and *TERMINATING FLOWER* Regulate Leaf Axil Patterning Along the Proximal-Distal Axes. *Front. Plant Sci.* **9**: 1126.

- Jun, J.H., Ha, C.M., and Fletcher, J.C.** (2010). BLADE-ON-PETIOLE1 Coordinates Organ Determinacy and Axial Polarity in *Arabidopsis* by Directly Activating ASYMMETRIC LEAVES2. *Plant Cell* **22**: 62–76.
- Katoh, K.** (2002). MAFFT: a novel method for rapid multiple sequence alignment based on fast Fourier transform. *Nucleic Acids Res.* **30**: 3059–3066.
- Liu, J., Rutten, L., Limpens, E., van der Molen, T., van Velzen, R., Chen, R., Chen, Y., Geurts, R., Kohlen, W., Kulikova, O., and Bisseling, T.** (2019). A Remote *cis*-Regulatory Region Is Required for *NIN* Expression in the Pericycle to Initiate Nodule Primordium Formation in *Medicago truncatula*. *Plant Cell* **31**: 68–83.
- Magne, K., George, J., Berbel Tornero, A., Broquet, B., Madueño, F., Andersen, S.U., and Ratet, P.** (2018). *Lotus japonicus* NOOT-BOP-COCH-LIKE1 is essential for nodule, nectary, leaf and flower development. *Plant J.* **94**: 880–894.
- McKim, S.M., Stenvik, G.-E., Butenko, M.A., Kristiansen, W., Cho, S.K., Hepworth, S.R., Aalen, R.B., and Haughn, G.W.** (2008). The *BLADE-ON-PETIOLE* genes are essential for abscission zone formation in *Arabidopsis*. *Development* **135**: 1537–1546.
- Muhr, M., Paulat, M., Awwanah, M., Brinkkötter, M., and Teichmann, T.** (2018). CRISPR/Cas9-mediated knockout of *Populus BRANCHED1* and *BRANCHED2* orthologs reveals a major function in bud outgrowth control. *Tree Physiol.* **38**: 1588–1597.
- Muhr, M., Prüfer, N., Paulat, M., and Teichmann, T.** (2016). Knockdown of strigolactone biosynthesis genes in *Populus* affects *BRANCHED1* expression and shoot architecture. *New Phytol.* **212**: 613–626.
- Norberg, M.** (2005). The *BLADE ON PETIOLE* genes act redundantly to control the growth and development of lateral organs. *Development* **132**: 2203–2213.
- Sjödin, A., Street, N.R., Sandberg, G., Gustafsson, P., and Jansson, S.** (2009). The *Populus* Genome Integrative Explorer (PopGenIE): A new resource for exploring the *Populus* genome. *New Phytol.* **182**: 1013–1025.
- Tavakol, E. et al.** (2015). The Barley *Uniculme4* Gene Encodes a BLADE-ON-PETIOLE-Like Protein That Controls Tillering and Leaf Patterning. *Plant Physiol.* **168**: 164–174.
- Teichmann, T. and Muhr, M.** (2015). Shaping plant architecture. *Front. Plant Sci.* **6**: 233.
- Toriba, T., Tokunaga, H., Shiga, T., Nie, F., Naramoto, S., Honda, E., Tanaka, K., Taji, T., Itoh, J.-I., and Kyoizuka, J.** (2019). *BLADE-ON-PETIOLE* genes temporally and developmentally regulate the sheath to blade ratio of rice leaves. *Nat. Commun.* **10**: 619.
- van Velzen, R. et al.** (2018). Comparative genomics of the nonlegume *Parasponia* reveals insights into evolution of nitrogen-fixing rhizobium symbioses. *Proc. Natl. Acad. Sci. U. S. A.* **115**: E4700–E4709.
- Wang, B., Smith, S.M., and Li, J.** (2018). Genetic Regulation of Shoot Architecture. *Annu. Rev. Plant Biol.* **69**: 437–468.
- Wang, J., Tian, Y., Li, J., Yang, K., Xing, S., Han, X., Xu, D., and Wang, Y.** (2019). Transcriptome sequencing of active buds from *Populus deltoides* CL and *Populus × zhaiguanheibaiyang* reveals phytohormones involved in branching.

- Genomics **111**: 700–709.
- Wang, Q., Hasson, A., Rossmann, S., and Theres, K.** (2016). *Divide et impera*: Boundaries shape the plant body and initiate new meristems. *New Phytol.* **209**: 485–498.
- Ward, S.P., Salmon, J., Hanley, S.J., Karp, A., and Leyser, O.** (2013). Using Arabidopsis to Study Shoot Branching in Biomass Willow. *Plant Physiol.* **162**: 800–811.
- Wardhani, T.A., Purwana Roswanjaya, Y., Dupin, S., Li, H., Linders, S., Hartog, M., Geurts, R., and van Zeijl, A.** (2019). Genome Editing and Phenotyping the Nitrogen-fixing Tropical Cannabaceae Tree *Parasponia andersonii*. *J. Vis. Exp.*: 59971.
- Xu, C., Park, S.J., Van Eck, J., and Lippman, Z.B.** (2016). Control of inflorescence architecture in tomato by BTB/POZ transcriptional regulators. *Genes Dev.* **30**: 2048–2061.
- Žádníková, P. and Simon, R.** (2014). How boundaries control plant development. *Curr. Opin. Plant Biol.* **17**: 116–125.
- van Zeijl, A., Wardhani, T.A.K., Seifi Kalhor, M., Rutten, L., Bu, F., Hartog, M., Linders, S., Fedorova, E.E., Bisseling, T., Kohlen, W., and Geurts, R.** (2018). CRISPR/Cas9-Mediated Mutagenesis of Four Putative Symbiosis Genes of the Tropical Tree *Parasponia andersonii* Reveals Novel Phenotypes. *Front. Plant Sci.* **9**: 1–14.



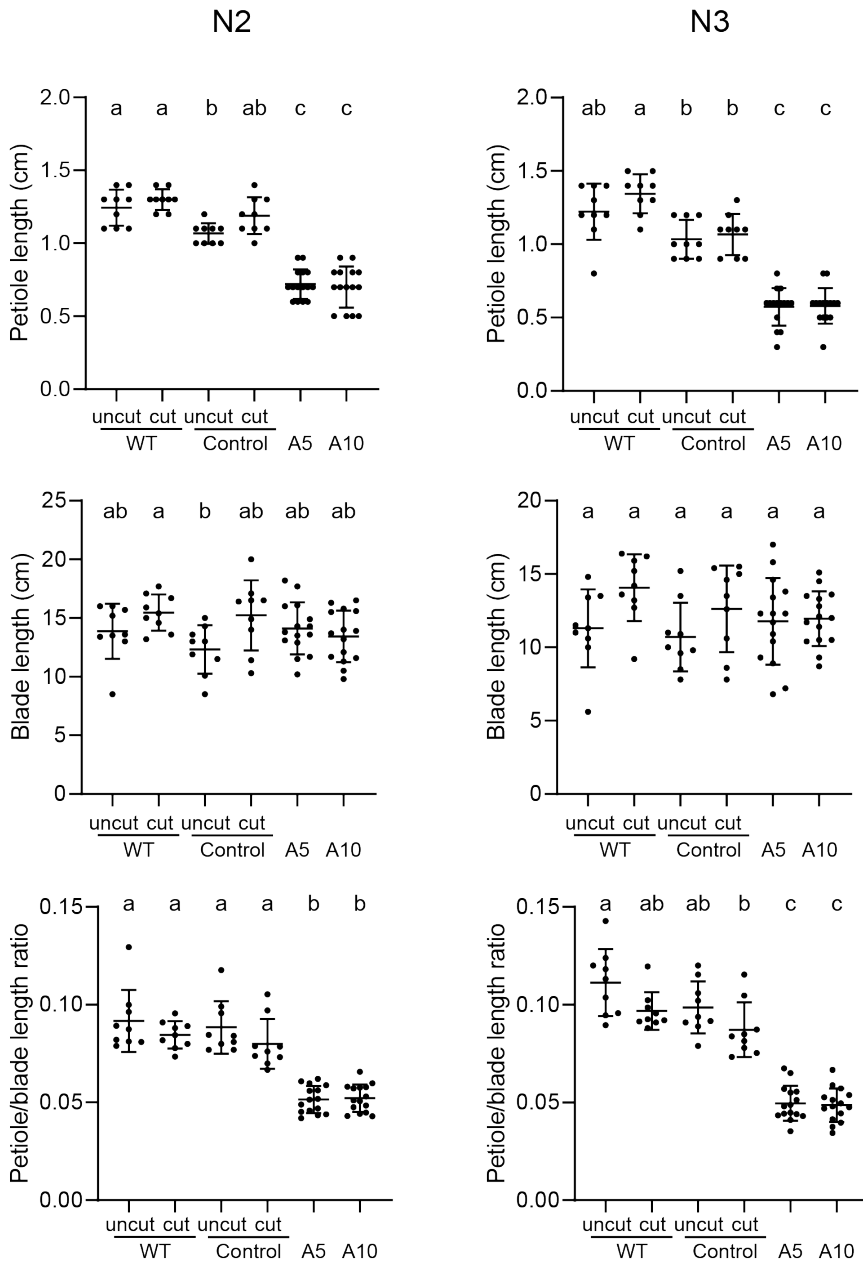
Continued on next page



Supplementary Figure 2. The overall branch length is reduced in the *Pannoot1* mutants. **(A)** A representation of the shoot tip region of a transgenic control line plant grown in soil for 10 weeks. The nodes (N0-N4) are indicated. **(B)** The overall branch length of the two independent *Pannoot1* mutants lines A5 and A10 is dramatically reduced, compared with wild-type and control line. The axillary branches of the *Pannoot1* mutants remain at small size at N1-N3, showing the outgrowth of axillary branches is delayed in the *Pannoot1* mutants. Data are mean \pm SD. One-way ANOVA with Tukey's multiple comparisons test was performed to assess significant differences. Lowercase letters indicate statistically different groups ($P < 0.0001$).

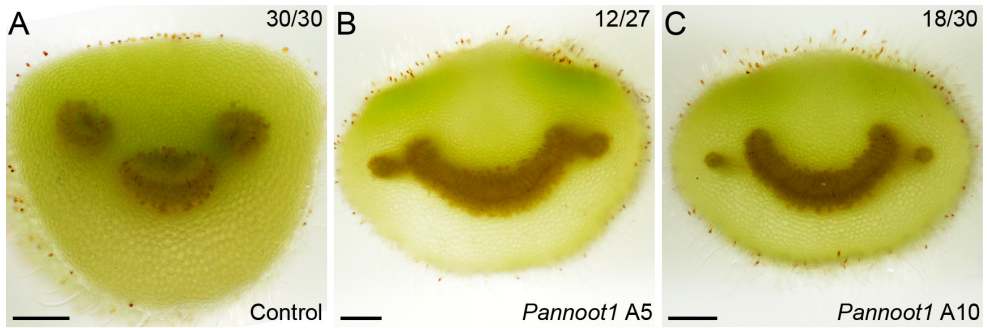
Continued

position starting from ATG. The sgRNA target sites and PAM (protospacer adjacent motif) sequences are highlighted in green and orange, respectively. The inserted nucleotides or deleted sequences in the *Pannoot1* mutant lines are highlighted in blue. Premature stop codons are highlighted in red, indicating that the *Pannoot1* mutant lines cannot produce functional PanNOOT1 protein.



Supplementary Figure 3. *Pannoot1* mutants form shorter petioles at N2 and N3. The petiole length and the ratio between the petiole and blade length is significantly reduced in the *Pannoot1* mutants, compared with of wild-type and the transgenic control line at N2 and N3, irrespectively of whether the axillary branches were cut or uncut. Therefore, the shorter petiole of the *Pannoot1* mutants is not caused by the arrested axillary branches. The blade length is not affected in the *Pannoot1*

Continued on next page



Supplementary Figure 4. The petioles of the *Pannoot1* mutants form abaxialized vasculatures. (A–C) Representative cross-sectional surfaces at the proximal region of petioles in the transgenic control line (A), and two *Pannoot1* mutant lines A5 (B) and A10 (C). Numbers at the corner denote the frequency of the shown phenotype. Scale bars: 500 μ m.

Supplementary Table 1. Primer sequences used in this study

Primer name	Sequence (5'-3')
<i>PanNOOT1</i> CRISPR Target 1-F	TGTGGTCTCAATTGTTGAGGTAATCCAACGACGTTTTAGAGCTAGAAATAGCAAG
<i>PanNOOT1</i> CRISPR Target 2-F	TGTGGTCTCAATTGAGCCGCCAAGATGCACCGGTGTTTTAGAGCTAGAAATAGCAAG
<i>PanNOOT1</i> CRISPR Target 3-F	TGTGGTCTCAATTGTCGTACCCAACCGAGTTCACGTTTTAGAGCTAGAAATAGCAAG
<i>PanNOOT1</i> CRISPR Target universal-R	TGTGGTCTCAAGCGTAATGCCAACTTTGTAC
<i>Pannoot1</i> mutant genotyping-F	AAGTTGATCCTCAGAACCCCTTT
<i>Pannoot1</i> mutant genotyping-R	GGGAACCAAATTTGCTGTTGA

Continued

mutants. Left panel represents the data on N2, right panel represents the data on N3. Each dot represents a measurement on a single plant (uncut wild-type: n=9, cut wild-type: n=9, uncut control: n=9, cut control: n=9, A5: n=15, A10: n=15). Data are mean \pm SD. One-way ANOVA with Tukey's multiple comparisons test was performed to assess significant differences. Lowercase letters indicate statistically different groups ($P < 0.05$).

CHAPTER 6

General Discussion

Defeng Shen

Laboratory of Molecular Biology, Department of Plant Sciences, Wageningen University, Droevendaalsesteeg 1, 6708 PB Wageningen, The Netherlands.



Recent Phylogenomics Studies on Root Nodule Evolution

Nitrogen-fixing root nodule symbiosis exclusively occurs in plant species belonging to four orders that together form the nitrogen-fixing clade (NFC). As the occurrence of nodulating species is rather scattered within this clade, it has been hypothesized that nodulation evolved several times within this clade (Soltis et al., 1995; Swensen, 1996). Further, since all nodulating species belong to the NFC, it has been hypothesized that the common ancestor of this clade obtained a predisposition to evolve the nodulation trait (Soltis et al., 1995; Swensen, 1996). However, two recent phylogenomic studies questioned these hypotheses. These studies revealed that several genes essential for establishing root nodule symbiosis are independently lost or pseudogenized in the non-nodulating relatives of nodulating species in the NFC. The first study compared the genome sequence of *Parasponia* species with that of its closely related non-nodulating sister genus *Trema* (Cannabaceae, order Rosales). This showed that *NFP/NFR5*, *NIN* and *RPG*, which are essential for nodulation, are lost or pseudogenized in the genomes of *Trema* species. A similar loss or pseudogenization has occurred in more distantly related non-nodulating Rosales species (van Velzen et al., 2018). The second study compared genomes of multiple nodulating and non-nodulating plants across the four orders of the NFC. This revealed the independent loss or pseudogenization of *NIN* and/or *RPG* in the non-nodulating species (Griesmann et al., 2018). As these pseudogenized/lost symbiosis genes are orthologues of genes specifically involved in nodule symbiosis, these findings suggest that massive loss of nodulation occurred in the NFC and challenge the view that nodulation evolved several times in parallel.

This massive loss of the nitrogen-fixing nodule trait is counter-intuitive as nitrogen fixation is considered to be beneficial for the host plant. However, the massive loss of nodulation suggests that this trait became less favorable during the period that loss occurred. The occurrence of widespread loss of nodulation can be best explained by environmental factors that changed on a global scale. Such factor could be the level of atmospheric CO₂, which is important for photosynthesis. Global atmospheric CO₂ levels have generally been decreasing in the last 100 million years, so a period which coincides with the evolution of species within the four orders of the NFC. During the general decrease of CO₂ levels, there were several geological periods with particularly steep decline of CO₂ levels. Nitrogen fixation is a high energy demanding process and therefore it requires a high level of photosynthesis. Therefore, the reduced atmospheric CO₂ levels

could have become a limiting factor for plant growth, which made nodulation a less favorable trait (van Velzen et al., 2019). Reduced photosynthesis does block nodulation (Taylor and Menge, 2018). So in the periods with decreasing CO₂ levels nodulation might have been blocked and there would have been no pressure to maintain this trait, by which it could have been massively lost. Decreasing CO₂ levels can not only explain the occurrence of massive loss of nodulation in diverse lineages, but also the differences in the timing of loss, from very recent (such as *Trema*) to more ancient (such as *Prunus*) (van Velzen et al., 2019).

The massive loss of nodulation has led to the hypothesis that the common ancestor of the NFC did not evolve a predisposition for nodulation, but evolved a symbiosis with nitrogen-fixing bacteria. In all nitrogen-fixing root nodule symbiosis, the bacteria are hosted intracellularly and always surrounded by a plant-derived membrane. Based on this, it was proposed that the common ancestor of the NFC can form an intracellular symbiosis in existing root cells. Subsequently, nodulation evolved independently in different lineages (Parniske, 2018). The latter was proposed because of the fundamental differences in nodule ontogeny of, for example, legume-type and actinorhizal-type nodules. In contrast, van Velzen et al. (2019) proposed a single gain of nodulation by the common ancestor of the NFC. However, such single gain of nodulation hypothesis did not take account of the proposed fundamental differences regarding the ontogeny of the two nodule types.

The Actinorhizal Nodule Type Is Most Likely Ancestral to the Legume Nodule Type

Our study revealed that actinorhizal-type nodules and legume-type nodules are more similar than previously described. The property that they share is that in both cases cells derived from the mitotically activated root cortex form the infected tissue of the nodule, in which bacteria are hosted intracellularly (CHAPTER 3).

The major difference between the legume-type and actinorhizal-type nodules is the ontogeny of the nodule vascular bundles. In case of the actinorhizal-type nodules, they are formed from pericycle-derived cells, whereas the legume nodule vasculatures are derived from cortical cells. Furthermore, I showed that a loss-of-function mutation in *Medicago truncatula* (*Medicago*) *MtNOOT1* led



to the formation of nodule vasculatures from pericycle-derived cells. So an ontogeny similar to that of actinorhizal-type nodule vasculatures. Therefore, knockout of *MtNOOT1* causes a (partial) homeotic switch from a legume-type nodule to an actinorhizal type (CHAPTER 3).

So on one hand, I showed that the ontogeny of the two nodule types is more similar as in both cases cortex-derived cells form the infected nodule tissue. Further, as homeotic mutations often cause a reversion to an ancestral phenotype (Garcia-Bellido, 1977; Wellmer et al., 2014), this suggests that legume-type nodules evolved from actinorhizal-type nodules. These findings support the hypothesis that the common ancestor of the NFC evolved the nodulation trait (single gain), and this was an actinorhizal-type nodule.

When nodulation evolved in the common ancestor of the NFC, it was most likely induced by *Frankia* bacteria. This implies that there was a switch from *Frankia*-induced nodulation to rhizobium-induced nodulation in *Parasponia* and in legumes. A striking difference between legume-type and actinorhizal-type nodules is that in general rhizobia are released from infection threads in legume nodules and are present as organelle-like structures in the cytoplasm of host cells. In contrast, bacteria are not released from infection threads in actinorhizal nodules, but stay present in fixation threads that remain connected to the infection threads (reviewed in Pawlowski and Demchenko, 2012). This seems not very surprising for the filamentous *Frankia* bacteria. However, also in *Parasponia* nodules the rhizobia are hosted in fixation threads. Rhizobia cannot be released in *Parasponia* nodules, because the fixation thread is surrounded by a (thin) cell wall (Lancelle and Torrey, 1984, 1985). In the nodule cells of most legumes cell wall free droplets are formed at the tip of infection threads, by which the rhizobia can be pinched off and become encapsulated by a host membrane (reviewed in Ivanov et al., 2010). However, rhizobia are not released from infection threads in nodules of some *Chamaecrista* species and fixation threads are formed (Naisbitt et al., 1992). This suggests that this basal legume maintained some characteristics of actinorhizal-type nodules, supporting the hypothesis that legume-type nodules evolved from actinorhizal-type nodules.

Evolution of Hemoglobin Genes to Facilitate Oxygen Supply in Nodules

All root nodules face a so-called oxygen dilemma of nitrogen fixation. In the infected cells the oxygen requirement of rhizobia/*Frankia* is high to produce sufficient ATP for reduction of atmospheric nitrogen to ammonia. However, nitrogenase is sensitive to oxygen, which can irreversibly denature nitrogenase. To solve this dilemma, symbiotic hemoglobin genes have evolved that are specifically expressed in nodules. These genes evolved from non-symbiotic hemoglobin genes that plants use to modulate levels of toxic NO and redox potentials, and oxygen transportation at low levels (Vázquez-Limón et al., 2012). These non-symbiotic hemoglobin genes have been divided in class I and class II types. Legumes (precisely species of Papilionoideae subfamily) use leghemoglobins to facilitate the transportation of oxygen to the rhizobia at low oxygen concentrations. These have evolved from class II hemoglobin genes (Ott et al., 2005). *Chamaecrista fasciculata* is a species from the legume subfamily Caesalpinioideae. It has been suggested that the property of *C. fasciculata* hemoglobin (ppHb) is intermediate between that of class I hemoglobin and leghemoglobin, suggesting that ppHb evolved independently from the leghemoglobins of Papilionoideae species (Gopalasubramaniam et al., 2008). In line with this, the majority of actinorhizal plants (*Alnus firma*, *Myrica gale* (order Fagales), *Datisca glomerata* (order Cucurbitales) and *Ceanothus thyrsifloru* and *Parasponia* (order Rosales)) evolved (nodule-specific) hemoglobins from class I hemoglobins for oxygen supply in their nodules (Heckmann et al., 2006; Sasakura et al., 2006; Pawlowski et al., 2007; Sanz-Luque et al., 2015; Salgado et al., 2018). In the actinorhizal species *Casuarina glauca* (order Fagales), a nodule hemoglobin evolved from a class II hemoglobin. Taken together, it shows that there has been pressure to evolve a hemoglobin-based oxygen supply system and this most likely evolved independently several times.

The *Parasponia* species all have a symbiotic hemoglobin gene (*HB1*) that is derived from a class I hemoglobin. This is the result of *Parasponia*-specific gain-of-function adaptations in *HB1*, which did not occur in *Trema* hemoglobin genes (Sturms et al., 2010; Kakar et al., 2011; van Velzen et al., 2018). This suggests that the common ancestor of *Parasponia* and *Trema* made nodules, but lacked symbiotic hemoglobins. These did evolve in the *Parasponia* branch, but not in the *Trema* branch. This suggests that nitrogen-fixing efficiency within the *Trema* branch was markedly lower than in the *Parasponia* branch. This might have contributed to the loss of the nodulation trait in the *Trema* branch.

It will be interesting to study whether non-nodulating species within the NFC had symbiotic hemoglobin genes. This can provide insight into what extend the lack of symbiotic hemoglobin genes could have contributed to the loss of the nitrogen-fixing trait.

Tissue Organization of Nodule Vasculatures in Legume- and Actinorhizal-type Nodules

In actinorhizal-type nodules, vasculatures have a central position and are surrounded by infected cells. In contrast, legume-type nodules have a central infected tissue which is surrounded by peripheral vasculatures. I hypothesize that this different spatial organization of vasculatures and infected tissue led to the evolution of different tissue organization of nodule vasculatures to support efficient nutrient exchange. In actinorhizal-type nodules, the central vasculature consists of multiple xylem and phloem poles. This organization seems well adapted to nutrient exchange (e.g. ammonia and carbohydrates) between the surrounding infected cells and the host plant through this central nodule vasculature (Figure 1A-B). In legume-type nodules, the peripheral vasculature is composed of one xylem pole and one phloem pole (Guinel, 2009) (Figure 1C). This relatively simple organization seems sufficient for an efficient exchange of nutrients between the central tissue with infected cells and the host plant through the peripheral vascular system. The ontogeny of the nodule vasculatures in these two nodule types is different, pericycle-derived in actinorhizal-type nodules, cortex-derived in legume-type nodules. Therefore, the different tissue organization between the actinorhizal-type and legume-type nodule vasculatures could be due to their different ontogeny. *Medicago Mtnoot1* mutants provide a possibility to test this hypothesis as the ontogeny of their nodule vasculatures has become more actinorhizal-like.

The nodule vasculature of wild-type *Medicago* consists of one phloem and one xylem pole, with the xylem pole facing the exterior of nodules and the phloem pole facing the infected cells (Figure 1C). In contrast, in *Medicago Mtnoot1* mutant nodules a file of xylem cells with a xylem pole at both ends is formed in the middle of the vasculature and this is sandwiched by two phloem poles. This results in a diarchy patterning. One of the phloem poles faces the exterior of the nodule, the other one facing the interior of the nodule (Figure 1D). These results show that the tissue organization of *Mtnoot1* nodule vasculatures becomes more complicated, resembling the vascular patterning in actinorhizal-type

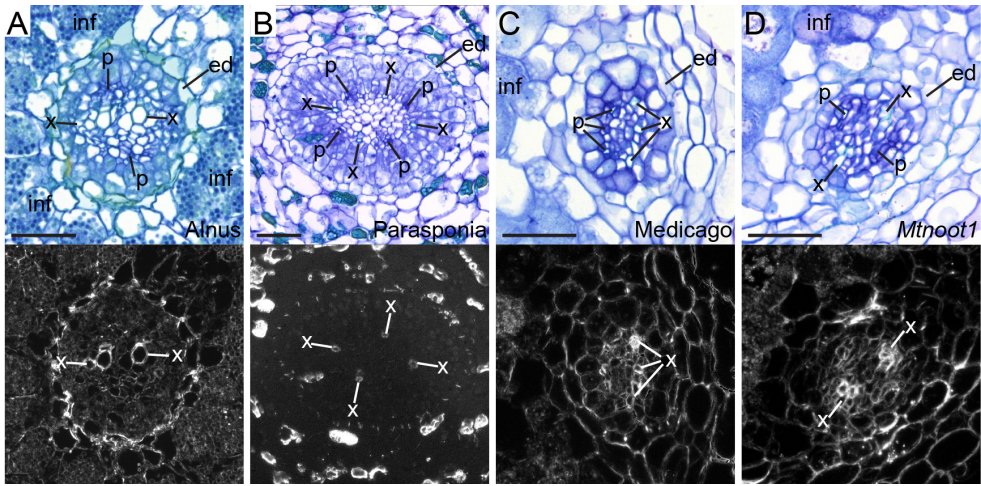


Figure 1. The Tissue Organization of Nodule Vasculature in Different Nodules. (A–D) Cross sections of nodules formed by *Alnus glutinosa* (Alnus) (A), *Parasponia andersonii* (Parasponia) (B), *Medicago truncatula* (Medicago) (C), and *Mtnoot1* mutants (D). Below are dark field images to visualize xylem cells. (A, B) In actinorhizal-type nodules, vasculature is centrally localized, surrounded by infected cells (inf). The nodule vasculatures have multiple poles of xylem (x) and phloem (p) cells. (C) In Medicago nodules, the peripheral vasculatures show a collateral organization of xylem and phloem tissues, with one phloem pole facing the infected cells and one xylem pole facing the exterior of nodule. (D) In *Mtnoot1* nodules, a file of xylem cells with a xylem pole at both ends is formed in the middle of the vasculature. The xylem cell file is sandwiched by two phloem poles. One of the phloem poles faces the infected cells, the other one faces the exterior of nodule. ed, endodermis of nodule vasculature. Scale bars: 50 μ m.

nodules. This supports the hypothesis that the ontogeny of nodule vasculatures contributes to their tissue organization. In line with this, the tissue organization of *Lotus japonicus noot-bop-coch-like1* mutant (mutation in the ortholog of *MtNOOT1* in *L. japonicus*) nodule vasculature also becomes more complicated (Magne et al., 2018b), similar to that of Medicago *Mtnoot1* and actinorhizal-type nodule vasculatures.

So why would a nodule vasculature with a simpler tissue organization have evolved in legumes? I hypothesize that creating unnecessary xylem and phloem poles causes a waste of energy. Therefore, simpler nodule vasculatures induced by legume NOOT1 might be an advantage.

Evolution of Legume-type Nodules

I hypothesize that the evolution of legume-type nodules from actinorhizal-type nodules is (at least) a two-step process: 1) actinorhizal-type vasculatures formed at the periphery of nodules, similar to legume *noot1* nodules; 2) creating legume-type nodule vasculatures by recruiting legume *NOOT1*.

The second step requires repression of cell division in the pericycle-derived cells. In line with this, we showed that the expression of *MtNOOT1* is induced in the pericycle-derived cells in Medicago nodule primordia. Combined with the phenotype of *Mtnoot1* mutants, I suggested that Medicago *MtNOOT1* fulfills a cell-autonomous function in repressing cell division in the pericycle-derived cells. In line with this, *PanNOOT1*, an ancestral *NOOT1*, is not expressed in the pericycle-derived cells of nodule primordia of *Parasponia andersonii* (Parasponia). This suggests neofunctionalization of the *cis*-regulatory elements after the duplication of *NOOT* in legumes. The comparison with Parasponia suggests that it maintained its original/ancestral expression in the meristem of the nodule and it acquired a new expression domain in the pericycle-derived cells. The latter led to the evolution of legume-type nodules.

Then, what could drive the proposed first step of legume-type nodule evolution, which positioned vasculatures at the periphery of the nodule? We observed that the vasculatures of *Mtnoot1* nodules can originate at the central basal part, but grow towards the peripheral region of the nodule and seem unable to grow in between the cells that will form the infected tissue (Figure 2). This could be (partly) due to the characteristics of legume infected tissue, which is more compact, compared with the infected tissue of actinorhizal-type nodules. I hypothesize that the characteristics (e.g. patterning of cell division) of cells that form the infected tissue can control the positioning (central vs. peripheral) of the nodule vasculature in these two types of nodules, and this is independent of legume *NOOT1*.

Nodulation is very common in legumes, the peripheral positioning of nodule vasculatures has been proposed to be one of the reasons that legume nodulation is so successful (Downie, 2014). In the cells of nodule vasculature, oxygen is required to generate ATP to satisfy the energy demands of the vasculature. In case of central nodule vasculature, it is surrounded by infected cells that consume a lot of oxygen. Further, in these cells leghemoglobin facilitates the transport of oxygen to the mitochondria at a low oxygen concentration. As

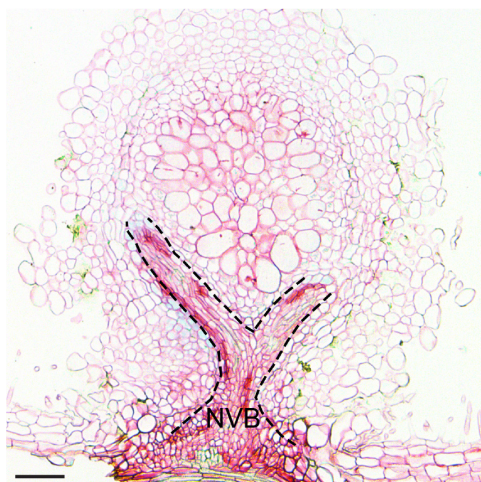


Figure 2. Nodule Vasculatures Migrate to the Peripheral Region of Medicago *Mtnoot1* Nodules. Longitudinal section of a transgenic *Mtnoot1* nodule (10 dpi) expressing *AtCASP1::GUS* (see METHODS in CHAPTER 3 for details). This shows that nodule vasculature originates at central basal region of the nodule, then migrates to the peripheral region. Dotted line outlines nodule vasculature (NVB). Scale bar: 100 μ m.

leghemoglobin binds oxygen it even further decreases the availability of oxygen to nodule vascular cells. Therefore, it has been proposed that peripheral vasculature is an advantage as oxygen will be more available (Downie, 2014).

The Ancestral Symbiotic Function of NOOT1 in the NFC

A key difference between *Parasponia* PanNOOT1 and *Medicago* NOOT1 is that the latter suppresses divisions in the pericycle-derived cells in nodule primordia, whereas PanNOOT1 does not (CHAPTER 3). A similarity between both *NOOT1* genes is that they are expressed in the apical region (meristem and infection zone) of nodules and the function in this region could be conserved. In line with this, NOOT1 is required for the maintenance of nodule identity of the vascular meristem in *Parasponia* and *Medicago*, as knocking out of *NOOT1* genes in both species leads to the formation of nodule roots. Further, nodule meristem formation is disturbed in *Medicago Mtnoot1* mutants. Meristems can be formed in *Parasponia Pannoot1* mutants, however, the maintenance of nodule meristem activity is disturbed. Therefore, in both species NOOT1 is important for nodule meristem activity. Bacterial colonization is disrupted in both *Pannoot1* and *Mtnoot1* mutants, and is aggravated in *Mtnoot1Mtnoot2* double mutants, indicating that *Parasponia* PanNOOT1 and two *Medicago* NOOT genes are required for intracellular hosting of bacteria (CHAPTER 4). How NOOT genes of *Parasponia* and *Medicago* regulate this process remains unclear. One indication could be that *PanNOOT1* and *MtNOOT1* are expressed in the infection zone, they might repress defense responses in the infected cells. In line with this, early

senescence is induced the Parasponia *Pannoot1* mutant nodules (CHAPTER 4) and defense response genes are induced in the Medicago *Mtnoot1* and *Mtnoot1Mtnoot2* double mutant nodules (Magne et al., 2018a). More clues can be obtained by examining the expression level of genes involved in repressing defense responses, such as *NAD1*, *SymCRK* and *DNF2*.

Similar to Parasponia, most actinorhizal plants with available genome sequence (e.g. *Alnus glutinosa*, *Casuarina glauca* and *Discaria trinervis*) only have one putative *NOOT* gene (Griesmann et al., 2018). Recent transcriptome studies showed that the putative ortholog(s) of *BOP* is/are expressed in *D. glomerata* (Datiscaceae, order Cucurbitales) nodules (Salgado et al., 2018). As Parasponia PanNOOT1 and Medicago MtNOOT1 (and its paralog MtNOOT2) share a function in the maintenance of nodule identity of the vascular meristem, nodule meristem functioning and intracellular colonization of symbionts in the host cells, I hypothesize that this is the ancestral function of NOOT1 in root nodules, and this is also the function of NOOT1 in nodules of other actinorhizal plants

NOOT1 Functions as a Boundary Specification Gene

To better understand the symbiotic functions of NOOT1, we also studied the non-symbiotic functions of *NOOT1* genes in Medicago and Parasponia. This confirmed that NOOT1 plays a general role in specifying boundary formation in various developmental contexts.

The shoot apical meristem (SAM) generates all aerial organs of plant. To initiate new organs from the SAM, a meristem-to-organ boundary with restricted growth is created to physically separate the SAM and the newly formed organs. Impairment of boundaries often leads to organ fusion. Also at sites where abscission takes place boundaries are formed (Hepworth and Pautot, 2015). In Arabidopsis, *AtBOP1* and *AtBOP2* encode co-transcription factors involved in the gene regulatory network required for plant boundary formation (reviewed in Khan et al., 2014; Žádníková and Simon, 2014; Hepworth and Pautot, 2015; Wang et al., 2016). They function at lateral organ boundaries, regulating abscission and the morphogenesis of leaves, inflorescences, fruits, and flowers. Knockout of *AtBOP1* and *AtBOP2* leads to a plethora of defects, including leafy petioles, fused organs, disturbed floral patterning, and loss of abscission (Ha et al., 2003, 2004; Norberg, 2005; Hepworth et al., 2005; McKim et al., 2008; Xu et al., 2010; Khan et al., 2012). Similarly in Parasponia, *PanNOOT1* is expressed

at the boundary between the SAM and leaf primordia. Knockout of *PanNOOT1* leads to organ fusion between petiole and stem, indicating that boundary formation is disturbed. Axillary buds are formed at the boundary, therefore, the disturbed boundary formation could explain the shifted position of axillary buds in the *Pannoot1* mutants. So our studies on *Parasponia* confirmed that NOOT1 plays a conserved role in boundary formation (CHAPTER 5).

During (primary) root development such boundary is also formed. The transition zone serves as a boundary separating actively dividing meristematic cells and rapidly elongating cells. The expression of *MtNOOT1* in the transition zone suggests that *MtNOOT1* suppresses cell division of meristematic cells, by which they enter the elongation and differentiation zone. In line with this, knockout of *MtNOOT1* leads to a longer root apical meristem with more meristematic cells (CHAPTER 2). During nodule formation a boundary is also formed at the base of the nodule primordia. The mitotic activity of pericycle- and endodermis-derived cells is suppressed at an early stage of nodule primordium formation. These cells serve as a boundary separating the infected cortical cells from the root vasculature. The suppressed mitotic activity of these cells inhibits formation of actinorhizal-type vasculatures. It is plausible that such boundary is a prerequisite for the formation of legume-type nodule vasculatures. Therefore, NOOT1 functions as a boundary specification gene in various developmental processes.

Concluding Remarks

In this thesis I showed that legume-type and actinorhizal-type nodules could share a common evolutionary origin, and the actinorhizal type is mostly like ancestral. In these two types of nodules NOOT1 is required for the maintenance of nodule identity of the vascular meristem. I further showed that NOOT1 plays a general role in boundary formation in diverse developmental processes. The regulator(s) of *NOOT1* and its interactor(s) during nodule formation remain unclear, this can be the target of future research.



REFERENCES

- Downie, J.A. (2014). Legume nodulation. *Curr. Biol.* **24**: R184–R190.
- Garcia-Bellido, A. (1977). Homoeotic and atavic mutations in insects. *Am. Zool.* **17**: 613–629.
- Gopalasubramaniam, S.K., Kovacs, F., Violante-Mota, F., Twigg, P., Arredondo-Peter, R., and Sarath, G. (2008). Cloning and characterization of a caesalpinoid (*Chamaecrista fasciculata*) hemoglobin: The structural transition from a nonsymbiotic hemoglobin to a leghemoglobin. *Proteins Struct. Funct. Genet.* **72**: 252–260.
- Griesmann, M. et al. (2018). Phylogenomics reveals multiple losses of nitrogen-fixing root nodule symbiosis. *Science* **361**: eaat1743.
- Guinel, F.C. (2009). Getting around the legume nodule: I. The structure of the peripheral zone in four nodule types. *Botany* **87**: 1117–1138.
- Ha, C.M., Jun, J.H., Nam, H.G., and Fletcher, J.C. (2004). *BLADE-ON-PETIOLE1* Encodes a BTB/POZ Domain Protein Required for Leaf Morphogenesis in *Arabidopsis thaliana*. *Plant Cell Physiol.* **45**: 1361–1370.
- Ha, C.M., Kim, G.-T., Kim, B.C., Jun, J.H., Soh, M.S., Ueno, Y., Machida, Y., Tsukaya, H., and Nam, H.G. (2003). The *BLADE-ON-PETIOLE 1* gene controls leaf pattern formation through the modulation of meristematic activity in *Arabidopsis*. *Development* **130**: 161–72.
- Heckmann, A.B., Hebelstrup, K.H., Larsen, K., Micaelo, N.M., and Jensen, E. (2006). A single hemoglobin gene in *Myrica gale* retains both symbiotic and non-symbiotic specificity. *Plant Mol. Biol.* **61**: 769–779.
- Hepworth, S.R. and Pautot, V.A. (2015). Beyond the Divide: Boundaries for Patterning and Stem Cell Regulation in Plants. *Front. Plant Sci.* **6**: 1052.
- Hepworth, S.R., Zhang, Y., McKim, S., Li, X., and Haughn, G.W. (2005). *BLADE-ON-PETIOLE*-dependent signaling controls leaf and floral patterning in *Arabidopsis*. *Plant Cell* **17**: 1434–48.
- Ivanov, S., Fedorova, E., and Bisseling, T. (2010). Intracellular plant microbe associations: secretory pathways and the formation of perimicrobial compartments. *Curr. Opin. Plant Biol.* **13**: 372–7.
- Kakar, S., Sturms, R., Tiffany, A., Nix, J.C., DiSpirito, A.A., and Hargrove, M.S. (2011). Crystal Structures of *Parasponia* and *Trema* Hemoglobins: Differential Heme Coordination Is Linked to Quaternary Structure. *Biochemistry* **50**: 4273–4280.
- Khan, M., Xu, H., and Hepworth, S.R. (2014). *BLADE-ON-PETIOLE* genes: Setting boundaries in development and defense. *Plant Sci.* **215–216**: 157–171.
- Khan, M., Xu, M., Murmu, J., Tabb, P., Liu, Y., Storey, K., McKim, S.M., Douglas, C.J., and Hepworth, S.R. (2012). Antagonistic interaction of *BLADE-ON-PETIOLE1* and 2 with *BREVIPEDECELLUS* and *PENNYWISE* regulates *Arabidopsis* inflorescence architecture. *Plant Physiol.* **158**: 946–60.
- Lancelle, S.A. and Torrey, J.G. (1984). Early Development of *Rhizobium*-Induced Root-Nodules of *Parasponia rigida*. I. Infection and Early Nodule Initiation. *Protoplasma* **123**: 26–37.
- Lancelle, S.A. and Torrey, J.G. (1985). Early development of *Rhizobium*-induced root nodules of *Parasponia rigida*. II. Nodule morphogenesis and symbiotic

- development. *Can. J. Bot. Can. Bot.* **63**: 25–35.
- Magne, K. et al.** (2018a). *MtNODULE ROOT1* and *MtNODULE ROOT2* Are Essential for Indeterminate Nodule Identity. *Plant Physiol.* **178**: 295–316.
- Magne, K., George, J., Berbel Tornero, A., Broquet, B., Madueño, F., Andersen, S.U., and Ratet, P.** (2018b). *Lotus japonicus* *NOOT-BOP-COCH-LIKE1* is essential for nodule, nectary, leaf and flower development. *Plant J.* **94**: 880–894.
- McKim, S.M., Stenvik, G.-E., Butenko, M.A., Kristiansen, W., Cho, S.K., Hepworth, S.R., Aalen, R.B., and Haughn, G.W.** (2008). The *BLADE-ON-PETIOLE* genes are essential for abscission zone formation in *Arabidopsis*. *Development* **135**: 1537–1546.
- Naisbitt, T., James, E.K., and Sprent, J.I.** (1992). The evolutionary significance of the legume genus *Chamaecrista*, as determined by nodule structure. *New Phytol.* **122**: 487–492.
- Norberg, M.** (2005). The *BLADE ON PETIOLE* genes act redundantly to control the growth and development of lateral organs. *Development* **132**: 2203–2213.
- Parniske, M.** (2018). Uptake of bacteria into living plant cells, the unifying and distinct feature of the nitrogen-fixing root nodule symbiosis. *Curr. Opin. Plant Biol.* **44**: 164–174.
- Pawlowski, K. and Demchenko, K.N.** (2012). The diversity of actinorhizal symbiosis. *Protoplasma* **249**: 967–979.
- Pawlowski, K., Jacobsen, K.R., Alloisio, N., Ford Denison, R., Klein, M., Tjepkema, J.D., Winzer, T., Sirrenberg, A., Guan, C., and Berry, A.M.** (2007). Truncated Hemoglobins in Actinorhizal Nodules of *Datisca glomerata*. *Plant Biol.* **9**: 776–785.
- Salgado, M.G., van Velzen, R., Nguyen, T. Van, Battenberg, K., Berry, A.M., Lundin, D., and Pawlowski, K.** (2018). Comparative Analysis of the Nodule Transcriptomes of *Ceanothus thyrsiflorus* (Rhamnaceae, Rosales) and *Datisca glomerata* (Datiscaceae, Cucurbitales). *Front. Plant Sci.* **9**: 1629.
- Sanz-Luque, E., Ocaña-Calahorra, F., De Montaigu, A., Chamizo-Ampudia, A., Llamas, Á., Galván, A., and Fernández, E.** (2015). THB1, a truncated hemoglobin, modulates nitric oxide levels and nitrate reductase activity. *Plant J.* **81**: 467–479.
- Sasakura, F., Uchiumi, T., Shimoda, Y., Suzuki, A., Takenouchi, K., Higashi, S., and Abe, M.** (2006). A Class 1 Hemoglobin Gene from *Alnus firma* Functions in Symbiotic and Nonsymbiotic Tissues to Detoxify Nitric Oxide. *Mol. Plant-Microbe Interact.* **19**: 441–450.
- Soltis, D.E., Soltis, P.S., Morgan, D.R., Swensen, S.M., Mullin, B.C., Dowd, J.M., and Martin, P.G.** (1995). Chloroplast gene sequence data suggest a single origin of the predisposition for symbiotic nitrogen fixation in angiosperms. *Proc. Natl. Acad. Sci. U. S. A.* **92**: 2647–2651.
- Sturms, R., Kakar, S., Trent, J., and Hargrove, M.S.** (2010). *Trema* and *Parasponia* Hemoglobins Reveal Convergent Evolution of Oxygen Transport in Plants. *Biochemistry* **49**: 4085–4093.
- Swensen, S.M.** (1996). The evolution of actinorhizal symbioses: evidence for multiple origins of the symbiotic association. *Am. J. Bot.* **83**: 1503–1512.
- Taylor, B.N. and Menge, D.N.L.** (2018). Light regulates tropical symbiotic nitrogen

- fixation more strongly than soil nitrogen. *Nat. Plants* **4**: 655–661.
- Vázquez-Limón, C., Hoogewijs, D., Vinogradov, S.N., and Arredondo-Peter, R.** (2012). The evolution of land plant hemoglobins. *Plant Sci.* **191–192**: 71–81.
- van Velzen, R. et al.** (2018). Comparative genomics of the nonlegume *Parasponia* reveals insights into evolution of nitrogen-fixing rhizobium symbioses. *Proc. Natl. Acad. Sci. U. S. A.* **115**: E4700–E4709.
- van Velzen, R., Doyle, J.J., and Geurts, R.** (2019). A Resurrected Scenario: Single Gain and Massive Loss of Nitrogen-Fixing Nodulation. *Trends Plant Sci.* **24**: 49–57.
- Wang, Q., Hasson, A., Rossmann, S., and Theres, K.** (2016). *Divide et impera*: Boundaries shape the plant body and initiate new meristems. *New Phytol.* **209**: 485–498.
- Wellmer, F., Graciet, E., and Riechmann, J.L.** (2014). Specification of floral organs in *Arabidopsis*. *J. Exp. Bot.* **65**: 1–9.
- Xu, M., Hu, T., McKim, S.M., Murmu, J., Haughn, G.W., and Hepworth, S.R.** (2010). Arabidopsis BLADE-ON-PETIOLE1 and 2 promote floral meristem fate and determinacy in a previously undefined pathway targeting *APETALA1* and *AGAMOUS-LIKE24*. *Plant J.* **63**: 974–989.
- Žádníková, P. and Simon, R.** (2014). How boundaries control plant development. *Curr. Opin. Plant Biol.* **17**: 116–125.



SUMMARY

Nitrogen-fixing root nodule symbiosis can sustain the development of the host plants under nitrogen limiting conditions. Such symbiosis only occurs in a clade of angiosperms known as the nitrogen-fixing clade (NFC). It has long been proposed that root nodule symbiosis evolved several times (in parallel) in the NFC. There are two main arguments supporting this parallel hypothesis. First, the occurrence of root nodule symbiosis is scattered across the NFC, hypothesizing a single origin is evolutionarily unparsimonious as this would require massive loss of the trait. Second, legume-type and actinorhizal-type nodules are fundamentally different. Two recent phylogenomic studies compared the genomes of nodulating and related non-nodulating species across the four orders of the NFC and found that genes essential for nodule formation are lost or pseudogenized in the non-nodulating species. As these symbiosis genes are specifically involved in the symbiotic interaction, it means that the presence of pseudogenes and the loss of symbiosis genes strongly suggest that their ancestor that still had functional genes most likely formed the nodule symbiosis. Therefore, the first argument supporting the parallel hypothesis is disproved.

Actinorhizal-type nodules have long been regarded as modified lateral roots, originating from root pericycle cells, with newly formed cortical cells being infected by bacteria. Here, we compared the lateral root and nodule development in two plant species forming actinorhizal-type nodules (*Parasponia andersonii* (Parasponia) and *Alnus glutinosa* (Alnus)). We showed that in Parasponia and Alnus, lateral roots are mainly originated from pericycle-derived cells, endodermis cells only form the outmost layer of the lateral root cap. During the formation of Parasponia and Alnus nodules, pericycle-derived cells only form the nodule vasculature, instead of a lateral root (as was previously reported for these species). In both cases, parental root cortical cells are mitotically activated and are infected by bacteria. This is similar to the origin of infected tissue in legume nodules. This finding shows that actinorhizal-type nodules are not modified lateral roots, they are more similar to legume-type nodules than previously described. Therefore, the second argument supporting the parallel hypothesis is also disproved.

We further showed that a legume-type nodule can be (partially) converted to actinorhizal type by knocking out a gene, namely *Medicago truncatula* (Medicago) *NODULE ROOT1* (*MtNROOT1*). In Medicago *Mtnoot1* mutants, the

Summary

nodule vasculature is derived from pericycle cells, similar to the ontogeny of actinorhizal-type nodule vasculature. As homeotic mutants usually revert to an ancestral phenotype, we proposed that actinorhizal-type and legume-type nodules share a common evolutionary origin, and actinorhizal type is ancestral. Our study supports the single origin hypothesis that nodulation of actinorhizal type evolved once in the common ancestor of the NFC.

It has been suggested that *MtNOOT1* maintains nodule identity of the vascular meristem in a cell autonomous manner. However, our study implies that *MtNOOT1* can indirectly maintain nodule identity by repressing actinorhizal-type ontogeny of nodule vasculature. It remains unclear whether *MtNOOT1* has a direct effect on maintaining nodule identity of the vascular meristem. To investigate this, we generated CRISPR/Cas9 mutants in the *MtNOOT1* orthologous gene in *Parasponia*, named *PanNOOT1*. We showed that in *Parasponia Pannoot1* mutants roots can be formed at the nodule apex, similar to legume *noot1* mutants. Both *MtNOOT1* and *PanNOOT1* are expressed in the nodule vascular meristem, suggesting that *Medicago MtNOOT1* and *Parasponia PanNOOT1* share a conserved function in maintaining nodule identity of the vascular meristem in a cell autonomous manner. We further showed that *MtNOOT1* and *PanNOOT1* are required for the intracellular colonization of bacteria in the host cells. The functional analysis of *PanNOOT1* could bring insight to the ancestral symbiotic function of *NOOT1* in the NFC.

Medicago MtNOOT1 has been described as a nodule identity gene. It is also highly expressed in *Medicago* roots, where its function remains unclear. We showed that knockout of *MtNOOT1* leads to accelerated primary root growth due to an enlarged root apical meristem. We further revealed that *MtNOOT1* is expressed in the transition zone of roots, suggestive of a promotive role in inducing cell differentiation between two cell groups with different fates (root apical meristem vs. elongation/differentiation zone). This is similar to the function of *MtNOOT1* orthologs in *Arabidopsis thaliana* (*Arabidopsis*)- *AtBOP1* and *AtBOP2*-setting the boundary of restricted growth between shoot apical meristem and differentiating/elongating leaf primordia. In *Arabidopsis*, *AtBOP1* and *AtBOP2* promote cell differentiation in the stem by inducing lignin biosynthesis. Similarly, in *Medicago* roots *MtNOOT1* promotes xylem cell differentiation by inducing a cascade of genes involved in xylem cell differentiation at proper distance from the root tip. A general role played by *MtNOOT1* is to promote cell differentiation along the apical-basal axis during root development. These findings indicate that *MtNOOT1* is required for a coordinated root development along the apical-

basal axis.

Shoot architecture of plants is modified by branching. Previous studies have shown that *Arabidopsis* AtBOP1 and AtBOP2 orthologs in monocot species (*Hordeum vulgare* and *Zea mays*) are involved in modulating shoot branching. We showed that in the tropical tree *Parasponia* PanNOOT1 regulates axillary branch development. Knock-out of *PanNOOT1* reduces axillary branch growth, due to delayed axially bud emergence and outgrowth. We further showed that PanNOOT1 functions in boundary specification between the petiole and the stem, and in stipule formation and leaf patterning, in a similar fashion as *BOP* genes in herbaceous (model) species. This indicates that *PanNOOT1* is a *BOP* gene, playing a conserved role in stipule formation and leaf patterning. This is the first time that the function of a *BOP* gene is characterized in a tree, revealing a novel role in shoot branching.

I discussed the findings obtained in this thesis together with related published studies. I proposed the evolutionary trajectory of legume-type nodules, and the role of legume NOOT1 in this process. NOOT1 is required for the maintenance of nodule identity in actinorhizal-type and legume-type nodules. I further hypothesized the ancestral symbiotic function of NOOT1 in the NFC, and discussed the general function of NOOT1 under various developmental contexts.

ACKNOWLEDGMENTS

Ton, thank you for the recruitment, for your guidance and patience. Because of you, it has been an inspiring journey. I also must thank you for the financial support in the last two years. Without it I would not be able to finish the project. Ton, it is such a honor to be your student, I am deeply indebted to you.

René, I still remember the first encounter with you, Tian and Fengjiao in CAAS. Thank you for picking me up at the airport when I first arrived; thank you for the Christmas dinner at your home. Thank you for everything you did for me.

Olga, thank you for all the supports you have been giving to me in the past years. Thank you, Henk. I am very glad to know you, I know that I can always count on you when I am in need.

Thank you, Tingting and Huchen. You are the go-to persons when I am in difficulty. Thank you two for the efforts you made to generate a harmonious atmosphere for the Chinese community in the lab. I still remember the barbecue by the lake, the Malta trip, the Königssee trip, Miumiu...

Many thanks to my colleagues and friends: Maria, Marie-Jose, Jan V., Elena, Wouter, Renze, Marijke, Carolien, Joan, Erik, Robin, Jan H., Viola, Norbert; Arjan, Rik, Rens, Titis, Yuda, Luuk, Jelle, Asma, Menno, Lucas, Martinus, Trupti, Jorge, Kavya, Bandan, Adam, Toolbox 56...Without your help and warmth, my PhD journey would have been a misery.

Many thanks to the Chinese community who have been incredibly supportive of me: Fengjiao, Tian; Wenkun, Xu, Jieyu, Guiling, Peng, Zhichun, Jing, Minggang, Jianyong, Yinshan, Jun, Fuxi, Jundi, LuLu, Liguu, DuDu, I-Chiao, Mengmeng, Yuchen, Han; Li Jinling, Zhao Tao, Lin Xiao, Shi Wenbiao, Bao Man, Zhang Yanxia, Song Wei, Wu Jinbing, Zhang Yunmeng, Song Yin, Song Shuang, Bai Bing, Zhang Jianhua, He Jun, Li Tao, Chen Baojian, Wang Ruwang...

妈，爸，感谢你们一直以来的支持，让我去追求自己的梦想。过去十三年，特别是最近六年，一直没能多多陪在你们身边，你们辛苦了。

媛园，你赋予了我这个地方另一个意义，期待和你的未来。

I wish you all the bests, 愿诸位万事遂意,

Defeng 德峰

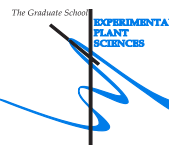
in Wageningen, Autumn 2019

CURRICULUM VITAE

Defeng Shen was born on June 2nd 1987, in Shuangyashan City, China. In 2006 he was admitted to Northeast Forestry University in Harbin. There he majored in Life Sciences, and graduated with honor in 2010. Then he moved to Beijing Normal University, studying the function of microRNAs during caryopsis development in rice. Under the supervision of Prof. Yingdian Wang, he obtained Master of Science Degree in 2013. Thereafter he moved to Wageningen University for doctoral training, supported by China Scholarship Council. He studied the evolution of legume nodule type, with Prof. Ton Bisseling as Promotor and Dr. René Geurts as Co-Promotor. Key findings obtained during his doctoral study are presented in this thesis.

Education Statement of the Graduate School

Experimental Plant Sciences



Issued to: Defeng Shen
 Date: 02 December 2019
 Group: Laboratory of Molecular Biology
 University: Wageningen University & Research

1) Start-Up Phase	<u>date</u>	<u>cp</u>
► First presentation of your project Mechanisms controlling 2 key steps in the legume Rhizobium symbiosis	14 Mar 2014	1.5
► Writing or rewriting a project proposal Mechanisms controlling 2 key steps in the legume Rhizobium symbiosis	Sep-Nov 2013	3.0
► Writing a review or book chapter		
► MSc courses		

Subtotal Start-Up Phase

4.5

2) Scientific Exposure	<u>date</u>	<u>cp</u>
► EPS PhD student days Get2Gether Event, Soest	29-30 Jan 2015	0.6
► EPS theme symposia EPS theme 1 Symposium Developmental Biology of Plants, Wageningen	24 Jan 2014	0.3
EPS theme 1 Symposium Developmental Biology of Plants, Leiden	08 Jan 2015	0.3
EPS theme 1 Symposium Developmental Biology of Plants, Wageningen	21 Jan 2016	0.3
EPS theme 1 Symposium Developmental Biology of Plants, Leiden	28 Feb 2017	0.3
EPS theme 1 Symposium Developmental Biology of Plants, Wageningen	30 Jan 2018	0.3
► Lunteren Days and other national platforms Annual meeting Experimental Plant Sciences, Lunteren, the Netherlands	14-15 Apr 2014	0.6
Annual meeting Experimental Plant Sciences, Lunteren, the Netherlands	13-14 Apr 2015	0.6
Annual meeting Experimental Plant Sciences, Lunteren, the Netherlands	11-12 Apr 2016	0.6
Annual meeting Experimental Plant Sciences, Lunteren, the Netherlands	10-11 Apr 2017	0.6
Annual meeting Experimental Plant Sciences, Lunteren, the Netherlands	9-10 Apr 2018	0.6
Annual meeting Experimental Plant Sciences, Lunteren, the Netherlands	8-9 Apr 2019	0.6
► Seminars (series), workshops and symposia Start symposium Plant Developmental Biology	14 Oct 2013	0.3
Seminar, Jos Raaijmakers, Wageningen	7 Jan 2014	0.1
Seminar, Toby Kiers & Rene Geurts, Wageningen	11 Mar 2014	0.2
EPS Flying Seminar, Noah K. Whiteman, Wageningen	17 Jul 2014	0.1
Seminar, Micheal Djordjevic, Wageningen	15 Sep 2014	0.1
EPS Flying Seminar, Ortrun Mittelsten Scheid, Wageningen	19 Nov 2014	0.1
EPS Flying Seminar, George Coupland, Wageningen	19 Jan 2015	0.1
EPS Flying Seminar, Yves van de Peer, Wageningen	3 Feb 2015	0.1
EPS Flying Seminar, Jeff Doyler, Wageningen	12 May 2015	0.1
EPS Mini Symposium, Root development and rhizosphere, Wageningen	20 May 2015	0.2
Seminar, Alain Goossens, Wageningen	8 Dec 2015	0.1
Seminar, Jan Ruijter, Wageningen	14 Mar 2016	0.1
Seminar, Pierre-Marc Delaux, Wageningen	8 Apr 2016	0.1
Seminar, Raffaele Dello Ioio, Wageningen	29 Aug 2016	0.1
Seminar, Stephanie Porter, Wageningen	22 Sep 2016	0.1
EPS Flying Seminar, Hans Thordal-Christensen, Wageningen	12 Dec 2016	0.1
Seminar, Annet Westhoek & Roland Boer, Wageningen	9 Jan 2017	0.2
Symposium, Publish for Impact, Wageningen	7 Feb 2017	0.2
Symposium, The Undergrond Labyrinth: Roots, Friends and Foes, Wageningen	8 Feb 2017	0.2
Seminar, Ford Denison, Wageningen	10 May 2017	0.1
EPS Flying Seminar, Gerben van Ooijen, Wageningen	29 May 2017	0.1
Seminar, Herman Hofte, Wageningen	30 May 2017	0.1
EPS Flying Seminar, Martin Cann, Wageningen	11 Jul 2017	0.1
WEES Seminar, Richard Lenski, Wageningen	31 Aug 2017	0.1
Seminar, Jean-Francois Arrighi, Wageningen	18 Oct 2017	0.1
Seminar, Magdalena Bezanilla, Wageningen	6 Nov 2017	0.1
Seminar, Jijie Chai, Wageningen	5 Jun 2019	0.1
Public lecture, Alga Zuccaro and Ikram Bllou, Wageningen	10 Sep 2019	0.2
Public lecture, Jürgen Kleine-Vehn, Wageningen	28 Oct 2019	0.1
► Seminar plus		
► International symposia and congresses European Plant Science Retreat 2015, Paris, France	10-13 Jul 2015	1.2
20th International Congress on Nitrogen Fixation (ICNF), Granada, Spain	3-7 Sep 2017	1.5
► Presentations Poster presentation, 20th ICNF, Granada	3-7 Sep 2017	1.0
Presentation at EPS theme 1 Symposium Developmental Biology of Plants, Wageningen	30 Jan 2018	1.0
► IAB interview		

CONTINUED ON NEXT PAGE

► Excursions		
Excursion to company Enza Zaden	12 Jun 2015	0.2
<i>Subtotal Scientific Exposure</i>		14.3

3) In-Depth Studies	<i>date</i>	<i>cp</i>
► Advanced scientific courses & workshops		
PhD Course, Bioinformatics-A User's Approach	25-29 Aug 2014	1.5
WIAS Advanced Statistics Course, Design of Experiments	8-10 Oct 2014	1.0
EPS course, Data Analyses and Visualizations in R	8-9 May 2018	0.6
► Journal club		
Member of literature discussion at MolBi	2014-2019	3.0
► Individual research training		
Laser capture microdissection training with Dr. Hooiveld in Division of Human Nutrition, WUR	16 Jul 2014	0.2
<i>Subtotal In-Depth Studies</i>		6.3

4) Personal Development	<i>date</i>	<i>cp</i>
► General skill training courses		
PhD Course, Information Literacy PhD including EndNote Introduction	9-10 Jun 2015	0.6
PhD Course, Reviewing a Scientific Paper	17 Sep 2015	0.1
PhD Course, Project- and Time Management	10 Feb - 23 Mar 2016	1.5
PhD Course, Scientific Writing	10 Jan - 7 Mar 2017	1.8
PhD Course, Scientific Publishing	19 Oct 2017	0.3
PhD Course, Brain Training	8 Nov 2017	0.3
PhD Course, Research Integrity	30 Nov - 1 Dec 2017	0.6
► Organisation of meetings, PhD courses or outreach activities		
► Membership of EPS PhD Council		
<i>Subtotal Personal Development</i>		5.2

TOTAL NUMBER OF CREDIT POINTS*		30.3
Herewith the Graduate School declares that the PhD candidate has complied with the educational requirements set by the Educational Committee of EPS with a minimum total of 30 ECTS credits.		
* A credit represents a normative study load of 28 hours of study.		

This research was performed in Laboratory of Molecular Biology, Wageningen University, with support from European Research Council (ERC-2011-AdG-294790), from NWO-VICI grant (865.13.001), and from China Scholarship Council (201306040120).

Cover Design and Thesis Layout: Defeng Shen.